UNIVERSIDADE DO VALE DO RIO DOS SINOS-UNISINOS
UNIDADE ACADÊMICA DE PESQUISA E PÓS-GRADUAÇÃO
PROGRAMA DE PÓS-GRADUAÇÃO EM GEOLOGIA
NÍVEL DOUTORADO

DAIANE CEOLIN

TAXONOMIA E ASPECTOS PALEOECOLÓGICOS DOS OSTRACODES DO MAASTRICHTIANO – DANIANO (FORMAÇÕES JAGÜEL E ROCA) DA SEÇÃO DE CERRO AZUL, GENERAL ROCA, BACIA DE NEUQUÉN, ARGENTINA.

SÃO LEOPOLDO
2015

Daiane Ceolin

TAXONOMIA E ASPECTOS PALEOECOLÓGICOS DOS OSTRACODES DO MAASTRICHTIANO – DANIANO (FORMAÇÕES JAGÜEL E ROCA) DA SEÇÃO DE CERRO AZUL, GENERAL ROCA, BACIA DE NEUQUÉN, ARGENTINA.

Tese de Doutorado apresentada como requisito parcial para obtenção do título de Doutor, pelo Programa de Pós-Graduação em Geologia da Universidade do Vale do Rio dos Sinos – UNISINOS

Área de concentração: Geologia Sedimentar

Linha de Pesquisa: Paleontologia Aplicada

Orientador: Dr. Gerson Fauth

Co-orientadora: Dr[a]. Andrea Concheyro

BANCA EXAMINADORA:

Gabriela Catalina Cusminsky – Universidad Nacional del Comahue (UNCo)

João Carlos Coimbra – Universidade Federal do Rio Grande do Sul (UFRGS)

Cristianini Trescastro Bergue – Universidade do Vale do Rio dos Sinos (UNISINOS)

Ficha catalográfica

C398t Ceolin, Daiane
Taxonomia e aspectos paleoecológicos dos ostracodes do Maastrichtiano–Daniano (formações Jagüel e Roca) da seção de Cerro Azul, General Roca, Bacia de Neuquén, Argentina / por Daiane Ceolin. – 2015.
144 f.: il., 30 cm.

Tese (doutorado) — Universidade do Vale do Rio dos Sinos, Programa de Pós-Graduação em Geologia, 2015.
Orientação: Prof. Dr. Gerson Fauth ; Coorientação: Profa. Dra. Andrea Concheyro.

1. Bacia de Neuquén. 2. Ostracode. 3. Cretáceo-Paleógeno. 4. Formação Jagüel. 5. Formação Roca. 6. Argentina. I. Título.

CDU 595.33

Catalogação na Fonte:
Bibliotecária Vanessa Borges Nunes - CRB 10/1556

UNISINOS

UNIVERSIDADE DO VALE DO RIO DOS SINOS
Ciências Exatas e Tecnológicas
Programa de Pós-Graduação em Geologia

A tese de doutorado

"TAXONOMIA E ASPECTOS PALEOECOLÓGICOS DOS OSTRACODES DO MAASTRICHTIANO-DANIANO (FORMAÇÕES JAGÜEL E ROCA) DE SEÇÃO DE CERRO AZUL, GENERAL ROCA, BACIA DE NEUQUÉN, ARGENTINA"

apresentada por **Daiane Ceolin**

foi aceita e aprovada como atendimento parcial aos requisitos para a obtenção do grau de

DOUTOR EM GEOLOGIA pela seguinte banca examinadora:

Dr. Cristianini Trescastro Bergue
Universidade do Vale do Rio dos Sinos

Prof.ª Dr.ª Gabriela Catalina Cusminsky
Instituto de Investigaciones de Biodiversidad y Medio Ambiente (Argentina)

Prof. Dr. João Carlos Coimbra
Universidade Federal do Rio Grande do Sul

Prof. Dr. Gerson Fauth
Presidente da Banca Examinadora
Universidade do Vale do Rio dos Sinos

São Leopoldo, 20 de março de 2015.

Av. Unisinos, 950 - Caixa Postal 275 - CEP 93022-000 - São Leopoldo - Rio Grande do Sul - Brasil
Fone: (51) 3590-8174 - Fax: (51) 3590-8162 - ppggelogia@unisinos.br - www.unisinos.br

Dedico este estudo...

à Sara Ballent (*in memorian*) que foi a grande mentora deste projeto e que não pôde estar aqui para presenciar a conclusão desta pesquisa. Meu eterno obrigado!

AGRADECIMENTOS

Primeiramente quero agradecer à Deus pela vida.

Agradeço à UNISINOS pela concessão da bolsa de estudos Padre Milton Valente e à CAPES pela bolsa de doutorado sanduíche (CAPES - Proc. BEX 2696/14-2).

Quero agradecer profundamente aos professores que acompanharam o meu estudo durante esses quatro anos, principalmente ao meu orientador, Prof. Dr. Gerson Fauth, pelo apoio e incentivo durante a realização desta tese.

À minha co-orientadora, professora Dr[a.] Andrea Concheyro da Universidad de Buenos Aires por toda ajuda e tempo dedicado à realização deste estudo; bem como à Dr[a]. Telma Musso da Universidad Nacional del Comahue, Neuquén, pelas amostras concedidas para a realização deste doutorado e ao suporte na atividade de campo. Agradeço também aos demais profissionais da Universidade de Buenos Aires que contribuíram de alguma forma para a realização deste trabalho.

Ao professor Dr. Robin Whatley da Aberystwyth University, UK, pelo tempo dedicado e pelos ensinamentos ao longo do desenvolvimento desta tese durante o doutorado sanduíche.

Aos meus colegas do itt Fossil, especialmente à Marlone Bom, Patrícia Krauspenhar, Rodrigo Guerra, Karlos Kochhan e Simone Fauth pelo apoio, ajuda, incentivo, troca de ideias e descontrações. Aos demais colegas do instituto, obrigada pelas experiências e momentos compartilhados.

Aos meus pais, irmãs e familiares, pelo apoio, orações e palavras de incentivo durante esta longa caminhada dedicada aos estudos e à pesquisa.

E, por fim, agradeço ao meu querido e grande incentivador, Cristiano, que sem seu apoio eu não teria chegado até aqui. Obrigada pela compreensão, paciência, companheirismo, pelo carinho e pelo amor.

RESUMO

A Bacia de Neuquén é conhecida por apresentar um rico e bem preservado conteúdo fossilífero exposto em seções completas e com registros sedimentológicos excelentes, constituindo um local ideal para o estudo do evento de extinção do limite K–Pg. Apesar do grande número de trabalhos já publicados, recentemente novas seções foram descobertas, entre as quais, a seção de Cerro Azul que possui uma fauna de ostracodes abundante, bem preservada e registra a passagem do limite K–Pg. No presente estudo, foram analisadas 27 amostras pertencentes às formações Jagüel e Roca (Maastrichtiano–Daniano) da seção de Cerro Azul, Bacia de Neuquén. O estudo faunístico permitiu o reconhecimento de 113 espécies, pertencentes à 51 gêneros e 11 famílias. Destes, 10 gêneros e 41 espécies novas são descritas, além da nova subfamília Nodoconchiinae. As espécies novas são: *Cytherella saraballentae*, *Cytherella semicatillus*, *Paracypris bertelsae*, *Paracypris imaguncula*, *Argilloecia abnormalis, Argilloecia concludus*, *Argilloecia hydrodynamicus*, *Bythoceratina cheleutos*, *Phelocyprideis acardomesido* (novo gênero e espécie), *Eucythere dinetos*, *Krithe crepidus*, *Cytheropteron hyperdictyon*, *Cytheropteron bidentinos*, *Cytheropteron translimitares*, *Aversovalva glochinos*, *Eucytherura stibaros*, *Hemingwayella verrucosus*, *Heinia prostratopleuricos*, *Loxoconcha* (s.l.) *posterocosta*, *Keijia circulodictyon*, *Keijia kratistos*, *Paramunseyella epaphroditus*, *Munseyella costaevermiculatus*, *Ameghinocythere archaios*, *Aleisocythereis polikothonus*, *Castillocythereis multicastrum* (novo gênero e espécie), *Castillocythereis albertoriccardii*, *Cythereis stratios*, *Cythereis clibanarius*, *Cythereis trajectiones*, *Henryhowella (Wichmannella) praealtus*, *Hysterocythereis paredros* (novo gênero e espécie), *Hysterocythereis coinotes*, *Hysterocythereis diversotuberculatus*, *Orthrocosta decores* (novo gênero e espécie), *Orthrocosta atopos*, *Orthrocosta phantasia*, *Sthenarocythereis erymnos* (novo gênero e espécie), *Nodoconcha polytorosa*, *Nodoconcha sanniosis*, *Nodoconcha upsilon* e *Ectonodoconcha lepidotus* (novo gênero e espécie). Os demais gêneros novos *Aleisocythereis*, *Apatoleberis*, *Mimicocythereis* e *Petalocythereis* foram propostos para acomodar algumas espécies previamente descritas para a Bacia de Neuquén. Alguns aspectos evolutivos da fauna identificada, principalmente das subfamílias Trachyleberidinae e Nodoconchiinae são discutidos. A interpretação paleoecológica para a seção de Cerro Azul, baseada na associação faunística, permite inferir um ambiente marinho de plataforma média a interna, sendo a família Trachyleberididae a mais abundante tanto no

Maastrichtiano quanto no Daniano. A passagem do limite K–Pg é marcada por uma considerável mudança faunística, caracterizada pelo surgimento de uma nova fauna mais rica e abundante no Daniano, além da presença de 21 espécies sobreviventes. Além disso, é observada a presença de predação nas carapaças, possivelmente causada por Naticídeos, especialmente no Daniano.

Palavras-chave: Bacia de Neuquén. Ostracode. Cretáceo–Paleógeno. Formação Jagüel. Formação Roca. Argentina.

ABSTRACT

The Neuquén basin is known by its rich and well preserved fossil content exposed in a complete and excellent sedimentological records, constituting an ideal location for study of the K–Pg boundary. Despite of the large number of published works in the area, recently new sections have been discovered. Among these, the Cerro Azul section is of great importance due to its abundant and well preserved ostracod fauna which spans the K–Pg boundary. In the present study, a total of 27 samples from the Jagüel and Roca formations (Maastrichtian-Danian) of the Nequén basin were analysed. The faunal study allowed the recognition of 113 species, belonging to 51 genera and 11 families. From these, 10 new genera, 41 new species and a new subfamily Nodoconchiinae, were described. The new species are: *Cytherella saraballentae*, *Cytherella semicatillus*, *Paracypris bertelsae*, *Paracypris imaguncula*, *Argilloecia abnormalis, Argilloecia concludus*, *Argilloecia hydrodynamicus*, *Bythoceratina cheleutos*, *Phelocyprideis acardomesido* (new genus and species), *Eucythere dinetos*, *Krithe crepidus*, *Cytheropteron hyperdictyon*, *Cytheropteron bidentinos*, *Cytheropteron translimitares*, *Aversovalva glochinos*, *Eucytherura stibaros*, *Hemingwayella verrucosus*, *Heinia prostratopleuricos*, *Loxoconcha* (s.l.) *posterocosta*, *Keijia circulodictyon*, *Keijia kratistos*, *Paramunseyella epaphroditus*, *Munseyella costaevermiculatus*, *Ameghinocythere archaios*, *Aleisocythereis polikothonus*, *Castillocythereis multicastrum* (new genus and species), *Castillocythereis albertoriccardii*, *Cythereis stratios*, *Cythereis clibanarius*, *Cythereis trajectiones*, *Henryhowella (Wichmannella) praealtus*, *Hysterocythereis paredros* (new genus and species), *Hysterocythereis coinotes*, *Hysterocythereis diversotuberculatus*, *Orthrocosta decores* (new genus and species), *Orthrocosta atopos*, *Orthrocosta phantasia*, *Sthenarocythereis erymnos* (new genus and species), *Nodoconcha polytorosa*, *Nodoconcha sanniosis*, *Nodoconcha upsilon* and *Ectonodoconcha lepidotus* (new genus and species). The new genera *Aleisocythereis*, *Apatoleberis*, *Apobradleya* and *Petalocythereis* were proposed to accomodate species previously described for Neuquén Basin. Some evolutionary aspects of the identified fauna, mainly regarding the Trachyleberidinae and Nodoconchiinae subfamilies, are discussed. The paleoecological interpretation based on the faunal association present in the Cerro Azul section allows the inference of a marine, inner to mid-shelf environment, with a dominance of the family Trachyleberididae in both Maastrichtian and Danian rocks. The K–Pg boundary is marked by a considerable faunal change, characterized by the appearance of a

richer and more abundant Danian fauna alongside 21 species which survived the extinction event. The presence of predation on the carapaces is documented, possibly caused by naticid snails.

Key words: Neuquén Basin. Ostracod. Cretaceous–Paleogene. Jagüel Formation. Roca Formation. Argentina.

LISTA DE FIGURAS

SUMÁRIO

1. INTRODUÇÃO

O limite Cretáceo–Paleógeno representa um dos maiores eventos de extinção ocorridos na história da Terra e um dos acontecimentos do passado geológico com maior volume de estudos. As causas deste evento são ainda muito discutidas e não há consenso se foi um evento único ou vários, mas as hipóteses mais aceitas se referem a possível queda de um meteorito (e.g., Alvarez *et al*. 1980a, Ward *et al*. 1995), a intensa atividade vulcânica ocorrida na Índia (e.g., Keller 2003, 2005, 2008) ou a mudanças climáticas com flutuações no nível do mar (e.g., Officer & Drake 1983, Alegret *et al*. 2003, Hay 2008).

A Bacia de Neuquén, desde o início do século XX tem sido objeto de numerosos estudos, tanto estratigráficos quanto paleontológicos (e.g., Uliana & Dellapé 1981, Nañez & Concheyro 1996, Gasparini *et al*. 2007). Entre as décadas de 1960 e 1990, a exploração de hidrocarbonetos levou a significativos avanços no entendimento da bacia (Howell *et al*. 2007) e, a partir disso, um refinamento bioestratigráfico passou a ser realizado em várias seções destacando-se as que registram o limite K–Pg, devido à completude e continuidade das seções aflorantes e à excelente preservação e abundância de vários grupos fósseis (Bertels 1975a, 1980, Concheyro *et al*. 2002).

Estudos pioneiros com ostracodes para esta bacia foram realizados por Bertels (1964, 1973, 1974, 1975a) com enfoque micropaleontológico e paleoecológico, revelando uma excelente fauna em termos de preservação e riqueza. Os trabalhos com nanofósseis, foraminíferos e outros grupos fósseis também se destacam pelas importantes contribuições bioestratigráficas, paleoecológicas e paleoambientais e, por isto, esta bacia constitui-se em uma região ideal para novas pesquisas sobre as causas e efeitos da extinção no final do Cretáceo (Nañez & Concheyro 1996, Concheyro *et al*. 2002, Casadío *et al*. 2004, Howell *et al*. 2007).

A seção de Cerro Azul representa um novo registro estratigráfico do limite K–Pg na Bacia de Nequén. Os estudos desenvolvidos são pioneiros para esta seção, localizada na porção centro-oeste da bacia, sendo que anteriormente somente Musso *et al*. (2012) realizaram um trabalho sobre a mineralogia das argilas e os nanofósseis calcários, caracterizando as condições climáticas vigentes.

O estudo taxonômico e paleoecológico dos ostracodes desta seção fornecem dados novos que podem contribuir para a melhor compreensão da evolução da bacia, permitindo a realização de interpretações sobre o comportamento da fauna de ostracodes durante este

evento de extinção, além de ampliar o conhecimento sobre a distribuição das espécies na Bacia de Neuquén.

1.1 Objetivos

Os objetivos deste estudo estão relacionados a propósitos taxonômicos e, a partir destes, inferir sobre aspectos paleoecológicos relacionados ao evento de extinção do limite K–Pg na Bacia de Neuquén, especificamente na seção de Cerro Azul.

Os objetivos específicos deste trabalho incluem:

- refinar a taxonomia dos ostracodes para o intervalo Maastrichtiano–Daniano, na seção de Cerro Azul, descrevendo os novos táxons, a fim de proporcionar um melhor conhecimento sobre a fauna existente na Bacia de Neuquén;
- analisar a distribuição estratigráfica dos ostracodes durante este intervalo objetivando o reconhecimento do comportamento faunístico frente ao evento de extinção K–Pg;
- realizar inferências paleoecológicas para esta nova seção, com base na fauna de ostracodes identificada.

1.2 Organização da Tese

A presente tese de doutorado está composta pelos seguintes temas: introdução, contextualização geológica do local de estudo, revisão dos principais temas que norteiam este trabalho, resultados, discussões e conclusões.

No item contextualização geológica estão descritos, de forma geral, os principais aspectos sobre a área de estudo bem como sobre a metodologia utilizada na preparação das amostras, além da revisão dos estudos anteriores desenvolvidos na Bacia de Neuquén. No item eventos de extinção são abordados os principais aspectos relacionados ao evento do limite K–Pg. As considerações paleoecológicas realizadas para a seção, baseada na fauna de ostracodes identificada, estão apresentadas no capítulo final. Este último tópico será tema de uma futura publicação.

O resultado taxonômico obtido neste trabalho está compilado na forma de dois artigos científicos que foram submetidos aos periódicos *Palaeontology* e *Journal of*

Micropaleontology e, portanto, já se encontram finalizados e de acordo com as normas das respectivas revistas. A seguir, apresenta-se o título de cada artigo e uma breve descrição sobre os aspectos abordados:

1) *New genera and species of Ostracoda from the Maastrichtian and Danian of the Neuquén Basin, Argentina*. Este artigo apresenta o estudo taxonômico do perfil Cerro Azul, com a identificação de 113 espécies pertencentes a 54 gêneros, dos quais, nove são novos, 38 novas espécies e 28 espécies foram deixadas em nomenclatura aberta. O artigo também apresenta uma breve abordagem sobre os aspectos da origem e evolução da fauna, principalmente da subfamília Trachyleberidinae.
2) *The Nodoconchiinae, a new Subfamily of Cytheridae (Crustacea, Ostracoda)*. Este artigo apresenta a determinação de uma nova Subfamília de ostracodes para acomodar três gêneros: *Austrocythere* Hartmann, *Nodoconha* Hartmann e *Ectonodoconcha* gen. nov., sendo este último um gênero novo com sua respectiva espécie nova. No artigo foram identificadas sete espécies do gênero *Nodoconcha* Hartmann, sendo que destas, três são novas e estão devidamente descritas. Ao final é apresentada uma discussão sobre a possível evolução filogenética destas espécies.

2. CONTEXTUALIZAÇÃO GEOLÓGICA

2.1 A Bacia de Neuquén

A Bacia de Neuquén é limitada na margem nordeste e sul pelo maciço de Serra Pintada e o maciço do Norte Patagônico respectivamente. A sucessão inclui rochas compostas por sedimentos siliciclásticos, carbonáticos e evaporíticos que se depositaram em diferentes regimes tectônicos. Além disso, possui um espesso pacote de sedimentação marinha depositado entre o Jurássico e o Cretáceo (Howell *et al*. 2007, Musso *et al.* 2012).

A bacia está localizada na região centro-oeste da Argentina entre 32º e 40ºS de latitude, abrangendo parte das províncias de Mendoza, Neuquén, Río Negro e La Pampa (Fig.1). Na latitude 35ºS, a bacia se expande e forma o embaiamento Neuquino, que compreende 600 km de extensão em sentido norte-sul e 300-400 km em sentido leste-oeste. Em sua totalidade, registra um pacote de 7.000 m de espessura de rochas sedimentares marinhas e continentais que abrange desde o Jurássico Superior até o Paleoceno (Howell *et al*. 2007, Aguirre-Urreta *et al*. 2008).

O desenvolvimento sedimentar da Bacia de Neuquén pode ser dividido em três grandes ciclos, denominados Jurássico (Triássico Superior–Jurássico Superior: fase *synrift*), Ândico (Jurássico Superior–Cretáceo Inferior: *postrift*) e Riograndídico (Cretáceo Superior–Paleógeno: *foreland*). Este último foi dividido em dois subciclos, o inferior, integrado pelo Grupo Neuquén (Cenomaniano–Campaniano) de caráter continental e o superior denominado Malalhueyano, entre o Maastrichtiano e o Paleoceno de caráter marinho (Groeber 1946).

Nesta última fase, o sistema deposicional da bacia foi fortemente controlado pelo regime compressivo como consequência do movimento extensional do Atlântico Sul e da reorganização da placa do Pacífico. Isto resultou no desenvolvimento de um regime tectônico compressional que causou a inversão de estruturas extensionais prévias. Neste momento houve a primeira transgressão marinha do Oceano Atlântico, mais precisamente no intervalo Maastrichtiano, que foi influenciada também pelo alto nível do mar nesta época, originando um mar relativamente raso que cobriu grande parte da Patagônia extra-andina e que persistiu até o Daniano (Camacho 1992, Parras *et al*. 1998, Malumián 1999, Prámparo & Papú 2006, Howell *et al*. 2007, Nañez & Malumián 2008, Aguirre-Urreta *et al*. 2010). Esta transgressão está relacionada ao afundamento da margem passiva patagônica ocasionado pelo resfriamento litosférico e sobrecarga de sedimentos, associado à subsidência da bacia devido ao evento de

soerguimento dos Andes durante a fase Laramica (Uliana & Bidde 1988, Gasparini *et al.* 2001) (Fig. 2).

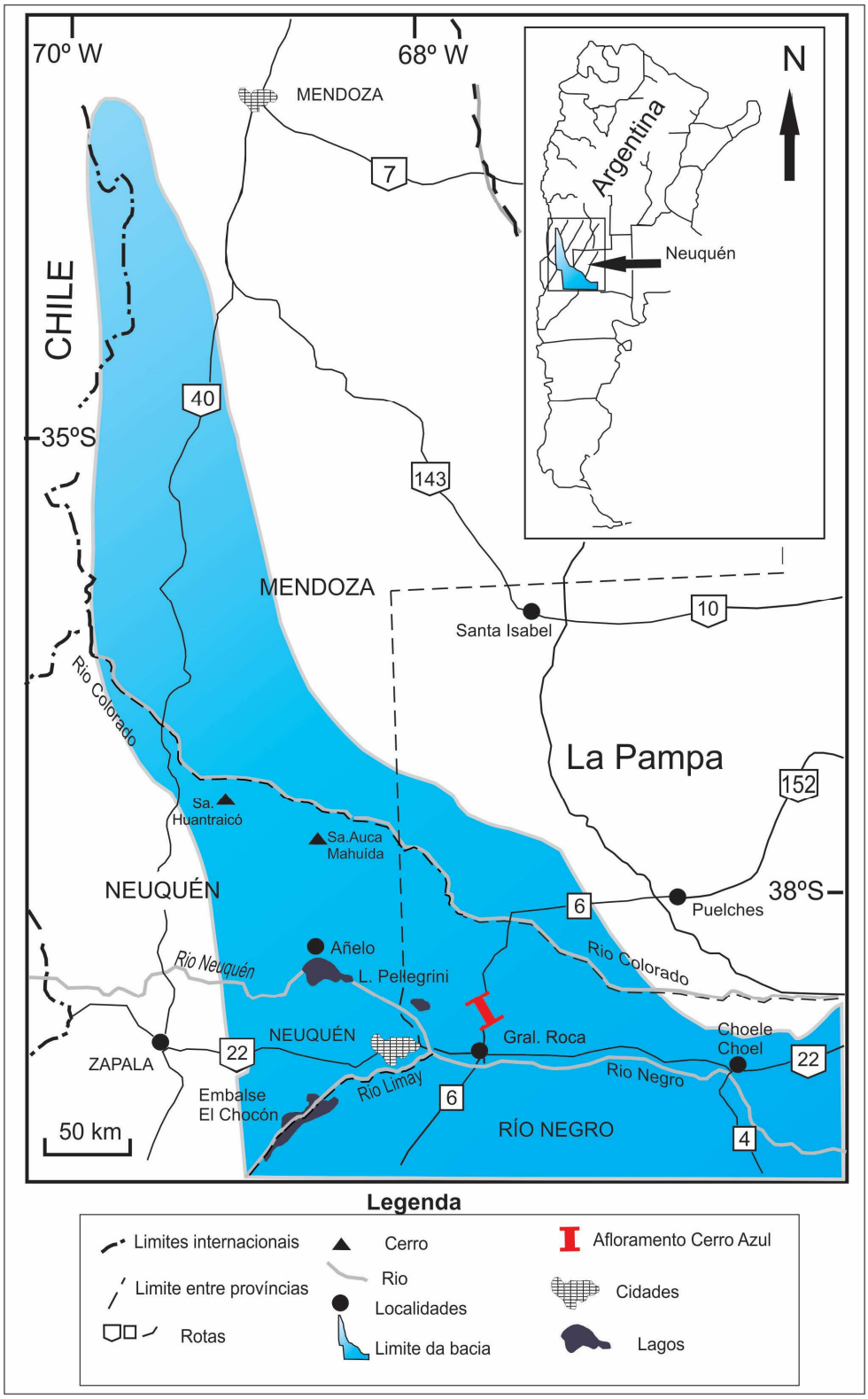

Figura 1: Mapa da Bacia de Neuquén com a localização da seção estudada. (Modificado de Del Río *et al.* 2011).

O subciclo Malalhueyano está representado pelas litologias do Grupo Malargüe que é composto, na região oriental, pelas Formações Allen, Jagüel, Roca e El Carrizo. As formações Allen e El Carrizo são constituídas por sedimentos de origem continental, enquanto que Jagüel e Roca por sedimentos marinhos (Casadío *et al*. 1998, Gasparini *et al*. 2007, Fernández *et al.* 2008). Estas duas últimas formações são objeto deste estudo e foram depositadas no intervalo Maastrichtiano e Daniano.

2.1.1. FORMAÇÃO JAGÜEL (WINDHAUSEN 1914).

A Fm. Jagüel contém rochas correspondentes aos intervalos Maastrichtiano e Daniano, caracterizados por importantes mudanças climáticas e paleoambientais evidenciadas na fauna presente no Grupo Malargüe (Casadío *et al*. 2005). Esta formação apresenta distribuição nos setores mais internos da bacia e aflora com boas exposições no setor pampeano e rionegrense. Devido a sua litologia fina e homogênea, os afloramentos apresentam pouca variação morfológica (Rodrigues 2011).

Grande parte dos autores que estudaram esta formação salientam que o pacote sedimentar é constituído por uma sequência monótona de siltitos e argilitos pouco estratificados de tonalidades cinza-amarelados e castanho-esverdeados, intercalados por finas camadas de gesso diagenético, que representam um ambiente marinho de plataforma interna à externa com condições de baixa energia e boa circulação (e.g., Concheyro 1995, Papú *et al*. 1999, Parma & Casadío 2005). Esta formação é limitada na base pela camada de gipsita da Fm. Allen e, ao topo, pela primeira camada de calcário organogênico da Fm. Roca (Uliana & Dellapé 1981, Papú *et al*. 1999, Scasso *et al*. 2005) (Fig. 3).

2.1.2. FORMAÇÃO ROCA (IHERING 1903).

Vários autores estudaram a Fm. Roca, de idade daniana, desde o início do século passado, abordando principalmente a análise de fácies e o conteúdo fossilífero (e.g., Uliana & Dellapé 1981, Bertels 1964, 1969a, 1970, 1975a, 1980, Concheyro 1995). Os depósitos desta formação se encontram distribuídos em uma extensa área da Patagônia setentrional (Bertels 1980) (Fig. 3) e são considerados ambientes de deposição mais rasos e com uma litologia que apresenta variações mais expressivas se comparada com a Fm. Jagüel (Nañez & Concheyro 1996).

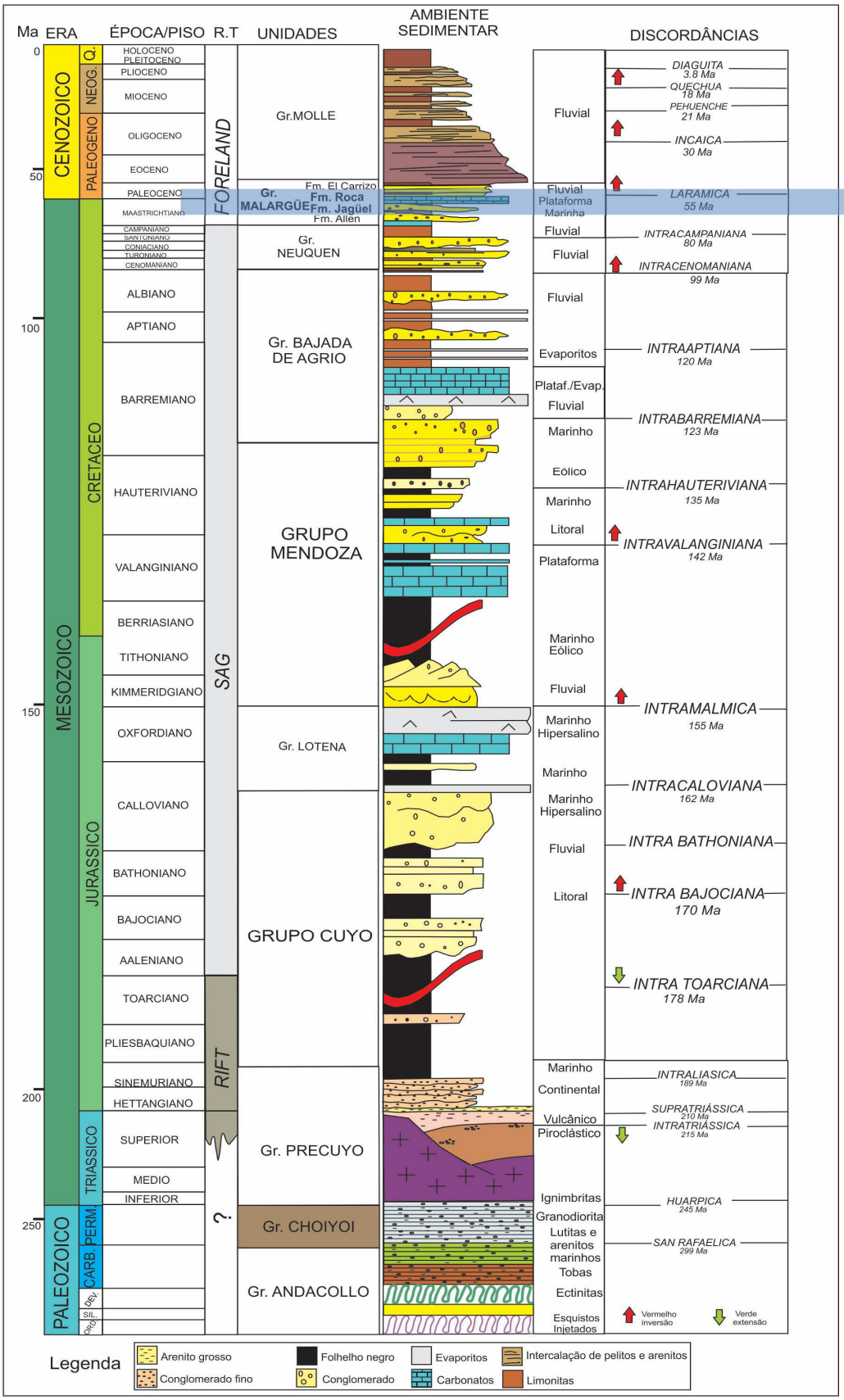

Figura 2: Coluna estratigráfica da Bacia de Neuquén destacando o intervalo estudado. (Modificado de Arregui *et al*. 2011).

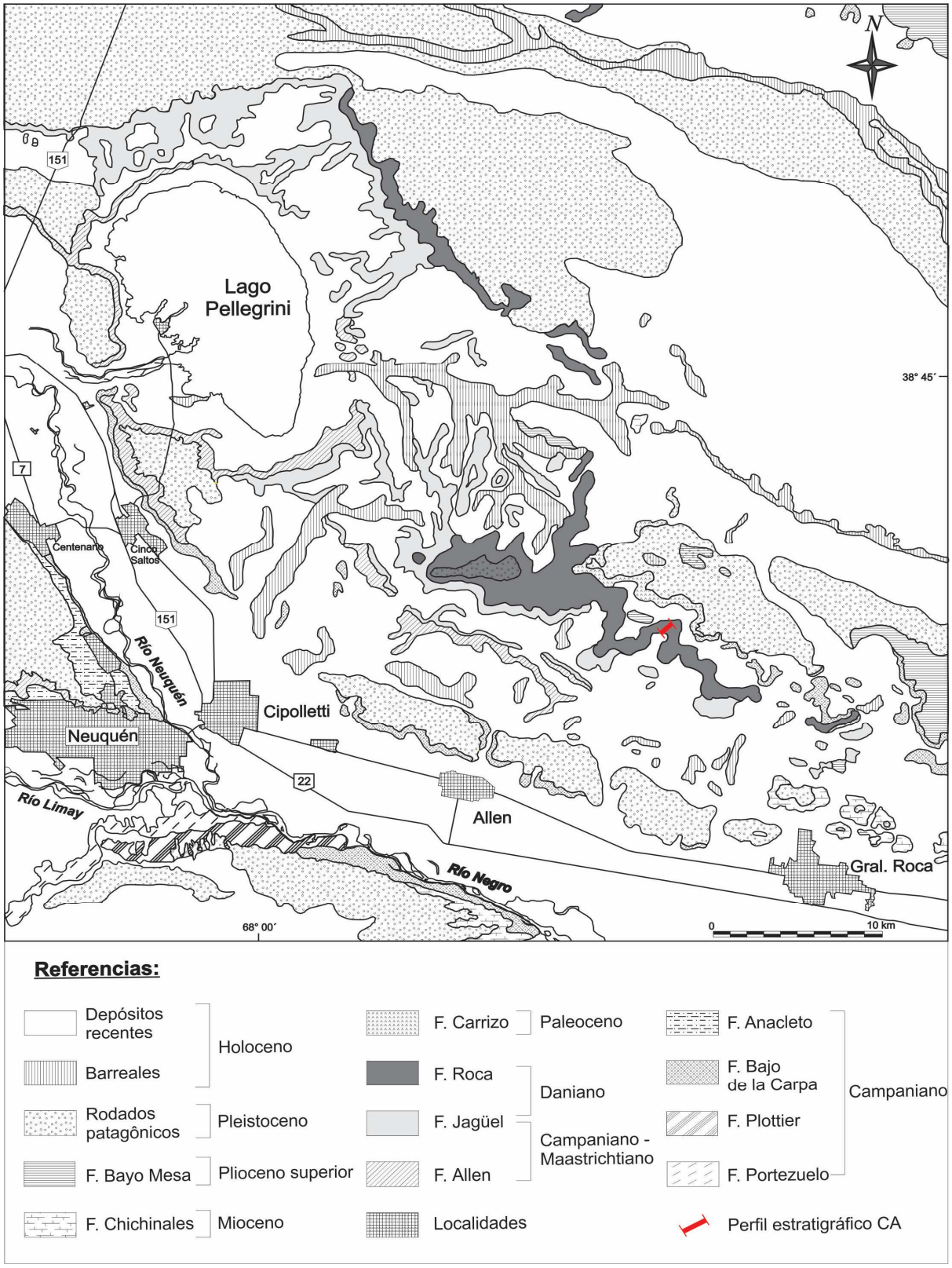

Figura 3: Mapa geológico da área de estudo com o posicionamento do perfil de Cerro Azul. (Adaptado de Musso *et al*. 2012).

O pacote sedimentar varia desde carbonatos até intercalações de arenito e lamito calcários, *mudstones* e *limestones* de coloração cinza-esverdeado, associados a abundantes fragmentos esqueletais, dependendo da região onde a formação está exposta (Del Río *et al*. 2011). Casadío *et al*. (2005) e Parras *et al*. (1998) definem esta unidade como sendo constituída por bioclásticos *packstones*, *grainstone* e margas depositados em ambientes com influência de marés. A Fm. Roca apresenta relação de concordância com a Fm. Jagüel e ambas unidades são consideradas como pertencentes a um mesmo ciclo sedimentar (Uliana & Dellapé 1981). Um histórico mais detalhado sobre estas duas formações pode ser encontrado em Rodrigues (2011).

2.2 Material e Métodos

Para a realização do presente estudo foram utilizadas 27 amostras de rochas coletadas em 70 m da seção de Cerro Azul, província de Río Negro onde afloram as formações Jagüel e Roca de idade maastrichtiana-daniana. Musso *et al.* (2012) descreveram a litologia desta seção, caracterizando a Formação Jagüel como sendo homogênea e constituída por argilito calcário amarelo acinzentado. A Formação Roca apresenta uma alternância de rochas carbonáticas e argilitos calcários cinza esverdeados e a base é definida pelo primeiro aparecimento de calcário organogênico (Uliana & Dellapé 1981). As amostras utilizadas neste estudo possuíam em média 20 g e eram compostas basicamente por argilitos e carbonatos (Fig. 4).

Estas amostras foram gentilmente cedidas pela professora Drª. Andrea Concheyro da Facultad de Ciencias Exactas y Naturales, Universidad de Buenos Aires – UBA e foram coletadas em atividade de campo, no ano de 2008, pelas Drª Telma Musso da Universidad Nacional del Comahue, Neuquén e Drª Andrea Concheyro.

2.2.1 PREPARAÇÃO DAS AMOSTRAS

A preparação das amostras foi efetuada no Instituto Tecnológico de Micropaleontologia, itt Fossil da UNISINOS. Aproximadamente 20 g de cada amostra foram preparadas de acordo com a metodologia de Sohn *et al*. (1965) detalhada em Slipper (1997), adaptado para microfósseis calcários. O procedimento seguiu as seguintes etapas:

- aproximadamente 20 g de rocha (fragmentadas quando necessário) foram pesadas em balança semi-analítica e transferidas para béqueres de forma alta (600 mL de capacidade);
- na sequência, adicionou-se cerca de 200 mL de peróxido de hidrogênio (H_2O_2) P.A, por um período de 24 h com a finalidade de eliminar a matéria orgânica. Quanto maior o teor de matéria orgânica na rocha, maior será a reação do oxigênio liberado pelos produtos orgânicos, gerando um aumento de calor. Para controlar esta reação exotérmica, utiliza-se o etanol que reduz a tensão superficial das bolhas;
- após este período, as amostras foram lavadas em uma peneira de malha 45 µm e a fração restante foi devolvida ao béquer;
- na sequência, foi adicionado 200 mL de H_2O_2 P.A. e aquecido em banho de areia a 60 ºC por 2 h, com a finalidade de eliminar qualquer resquício de matéria orgânica que não tenha sido eliminada na etapa anterior;
- posterior a este período, as amostras foram lavadas em água corrente utilizando peneiras superpostas de malhas 250, 180 e 63 µm para a separação das frações granulométricas;
- o material recuperado nas peneiras foi transferido para cápsulas de porcelana devidamente identificadas e levadas para secagem em estufa a 60 °C;
- depois de seco, o material foi transferido para pequenos recipientes de acrílico etiquetados;
- posteriormente, o material foi triado sob microscópio estereoscópico V8 ZEIS e os espécimes separados por morfotipos.

2.2.2 PROCEDIMENTOS PARA O ESTUDO TAXONÔMICO

Os melhores exemplares de cada morfotipo foram metalizados e imageados em microscópio eletrônico de varredura (MEV-EVO MA15, ZEIS) no itt Fossil, para a identificação taxonômica, que seguiu a classificação supragenérica de Moore & Pitrat (1961) com algumas modificações.

As discussões taxonômicas foram realizadas sob a supervisão do professor Dr. Robin Whatley da Aberystwyth University, no País de Gales, UK durante o desenvolvimento do

doutorado sanduíche (5 meses) do programa PDSE da CAPES. Na oportunidade foram desenvolvidos os dois artigos científicos apresentados nesta tese.

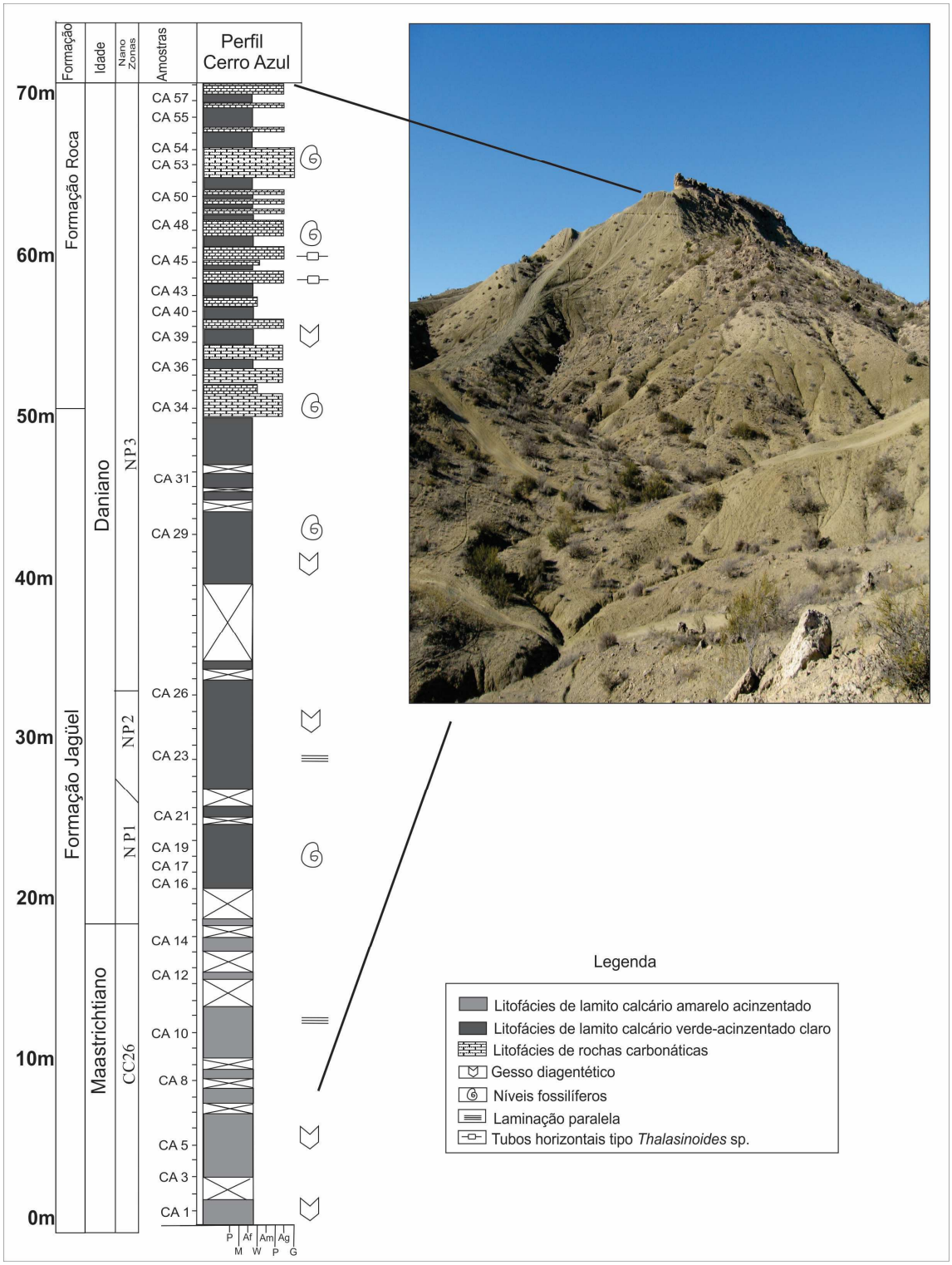

Figura 4: Perfil litológico de Cerro Azul com as amostras estudadas e o local de coleta. (Modificado de Musso *et al*. 2012).

2.3 Estudos micropaleontológicos prévios sobre o Maastrichtiano–Daniano na Bacia de Neuquén.

2.3.1 OSTRACODES

A fim de resolver problemas estratigráficos existentes para o limite K–Pg na Bacia de Neuquén, Bertels (1968b,1969a) desenvolveu um estudo na Patagônia setentrional, analisando a fauna de ostracodes presente em várias seções, inclusive em Barranca de Jagüel, considerada a melhor exposição do limite K–Pg na bacia e a seção tipo para a Fm Jagüel. Em Cerro Huantrai-co e em outras seções próximas de Fortín General Roca, estudos taxonômicos com ostracodes foram desenvolvidos (Bertels 1968b, 1969a, 1973, 1974) possibilitando a identificação de aproximadamente 61 espécies para o Maastrichtiano e 53 para o Daniano.

Na passagem do limite K–Pg, Bertels (1973, 1975c) observou uma mudança faunística abrupta com a completa substituição da fauna de ostracodes. Além disso, a autora sugeriu a existência de um possível hiato no Maastrichtiano superior e que, em algumas localidades, aparecem superfícies de paraconformidades que aparentemente não estão evidenciadas na litologia (Bertels 1973).

Bertels (1975c) estabeleceu alguns fatores ecológicos que influenciaram a distribuição dos ostracodes marinhos durante o Cretáceo-Superior e o Cenozóico. Aspectos como salinidade e temperatura foram avaliados, sugerindo um ambiente com temperaturas quentes e salinidade normal para o intervalo Cretáceo–Paleógeno na bacia. Além disso, foi evidenciado um ciclo transgressivo-regressivo na Formação Roca.

Além dos estudos com ostracodes marinhos, destaca-se a importância dos estudos com ostracodes não-marinhos na Bacia de Neuquén, especialente para o Cretáceo. Dados mais completos sobre este trabalhos podem ser encontrados em Carignano (2011) e Ballent *et al*. (2011).

2.3.2 FORAMINÍFEROS

Bertels (1970, 1980) realizou estudos com foraminíferos planctônicos e bentônicos da localidade tipo da Fm. Roca, em General Roca, e da localidade tipo da Fm. Jagüel, em Barranca de Jagüel, respectivamente. Um zoneamento bioestratigráfico para foraminíferos foi

utilizado para determinar a idade das rochas das formações Jagüel e Roca. Foi observado um hiato paleontológico entre as duas formações, possivelmente equivalente a uma biozona.

Com relação a passagem do limite K–Pg, Bertels (1970, 1975c) observou uma mudança faunística abrupta para os foraminíferos planctônicos, inclusive com a redução no tamanho das testas; e um padrão de extinção gradual para a fauna bentônica. Keller *et al*. (2007) também estudando os foraminíferos planctônicos de Barranca de Jagüel para o limite, evidenciaram condições de alto estresse marinho, provavelmente desencadeado pelo influxo de nutrientes, dos movimentos tectônicos na bacia e também pela presença de espécies oportunistas do gênero *Guembelitria* e *Heterohelix*. Além disso, observaram a presença de uma superfície erosional no limite K–Pg.

Uma proposta de reconstituição paleoambiental foi sugerida por Bertels (1970, 1980, 1975c) para os estratos do Maastrichtiano e do Daniano. A associação Maastrichtiana revelou ambiente marinho de águas profundas (150-300 m), evidenciada pela abundância de foraminíferos planctônicos, que foi progressivamente raseando a medida em que chegavam nos estratos superiores da Fm. Roca (Daniano), caracterizando um ambiente de plataforma interna com profundidades variando entre 80 e 100 m. Esta tendência também foi evidenciada por Concheyro *et al*. (2002) em Trapalcó. Além destes, o trabalho de Nañez & Concheyro (1996) contribuiu para a identificação do limite K–Pg em várias seções na bacia com foraminíferos e nanofósseis calcários.

2.3.3 NANOFÓSSEIS CALCÁRIOS

A rápida evolução dos nanofósseis permitiu estabelecer uma detalhada zonação mundial e apontar dados sobre as consequências do evento de extinção para este grupo. O estudo de oito perfis litológicos na Bacia de Neuquén realizado por Nañez & Concheyro (1996), permitiu o refinamento bioestratigráfico das formações Jagüel e Roca para esta região. A Fm. Jagüel compreende as zonas CC26, Maastrichtiano e a zona NP1, confirmando o Daniano inferior na mesma formação. Esta confirmação ajudou a esclarecer algumas das confusões que existiam sobre a idade das mencionadas formações, pois acreditava-se que a Fm. Jagüel era somente maastrichtiana (e.g., Bertels 1974, 1975c). A zona NP4 foi determinada para o Daniano superior na Fm. Roca.

Além desses, outros estudos foram realizados para identificar o limite K–Pg (e.g., Concheyro & Nañez 1994, Concheyro 1995, Concheyro & Villa 1996, Concheyro 2004)

registrando uma considerável mudança na fauna de nanofósseis calcários. Keller *et al*. (2007) relacionaram a extinção das espécies de nanofóssies, em Barranca de Jagüel, ao estresse ambiental evidenciado pelo domínio da espécie *Micula decussata,* que é resistente à condições de alterações ecológicas no ambiente. A ausência da zona NP1a representa a presença de uma base erosiva na seção de Barranca de Jagüel, no limite K–Pg.

A flora de nanofósseis calcários também ajudou na identificação de um retrabalhamento de idade hauteriviana em rochas do Daniano que pode estar relacionado ao tectonismo no lado oeste da bacia (Concheyro & Villa 1996).

Nas localidades de El Matuasto e Cerro Azul, próximos a região de Cipolleti, os estudos micropaleontológicos são relativamente recentes e únicos. Concheyro *et al*. (2002) e Musso *et al*. (2012) posicionaram o limite K–Pg dentro do pacote sedimentar da Fm. Jagüel, e reconheceram uma mudança na fauna de nanofósseis e foraminíferos planctônicos. Além disso, a análise mineralógica dos sedimentos também contribuiu para inferências paleoecológicas, especialmente para a seção de Cerro Azul.

2.3.4 OUTROS GRUPOS FÓSSEIS

A partir destes estudos, iniciou-se uma investigação sobre o comportamento de outros grupos fósseis na passagem do limite K–Pg. Em Barranca de Jagüel foi realizado uma análise bioestratigráfica com cistos de dinoflagelados (Palamarkzuk 2006) que registrou uma mudança faunística e o aumento da riqueza durante o Daniano. Em Cerro Butaló foi identificado o Maastrichtiano superior para Fm. Jagüel, baseado neste mesmo grupo fóssil, e sugerido um ambiente mais profundo para o Maastrichtiano e mais raso para o Daniano (Prámparo & Papú 2006). Barreda *et al*. (2004) observaram uma redução nos palinomorfos terrestres próximo à camada do limite K–Pg e um dramático aumento na abundância das gimnospermas e de esporos após o evento, suportando a ideia de um declínio global na vegetação que antecede a extinção. Outros estudos com palinologia sugerem essa mesma tendência (Palamarczuk 2002, Papú *et al*. 1999).

Estudos com equinóides (Del Río *et al*. 2007), amonóides (Casadío & Leanza 1991), ostras (Casadío 1998) e recifes microbiais (Kiessling *et al*. 2006) foram realizados com o objetivo de melhorar a resolução estratigráfica do limite K–Pg, e fornecer interpretações paleoecológicas. De uma maneira geral, as mudanças observadas na fauna marinha durante

este evento são consideradas reflexo das alterações ambientais, como a mudança de temperatura e a queda no nível do mar no Daniano.

3 EVENTOS DE EXTINÇÃO

Eventos de extinção são o resultado de uma perturbação global do ambiente físico que geram uma redução da biodiversidade e da abundância dos seres vivos. Basicamente existem dois modelos de extinção em massa: extinção em massa gradual e extinção em massa catastrófica ou súbita. A duração de uma extinção em massa gradual pode chegar a superar milhões de anos enquanto que uma extinção em massa súbita pode acontecer em menor intervalo de tempo (Molina 2006).

Eventos climáticos, distúrbios de hábitat ou introdução de novos predadores são alguns dos fatores apontados como capazes de eliminar espécies principalmente se elas apresentarem limitada distribuição geográfica ou endemismo. A competição por um nicho, alterações nos sistemas de correntes oceânicas e mudanças no fornecimento de nutrientes também são fatores que contribuem para o desequilíbrio e, consequentemente, a extinção de espécies (Brenchley & Harper 1998, Apesteguía & Ares 2010).

Para serem produzidos eventos de extinções em massa, uma grande quantidade de espécies deve ser eliminada, inclusive as endêmicas. Para tanto, as condições ambientais devem estar em um nível de estresse elevado, serem extremamente severas e atingirem de maneira rápida uma ampla área (Brenchley & Harper 1998, Molina 2006, Lavina & Fauth 2011). De um ponto de vista biológico, as extinções representam uma oportunidade para a evolução das espécies ao ponto que, quando uma espécie é extinta, um novo nicho se torna disponível para que uma nova espécie o ocupe (Rydley 2006, Apesteguía & Ares 2010). Isto significa que as extinções em massa são seletivas e afetam de maneira diferente cada espécie.

Segundo Kauffman & Harries (1996) e MacLeod *et al*. (1997), durante um evento de extinção em massa, podem ser identificadas algumas fases, com extinção, sobrevivência e surgimento. Os táxons reagem de maneira diferente, como por exemplo, se extinguindo no momento do evento ou um pouco depois, aproveitando as condições críticas para se desenvolverem (espécies oportunistas), fugindo das condições ambientais alteradas e retornando quando estas estiverem normais (efeito Lázarus) ou ainda resistindo às condições alteradas do meio (sobreviventes) (Fig. 5).

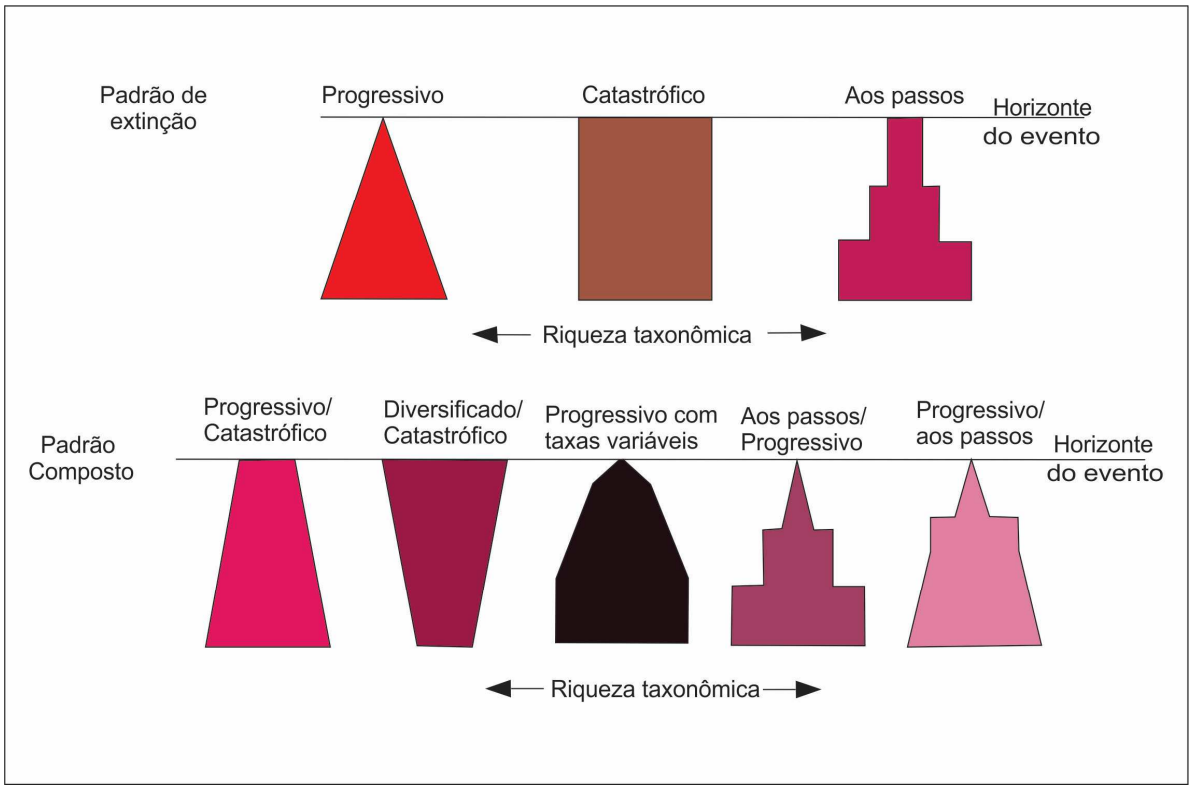

Figura 5: Padrões teóricos de extinção em massa no registro fóssil. O padrão de extinção indica diferentes mecanismos que causaram mudanças ambientais a longo prazo (Progressivo), abrupto (Catastrófico) ou moderados e episódicos (aos passos). Padrões compostos indicam a ação de múltiplas causas. (Modificado de MacLeod *et al*. 1997).

Segundo Krug *et al*. (2009) embora as extinções em massa sejam bem conhecidas por suas consequências nefastas, elas irreversivelmente reestruturaram a composição taxonômica da biota global. Admite-se atualmente que, ao longo do Fanerozóico, cinco grandes eventos de extinção foram registrados representando o desaparecimento de muitos táxons (Fig. 6).

No final do Ordoviciano, há 445 Ma, aproximadamente 85% da fauna marinha foi extinta. Mudanças climáticas, como eventos de glaciação, levaram à extinção famílias de braquiópodes, equinodermas, ostracodes e trilobitas (Benton & Harper 2009). O segundo maior evento de extinção ocorreu no final do Devoniano, quando 27% das famílias e 70% à 82% das espécies de organismos marinhos foram extintos, principalmente os recifes de coral, crinoides, estromatólitos, braquiópodes, ostracodes, placodermos, ostracodermos e trilobitas. As causas relacionadas são o resfriamento global associado a eventos de anoxia ou até mesmo a impactos massivos de objetos extraterrestres (Olempska 1997, Kaiser *et al*. 2006, Benton & Harper 2009, Robertson *et al*. 2013).

O final do Permiano foi o evento mais devastador do Fanerozóico. Em torno de 50% das famílias de animais marinhos e terrestres foram extintas, com a eliminação de 80% a 96% das espécies, sendo que somente 4-20% sobreviveram (Benton & Harper 2009). A causa mais aceita atualmente está relacionada ao extenso vulcanismo registrado na Sibéria e na China (Isozaki *et al*. 2007) e ao aumento dos níveis de CO_2 na atmosfera, o que produziria uma degradação ambiental e colapso ecológico. Esta crise biótica foi acompanhada por um evento anóxico oceânico que pode ter durado 8 Ma (Grice *et al*. 2005). Além disso, teria ocorrido uma drástica redução das plataformas continentais decorrentes da formação do Pangea reduzindo os ambientes costeiros (Erwin 1990, Brenchley & Harper 1998, Benton & Harper 2009).

O evento de extinção do final do Triássico, que ocorreu há ±200 Ma, é caracterizado pela redução de muitas famílias de amonóides, braquiópodes, bivalves, gastrópodes e répteis marinhos. O impacto de um meteorito tem sido atribuído como a possível causa desta extinção em massa, mas outras suposições apontam para anoxia e aquecimento global, seguido por erupções vulcânicas (Benton & Harper 2009, Apesteguía & Ares 2010, Lavina & Fauth 2011).

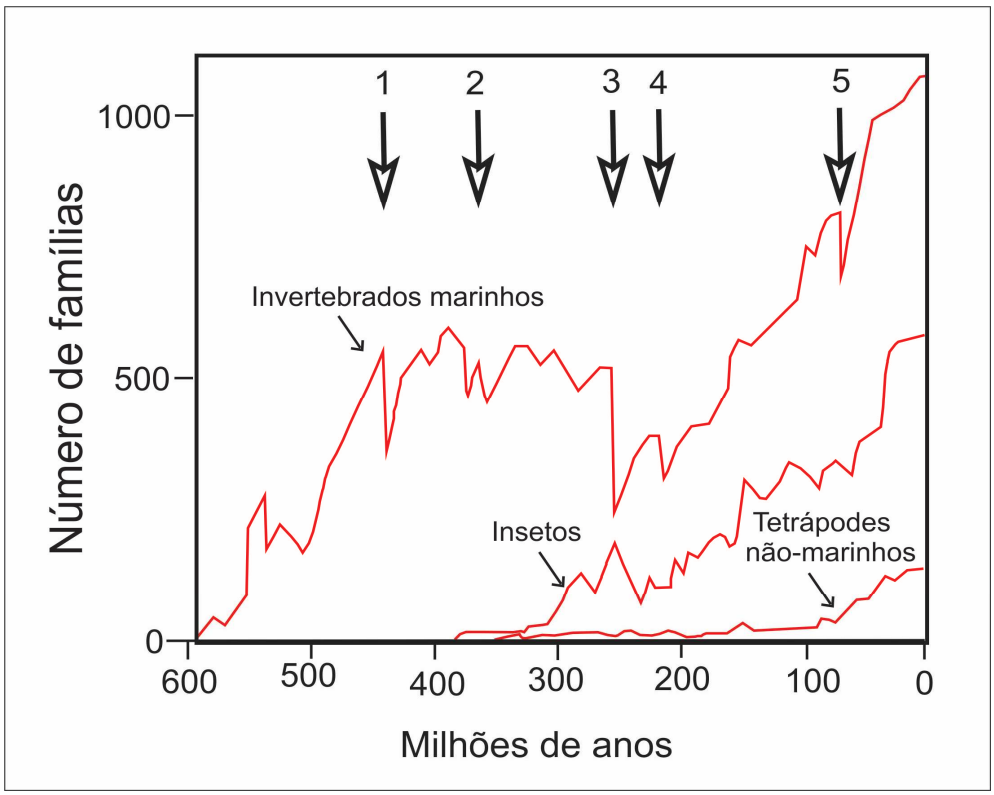

Figura 6: Posição dos cinco maiores eventos de extinção indicadas pelas setas (1, final do Ordoviciano; 2, final do Devoniano; 3, final do Permiano; 4, final do Triássico; 5, K–Pg). (Modificado de Benton 2001).

3.1 Cretáceo–Paleógeno (K–Pg)

Este evento de extinção em massa é o mais estudado e o mais controverso de todos. Apesar de não ser a maior extinção da história geológica da Terra, é a mais conhecida devido ao desaparecimento dos grandes répteis. Este evento vitimou cerca de 26% das famílias e 75% das espécies tanto terrestres quanto marinhas (Rydley 2006). A polêmica consiste em saber se esta extinção foi instantânea (Tappan 1979) ou gradual (Gamper 1977, Keller *et al*. 1993, Coccioni & Galeotti 1994, Skelton 2003, Ridley 2006); e as hipóteses a respeito do que realmente teria ocorrido foram e ainda são tema de muitas discussões. As pricipais teorias estão relacionadas a mudanças climáticas (e.g., Bramlette 1965, Tappan 1979), queda de um ou mais meteoritos (e.g., Alvarez *et al*. 1980a, Alvarez 1987, Kent 1981, Smit 1990, Canudo *et al*. 1991, Olsom *et al*. 1997), extenso vulcanismo (e.g., Zoller *et al*. 1983, Hallan 1987, McLean 1985, Baksi *et al*. 1994, Keller *et al*. 2008, Keller *et al*. 2011) e também múltiplas causas (e.g., Ward *et al*. 1995, Hallam 2005, Alegret *et al*. 2012).

Este evento que ocorreu em torno de 66 Ma e marca o final do período Cretáceo e o início do Paleógeno, teve um importante impacto na biodiversidade da Terra, vitimando boa parte dos seres vivos da época, incluindo os dinossauros não-avianos e amonites (Alvarez *et al*. 1980a, Surlyk 1990, Gradstein *et al*. 2012).

Neste período, houve mudanças ambientais catastróficas na vida de todo planeta (e.g., Skelton 2003, Keller 2003) e o registro estratigráfico mostra que o desaparecimento abrupto das espécies coincide com um nível de argilas que apresenta quartzos metamorfizados, microtectitos e uma milimétrica camada rica em irídio, um elemento químico geralmente associado a corpos extraterrestres ou a vulcanismos (Alvarez *et al*. 1980b, Alvarez 1987, Officer & Drake 1985).

3.1.1 EVIDÊNCIAS DO LIMITE CRETÁCEO–PALEÓGENO

As hipóteses levantadas para o evento que marca o final do Cretáceo, além das extinções registradas, são baseadas em significativas variações na composição geoquímica e mineralógica dos sedimentos que marcam o limite K–Pg. Estas alterações constituem evidências que ajudam a entender o que realmente teria desencadeado este evento de extinção e como poderia ter ocorrido. De acordo com Kyte (2002), o influxo de material extraterrestre

é dominado por dois tipos de frações: poeira interplanetária e impactos de asteroides e cometas.

3.1.1.1 Anomalia de irídio

Anomalias geoquímicas têm sido detectadas em seções onde o limite K–Pg está bem preservado. O elemento químico irídio (Ir) e outros elementos pertencentes ao grupo da platina (e.g., Ru, Rh, Pd, Os e Pt) são extremamente raros na crosta terrestre, entretanto apresentam concentrações 10.000 vezes maiores em meteoritos e asteroides, por isso o irídio tem sido o elemento mais comumente usado como marcador de origem extraterrestre (e.g., Alvarez *et al*. 1980a,b, 1982, Alvarez 1983, Zoller *et al*. 1983, Yalcin & Bozkaya 1996, Abdelkader *et al*. 1997, Kyte 2002, Ruddiman 2008). Em sua primeira descoberta da anomalia de Ir, Alvarez *et al*. (1980b) identificaram uma quantidade de 9 p.p.m. em Gubbio, Itália. As concentrações de Ir foram registradas tanto em sedimentos de origem marinha quanto continental.

3.1.1.2 Mineralógicas

Quartzo metamorfizado ou quartzo de impacto, como é usado por alguns autores, é uma forma estruturalmente alterada de quartzo que foi modificado a partir de uma aplicação súbita de alta pressão (Alvarez *et al*. 1995, Ruddiman 2008). Quartzo é um mineral composto basicamente por sílica e muito abundante na Terra. Ao passar por processos de pressão extremamente alta, como os relacionados a impactos meteoríticos, podem adquirir feições de interseções lamelares e são frequentes em sequências que registram o limite (Jablonski & Raup 1995).

Mineral de quartzo metamorfizado também pode ser encontrado próximo a erupções vulcânicas explosivas, mas sem a característica multilamelar e de ampla distribuição como são os provenientes do impacto (Alvarez 1987).

3.1.1.3 Sedimentológicas (tectitos e esférulas)

Tectitos e microtectitos são partículas vítreas esféricas, de tamanho variado, originados por gotas de material rochoso fundido no impacto de meteoritos. Sua cor

variavelmente escura e sua forma geralmente esférica mostram superfícies onduladas erodidas e apresentam a aparência de que foram formados no ar a tempo de resfriarem antes de serem depositados (Jablonski & Raup 1995). Os microtectitos são bem conhecidos por terem baixas concentrações de Ir. Sua composição é rica em sílica e pobre em água, o que justifica sua origem terrestre oriunda de materiais atingidos por impactos (Smit & Romein 1985, Kyte 2002), embora uma origem lunar também pode ser sugerida (Alvarez *et al*. 1982).

Esférulas podem ter origem cósmica ou de impacto. Esférulas cósmicas foram descobertas pela primeira vez em sedimentos marinhos profundos (Ganapathy *et al*. 1978) e são derivadas primariamente da ablação de grãos de poeira interplanetária, ou seja, pelo material superficial que é perdido de um meteorito devido ao aquecimento quando este atravessa a atmosfera (Kyte 2002). As esférulas comumente encontradas no ambiente de impacto não apresentam uma composição significativa de elementos extraterrestres, por isso, embora estas possam ser marcadoras de eventos de impacto pela deformação do material silicoso, elas não são necessariamente oriundas de meteoritos (Kyte 2002). Estes materiais silicosos deformados também podem ser provenientes de erupções vulcânicas devido ao choque de ondas com temperaturas altas (Carter *et al.* 1990).

3.1.1.4 Geoquímicas

A geoquímica isotópica é uma técnica que tem sido utilizada para detectar indícios das prováveis causas deste evento e auxiliar nas interpretações paleontológicas. Os dados de isótopos de carbono e oxigênio ($\delta^{13}C$ e $\delta^{18}O$) têm sido utilizados para inferir parâmetros como temperatura da água, salinidade, produtividade e disponibilidade de nutrientes, permitindo realizar reconstituições paleoambientais e detecção de períodos de anoxia e glaciação (Stüben *et al*. 2002, Rodrigues & Fauth 2013).

Alguns estudos utilizando a análise de isótopo $\delta^{13}C$ em testas de foraminíferos planctônicos e bentônicos mostraram valores negativos de $\delta^{13}C$ no Maastrichtiano superior, indicando uma rápida redução na produtividade primária, principalmente da fauna planctônica (e.g., Arthur *et al*. 1987, Hsü *et al*. 1982, Keller 1993, Barrera & Keller 1994, Keller *et al*. 1997). Já nos foraminíferos presentes no início do Paleógeno, são registrados valores positivos de $\delta^{13}C$ indicando um significativo aumento da mesma (Martínez-Ruíz *et al*. 1994).

Isótopos de oxigênio ($\delta^{18}O$) podem ser utilizados para indicar flutuações na temperatura dos oceanos. Smit (1990) realizou análise em carbonatos pelágicos em rochas do

limite K–Pg e estimou um aumento na temperatura superficial do oceano em 8 °C no Daniano, evidenciando que o efeito estufa sucedeu o evento do impacto e poderia ter durado milhares de anos. A análise de $\delta^{18}O$ em minerais e esmectitas do limite K–Pg em Stevens Klint, Dinamarca, possibilitou a determinação da origem dos mesmos como produto do impacto do meteorito (Kastner *et al*. 1984).

Além da análise de isótopos de carbono e oxigênio, outro elemento utilizado para auxiliar nas interpretações ambientais são os isótopos de argônio ($^{40}Ar/^{39}Ar$) e estrôncio ($^{87}Sr/^{86}Sr$). Um exemplo do uso $^{40}Ar/^{39}Ar$ foi estudado por Javoy & Curtillot (1989) que atribuíram os níveis de argônio ao vulcanismo explosivo ácido que teria desencadeado chuva ácida e mudanças climáticas. Mais recentemente Renne *et al*. (2013) determinaram, através da análise de alta precisão de $^{40}Ar/^{39}Ar$, uma sequência para os eventos do limite K–Pg. A contribuição deste estudo foi refutar a hipótese de que o impacto em Chicxulub, México, teria pré-datado o evento de extinção.

Flutuações oceânicas nas quantidades de $^{87}Sr/^{86}Sr$ têm sido atribuídas ao aumento de Sr radiogênico produzido pela chuva ácida depois do impacto (Martínez-Ruíz *et al*. 1994, Ortega-Huertas *et al*. 2002). Devido às grandes quantidades de óxido de nitrogênio que foram liberadas na atmosfera, gerando a chuva ácida, houve um aumento da desagregação no continente e, consequentemente, um aumento da quantidade de estrôncio no mar (Macdougall 1988).

3.1.1.5 Microfósseis

Os microfósseis têm sido valorosos nas interpretações paleoambientais e estratigráficas das seções com o limite K–Pg, pois revelam as mudanças faunísticas sofridas em cada grupo fóssil em resposta ao evento de extinção. A magnitude de um evento é determinada pela quantidade de espécies que são extintas num determinado intervalo de tempo, mas também depende do intervalo entre uma amostra e outra e se o registro fóssil está completo (MacLeod *et al*. 1997).

Um bom registro sedimentológico é importante para não gerar identificações incorretas de padrões de extinção (Smith 1994). A presença de hiatos, níveis de retrabalhamento, mudanças de fácies e a qualidade amostral, devem ser levados em consideração quando se propõe uma interpretação à luz de um evento de extinção. Isto pode refletir em interpretações incorretas, como por exemplo, se o evento de extinção foi gradual

ou catastrófico (efeito Signor-Lipps e efeito Lázarus) (Signor & Lipps 1982, Brenchley & Harper 1998) (Fig. 7).

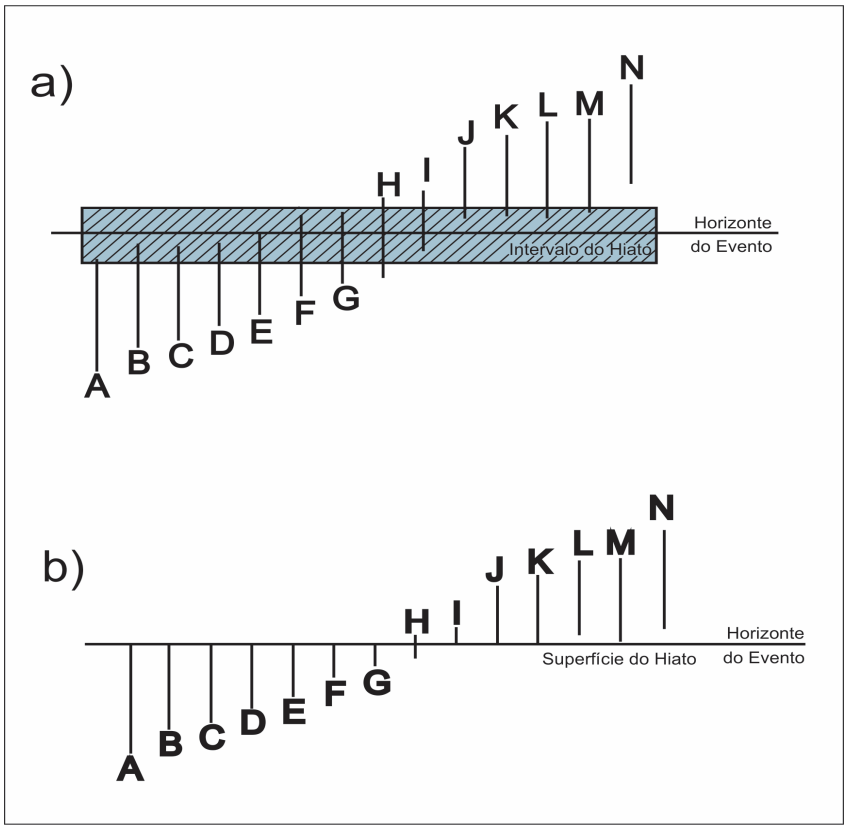

Figura 7: Hiato deposicional: a presença de um hiato pode sugerir um evento catastrófico. Em a) distribuição hipotética bioestratigráfica dos táxons A-N através de um horizonte de evento. Em b) como seriam observadas a distribuição estratigráfica se existisse um hiato deposicional. (Modificado de MacLeod *et al*. 1997).

Para tanto, são utilizados zoneamentos bioestratigráficos mundiais, baseados em foraminíferos planctônicos e nanofósseis calcários, pois esses organismos sofreram drasticamente os efeitos da crise ambiental desencadeada no evento de extinção e responderam de uma maneira mais rápida à ela (e.g., Koutsoukos 1997, Keller *et al*. 2002, Keller *et al*. 2007, Bernaola & Monechi 2007, Alegret 2007, Alegret *et al*. 2003, Tantawy *et al*. 2009, Jiang *et al*. 2010). Estes zoneamentos, aliados aos indícios sedimentológicos e as análises isotópicas, são valiosas ferramentas que contribuem para um melhor entendimento sobre como os eventos catastróficos afetaram a vida, principalmente no ambiente marinho, e como ele está representado no registro geológico (Fig. 8).

A presença, por exemplo, de espécies consideradas oportunistas, como é o caso do nanofóssil *Micula decussata* e do foraminífero *Guembelitria cretacea*, auxiliam na

caracterização da instabilidade ambiental pelo fato de estas espécies serem resistentes e abundantes em condições de estresse (Keller & Pardo 2004, Scasso *et al*. 2005, Keller 2005, Keller *et al*. 2012). Adicionalmente, os organismos bentônicos também foram afetados pela instabilidade do ambiente, em consequência da diminuição do fitoplâncton, em decorrência da supressão da fotossíntese que seguiu o impacto (Robertson *et al*. 2013).

Os zoneamentos bioestratigráficos utilizados para determinar o limite K–Pg com nanofósseis calcários são os de Perch Nielsen (1985) para o Cretáceo e Martini (1971) para o Paleógeno e estão demostrados na figura 8. Em Cerro Azul o Maastrichtiano é marcado pela zona CC26 de nanofósseis calcários e o Daniano pelas zonas NP1, NP2 e NP3. Até o momento, nos estudos bioestratigráficos realizados com nanofósseis, não foi possível realizar o detalhamento da zona NP1. Possivelmente exista um hiato bioestratigráfico pela ausência da zona NP1a e também a zona P0 de foraminíferos planctônicos.

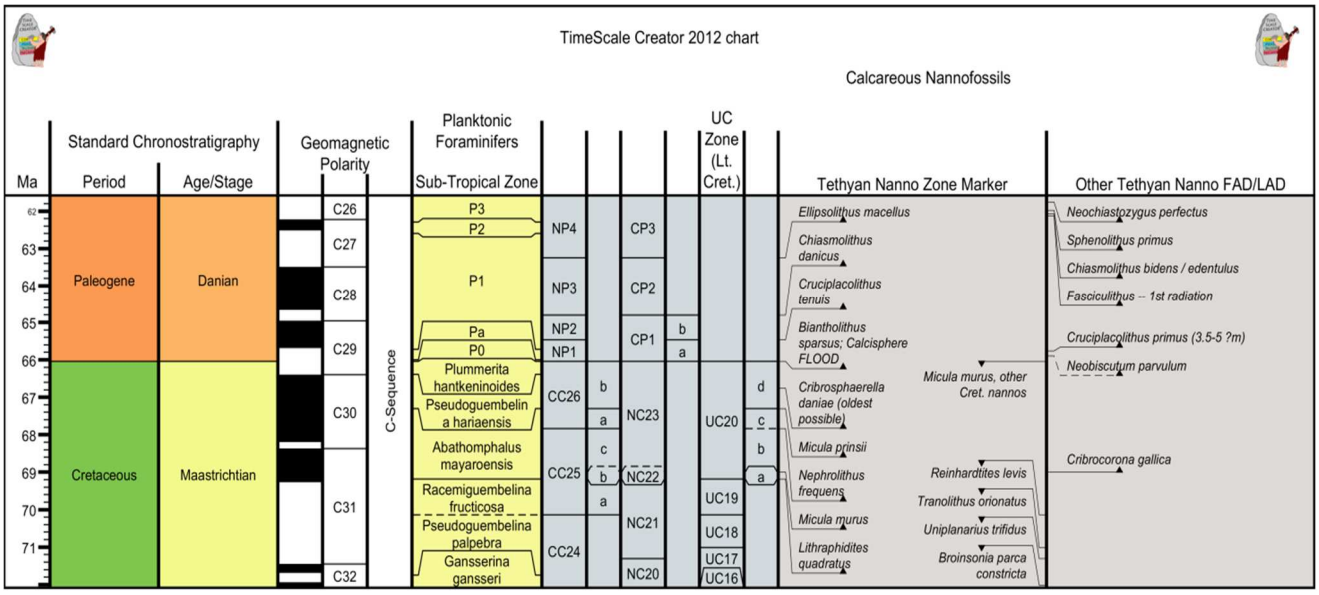

Figura 8: Biozoneamentos estratigráficos para nanofósseis calcários e foraminíferos. (Gerado em Time Scale Creator 2012).

3.2 Principais teorias

As teorias que explicam o evento de extinção do limite K–Pg estão relacionadas principalmente às mudanças climáticas, impactos de meteorito, eventos vulcânicos e alterações ambientais. Estas alterações ambientais podem ser físicas ou químicas ou ambas e são as principais causas das discussões e das proposições hipotéticas pelos autores que

estudam esta extinção. Na sequência é apresentado um resumo das principais teorias existentes que tentam explicar o que teria ocorrido neste episódio.

3.2.1 MUDANÇAS CLIMÁTICAS

Os primeiros estudos que abordaram o limite Cretáceo–Paleógeno na década de 1960 delineavam hipóteses sobre possíveis mudanças climáticas que poderiam ter desencadeado este evento de extinção. Bramlette (1965) considerou este evento como resultado de uma excessiva radiação que se espalhou e afetou a vida em todo o planeta. A extinção dos foraminíferos planctônicos e nanofósseis calcários teria sido tão abrupta que o registro no estrato ainda estava obscuro. Esta ausência de um zoneamento estratigráfico conhecido para os foraminíferos planctônicos na época, e de evidências físicas, dificultou a determinação do limite K–Pg no México, onde existem seções com o limite (Gamper 1977).

Outra hipótese proposta foi a migração da CCD (zona de compensação de carbonato de cálcio) para a superfície dos oceanos, resultante da depleção de carbonato durante o Cretáceo e que teria afetado diretamente os organismos planctônicos (Windle *et al*. 1971, Worsley 1974).

Gartner & Keany (1978), Gartner & McGuirk (1979) e Tappan (1979) propuseram que a extinção dos nanofósseis e foraminíferos planctônicos teria sido ocasionada pela mudança na salinidade dos oceanos durante a separação do Ártico. Esta, por sua vez, teria desencadeado uma série de mudanças climáticas incluindo baixas temperaturas e precipitações que afetaram radicalmente a distribuição da vegetação na terra e a consequente extinção dos grandes répteis.

3.2.2 IMPACTO DE METEORITO

As primeiras especulações a respeito da hipótese sobre a queda do meteorito, que é um fragmento de um asteroide que sobreviveu a passagem pela atmosfera e atingiu a superfície (AMS 2014) foram abordados por Ganapathy *et al*. (1978) ao encontrarem esférulas de silicatos em sedimentos de fundo oceânico, entretanto esta teoria somente foi proposta por Alvarez *et al*. (1980a). A partir de então, iniciou-se uma busca por evidências em diversas seções no mundo que geraram grandes discussões a respeito da validade da mesma.

Alvarez *et al*. (1980b) propuseram que impactos de grandes asteroides poderiam ter ejetado uma enorme quantidade de material e que, por conseguinte, uma nuvem de poeira e fuligem teria sido gerada, resultando no escurecimento da Terra. Isto poderia ter desencadeado o que Robertson *et al*. (2013) chamou de "impacto de inverno". Sem a luz solar por um longo período (meses ou anos), o frio e a escuridão poderiam ter levado ao comprometimento da fotossíntese, desestabilizando o ambiente e causando a extinção.

Simulações virtuais sugeriram que o impacto de um meteorito desta magnitude gera uma energia cinética equivalente a 10.000 vezes o arsenal nuclear existente hoje, suficiente para gerar uma cratera de 150-200 km de diâmetro e ondas de choque que fundem e vaporizam tanto as rochas do impactante como as impactadas (Alvarez *et al*. 1995).

Alvarez *et al*. (1980a) e Alvarez (1983) publicaram um manuscrito que detalhava as condições em que a camada de irídio foi encontrada e coincidentemente com ela os níveis de microtectitos e esférulas. Além disso, realizaram um experimento que estimava o diâmetro deste meteorito (10 km) e a velocidade (25 km/s) com que teria atingido a Terra.

Até o início dos anos 90, os pesquisadores contrários à teoria do impacto alegavam que uma cratera adequada à magnitude do evento não teria sido encontrada. Hildebrand *et al*. (1991) através de levantamentos sísmicos nas proximidades da península de Yucatán no México, encontraram a cratera do impacto, a cratera Chicxulub.

A partir desta descoberta, vários estudos foram realizados buscando corroborar a hipótese da queda do meteorito (Fig. 9). Bohor *et al*. (1984, 1987), Albertão (1996) analisaram grãos de quartzo provenientes de seções com o limite preservado, encontrando evidências de metamorfismo gerado por altas temperaturas. Smit (1990) sugeriu ter ocorrido a queda de um meteorito em terra e outro no mar pela presença de quartzo chocado com características de rápido resfriamento e algumas texturas cristalinas (quiropiroxênio); enquanto que a presença de quartzo chocado e shistovita favorecem um impacto continental. Esta hipótese também foi reforçada pelos indícios de tsunamis encontrados em seções marinhas que poderiam ter sido desencadeados pelo impacto do meteorito na água (Bourgeois *et al*. 1988, Albertão 1994, Scasso *et al*. 2005).

Alguns autores (Wolbach *et al*. 1985, Albertão 1996, Kring 2007) propuseram a existência de incêndios após a queda do meteorito, baseados em evidências sobre uma fina camada de fuligem identificada nos depósitos do limite K–Pg nas seções de Stevens Klint (Dinamarca), Caravaca (Espanha), Woodside Creek (Nova Zelândia). Wolbach *et al*. (1985) propuseram que o efeito da fumaça proveniente deste incêndio junto com a poeira cósmica,

teriam sido muito eficiente para bloquear a radiação solar e gerar a queda na temperatura superficial da Terra. Entretanto, Cisowski *et al*. (1986) contestaram estas evidências, pois as variáveis necessárias para se manter um incêndio de grandes proporções, tais como, mudanças na direção dos ventos, taxa de queima, presença de chuva e rios que poderiam parar o fogo, não foram levadas em consideração pelos autores.

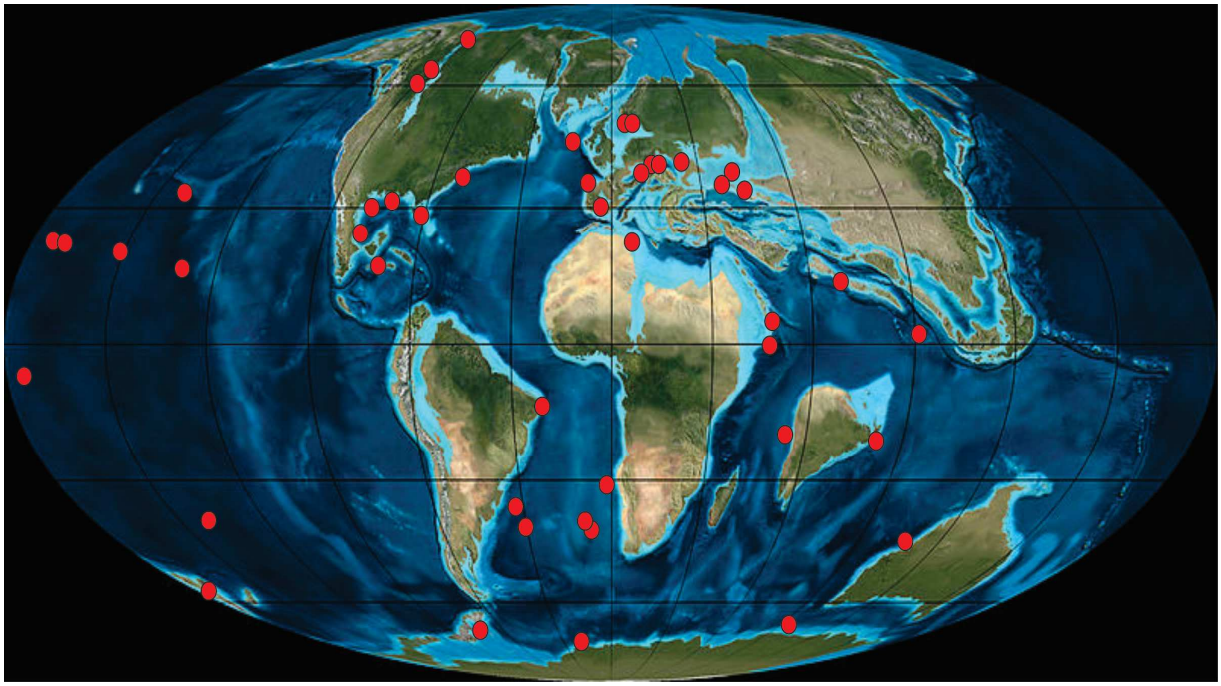

Figura 9: Localização das seções sedimentares com o limite K–Pg e anomalia de Irídio em diferentes concentrações. (Adaptado de Claeys *et al*. 2002).

Nesta mesma época, foram desenvolvidos estudos para avaliar as consequências que certos elementos químicos, associados à queda do meteorito, poderiam gerar na vida dos oceanos. Uma das ideias é que o fluxo de elementos meteoríticos poderia ter sido grande o suficiente para causar uma seletiva intoxicação da biota marinha e com isso, a extinção, sendo a chuva ácida um exemplo (Erickson & Dickson 1987).

A chuva ácida seria o resultado da grande quantidade de óxido de nitrogênio, resultante do impacto que aqueceu a atmosfera, aumentando o intemperismo no continente e a quantidade de estrôncio no mar (Macdougall 1988). A associada redução na produtividade levaria a uma transferência parcial de dióxido de carbono dos oceanos para a atmosfera, elevando a temperatura (Hsü *et al*. 1982, Hildebrand *et al*. 1991, Alvarez *et al*. 1995, Arthur *et al*. 1987, Smith 1997).

A redução do fitoplâncton ocasionou a eliminação seletiva de organismos que dependiam diretamente do fluxo de matéria orgânica na zona fótica. Grupos de filtradores e suspensívoros (moluscos, corais, braquiópodes, briozoários, crinoides) teriam uma queda rápida. Já os organismos detritívoros ou com hábitos infaunais, teriam tido mais sorte e não sofreriam tanto, pois são menos dependentes do suprimento de comida (Hansen *et al*. 1987, Alegret *et al*. 2001, Alegret *et al*. 2003). Exemplos de estudos micropaleontológicos que relacionaram a extinção com a queda do meteorito podem ser encontrados em Canudo *et al.* (1991), Albertão *et al*. (1994), Keller *et al*. (1993), Keller *et al*. (1995), Smith (1997), López-Oliva *et al*. (1998), Bown (2005), Koutsoukos (2005), dentre outros.

Recentemente foi proposta uma outra hipótese sugerindo que a queda do meteorito ocorrido na Península de Yucatán, México, teria predatado o limite K–Pg em aproximadamente 300 mil anos (Keller *et al*. 2003, Keller *et al*. 2007), mas que não somente um, mas três impactos teriam ocorrido e estariam ainda associados ao evento do vulcanismo em Deccan, na Índia. Renne *et al*. (2013) e Schulte *et al*. (2010), utilizaram a análise de $^{40}Ar/^{39}Ar$ para tentar resolver a relação entre o impacto do meteorito e a extinção, e constataram que esta teoria não se mantém, pois verificaram um sincronismo entre a queda do meteorito em Yucatán e os níveis de extinção das espécies. Pälike (2013) apresentou uma discussão geral sobre a queda do meteorito e a questão do vulcanismo, chegando a conclusão que o impacto não teria pré-datado o evento como abordado por Keller *et al*. (*op*. *cit*), mas que a recuperação da fauna no Daniano teria ocorrido por migração a partir de zonas de refúgios, mais do que por radiação evolutiva.

3.2.3 VULCANISMO

Alguns autores, contrários à hipótese do impacto, buscaram outra explicação para a origem deste material dito anômalo. A identificação de irídio em lavas vulcânicas provenientes do vulcão Kilauea foi realizado por Zoller *et al*. (1983). O vulcanismo estaria relacionado a uma grande perturbação do ciclo de carbono na Terra e o processo de extinção teria sido relativamente gradual e por isso as causas seriam endógenas. Officer & Drake (1985) estimaram que erupções vulcânicas como as do Krakatoa, Kilauea e Deccan, por exemplo, teriam sido capazes de depositar irídio em quantidades semelhantes ao que seria depositado pelo impacto do meteorito. Os autores defenderam que os elementos do grupo da platina, além de estarem presentes em corpos extraterrestres, também estariam presentes no

manto. Baseados em dados de paleomagnetismo e geocronologia, Courtillot *et al*. (1986) sugeriram que esta atividade vulcânica poderia ter durado menos de um milhão de anos.

Ao analisarem a composição mineralógica da camada de argila do limite K–Pg em Walvis Ridge, Robert & Chamley (1990) identificaram um aumento na quantidade de esmectita, caolinita e ilita. Esta combinação sugere um aumento na taxa de erosão e predomínio de rochas vulcânicas.

Picos de estrôncio encontrados por Javoy & Courtillot (1989), normalmente atribuídos a meteoritos e a chuva ácida ou à regressão do nível do mar, são explicados como sendo oriundos do vulcanismo explosivo ácido procedente de Deccan Traps. Este pode ter sido responsável pelas mudanças climáticas, pelos minerais metamorfizados e pela possível anomalia de Ir registrada em todo o mundo.

Mais recentemente, Keller *et al*. (2011) e Keller *et al*. (2012), estimaram que o vulcanismo registrado em Deccan Traps, na Bacia Krishna-Godavari, teria coberto uma área equivalente a França ou ao estado do Texas (Fig. 10). Quatro eventos de fluxos de lava foram identificados, sendo que o último teria ocorrido próximo do limite K–Pg (baseado em dados paleomagnéticos). A resposta biológica foi devastadora revelando uma extinção de 50% da fauna de foraminíferos planctônicos no primeiro evento de extinção (Maastritchiano) e os sobreviventes desapareceram nos eventos sucessivos. A última erupção foi no Daniano e associado a este evento também teriam ocorrido as mudanças climáticas. Uma revisão geral sobre as implicações do vulcanismo registrado em Deccan são discutidas em Punekar *et al*. (2014).

3.2.4 MÚLTIPLAS CAUSAS

Concomitante com todas estas discussões, alguns autores acreditam que o evento de extinção seja o reflexo de alterações ambientais que atuaram em conjunto. Keller (1988) estudou os foraminíferos planctônicos na seção tipo do limite K–Pg, em El Kef e sugeriu que, pelo longo período necessário para a recuperação do ecossistema depois do impacto do meteorito, múltiplas causas poderiam ter sido responsáveis pela extinção tais como, mudanças climáticas, vulcanismo em várias províncias ígneas, queda do nível do mar, aquecimento dos oceanos e as consequências de um aumento de salinidade. Em 1989, Keller correlacionou os padrões de extinção e abundância relativa de espécies de foraminíferos planctônicos de Brazos River e El Kef na tentativa de encontrar indícios da queda do meteorito. A mesma

concluiu que a extinção das espécies foi causada por um aumento de estresse ecológico como consequência da regressão do nível do mar no final do Maastrichtiano.

Figura 10: Distribuição global das províncias vulcânicas continentais e dos platôs oceânicos. (Modificado de Wignall 2001).

Esta mesma constatação foi sugerida po Canudo *et al*. (1991) que estudaram o padrão de extinção dos foraminíferos planctônicos nas seções de Caravaca e Agost, Espanha, e observaram que a extinção foi seletiva e eliminou espécies geograficamente restritas, grandes, complexas e de águas profundas, favorecendo a sobrevivência de espécies cosmopolitas, pequenas e de superfície, possivelmente refletindo a regressão do nível do mar. O impacto do meteorito poderia ter acelerado a morte da fauna cretácea em declínio e a transição do limite K–Pg não teria sido causada por um único evento instantâneo, mas por um conjunto de fatores complexos e inter-relacionados.

Keller (1993) e Keller *et al*. (1997) propuseram que o declínio dos foraminíferos planctônicos durante os últimos 300 mil anos do Maastrichtiano seria reflexo de anoxia somado ao intenso vulcanismo, mudanças no nível do mar e da temperatura. Um evento

catastrófico gerado por impacto ou vulcanismo, estaria superimposto as outras causas e pode ter acelerado a extinção em massa.

Keller (2003) e Keller *et al*. (2003) estudaram as seções do México, Guatemala, Belize e Haiti e propuseram a existência de um cenário de múltiplos impactos de meteorito. O primeiro estaria associado ao maior vulcanismo em Deccan e provavelmente teria contribuído para o rápido aquecimento global de 3 °C a 4 °C entre 65.4 e 65.2 Ma, terminando com o declínio da população de foraminíferos planctônicos. O segundo é conhecido como o evento do limite sendo representado pela morte de todos os foraminíferos planctônicos tropicais e subtropicais e pela queda na produtividade primária. O terceiro impacto teria ocorrido 100 anos depois do limite e teria sido responsável pela morte dos sobreviventes. A crise na flora de nanofósseis calcários também tem sido atribuída a consequências do vulcanismo associado as mudanças ambientais (Tantawy *et al*. 2009).

A descoberta de outras pequenas crateras de impacto, duas no Maastrichtiano do Mar do Norte (Kelley & Gurov 2002, Stewart & Allen 2002) e duas com anomalias de Ir em Oman (Ellwood *et al*. 2003) favorecem a hipótese de múltiplos impactos. De acordo com Keller (2005, 2008) impactos de meteoritos e vulcanismos podem desencadear catástrofes ambientais de mesma magnitude. Segundo MacLeod (2003) as extinções registradas podem ser originadas de uma variedade de mudanças ambientais relacionadas ao tectonismo e a fatores ecológicos evolutivos.

3.3 Os ostracodes e o limite K–Pg

Nas últimas décadas, como já mencionado anteriormente, as seções com o limite K–Pg têm sido estudadas a partir de diversos grupos de microfósseis, entretanto, poucas delas contém ostracodes. De uma maneira geral, os estudos com ostracodes estão mais concentrados nas regiões equatoriais (Fig. 11). Os trabalhos realizados na África estão concentrados próximo a El Kef, na Tunísia, considerada a seção-tipo para o limite K–Pg, demonstram uma variação de padrões de extinção. No estudo realizado por Donze *et al*. (1982) a extinção foi catastrófica com a identiciação de crise no final do Maastrichtiano. Entretanto, espécies sobreviventes também foram registradas.

Os ostracodes do Campaniano ao Eoceno inferior da localidade de Ellès, na Tunísia, foram estudados por Said-Benzarti (1988), revelando que a fauna do Maastrichtiano foi

reduzida e somente uma fauna pontual e pobre existiu no Daniano, aumentando sua diversificação ao longo do Paleoceno.

Os ostracodes do Maastrichtiano e Paleoceno de Djebel Dry, no leste da Argélia, foram estudados por Damotte e Fleury (1987) que encontraram semelhanças com a fauna de ostracodes de El Kef, Tunísia, porém com menor diversidade, refletindo um padrão de extinção não catastrófico (Damotte 1991, 1993).

A fauna de ostracodes do K–Pg de Mali, oeste da África, foi reportada por Colin *et al*. (1998), mas devido ao registro sedimentar incompleto, não foi possível sugerir nenhuma interpretação sobre a existência da crise faunística como observada em outras bacias.

Na América do Norte, este evento foi estudado por Maddocks (1985), no Texas, que analisou a fauna de ostracodes marinhos nas três maiores seções: Litting Quarry, Walkers Creek e Brazos River. Não foi observado nenhuma descontinuidade na fauna de ostracodes, caracterizando uma passagem gradual do Cretáceo para o Paleógeno, mesmo em seções com reconhecidas descontinuidades.

Uma fauna bem preservada do norte do Alaska, correspondente aos intervalos Maastrichtiano e Daniano, foi estudada por Browers & De Deckker (1993). Esta seção constituiu a única oportunidade para realizar a reconstrução de um paleoambiente ártico, já que faunas de latitudes altas desta idade são pouco conhecidas. Neste estudo foram definidas quatro assembleias de ostracodes. Os estratos do Maastrichtiano foram depositados em planícies de inundação e os do Daniano foram considerados predominantemente marginal-marinhos a marinho raso. A fauna não-marinha apresentou um *turnover* através do limite com o desaparecimento de algumas espécies no Maastrichtiano, embora outras tenham coexistido com a fauna típica do Daniano.

Na América Central, a assembleia de ostracodes batiais da margem distal do Demerara, no Suriname (Leg 207, sites 1260 e 1261) foi estudada por Guernet & Danelian (2006) que verificaram o desaparecimento de numerosas espécies de ostracodes batiais no limite K–Pg. Além disso, foi observada uma extinção seletiva que afetou mais os ostracodes com hábitos detritívoros do que os filtradores. Segundo os autores, isto pode estar refletindo a queda na produtividade da superfície marinha desencadeada pelo evento. No mar do Caribe, Aumond *et al*. (2009) estudaram os radiolários e ostracodes do ODP site 1001B, tendo havido uma baixa recuperação de ostracodes, tornando impossível a observação de uma tendência para o evento de extinção.

Na América do Sul, especialmente no Brasil, os estudos da passagem K–Pg com ostracodes são escassos pela falta de seções preservadas que registrem este período. Fauth *et al*. (2005) e Rodrigues *et al*. (2014) realizaram estudos taxonômicos, bioestratigráficos e geoquímicos nos ostracodes do limite K–Pg da pedreira Poty, em Pernambuco. Uma significativa mudança faunística foi registrada na passagem do Maastrichtiano para o Daniano com o registro de queda na produtividade primária. Depois de El Kef, esta é a segunda seção com ostracodes que apresenta o registro mais completo da passagem K–Pg no mundo.

Na Bacia de Pelotas, também foi realizado um estudo com ostracodes do Cretáceo–Paleógeno inferior, com amostras de calha. Mesmo com registro sedimentar incompleto, foi possível observar uma mudança faunística durante a passagem do limite K–Pg (Ceolin *et al*. 2011).

Na Argentina, os trabalhos realizados com ostracodes para o limite K–Pg já foram reportados no ítem 2.3.1.

De uma maneira geral, a escassez de estudos com ostracodes neste intervalo reflete a inexistência de seções conhecidas que contemplem o limite. As interpretações propostas pelos trabalhos até o momento desenvolvidos, refletem as condições locais do evento, pois dependem da completude do registro sedimentológico. Entretanto observa-se um padrão de extinção, não catastrófico, mas que registra uma mudança faunística, com espécies sobreviventes e uma fauna com maior diversidade no Daniano.

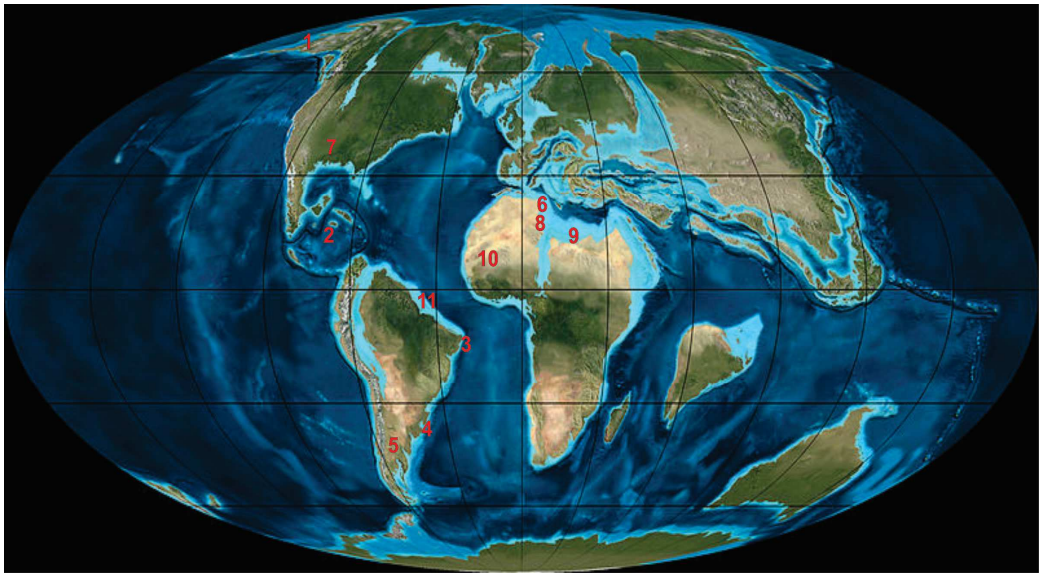

Figura 11: Localização das principais seções do limite K–Pg com estudos em ostracodes. 1-Alasca, 2- Mar do Caribe, 3- Bacia Potiguar, 4- Bacia de Pelotas, 5-Bacia de Neuquén, 6- Djebel Dry, Argélia, 7-Texas, 8- Ellès, Tunisia, 9- El Kef, Tunísia, 10- Tilemsi, Mali, 11- Suriname (Modificado de Scotese 2011).

4 RESULTADOS E DISCUSSÕES

4.1 Artigo 1

Título

New genera and species of Ostracoda from the Maastrichtian and Danian of the Neuquén Basin, Argentina.

Autores

DAIANE CEOLIN[1*], ROBIN WHATLEY[2], GERSON FAUTH[1] *and* ANDREA CONCHEYRO[3].

[1] Instituto Tecnológico de Micropaleontologia - itt Fossil, Universidade do Vale do Rio dos Sinos-UNISINOS, Avenida Unisinos, 950, CEP 93022-000, São Leopoldo-RS, Brazil; e-mail:daiaceolin@unisinos.br*, gersonf@unisinos.br

[2] Micropalaeontology Research Group, Institute of Earth Sciences, Aberystwyth University, Aberystwyth, Cardiganshire SY23 3DB, UK; e-mail: riw@aber.ac.uk

[3] IDEAN - Instituto de Estudios Andinos "Don Pablo Groeber". Consejo Nacional de Investigaciones Científicas y Técnicas. Facultad de Ciencias Exactas y Naturales, Universidad de Buenos Aires. Pabellón II. Ciudad Universitaria. CP 1428. Buenos Aires, Argentina. e-mail: andrea@gl.fcen.uba.ar

*Corresponding author

Periódico

Submetido à *Palaeontology*

OBS: o artigo já está formatado de acordo com as normas da revista.

New genera and species of Ostracoda from the Maastrichtian and Danian of the Neuquén Basin, Argentina.

by DAIANE CEOLIN[1*], ROBIN WHATLEY[2*], GERSON FAUTH[1] *and* ANDREA CONCHEYRO[3].

[1] Instituto Tecnológico de Micropaleontologia - itt Fossil, Universidade do Vale do Rio dos Sinos-UNISINOS, Avenida Unisinos, 950, CEP 93022-000, São Leopoldo-RS, BR; e-mails: daiaceolin@unisinos.br*, gersonf@unisinos.br

[2] Micropalaeontology Research Group, Institute of Earth Sciences, Aberystwyth University, Aberystwyth, Cardiganshire SY23 3DB, UK; e-mail:riw@aber.ac.uk*

[3] IDEAN – Instituto de Estudios Andinos "Don Pablo Groeber". Consejo Nacional de Investigaciones Científicas y Técnicas. Facultad de Ciencias Exactas y Naturales, Universidad de Buenos Aires. Pabellón II. Ciudad Universitaria. CP 1428. Buenos Aires, Argentina. e-mail: andrea@gl.fcen.uba.ar

*Corresponding authors

Abstract: A total of 113 species belonging to 54 genera are recovered from a study of the Maastrichtian and Danian deposits in the Cerro Azul section of the Neuquén Basin, West-Central Argentina. Of these, nine new genera, 38 new species and 28 species in open nomenclature are recorded. These form the basis of the present paper and are listed below: Genera - *Phelocyprideis* gen. nov., *Aleisocythereis* gen. nov., *Apatoleberis* gen. nov., *Mimicocythereis* gen. nov., *Castillocythereis* gen. nov., *Hysterocythereis* gen. nov., *Orthrocosta* gen. nov., *Petalocythereis* gen. nov. and *Sthenarocythereis* gen. nov. Species - *Cytherella saraballentae* sp. nov., *Cytherella semicatillus* sp. nov., *Paracypris bertelsae* sp. nov., *Paracypris imaguncula* sp. nov., *Argilloecia abnormalis* sp. nov., *Argilloecia concludus* sp. nov., *Argilloecia hydrodynamicus* sp. nov., *Bythoceratina cheleutos* sp. nov.,

Phelocyprideis acardomesido sp. nov., *Eucythere dinetos* sp. nov., *Krithe crepidus* sp. nov., *Cytheropteron hyperdictyon* sp. nov., *Cytheropteron bidentinos* sp. nov., *Cytheropteron translimitares* sp. nov., *Aversovalva glochinos* sp. nov., *Eucytherura stibaros* sp. nov., *Hemingwayella verrucosus* sp. nov., *Heinia prostratopleuricos* sp. nov., *Loxoconcha* (s.l.) *posterocosta* sp. nov., *Keijia circulodictyon* sp. nov., *Keijia kratistos* sp. nov., *Paramunseyella epaphroditus* sp. nov., *Munseyella costaevermiculatus* sp. nov., *Ameghinocythere archaios* sp. nov., *Aleisocythereis polikothonus* sp. nov., *Castillocythereis multicastrum* sp. nov., *Castillocythereis albertoriccardii* sp. nov., *Cythereis stratios* sp. nov., *Cythereis clibanarius* sp. nov., *Cythereis trajectiones* sp. nov., *Henryhowella (Wichmannella) praealtus* sp. nov., *Hysterocythereis paredros* sp. nov., *Hysterocythereis coinotes* sp. nov., *Hysterocythereis diversotuberculatus* sp. nov., *Orthrocosta decores* sp. nov., *Orthrocosta atopos* sp. nov., *Orthrocosta phantasia* sp. nov. and *Sthenarocythereis erymnos* sp. nov. The nature of the fauna and aspects of its evolution are discussed below.

Key words: Marine Ostracoda, Maastrichtian–Danian, Neuquén Basin, Argentina.

THE Neuquén Basin is located in West-Central Argentina between latitudes 32º and 40ºS. It occurs in the provinces of Mendoza, Neuquén, Río Negro and La Pampa. At latitude 35ºS, the basin extends to form the Neuquén embayment that comprises 600 km of extension in a north-south direction and 300-400 km east-west. It has a maximum thickness of 7.000 m of marine and non-marine sedimentary rocks, ranging from the Late Jurassic to the Paleocene (Howell *et al*. 2007; Aguirre-Urreta *et al*. 2011) (Figure 1).

During the Maastrichtian, the Neuquén Basin was flooded by the first transgression from the Atlantic Ocean. This extensive sea connected the basin to the South Atlantic and embraced an area from the present day Andes in the west to the eastern Atlantic Ocean. This basin is well-known from its well-preserved outcrops and rich fossil content. A summary of

the main micropalaeontological and geological studies can be found in Ballent *et al*. (2011) and Rodrigues *et al*. (2011) respectively.

The pioneer studies on Ostracoda in this basin were carried out by Bertels in the 1960's and 1970's in many outcrops of the Jagüel and Roca formations, mainly at Huntrai-co and Barranca de Jagüel, the latter being the type section of the K–T boundary in this basin. These studies provided an initial contribution to our knowledge of the biostratigraphy, palaeoecology and taxonomy of the Ostracoda of the northern part of the basin.

The Cerro Azul section is a relatively new site for micropalaeontological studies in the eastern sector of Lake Pellegrini, where sediments of the Jagüel (late Maastrichtian–early Danian) and Roca (Danian) formations can be seen at outcrop. Musso *et al*. (2012) studied the clay mineralogy, giving an environmental interpretation and identifying the transition between Upper Cretaceous and lower Danian based on calcareous nannofossils.

The present work presents a substantial new marine ostracod fauna from the Neuquén Basin in the Upper Cretaceous–lower Danian transition.

GEOLOGICAL SETTING

The Cerro Azul section is located at S38°50'48", W67°52'20" and is composed of calcareous siltstones and claystones from the Jagüel and Roca formations (Fig. 1). Musso *et al*. (2012) described the section they studied of the Jagüel Formation as being a homogenous lithology of grey calcareous mudstones. The Roca Formation was defined by an alternation of carbonate rocks and greenish grey calcareous mudstones and the base of the Roca Formation was defined, according to criteria adopted by Uliana and Dellape (1981), by the first appearance of organogenic limestones. The age was determined by calcareous nannofossils (Musso *et al.* 2012) (Fig. 2)

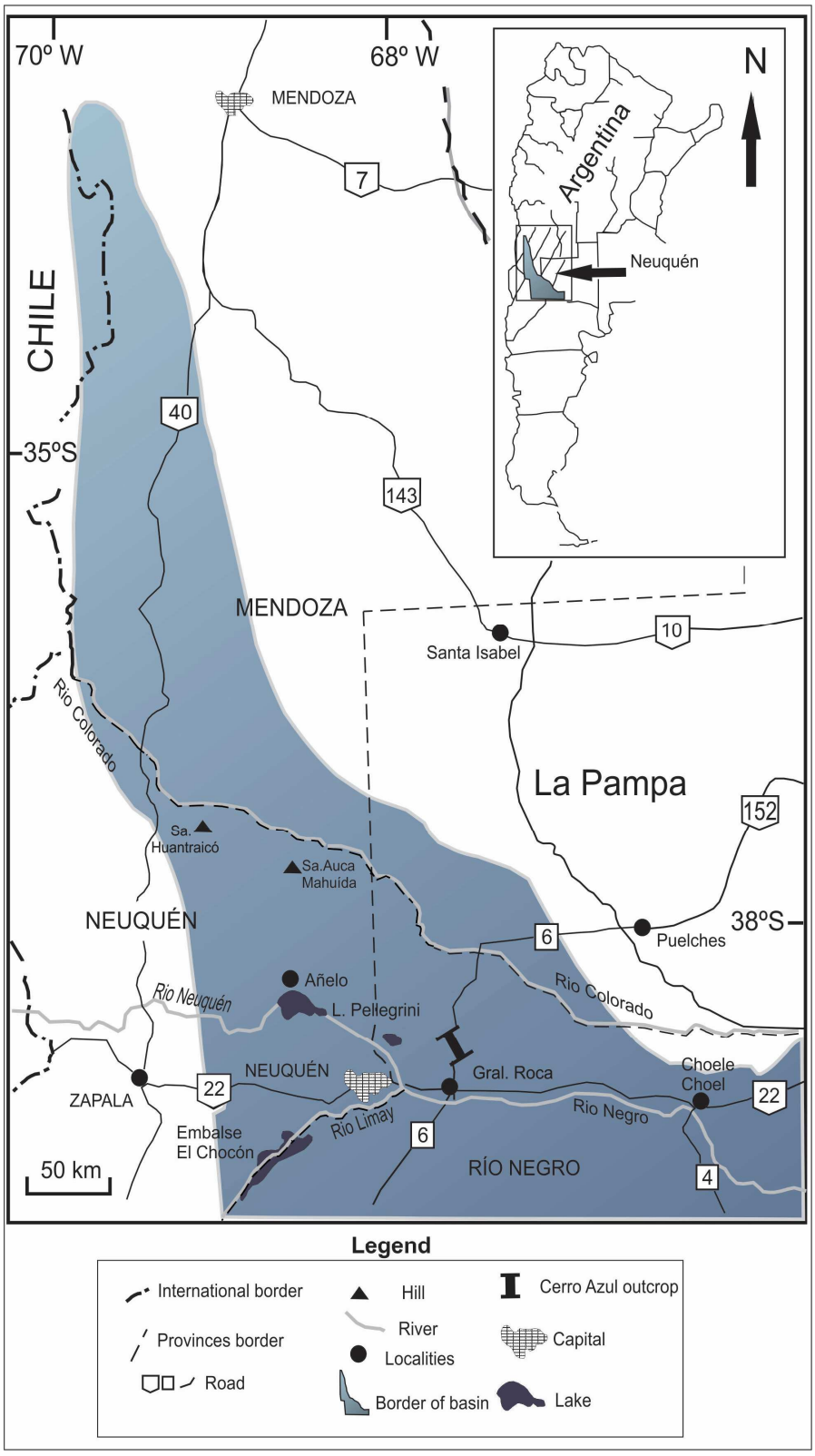

FIG. 1. Location map of Neuquén Basin with Cerro Azul section (modified from Del Río *et al*. 2011).

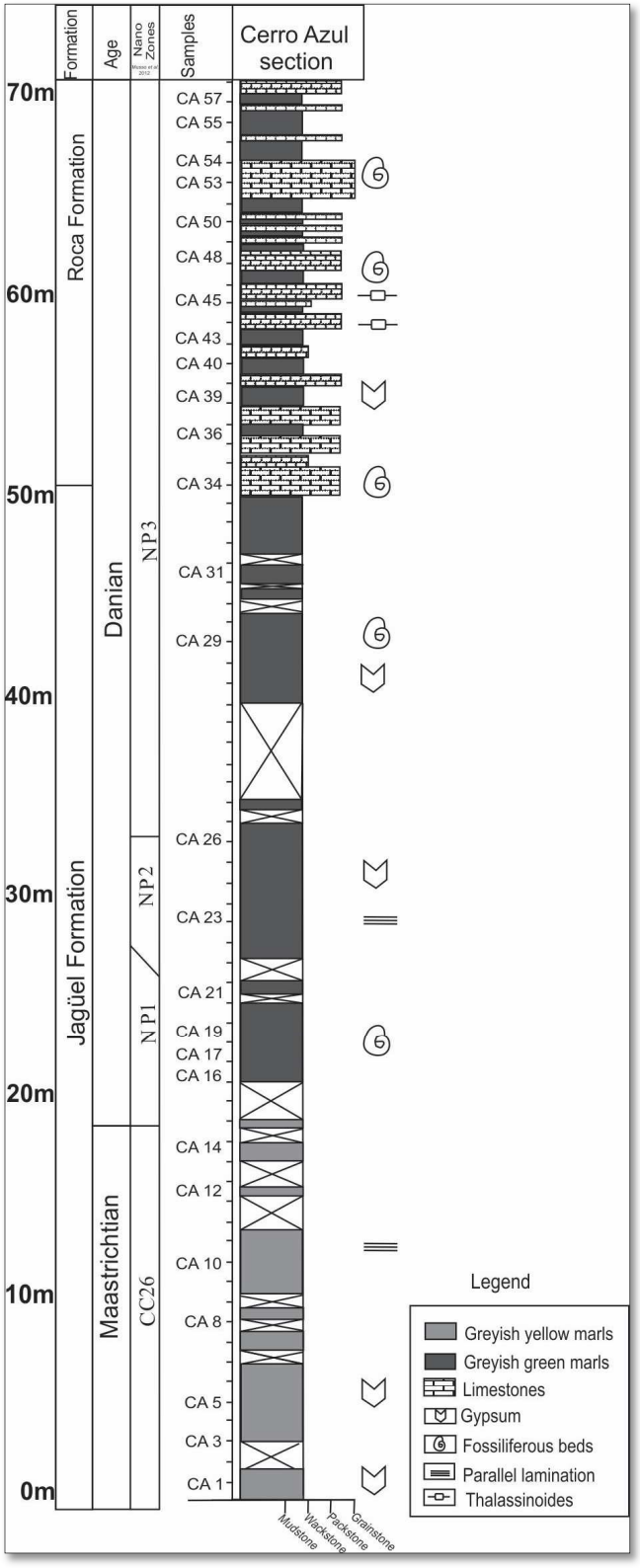

FIG. 2. Cerro Azul profile with samples position (modified from Musso *et al*. 2012).

MATERIAL AND METHODS

Twenty-seven outcrop samples were studied and approximately 20 g of dried rock was crushed and soaked in 200 mL of a hydrogen peroxide solution (H_2O_2) for 24 hours, at a concentration of 35 per cent. Residues were then washed and divided into grain fractions 63, 180, and 250 μm and dried at 60 ºC. All ostracods were hand-picked under stereo microscope from each size fraction. Selected specimens were imaged in a EVO MA15 Zeiss scanning electron microscope.

SYSTEMATIC PALAEONTOLOGY

This published work and the nomenclatural acts it contains, have been registered in Zoobank: http://zoobank.org/References/xxxxxxxxx. The suprageneric classification adopted is that proposed by Moore and Pitrat (1961) with some modifications. In the systematic descriptions, the following conventions are employed: L = length, H = height, W = width, RV= right valve, LV= left valve, CMS= central muscle scar. All dimensions are in mm. Size, based on length, is as follows: very small (<0.40 mm), small (0.41–0.5 mm), medium (0.51–0.7 mm), large (0.71–0.9 mm), very large (>0.9 mm). Type and figured specimens are deposited in the collections of the Facultad de Ciencias Exactas y Naturales, Laboratorio de Micropaleontología, Universidad de Buenos Aires, (UBA), Argentina, under their respective catalogue numbers LM-FCEN 3232-3310; 3400-3539.

Class OSTRACODA Latreille, 1806

Order PLATYCOPIDA Sars, 1866

Suborder PLATYCOPINA Sars, 1866

Family CYTHERELLIDAE Sars, 1866

Genus CYTHERELLA Jones, 1849

Type species. *Cytherina ovata* Röemer, 1840

Cytherella saraballentae sp. nov. Ceolin and Whatley

Figure 3A-E

LSID. urn:lsid:zoobank.org:act:xxxxxxxxx

1992 *Cytherella NC136* Colin and Hochuli. p. 273, pl. 4, fig.1

Derivation of name. In honour of the late Dr. Sara Ballent for her great contribution to the study of Ostracoda, and in particular to those of the Jurassic and Cretaceous of the Neuquén Basin, Argentina.

Type material. Holotype: one complete carapace, LM-FCEN 3232 (Fig. 3A, B); paratypes: LM-FCEN 3233-3234 (Figs 3C, D; 3E).

Material. 233 specimens, mainly juveniles from samples 1, 14; Maastrichtian; 16, 17, 19, 21, 23, 26, 29, 31, 34 and 39; Danian.

Diagnosis. A species of *Cytherella*, punctate over most of the valve in most specimens with a large smooth area mid-dorsally and centrally. A deep linear depression occurs between the two valves dorsally.

Dimensions. In mm:

		L	H	W	
Holotype, adult, female	LM-FCEN 3232	0.830	0.521	0.352	sample 23
Paratype, adult, male	LM-FCEN 3233	0.790	0.495	0.324	sample 19
Paratype, adult, female	LM-FCEN 3234	0.847	0.512	0.395	sample 21

Description. A large, very regularly elongate and subovate species with end margins almost equally rounded and with apex at mid-height. RV larger than LV with conspicuous overlap around the entire periphery, especially ventrally. Sagittate in dorsal view. Dorsal margin convex, with a small concavity at mid-length, that declines towards posterior margin. Ventral margin almost straight. Greatest length at about mid-height; greatest height and width at one-

third from the posterior margin. Surface essentially punctate, with puncta large, mainly circular and covering most of the valve except centrally, mid-ventrally and dorsally. There is some preferential orientation anteriorly and posteriorly parallel to those margins. Internally, females with the characteristic and conspicuous shallow concavity in the posterior part. Inner lamella with a contact groove in the larger right valve into which fits the edge of the smaller valve. Sexual dimorphism marked, with females more inflated posteriorly than males. CMS comprises a leaf-like pattern of two rows of five opposing scars typical of the suborder.

Remarks. This species differs from *Cytherella terminopunctata* Bertels, 1975*a* from the Maastricthian of the Neuquén Basin, also encountered in this study, in its much larger and more widely distributed puncta. It also differs from *Cytherella* sp. 4 from the Paleocene of the Pelotas Basin (Ceolin *et al*. 2011) in mainly by being more inflated in dorsal view and larger overall.

Stratigraphical range. Upper Cretaceous of eastern Niger (Colin and Hochuli 1992); Maastrichtian and Danian of Cerro Azul, General Roca.

Cytherella semicatillus sp. nov. Ceolin and Whatley

Figure 3F-I

LSID. urn:Isid:zoobank.org:act:xxxxxxxxx

Derivation of name. L. *semi*, half; plus *catillus*, a small plate. With reference to the shape of the anterior one-third of the left valve of this species which resembles one-half of a small plate.

Type material. Holotype: one complete carapace, LM-FCEN 3235 (Figs 3F, G, I); paratype: FCEN-LM 3236 (Fig. H).

Material. 176 specimens, mainly juveniles, from samples 3, 5 and 14; Maastrichtian; 16, 17, 21, 26 and 34. Danian.

Diagnosis. Carapace with a compressed, broadly rounded anterior margin with a structure similar to the edge of dinner plate. RV overlaps the LV less on the posteroventral margin where it is more inflated.

Dimensions. In mm:

		L	H	W	
Holotype, adult, female,	LM-FCEN 3235	0.798	0.542	0.375	sample 17
Paratype, juvenile,	LM-FCEN 3236	0.602	0.392	0.250	sample 19

Description. Large, subovate in lateral view. Subelliptical with anterior region acuminate in dorsal view. RV larger than LV with conspicuous overlap in lateral view around the entire periphery, except posteroventrally, which is obscured by valve tumidity. Anterior margin broadly rounded, compressed and with a subtle marginal rim in the left valve, which extends from anterodorsal margin to mid-ventrally. Apex at about mid-height. Posterior margin well rounded, but tumid with apex a little below mid-height. Dorsal margin gently convex in LV, medianly subumbonate in RV. Ventral margin almost straight in LV, gently convex in RV. Greatest height through "umbo"; greatest length about mid-height; greatest width in the posterior quarter. Surface smooth. There is a distinct marginal rim in LV. Selvage and flange visible anteriorly in the right valve. Other internal features not seen. Sexual dimorphism not observed.

Remarks. This species is similar to *Cytherella harmoniensis* Van den Bold, 1960 from the Lower Eocene of Sergipe, Brazil (Neufville 1973), mainly with respect to male specimens (fig. 2d), that differ in its more pronounced dorsal overlap and smaller size (*C. harmoniensis* L: 0.9-0.87).

Stratigraphical range. Maastrichtian and Danian of Cerro Azul, General Roca.

Order PODOCOPIDA Müller, 1894

Suborder PODOCOPINA Sars, 1866

Superfamily BAIRDIOIDEA Sars, 1888

Family BAIRDIIDAE Sars, 1888

Genus BAIRDOPPILATA Coryell, Sample and Jennings, 1935

Type species. *Bairdoppilata martyni* Coryell, Sample and Jennings, 1935

Bairdoppilata sp.

Figure 3J

Material. 16 specimens, mainly juveniles, from sample 21, Danian.

Dimensions. Adult valve, FCM-LM 3237, 1.110 (L), 0.642 (H).

Diagnosis. A very large, typically bairdioid species in lateral view, with a micropunctate ornament densely developed around the anterior margin and much more scarcely elsewhere.

Remarks. Although there are no complete carapaces, this species is similar to *Bairdoppilata triangulata* Edwards, 1944 from the Palaeogene and Miocene of the Pelotas Basin (Sanguinetti 1979; Ceolin *et al*. 2011) differing in its asymmetrically rounded anterior margin, being more elongate, and in the less symmetrical and more convex dorsal margin. It differs from *Bairdia anachoreta* Bertels 1968*b* in its more angular dorsal margin.

Bairdoppilata? sp.

Figure 3K

Material. 24 specimens from samples 16, 53, 55 and 57. Danian.

Dimensios. Adult carapace, LM-FCEN 3238, 0.782 (H), 0.63 (L), 0.335 (W).

Description. A large, subovate carapace with broadly rounded anterior margin and posterior margin sloping towards its rounded apex. Dorsal margin strongly convex with a slight

concavity present anterodorsally in RV. Ventral margin straight with a subtle concavity medianly in RV, LV overlaps RV, mainly ventrally and anterodorsally. Hinge adont. Calcified inner lamella wide anteriorly and posteriorly. CMS not seen.

Remarks. This species, although similar to what some authors have referred to as species of *Bythocypris* (i.e. *Bythocypris chapmani* Neale, 1975), does not belong to that genus due to its bairdioid shape mainly at anterodorsal margin. A more detailed classification is not possible due to absence of a well-preserved internal view.

Superfamily CYPRIDOIDEA Baird, 1845

Family PARACYPRIDIDAE Sars, 1923

Genus PARACYPRIS Sars, 1866

Type species. *Paracypris polita* Sars, 1866

Paracypris bertelsae sp. nov. Ceolin and Whatley

Figure 3L-O

LSID. urn:lsid:zoobank.org:act:xxxxxxxxx

1973 *Paracypris*? sp. Bertels, p. 314, pl. 1, fig. 7a–b.

Derivation of name. In honour of the late Dr. Alwine Bertels, in recognition of her important work on Ostracoda, especially those from the Maastrichtian and Danian of the Neuquén Basin.

Type material. Holotype: one complete carapace, LM-FCEN 3239 (Figs 3L, O); paratypes: LM-FCEN 3240-3241 (Figs 3M; 3N).

Material. 102 specimens from samples 16, 17, 19, 21, 23, 26, 29, 31, 34 and 45; Danian; and the "numerous" specimens referred to by Bertels (1973); Danian.

Diagnosis. A short and rather high species of *Paracypris* with strong overlap of LV over RV and arcuate dorsal margin with poorly defined cardinal angles.

Dimensions. In mm:

	L	H	W	
Holotype, adult, LM-FCEN 3239	0.955	0.480	0.368	sample 31
Paratype, adult, LM-FCEN 3240	0.953	0.527		sample 16
Paratype, adult, LM-FCEN 3241	0.913	0.501		sample 16

Description. Elongate, subovate to subtriangular in lateral view. In dorsal view, very regularly subovate and rather thick-shelled for the genus. Anterior margin narrowly rounded with apex below mid-height. Posterior margin sub-acute somewhat downturned and with subventral apex. Posterodorsal slope long, straight to slightly convex. Dorsal margin slightly concave anteriorly; anteromedianly slightly convex, then straight, but again convex posterodorsally. Ventral margin similarly gently sinuous with very slight oral incurvature. LV larger than RV with conspicuous overlap around entire periphery. Greatest length below mid-height; greatest height at anterior cardinal angle; greatest width in the middle one-third. Internally, the anterior and posterior calcified inner lamellae wide and vestibulate. CMS not seen. Hinge adont with a long smooth groove in the left valve, which is well-butressed ventrally.

Remarks. This species differs from *Paracypris imaguncula* sp. nov. in its dorsal slope being less acute and in its subovate to subtriangular shape and smaller size. It also differs from *Paracypris* sp. 1 Bertels, 1975*a*, from the Maastrichtian of Fortín General Roca, Río Negro Province, in being less elongate with a more convex dorsal margin, the less truncated posterior end and in being less acuminate.

Stratigraphical range. Danian of Fortín General Roca (Bertels 1973) and Danian of Cerro Azul, General Roca.

Paracypris imaguncula sp. nov. Ceolin and Whatley

Figure 3P-S

LSID. urn:lsid:zoobank.org:act:xxxxxxxxx

1973 *Paracypris* sp. Bertels, p. 315, pl. 1, fig. 8a.

Derivation of name. L. *imaguncula*, a copy. With reference to the general similarity of this species to the type of the genus, *Paracypris polita*, Sars.

Type material. Holotype: one complete carapace, LM-FCEN 3242 (Figs 3P, S); paratypes: LM-FCEN 3243-3244 (Figs 3Q; 3R).

Material: 36 specimens from samples 14; Maastrichtian; 16, 17, 21, 26, 29, 31, 34, 36, 39, 40, 53 and 57; Danian; and one specime referred to by Bertels (1973); Danian.

Diagnosis. A species of *Paracypris* of median length with posterior end acute and LV overlapping the RV around the entire margins, except anteriorly where the RV overlaps the LV.

Dimensions. In mm:

	L	H	W	
Holotype, adult, LM-FCEN 3242	1.041	0.480	0.256	sample 31
Paratype, adult, LM-FCEN 3243	1.070	0.468		sample 34
Paratype, adult, LM-FCEN 3244	1.106	0.532		sample 34

Description. Very large, elongate, subtriangular in lateral view. In dorsal view subeliptical with pointed posterior. LV overlapping the RV around entire periphery, strongly mid-ventrally and anterodorsally. Anterior margin narrowly but symmetrically rounded, extending beyond left valve, with apex below mid-height. Posterior margin acuminate subventrally. In both valves, posterodorsal slope long, straight or slightly concave. Dorsal margin concave anterodorsally, convex medianly and concave posterodorsally in the RV. LV convex

throughout and subumbonate anteromedianly. Ventral margin gently biconvex about a slight median incurvature. Surface smooth. There are a few, apparently simple, pore canals on the lateral surface. Internal features not seen.

Remarks. The present species is very similar to *Paracypris polita* Sars, 1866, differing in its less elongate shape, less acute posterior end and less pronounced concavity ventrally. It is also very similar to *P. umzambaensis* Dingle, 1969, from the Upper Senonian of the Pondoland Coast, South Africa, differing mostly in its pronounced ventral overlap, narrower anterior region and in its larger size (*P. umzambaensis* is L: 0.80, H: 0.33). It is also similar to *Paracypris* sp. Fauth *et al*., 2013, from the Upper Cretaceous of the Santos Basin, southeast Brazil, but differs in being more convex dorsally and in the greater degree of overlap around the entire margin, which in Fauth's species is absent in the mid-dorsal margin.

Stratigraphical range. Maastrichtian and Danian of Cerro Azul, General Roca and Danian of Fortín General Roca, Río Negro (Bertels 1973).

Paracypris? sp.

Figure 4A

Material. Six specimens from samples 21, 23, 29 and 36. Danian.

Dimensions. Adult carapace, LM-FCEN 3245, 0.523 (L), 0.25 (H).

Remarks. This species is tentatively classified in *Paracypris* althougth it lacks the very acute ventral to subventral posterior apex typical that genus. It is poorly preserved and distorted and its overlap relationship is difficult to assess.

Genus AGLAIOCYPRIS Sylvester-Bradley, 1946

Type species. *Aglaia pulchella* Brady, 1868*b*

Aglaiocypris? sp.

Figure 4B

Material. One specimen from sample 31. Danian.

Dimensions. Adult valve, LM-FCEN 3246, 0.591 (L), 0.244 (H).

Diagnosis. Median, elongate subovate in lateral view. Anterior margin rounded; posterior margin obliquely rounded. Dorsal margin convex with a slight concavity anterodorsally. Ventral margin gently concave medianly. Surface smooth. Internal features not seen.

Remarks. This specimen is only tentatively placed in the genus due to the fact that in the one poorly preserved valve it is impossible to see those internal features necessary to confirm the genus.

Family PONTOCYPRIDIDAE Müller, 1894

Genus ARGILLOECIA Sars, 1866

Type species. *Argilloecia cylindrica* Sars, 1866

Argilloecia abnormalis sp. nov. Ceolin and Whatley

Figure 4C-F

LSID. urn:Isid:zoobank.org:act:xxxxxxxxx

1973 *Bythocypris*? sp. Bertels, p. 313, pl. 1, fig 6a–b.

Derivation of name. L. *abnormalis*. With reference to the fact that this is the only species of the genus in which the smaller LV does not overreached the RV anteriorly.

Type material. Holotype: one complete carapace, LM-FCEN 3247 (Fig. 4C); paratypes: LM-FCEN 3248-3250 (Figs 4D; 4E; 4F).

Material. 232 specimens, mainly carapaces, from samples 8, 12 and 14; Maastrichtian; 16, 17, 19, 21, 23, 26, 29, 31, 36 and 39; Danian.

Diagnosis. A medium species of *Argilloecia* characterized by its less pointed posterior end and that the anterior margin of the LV does not overeach the RV, as in others species of the genus.

Dimensions. In mm:

		L	H	W	
Holotype, adult,	LM-FCEN 3247	0.528	0.207	0.165	sample 21
Paratype, adult,	LM-FCEN 3248	0.678	0.226		sample 23
Paratype, adult,	LM-FCEN 3249	0.533	0.212		sample 34
Paratype, adult,	LM-FCEN 3250	0.585	0.206	0.162	sample 21

Description. A medium, elongate subovate species in lateral view. In dorsal view subelliptical, with greatest width medianly and with pointed ends. Anterior margin symetrically rounded with apex a little above mid-height. Posterior margin narrower and obliquely rounded, with apex below mid-height. Dorsal margin more convex anterodorsally and almost straight but sloping in posterior margin. Ventral margin subconvex, with LV more concave in mid-ventral position. RV overlaps the LV and is least pronounced posterodorsaly. Surface smooth. Calcified inner lamella wide anteriorly and narrow posteriorly. CMS typical for the genus. Sexual dimorphism not seen.

Remarks. The decision to place this species in *Argilloecia*, is based on the valve overlap (RV larger than LV) and in the CMS being characteristic of *Argilloecia*.

Stratigraphical range. Danian of Fortín General Roca, Río Negro, (Bertels 1973); Maastrichtian and Danian of Cerro Azul, General Roca.

Argilloecia concludus sp. nov. Ceolin and Whatley

Figure 4G-J

LSID. urn:Isid:zoobank.org:act:xxxxxxxxx

Derivation of name. L. *concludo* end, close. With reference to its presence near the close of the Cretaceous.

Type material. Holotype: LM-FCEN 3251(Fig. 4G); paratypes: LM-FCEN 3252-3254 (Figs 4H; 4I; 4J).

Material. 12 specimens from samples 5 and 12. Maastrichtian.

Diagnosis. A proportionally rather short species of *Argilloecia* in which the carapace at one-third from the posterior margin is higher than in most other species. Dorsal margin convex and with strong RV over LV overlap. Oral incurvature stronger than many species.

Dimensions. In mm:

		L	H	W	
Holotype, adult,	LM-FCEN 3251	0.525	0.230	0.150	sample 5
Paratype, juvenile,	LM-FCEN 3252	0.485	0.222	0.135	sample 12
Paratype, juvenile,	LM-FCEN 3253	0.411	0.183		sample 12
Paratype, juvenile,	LM-FCEN 3254	0.502	0.200	0.151	sample 5

Description. A medium, elongate carapace in lateral view. Anterior margin narrowly rounded with apex below mid-height. Posterior margin acute with ventral apex. Dorsal margin symetrically convex and elongate; gently concave anterodorsally, mainly in LV. Ventral margin biconvex with pronounced anteroventral oral concavity. Greatest length below mid-height; greatest height at posterior one-third; greatest width medianly. RV overlaps the LV, mainly in dorsal one-third and around ventral margins. Surface smooth. Internal features not seen.

Remarks. The present species resembles *Argilloecia subcylindrica* Alexander, 1934 from the Eocene of Texas, but differs in being narrower anteriorly, the overlap is more developed postero- and anterodorsally and the posterodorsal region is higher.

Stratigraphical range. Maastrichtian of Cerro Azul, General Roca.

Argilloecia hydrodynamicus sp. nov. Ceolin and Whatley

Figure 4K-M

LSID. urn:Isid:zoobank.org:act:xxxxxxxxx

Derivation of name. Gr. *ύδρον* hydron, water; plus *δινα*μ*κυς* dynamicus, power, strongly. With reference to the supremely hydrodynamical outline and shape of this species.

Type material. Holotype: one carapace LM-FCEN 3255 (Fig. 4K); paratypes: LM-FCEN 3256-3257 (Figs 4L; 4M).

Material. 28 specimens, all carapaces from samples 16, 17, 21, 23 and 26. Danian.

Diagnosis. A very elongate, posteroventrally pointed species of *Argilloecia* with strong RV overlap anterodorsally and the reverse posterodorsally.

Dimensions. In mm:

		L	H	W	
Holotype, adult,	LM-FCEN 3255	0.432	0.178	0.125	sample 21
Paratype, juvenile,	LM-FCEN 3256	0.401	0.158		sample 21
Paratype, juvenile,	LM-FCEN 3257	0.386	0.135	0.122	sample 21

Description. Small, subtriangular, elongate in lateral view. Subelliptical in dorsal view. Anterior margin narrowly rounded with apex behind mid-height, posterior margin sub-acute with ventral apex. Dorsal margin convex with posterior one-third sloping towards the

posterior margin. Ventral margin almost straight with a weak oral concavity. Greatest length below mid-height; greatest height and width medianly. RV overlaps the LV along the ventral margin, mainly anteroventrally. Along the dorsal margin, the overlap is more pronounced anterodorsally and becomes less posteriorly and finally is not apparent. Surface smooth. Internal features not seen.

Remarks. Differs fom *Argilloecia concludus* sp. nov. mainly in being much narrower posteriorly, less incurved ventrally and more convex dorsally.

Stratigraphical range. Danian of Cerro Azul, General Roca.

Superfamily CYTHEROIDEA Baird, 1850

Family BYTHOCYTHERIDAE Sars, 1826

Genus BYTHOCERATINA Hornibrook, 1952

Type species. *Bythoceratina mestayerae* Hornibrook, 1952

Bythoceratina cheleutos sp. nov. Ceolin and Whatley

Figure 4N-Q

LSID. urn:Isid:zoobank.org:act:xxxxxxxxx

Derivation of name. Gr. *χελευτος*, cheleutos, netted. With reference to the net-like reticulum of this species.

Type material. Holotype: one carapace, LM-FCEN 3258 (Figs 4N, Q); paratype: LM-FCEN 3259 (Figs 4O, P).

Material. Six specimens from samples 34, 36, 39 and 53; Danian.

Diagnosis. An elongate, ovate species of *Bythocythere* with a well-pronounced median sulcus and anteromedian elevation. Ornament of chaotic reticulation centrally within a peripheral ring where the muri are preferentially aligned to the margins, giving an aspect of riblets surrounding the centre.

Dimensions. In mm:

	L	H	W	
Holotype, adult, LM-FCEN 3258	0.865	0.398	0.357	sample 34
Paratype, adult, LM-FCEN 3259	0.892	0.425	0.355	sample 29

Description. A large, elongate subovate species of *Bythoceratina* in lateral view. Dorsal view spindle-shaped with distinct median sulcus and laterally compressed posteriorly. Anterior margin broadly and regularly rounded with apex at about mid-height. Posterior margin subcaudate, slightly "upturned" with apex above mid-height. Posteroventral slope long, very gently convex; posterodorsal slope shorter and straight. Greatest length above mid-height; greatest height at anterior third; greatest width equal on either side of median sulcus. Dorsal margin straight to sinuous; ventral margin with gently incurvature at about one-third and posteriorly keel-like. LV slightly larger than RV, with dorsal overlap. Ornament centrally reticulate but rather chaotic with individual cells varying greatly in shape and size. Around the entire periphery, most notably antero- and posterodorsally, a series of five or six subparallel riblets formed from the muri, are developed. Median sulcus, which terminates a little below mid-height, extends in a vertical arc across the valve and is floored by reticulae. A large elevated tubercle occurs immediately anterior of this sulcus and is built up from coarse, well-developed muri, its apex is perforate. Small, rather low, usually conjunctive pore conuli are developed both on the muri, but also within the solae. All the pores seem to be simple.

Remarks. This species differs from *Bythocythere punctatula* Bertels, 1973, from the Danian of Fortín General Roca, Río Negro Province, mainly in its ornamentation pattern, which is reticulate, with a series of subparallel riblets around the entire periphery, while Bertels' species has small tubercles densely distributed across the entire surface.

Stratigraphical range. Danian of Cerro Azul, General Roca.

Bythoceratina rocana (Bertels, 1973) comb. nov.

Figure 4R-U

1973 *Bythocythere rocana* Bertels, p. 328, pl. 5, fig. 6a–b.

Material. Three carapaces from samples 19 and 29. Danian.

Dimensions. Adult carapace, LM-FCEN 3260 (Figs 4R, T) female, 0.677 (L), 0.304 (H), 0.362 (W); LM-FCEN 3261, (Figs 4S, U) male, 0.792 (L), 0.424 (H), 0.407 (W).

Remarks. *Bythoceratina rocana* (Bertels, 1973) does not resemble *Bythocythere* Sars as it in strongly nodose and has a developed reticulation pattern. This species has very strong sexual dimorphism that was not recognized by Bertels (1973). The female is lower and longer than males. The male is higher, rounder and narrower dorsally. The specimen figured by Bertels (1973) is female. Internal features are not seen.

S*tratigraphical range*. Danian of Fortín General Roca (Bertels 1973) and Cerro Azul.

Bythoceratina sp. aff. *Bythoceratina scaberrima* (Brady, 1887) Van den Bold 1957*a*

Figure 5A

1957*a Bythoceratina scaberrima* (Brady). Van den Bold, p. 246, pl. 2, fig. 8a–b.

Material. One specimen from sample 5. Maastrichtian.

Dimensions. Adult valve, LM-FCEN 3262 (lost), 0.591 (L), 0.415 (H).

Description. Subrhomboidal, but much modified by the position of the subdorsal caudal process and two large ventrolateral spines. Strongly reticulopunctate ornament with numerous rounded pore conuli, many conjunctive, some blind and some perforated. There is a distinct denticulate marginal rim around the free margins and on the dorsal margin, and a deep median sulcus.

Remarks. Differs from *Bythoceratina scaberrima* (Brady, 1887) in being more reticulate and lacking isolate conuli. This generic group are well-known in the deep sea and are an indicator of that environment.

Bythoceratina sp.

Figure 5B

Material. One specimen from sample 21. Danian.

Dimensions. A broken valve, LM-FCEN 3263, 0.773 (L), 0.433 (H).

Description. A broken LV of *Bythoceratina* with the usual large tubercles in the usual position of this genus and the large broken spine posteroventrally. Entire surface coverd by a net-like reticulum of low muri and mainly angular cells. Large numbers of pores on the muri or, if in solum, as eruptive conuli. Most are simple.

Remarks. Although this specimen is broken, it is possible to see the ventrolateral spinose projection, which allow us to classify it. It differs from *Bythoceratina incurvata* (Bertels, 1973) in having more numerous tubercles and in the net-type reticular pattern.

Genus PSEUDOCYTHERE Sars, 1866

Type species. *Pseudocythere caudata* Sars, 1866

Pseudocythere sp.

Figure 5C-D

Material. One adult carapace from sample 17. Danian.

Dimensions. Adult carapace, LM-FCEN 3264, 0.585 (L), 0.258 (H).

Description. A median, very elongate species of *Pseudocythere*. In lateral view, there are two well-developed ribs, one, the dorsal rib is a very strongly developed, almost flared rib, which extends onto the anterior and ventral margin peripherally where it acts as a marginal rim. This

rib has, just below it, another weaker rib, that extends from mid-dorsal just onto the anterodorsal surface and another shorter rib is developed mid-dorsally. These are very well seen in dorsal view. A linear inflated area extends across the valve from about mid-height to the caudal process. This is separated by a linear shallow area, below which a ventrolateral rib crosses the ventrolateral surface and falls away steeply to the ventral surface. Surface smooth.

Remarks. Differs from *Pseudocythere* sp. from the upper Senonian-lower Turonian of Morrocco (Andreu *et al*. 2013) in its more elongate and narrow outline and in the presence of ribs dorsally.

Genus TANYCYTHERE Cabral, Lord, Boomer and Malz, 2014.

Type species. *Tanycythere caudata* Cabral, Lord, Boomer and Malz, 2014.

Tanycythere sp.

Figure 5E

Material. Three specimens from samples 17 and 21. Danian.

Dimensions. Adult carapace, LM-FCEN 3265, 0.750 (L), 0.324 (H).

Diagnosis. A large, subrectangular to elongate subovate species of *Tanycythere* with anterior margin symmetrically rounded, with apex at mid-height; posterior margin caudate but broken, with apex above mid-height. Dorsal margin straight, ventral margin sinuous with median concavity. Surface smooth. RV overlaps the LV. Subeliptic in dorsal view.

Remarks. It differs from *Tanycythere praecaudata* Cabral and Loureiro, 2014 from the Jurassic of the Portugal in having a less inflated carapace, absence of a keel posteroventrally and being less rounded.

Family CYTHERIDEIDAE Sars, 1925

Subfamily CYTHERIDEINAE Sars, 1925

Genus PHELOCYPRIDEIS gen. nov. Ceolin and Whatley

LSID. urn:Isid:zoobank.org:act:xxxxxxxxx

Derivation of name. Gr. *φελο* deceitful; plus *Cyprideis*. With reference to the fact that this genus, while superficially resembling *Cyprideis* Jones, has a quite distinctly different hinge, which lacks the median element and which overall is diagonal to the edge of the hinge margin.

Type species. *Phelocyprideis acardomesido* gen. et sp. nov.

Diagnosis: A new genus of Cytherideidae typified by an unusual merodont hinge in which the terminal elements alternate in both structure and position relative to edge of the valve and the median element is absent. From the LV, for example, the anterior terminal element projects beyond the internal edge of the valve, and is mechanically positive (male) while the posterior terminal element is within the valve edge and is mechanically negative (female) and *vice versa* for the RV.

Remarks. The type of merodont hingement exhibited by this genus we name alternamerodont (from the Latin *alternos*) and from the fact that the terminal elements alternate in structure and function and in their relationship to the edge of the valve and because the entire structure seems to be diagonal to that edge. This hinge also lacks a median element. This Danian species is another element in the complex structure of this generic group throughout the Tertiary, leading to its final end product in the form of the genus *Cyprideis* Jones *via* such important genera as *Fossocytheridea* Swain & Brown, 1964 as outlined by Tibert *et al*. (2003). However, it does seem that *Phelocyprideis* is possibly the first genus in this important lineage leading directly to *Cyprideis* rather than *Fossocytheridea* and the first two authors of the present study intend to argue this case in a subsequent paper. One of us (RCW) has already described *Phraterfabanella* (Boomer *et al*. 2001) from the Italian Lower Jurassic, now acknowledged as the primitive genus of the entire Cytherideidae (see Tibert *et al*. Text fig. 6,

p. 213). *Phelocyprideis acardomesido* sp. nov. resembles none of the *Fossocytheridea* species described by Bergue *et al*. (2011) species from the Senonian of the Santos Basin in SE Brazil.

Description: As for the type species.

Phelocyprideis acardomesido sp. nov. Ceolin and Whatley

Figure 5F-L

LSID. urn:lsid:zoobank.org:act:xxxxxxxxx

Derivation of name. Gr. *α*, not, without; plus *καρλο*, hinge; plus *μεσιλο*, middle. With reference to the lack of a median hinge element in this species.

Type material. Holotype: LM-FCEN 3266 (Fig. 5F); paratypes: LM-FCEN 3267-3271(Figs 5G; 5H; 5I, J; 5K; 5L).

Material. 96 specimens from samples 34, 50 and 57. Danian.

Diagnosis. As for genus.

Dimensions. In mm:

		L	H	W	
Holotype, adult, female,	LM-FCEN 3266	0.583	0.364	0.268	sample 34
Paratype, adult, female	LM-FCEN 3267	0.523	0.317		sample 34
Paratype, adult, male,	LM-FCEN 3268	0.517	0.301	0.195	sample 34
Paratype, adult, female,	LM-FCEN 3269	0.557	0.345		sample 34
Paratype, adult, male,	LM-FCEN 3270	0.530	0.320	0.197	sample 57
Paratype, adult, female,	LM-FCEN 3271	0.524	0.325	0.249	sample 57

Description. A medium, very subovate species of *Phelocyprideis*. Subovate in dorsal view. LV overlaps the RV around entire periphery. Anterior margin broadly rounded with apex well below mid-height. Anterodorsal slope long and gently arcuate; anteroventral slope shorter and strongly convex. Posterior margin more narrowly rounded. Dorsal margin umbonate with apex anterior of the mid-length. Dorsal cardinal angles not marked. Ventral margin very

gently orally incurved in both valves. Greatest length below mid-height; greatest height anterior of mid-length; greatest width medianly. LV larger than RV with conspicuous overlap around entire periphery. Surface smooth. Numerous circular pits mark the normal pore canals; the smaller being simple and the larger sieve-type. Hinge alternamerodont and oblique to the margin. The anterior terminal element of the LV is a long structure bearing ten large teeth, all of which extend beyond the edge of the hinge margin. The median element is absent. The posterior terminal element comprises some ten large, rectangular locules, separated by vertical walls and all negative with respect to the edge of the valve. CMS a curved row of four adjacent scars and a small V-shape frontal scar. There is no fulcral point. Sexually dimorphic with males more elongate and less umbonate than females.

Remarks. An extensive search of the pertinent literature has failed to review any taxon resembling this in shape or hingement with which the present species could be compared. It differs from *Cyamocytheridea felix* Bertels, 1973 from the Danian of Fortín General Roca, Río Negro Province, in its more subrounded shape, alternamerodont hinge (Bertels' species has holomerodont hingement) and overlap around the entire periphery. Echevarría (1987) has identified *Cyamocytheridea rossiae* from the Miocene of Tierra del Fuego, but it differs from *P. acardomesido* sp. nov. in shape and in its hinge in which each valve has either an all positive or an all negative elements. The genus *Ovocytheridea* Grekoff has some similarities in shape of the carapace with *Phelocyprideis* gen. nov., however the hingement is completely different.

Stratigraphical range. Danian of Cerro Azul, General Roca.

Subfamily EUCYTHERIDEINAE Puri, 1954

Genus EUCYTHERE Brady, 1866

Type species. *Eucythere declivis* (Norman, 1865) Brady 1868*a*

Eucythere dinetos sp. nov. Ceolin and Whatley

Figure 5M-Q

LSID. urn:lsid:zoobank.org:act:xxxxxxxxx

Derivation of name. Gr. *δινετος*, dinetos. Whorled around. With reference to the circular disposition of the ribs on the valve surface that somewhat resemble a whirlpool.

Type material. Holotype: adult valve, LM-FCEN 3272 (Fig. 5M); paratypes: LM-FCEN 3273-3276 (Figs 5N; 5O; 5P; 5Q).

Material. 18 specimens from samples 3 and 5; Maastrichtian; 16, 21, 23 and 26; Danian.

Diagnosis. A medium, subtriangular species of *Eucythere* with ornamentation composed by six concentric ribs about a subovate median area that decrease in strength towards margins. Dorsal margin very umbonate.

Dimensions. In mm:

		L	H	W	
Holotype, adult, female,	LM-FCEN 3272	0.503	0.503		sample 21
Paratype, juvenile, female,	LM-FCEN 3273	0.340	0.187		sample 16
Paratype, adult, female,	LM-FCEN 3274	0.373	0.216		sample 23
Paratype, adult, male,	LM-FCEN 3275	0.308	0.134		sample 21
Paratype, juvenile, female,	LM-FCEN 3276	0.392	0.218	0.191	sample 16

Description. Median, subtriangular in lateral view. Anterior margin with a bluntly pointed apex well below mid-height; long, gently arcuate anterodorsal slope and shorter, more convex anteroventral slope. Posterior margin bluntly pointed with ventral downturned apex. Dorsal margin convex and umbonate in anterior part and long, gently convex and straight, in posterior part. Ventral margin with broad oral inflexion. Greatest length ventrally; greatest height through umbo; greatest width medianly. Ornament of six irregularly concentric ribs about a subovate, median area that decrease in strength towards margins. The ribs are

approximately parallel to one another and to the margins. There is a distinct perturbation anteroventrally. The median area contains pores that are rather, irregularly distributed between the ribs, many of them are sieve-type, other (smaller) are simple pores. Sexual dimorphism not observed. Internal features not seen.

Remarks. The present species is very similar to *Eucythere circumcostata* Whatley and Coles, 1987 from the early Pliocene of ODP Leg 34 in its pattern of concentric ribs, but differs in the dorsal margin that is much more arcuate and declines abruptly towards the posteroventral region. The present species is also larger than *E. circumcostata*. It differ from *Eucythere danica* Colin, 1987 described from the Danian of Sénégal, Africa, in its dorsal margin and posterior caudal process being more elongate.

Stratigraphical range. Maastrichtian and Danian of Cerro Azul, General Roca.

Subfamily KRITHINAE Mandelstam, 1958

Genus KRITHE Brady, Crosskey and Robertson, 1874

Type species. *Krithe bartonensis* (Jones, 1857*a*)

Krithe crepidus sp. nov. Ceolin and Whatley

Figure 5R, 6A-C

LSID. urn:lsid:zoobank.org:act:xxxxxxxxx

Derivation of name. Gr. *κρεπιλος*, a boot or shoe. Referring to the fanciful similarity of this species to a Greek boot or shoe.

Type material. Holotype: one complete carapace LM-FCEN 3277 (Fig. 5R; 6C); paratypes: LM-FCEN 3278-3279 (Figs 6A; 6B).

Material. 21 specimens from samples 3 and 5; Maastrichtian, 16, 21, 23 and 26; Danian.

Diagnosis. A large, elongate, subrectangular species of *Krithe*, LV strongly overlapping the RV around entire periphery. In posterodorsal view, the indentations strongly resemble the open torpedo tubes of a submarine.

Dimensions. In mm:

	L	H	W	
Holotype, adult, LM-FCEN 3277	0.805	0.404	0.347	sample 23
Paratype, adult, LM-FCEN 3278	0.693	0.327		sample 5
Paratype, adult, LM-FCEN 3279	0.709	0.337		sample 3

Description. In lateral view, a large, essentially smooth, subrectangular species of *Krithe*. In dorsal view, subovate, but very parallel sided in posterior-half. In this view, a posterior indentation of the lamella is very clearly seen, as is the very strong overlap of the LV over RV. In right lateral view, this seems to occur around the entire periphery. Anterior margin rather, narrowly, but symmetrically rounded about the apex at mid-height. Posterior margin obliquely truncated and tightly rounded subventrally. Dorsal margin straight in anterior two-third, more arcuate in posterior third. Ventral margin gently sinuous about oral concavity, best seen in right valve. Greatest length below mid-height; greatest height in posterior third; greatest width medianly. Surface smooth. Internally all the elements of the hinge are smooth. Anterior radial pore canals not seen due to crystallization of the shell. CMS with the most dorsal adductor being large and 'U'-shaped, frontal scar a broad forward facing 'U' which embraces a single smaller scar.

Remarks. This species differs from *Krithe rocanum* Bertels, 1973 from the Danian of the Neuquén Basin, in its more convex dorsal margin and more rounded and blunter posteroventral margin. It differs from *Krithe nibelaensis* Dingle, 1981 from the Campanian of southeast Africa mainly in its more rounded posterior region and narrower anterior.

Stratigraphical range. Maastrichtian and Danian of Cerro Azul, General Roca.

Krithe sp.

Figure 6D

Material. One carapace from sample 21. Danian.

Dimensions. Adult carapace, LM-FCEN 3280, 0.672 (L), 0.338 (H).

Diagnosis. A large, subrectangular species in lateral view with surface covered with a very degraded reticulum. In dorsal view, the posterior indentation of the lamella is very clear. Anterior margin rounded; posterior margin obliquely truncate and subrounded ventrally. Dorsal margin weakly convex and ventral margin almost straight, with a small concavity in the oral position. LV overlaps the RV around the entire margin, but most pronouncedly anteriorly. Greatest height just behind mid-length. Internal features not seen.

Remarks: This species differs from *K. crepidus* sp. nov. in its more regularly convex dorsal margin. It is less strongly truncate posteriorly and the surface of the carapace is covered with a subdued ghost reticulation. Differs from *K. rocanum* Bertels, 1973, from the Danian of Fortín General Roca, Río Negro Province, in its ornamented surface.

Subfamily NEOCYTHERIDEIDINAE Puri, 1957

Genus COPYTUS Skogsberg, 1939

Type species. *Copytus caligula* Skogsberg, 1939

Copytus sp.

Figure 6E-F

Material. Eight specimens from samples 3, 5; Maastrichtian; 21, 23 and 45; Danian.

Dimensions. Adult carapace, LM-FCEN 3281, 0.649 (L), 0.275 (H).

Diagnosis. A medium, subelliptical species with smooth surface and with an obliquely rounded anterior end. Dorsal and ventral margins straight and posterior end symmetrically rounded.

Remarks. The present species is similar to *Copytus cretaceous* described by Echevarría (1986) from the Maastrichtian of Chubut, Argentina, but differs in its smaller size and slight ventral rim.

Family CYTHERURIDAE Müller, 1894

Subfamily CYTHEROPTERINAE Hanai, 1957

Genus CYTHEROPTERON Sars, 1866

Type species. *Cythereis latissimum* (Norman, 1865) Brady 1867

Cytheropteron hyperdictyon sp. nov. Ceolin and Whatley

Figure 6G-J

LSID. urn:lsid:zoobank.org:act:xxxxxxxxx

Derivation of name. Gr. *ὑπερ* beyond, above; plus *λικτύον* net. With reference to the very great strength and intensity of the reticulation of this species.

Type material. Holotype: LM-FCEN 3282 (Fig. 6G); paratypes: LM-FCEN 3283-3285 (Figs 6H; 6I; 6J).

Material. 45 specimens from samples 21, 26, 29, 31, 34, 36, 39 and 40; Danian.

Diagnosis. A strongly, but not extendedly, alate species of *Cytheropteron*, carapace subovate with a very strong reticulation that ranges in size from small circular anteriorly to much larger centrally. Sagittate in dorsal view.

Dimensions. In mm:

		L	H	W	
Holotype, adult,	LM-FCEN 3282	0.641	0. 358		sample 29

Paratype, adult,	LM-FCEN 3283	0.632	0.365		sample 29
Paratype, adult,	LM-FCEN 3284	0.635	0.362	0.436	sample 26
Paratype, adult,	LM-FCEN 3285	0.612	0.390		sample 26

Description. A medium sized ostracod, thick-shelled for the genus, subovate, caudate posteriorly and strongly alate in lateral and dorsal views. Sagittate in dorsal view. Anterior margin broadly rounded with apex below mid-height and anterodorsal slope more gently convex that anteroventrally. Posterior margin with apex at above mid-height and slightly "upturned". Posteroventral slope long and slightly concave, ventral slope shorter and more convex. Dorsal margin straight sloping posteriorly, not overhung. Ventral margin completely obscured in lateral view by the alar process. Greatest length above mid-height; greatest height and greatest width through apex of ala. Ornament very strongly reticulate across entire valve surface. Individual cells ranging in size from small circles anteriorly and much larger ones centrally. The muri are almost smooth to micro-corrugate and bear a few, seemingly simple pore canals. There is some preferential orientation of the muri parallel to the free margins, but not apparent elsewhere. The solae seem mostly to be blind, but some possibly bears sieve plates, as suggested by the internal view of these structures. Hinge very strongly antimerodont. The right valve has a dentate bar with seven strong teeth anteriorly, some of which seems to be secondarily dentate dorsally and a bar with eight teeth posteriorly, also secondarily dentate. The median element is strongly locellate. Inner lamella wide. Surface marked with deep pores. CMS a curved row of four with an oval single scar anteriorly.

Remarks. The present species has similarities with *Cytheropteron rocanum* Bertels, 1973 from the Danian of Fortín General Roca, mainly in the pattern of ornamentation, but differs greatly in shape in dorsal view that is subtriangular, while *C. rocanum* is subovate.

Stratigraphical range. Danian of Cerro Azul, General Roca.

Cytheropteron bidentinos sp. nov. Ceolin and Whatley

Figure 6K-M

LSID. urn:lsid:zoobank.org:act:xxxxxxxxx

Derivation of name. L. *bi*, two, *dentino*, of teeth. With reference to the tooth-like apex of the alar process.

Type material. Holotype: one valve, LM-FCEN 3286 (Figs 6K, L); paratype: LM-FCEN 3287 (Fig. 6M).

Material. 17 specimens from samples 16, 17 and 21. Danian.

Diagnosis. A profoundly alate species of *Cytheropteron* in which both leading and trailing edges of alae are marked by parallel ribs and apex by a double spine. Peripheral surface smooth, remainder punctate.

Dimensions. In mm:

	L	H	
Holotype, adult, LM-FCEN 3286	0.458	0.240	sample 21
Paratype, adult, LM-FCEN 3287	0.496	0.319	sample 16

Description. Small, subrhomboidal and strongly alate species of *Cytheropteron*. Anterior margin broadly rounded with small, rounded marginal denticles medianly on the peripheral extended flange. Apex below mid-height. Posterior margin caudate with blunted subdorsal apex; posteroventral slope straight becoming convex and keel-like posteroventrally. Dorsal margins somewhat sinuous medianly, obscured by an arcuate rib. Ventral margin biconvex, but mostly obscured in lateral view by ventral tumidity and alar process. The large alar process has on its leading edge, three parallel ribs between which and on the flanks of external members, single rows of puncta. These ribs terminate at the base of the alar spine. The trailing edge is shorter and stronger with six ribs and rows of puncta; the most anterior being the

strongest. These ribs terminate in a bi-cuspate resembling the gaping bill of a bird. The remainder of the carapace, except for the area around the free margins, is covered by mainly concentric rows of rounded pores; these are smallest distally and largest proximally. The pores are absent from the area of the closing and frontal muscles. An arcuate rib with two roots anteriorly and posteriorly cross the valve dorsally, just behind mid-length. Internal features not seen.

Remarks. This species should not be confused with *Cytheroteron dividentum* Hornibrook, 1952, a species with strong vertical ribs, which name is seemingly associated with the double-toothed terminal hinge element. Differs from *Cytheropteron inornatun* Brady and Robertson, 1872 in having a longer posterodorsal caudal process, in its more arcuate rib posterodorsally and in its surface being more densely punctate. It is also similar to *Cytheropteron* sp. 2914 Dingle, Lord and Boomer, 1990, from the Quaternary of SW Africa, in having the alar spine, but differs in the shape of the caudal process, in the anterior margin being narrower and in its ornamentation.

Stratigraphical range. Danian of Cerro Azul, General Roca.

Cytheropteron translimitares sp. nov. Ceolin and Whatley

Figure 6N-R

LSID. urn:Isid:zoobank.org:act:xxxxxxxxx

Derivation of name. L. *trans*, across; plus *limitares*, boundary. With reference to the occurrence of this species on either side of the Maastrichtian-Danian boundary.

Type material. Holotype: one complete carapace, LM-FCEN 3288 (Figs 6N, Q); paratypes: LM-FCEN 3289-3291 (Figs 6O; 6P; 6R).

Material. 37 specimens from samples 1, 5 and 10; Maastrichtian; 16, 17, 21, 23, 26, 31 and 50; Danian.

Diagnosis. A subovate, reticulopunctate specimen with a short caudal process and strongly convex dorsal margin. Short alar process with ventrolateral ribs that are clearly seen ventrally.

Dimensions. In mm:

	L	H	W	
Holotype, adult, LM-FCEN 3288	0.368	0.244	0.392	sample 21
Paratype, adult, LM-FCEN 3289	0.403	0.221		sample 16
Paratype, adult, LM-FCEN 3290	0.612	0.390		sample 26
Paratype, adult, LM-FCEN 3291	0.410	0.340	0.189	sample 26

Description. Small, subovate, alate species of *Cytheropteron* with mainly punctate and, in part, reticulate ornament. Anterior margin well-rounded with apex at about mid-height. Posterior margin much more narrowly and asymmetrically rounded, with long, straight to gently convex posterior dorsal slope and shorter, more convex posteroventral. Dorsal margin strongly convex about an apex a little anterior of mid-length. Ventral margin with a very slight oral concavity in front of mid-length, only partially obscured in lateral view. Greatest length below mid-height; greatest height through dorsal apex; greatest width in posterior one-third. Puncta small peripherally and increasing in size somewhat towards to the centre and oriented parallel to margins. Puncta peripherally, but especially ventrally they occur in single rows associated with ventrolateral and ventral ribs. There is a slight marginal rim anteriorly and posteriorly. The alar process is defined by a number of ribs along the ventral surface and the ventrolateral rib. Intercostal areas smooth, except where valve has been abraded, resulting in a coarse, rough surface. Many of the puncta bear sieve-type pores. Some small simple pores occur between puncta. Internally, the hinge is antimerodont and in the right valve, the median element is a long, denticulate bar widest anteriorly. The terminal elements are strongly elevated with four or five teeth anteriorly and three or four posteriorly. CMS not seen. Calcified inner lamella wide around free margins.

Remarks. Differs from *Cytheropteron inops* Bertels, 1969*a* from the upper Cretaceous of Huantrai-co, Neuquén Province, in being more rounded, in its punctate surface and the presence of a ventrolateral rib that defines the alar process.

Stratigraphical range. Maastrichtian and Danian of Cerro Azul, General Roca.

Cytheropteron sp.

Figure 7A

Material. One specimen from sample 5. Maastrichtian.

Dimensions. Adult carapace, LM-FCEN 3292, 0.445 (L), 0.265 (H).

Diagnosis. A subovate, strongly alate species of *Cytheropteron* with main ornament of circular puncta and a number of small ribs that extend from a posterodorsal position onto the ventral surface under the alar process. Caudal process smooth, blunt at mid-height. Anterior apex also at mid-height.

Remarks. *Cytheropteron* sp. has similarities with *Cytheropteron crassipinatum* Whatley and Masson, 1980. It differs, however, in its alar process being more acuminate, dorsal margin more convex and in the ornamentation being circulo-punctate.

Genus AVERSOVALVA Hornibrook, 1952

Type species. Aversovalva aurea (Hornibrook, 1952) Crane, 1965

Aversovalva glochinos sp. nov. Ceolin and Whatley

Figure 7B-D

LSID. urn:lsid:zoobank.org:act:xxxxxxxxx

Derivation of name. Gr. *γλοχινος* glochinos, point of an arrow. With reference to the aspect of an arrowhead that this species presents in dorsal view.

Type material. Holotype: one valve, LM-FCEN 3293 (Fig. 7B) (lost); paratypes: LM-FCEN 3294-3295 (Figs 7C; 7D).

Material. Nine specimens from samples 3; Maastrichtian; 16 and 21; Danian.

Diagnosis. An elongate, subovate species of *Aversovalva* with a strong alar process bearing a reticulum, which is medianly subcircular, but which becomes extended and elongate-ovate on the alar process.

Dimensions. In mm:

		L	H	W	
Holotype, adult,	LM-FCEN 3293 (lost)	0.378	0.218		sample 22
Paratype, adult,	LM-FCEN 3294	0.384	0.265		sample 16
Paratype, adult,	LM-FCEN 3295	0.385	0.235	0.388	sample 3

Description. An elongate, subovate species with a very strong alar process in lateral view. Strongly sagittate in dorsal view. Anterior margin rounded but "downturned", with apex below mid-height. Posterior margin bluntly caudate at mid-height. Dorsal margin convex anteriorly and straight to the posterior cardinal angle. Ventral margin with pronounced oral incurvature. Ornament virtually smooth in anterior and posterior areas, elsewhere reticulate with large oval cells and low broad muri. Oval cells centrally become "stretched" on alar process. Alar process very strong with long leading edge, with three parallel ribs. Apex bluntly pointed posteroventrally and short trailing edge defined by three small ribs and intervening locules. Internal features as for genus.

Remarks. Differs from *Cytheropteron* (*Aversovalva*) *westaustraliense* Neale, 1975 from the Gingin Chalk (Santonian) of Western Australia, in the posterior caudal process being less abrupt and in the alar process more rounded. It also differs in reticulation pattern with better developed cells.

Stratigraphical range. Maastrichtian and Danian of Cerro Azul, General Roca.

Genus PEDICYTHERE Eagar, 1965

Type species. *Pedicythere tessae* Eagar, 1965

Pedicythere sp.

Figure 7E

Material. Three specimens from sample 5. Maastrichtian.

Dimensions: Adult valve, LM-FCEN 3296, 0.407 (L), 0.227 (H).

Description. *Pedicythere* with typical upturned blunt subdorsal caudal process. Alar process polygonal in base and conical at termination. Anterior margin deeply indented dorsally and with short radiate riblets in the ventral part. Surface smooth.

Remarks. The present species differs from *Pedicythere australis* Neale, 1975 from the Santonian of Gingin, Australia, in its more regular dorsal margin with "upturned"caudal process, which in Neale's species is straight; and in the posterior region that is slightly concave toward the caudal process, the opposite of *P. australis* that is convex.

Genus SEMICYTHERURA Wagner 1957

Type species. *Cythere nigrescens* Baird, 1838

Semicytherura argentinensis (Bertels, 1974) comb. nov.

Figure 7F

1974 *Cytherura argentinensis* Bertels, p. 391, pl. 2, fig. 9a–b.

Material. One specimen from sample 16. Danian.

Dimensions. Adult carapace, LM-FCEN 3297, 0.328 (L), 0.145 (H).

Remarks. On the basis of its external character alone, this species is clearly *Semicytherura*.

Stratigraphical range. Maastrichtian of Fortín General Roca (Bertels 1974) and Danian of Cerro Azul, General Roca.

Semicytherura sp. 1

Figure 7G

Material. Three specimens from samples 31, 39 and 50. Danian.

Dimensions. Adult carapace, LM-FCEN 3298, 0.310 (L), 0.139 (H).

Description. A very small species of *Semicytherura*, subovate, elongate and bluntly caudate in lateral view with straight dorsal margin. Anterior apex well-below mid-height; posterior apex at about mid-height. Marginal rim and posteroventral rib strongly developed. Anterior part with large reticulum of various shapes, posterior part with smaller, circular reticulum.

Remarks. This seems certainly to be a new species but is left *nomina aperta* due to paucity of material.

Semicytherura sp. 2

Figure 7H

Material. One specimen from sample 16. Danian.

Dimensions. Adult carapace, LM-FCEN 3299, 0.361 (L), 0.201 (H).

Description. Subovate *Semicytherura* with gently convex dorsal margin, caudal process above mid-height and anterior margin with apex at mid-height. Dorsal and ventrolateral ribs prominent and ornament reticulate with longitudinal muri dominant. Notable concavity above posteroventral rib and entirely below mid-height.

Remarks. This species differs from *Semicytherura* sp.1 of this study, mainly in its more rounded and less elongate shape and in the nature of reticulation and without strong ribs on the surface.

Semicytherura sp. 3

Figure 7I

Material. Seven specimens from samples 3, Maastrichtian; 16, 21, 39 and 53, Danian.

Dimensions. Adult carapace, LM-FCEN 3300, 0.361 (L), 0.177 (H).

Description. An elongate, subtriangular carapace in lateral view, with well-rounded anterior margin with apex below mid-height. Posterior margin very strongly caudate with apex at about mid-height. Dorsal margin obscured by crest-like rib. Ventral margin in part obscured by ornament, but biconvex about a considerable oral invagination. Several strong, but narrow ribs cross the lateral surface. Intercostal areas reticulopunctate with mainly circular cells.

Remarks. The present species differs from *Semicytherura cretae* Neale, 1975 from the Santonian of Gingin, Western Australia, in its well-developed ornamentation with ribs and intercostal cells and also with more elongate caudal process.

Semicytherura? sp.

Figure 7J

Material. One specimen from sample 21. Danian.

Dimensions. Adult valve, LM-FCEN 3301, 0.327 (L), 0.148 (H).

Description. Elongate, subrectangular with subtruncated anterior margin, with apex well-below mid-height. Posterior margin caudate with almost subventral apex. A series of large, very broad, interconnected, ribs cross the surface and the periphery, between which is a circular reticulum.

Remarks. Differs from other *Semicytherura* species in this study mainly in the posterior caudal process and in the presence of thick ribs around the entire margins and the valve surface. It is only tentatively included in this genus.

Genus EUCYTHERURA Müller, 1894

Type species. *Cythere complexa* Brady, 1866

Eucytherura stibaros sp. nov. Ceolin and Whatley

Figure 7K-O

LSID. urn:lsid:zoobank.org:act:xxxxxxxxx

Derivation of name: Gr. *δτιβαροϛ* strong. With reference to the strongly ornate carapace of this species.

Type material. Holotype: one complete carapace, LM-FCEN 3302 (Fig. 7K); paratypes: LM-FCEN 3303-3304 (Figs 7L, M, N; 7O).

Material. 15 specimens from samples 5 and 12; Maastrichtian; 16, 21, 23, 26 and 39; Danian.

Diagnosis. Subquadrate species of *Eucytherura* with hemispherical eye tubercle. Rather, subdued and dispersed subcentral tubercle, which is strongly reticulate as is the rest of the carapace. Dorsal rib crest-like posteriorly. Muri slightly microstriate, solae often bi, tri or quadrifoil and often bearing sieve plates. Very few pore conuli on muri.

Dimensions. In mm:

		L	H	W	
Holotype, adult,	LM-FCEN 3302	0.330	0.194		sample 3
Paratype, adult,	LM-FCEN 3303	0.358	0.206	0.187	sample 3
Paratype, adult,	LM-FCEN 3304	0.315	0.196		sample 3

Description. A very small, subquadrate, thick-shelled and heavily ornate species. Anterior margin broadly rounded with apex below mid-height. Anterodorsal slope long and gently convex; anteroventral slope shorter and more convex with five marginal denticles. Posterior margin very bluntly terminated with apex above mid-height. Posterodorsal slope concavo-convex; posteroventral straight, interrupted by four marginal denticles. Dorsal margin straight,

obscured posteriorly by dorsal rib, sloping gently posteriorly. Ventral margin biconvex about a shallow oral concavity, obscured in lateral view by ventral ribs. In dorsal view, subovate with a central constriction and end margins laterally compressed. Hemispherical eye tubercle very prominent. Greatest length above mid-height, greatest height through eye tubercle, greatest width at posterior one-quarter. Ornament of very coarse reticulation delimited by broad microtuberculate muri that are preferentially vertically orientated in anterior half and near the posterior margin, but more irregular elsewhere. Muri with rare, usually conjunctive, simple pores; solae with depressed sieve plates, with irregular, often trefoil or bifid outlines. The valve surface drops deeply onto the caudal area, which is largely smooth. A similar smooth area occurs along the anterior margin, separated below mid-height into cells by the muri whose distal extension form the anteroventral marginal denticles. The posterior termination of the ventrolateral rib is almost spinose and is subalate. Hinge strongly antimerodont with a well-defined, vertically orientated denticulations in a median element of the left valve. Calcified inner lamella wide specially at the ends. CMS not seen.

Remarks. Differs from *Eucytherura* sp. 2 of this study in the nature of its reticulation with sieve plates, its less truncate caudal process and in the well-developed hemispherical eye tubercle. Differs from *Eucytherura* sp.1 also of this study, in the absence of a subcentral tubercle, in the anteroventral rim being less inflated, in a bluntly reticulation pattern, and in the position of the eye tubercle.

Stratigraphical range. Maastrichtian and Danian of Cerro Azul, General Roca.

Eucytherura sp. 1

Figure 7P

Material. Three specimens from samples 21 and 23. Danian.

Dimensions. Adult carapace, LM-FCEN 3305 (lost), 0.306 (L), 0.168 (H).

Diagnosis. A very small species, subquadrate in lateral view with very heavily reticular ornament with strong muri, which intersect at right angle medianly, more irregularly elsewhere. Eye tubercle large, prominent; subcentral tubercle subcircular and strongly buttressed. Caudal process blunt and slightly downturned. Solae with trefoil to quadrifoil outlines, others polygonal. Large, simple pore conuli at mural intersections and sieve plates in solae together with incipient celation. Strong anteromarginal rim that passes into a strong ventrolateral rib that terminates in a subalar process.

Remarks. This species differs from *Eucytherura antipodum* Neale, 1975 (as figured on his page 111, fig. 1) from the Santonian of Australia, in its trefoil and quadrifoil reticulation pattern, in the absence of a posterodorsal rib and in a more subrectangular caudal process. It also differs from *Eucytherura cameloides* McKenzie, Reyment and Reyment, 1993, from the Eocene of Australia, in its less costellate surface, less pronounced eye tubercle and its ornamented caudal process.

Eucytherura sp. 2

Figure 7Q-R

Material. One valve from sample 3. Maastrichtian.

Dimensions. Adult valve, LM-FCEN 3306, 0.336 (L), 0.198 (H).

Diagnosis. A very small and subquadrate species of *Eucytherura* with distinctly subtruncate anterodorsal margin. Surface coarsely ornamented with well-developed muri, with scarce conjunctive simple pores, and solae of very variable shape, depressed sieve plates, with irregular, often simple, trefoil or bifid outlines. Short posterior caudal process and with a ventrolateral rib and non-prominent subalar process.

Remarks. Differs from *Eucytherura stibaros* sp. nov. of the present study in the shape of its anterior and posterior margins and the less well-developed eye tubercle, which is obscured by surface ornamentation, and more peripherally positioned than in *E. stibaros*.

Genus HEMIPARACYTHERIDEA Herrig, 1963

Type species. *Hemiparacytheridea oculta* (Herrig, 1963) Grüendel, 1975

Hemiparacytheridea sp.

Figure 8A

Material. Two specimens from samples 5 and 14. Maastrichtian.

Dimensions. Adult valve, LM-FCEN 3307 (lost), 0.248 (L), 0.125 (H).

Description. Elongate, subrectangular, well-rounded anterior margin with apex at mid-height. Posterior margin caudate with apex above mid-height. Dorsal margin straight to slightly sinuous and strongly inclined to posterior. Ventral margin with a strong oral concavity. Surface with four prominent elevations; one just behind an ocular position, another posteroventrolaterally and another posterodorsally. The fourth is the circular subcentral tubercle which is connected to the posteroventral tubercle by a pronounced sinuous ridge. There is a deep depressed area between this and the posterior margin which is compressed. Numerous large pore canals, all of with seem to be sieve-type.

Remarks. This species differs from *Hemiparacytheridea hemingwayi* Neale, 1975 of Guzel (2012) from the Cretaceous of Western Australia, by its shorter ventrolateral rib, well-developed subcentral tubercle and more distinct median vertical sulcus. It also differs from *Hemiparacytheridea ewingensis* Dingle, 1984 from the early-middle Albian of South Africa, in its less well-developed ornament, in lacking a caudal process and less well-developed antero-marginal rim and posterodorsal inflation.

Genus HEMINGWAYELLA Neale, 1975

Type species. *Hemingwayella* (*Parahemingwayella*) *barkeri* Dingle, 1984

Hemingwayella verrucosus sp. nov. Ceolin and Whatley

Figure 8B-D

LSID. urn:Isid:zoobank.org:act:xxxxxxxxx

Derivation of name. L. *verrucosus*, full of warts, many warts. With reference to the many wart-like protuberances on the surface of this species.

Type material. Holotype: adult valve, LM-FCEN 3308 (Fig. 8B) (lost); paratypes: LM-FCEN 3309-3310 (Figs 8C; 8D).

Material. Four specimens from sample 21. Danian.

Diagnosis. A typical species of *Hemingwayella*, except for its considerably strong reticulation, in which posteriorly the muri are preferentially elongated subhorizontally and interacting with vertical muri forming an open network. Anteriorly, in the dorsal two-thirds, the vertical muri are strongest. There are several parallel ribs on the ventral margin.

Dimensions. In mm:

		L	H	
Holotype, adult,	LM-FCEN 3308 (lost)	0. 429	0.171	sample 21
Paratype, juvenile,	LM-FCEN 3309	0.374	0.164	sample 21
Paratype, adult,	LM-FCEN 3310	0.382	0.134	sample 21

Description. Small, very elongate subrectangular, somewhat pointed posteriorly in lateral view. Subhexagonal and alate in dorsal view with compressed ends. Anterior margin broadly rounded with apex below mid-height; anteroventral part more convex and dentate, anterodorsal less convex without denticles. Posterior margin subcaudate and bluntly pointed a little above mid-height. Dorsal margin straight to gently sinuous only overhung by the dorsal

rib posterodorsally. Ventral margin notably sinuous. Greatest length a little above mid-height; greatest height anterior of eye tubercle; greatest width at one-fifth posteriorly. Ornament reticulocostate, strongly developed. The eye tubercle is proportionally very large, subcircular and essentially smooth. The subcentral tubercle is very large, rimmed by a riblet and bearing prominently the four elongate adductor scars clearly visible in external view. From an elevated ornate posterodorsal eminence, a short vertical rib extends down to about mid-height and a dorsal rib extends sinuously to a mid-dorsal prominence. Anterior of the subcentral tubercle, the muri of the reticulum are exaggerated in the vertical plane, but terminate in the sinuous ventrolateral rib that extends from the anterocentral margin, circumvents the subcentral tubercle ventrally and forms a distinct edge to the lateral surface before terminating posteroventrally in a sub-alar process. Beneath it, on the ventral surface, are a number of parallel ribs. There is a median sulcus between the eye tubercle and the median prominence and ending posterior of this structure. The reticulation comprises large angular reticular cells, ranging from quadrate to rectangular to polygonal, with the preferential orientation of the muri being horizontally. The extreme posterior surface is less ornamented, almost smooth. The surface is atuberculate although some small pore conuli open virtually flush with the surface.

Remarks. Differs from *Hemingwayella* sp. Guzel, 2012 in its less strongly developed pattern of reticulation and the absence of a hinge ear in LV. It also differs from the type-species *Hemingwayella pumilio* (Brady, 1880) in its more reticulate surface and its rounded caudal process. *H. verrucosus* is also higher. The present species exhibits similarities with *H. ornata* Bate, 1972 described from the Santonian of Gingin, Western Australia, but differs in the well-developed and reticulate caudal process and in its well-defined reticulation pattern. Differs from *H.* (*Parahemingwayella*) *barkeri* Dingle, 1984 from the early-middle Albian of South Africa, in having a discontinuous and less developed diagonal longitudinal rib to the posterior

cardinal angle and by absence of punctate regions. Differs from *Hemingwayella rionegrina* (Bertels, 1974) in being less inflated in dorsal view, in the absence of three strong horizontal ribs, in its spinose anterior and posterior margins.

Stratigraphical range. Danian of Cerro Azul, General Roca.

Family LOXOCONCHIDAE Sars, 1925

Genus HEINIA Van den Bold, 1985

Type species. *Heinia howei* Van den Bold, 1985

Heinia prostratopleuricos sp. nov. Ceolin and Whatley

Figure 8E-H

LSID. urn:Isid:zoobank.org:act:xxxxxxxxx

Derivation of name. Gr. *προστατος*, prostratos, to be laid flat; plus *πλεύικος*, plerikos, of the rib. With reference to the fact that the ribs of this species resemble a recumbent "U".

Type material. Holotype: one carapace, LM-FCEN 3400 (Fig. 8E); paratypes: LM-FCEN 3401-3402 (Figs 8F, G; 8H).

Material. Five specimens from sample 21. Danian.

Diagnosis. A small, elongate species of *Heinia* with surface ornament comprising a series of seven individual recumbent "U"-shaped ribs that do not achieve the anterior margin or posterior end. LV overlaps the RV.

Dimensions. In mm:

	L	H	W	
Holotype, adult, LM-FCEN 3400	0. 386	0.185	0.132	sample 21
Paratype, adult, LM-FCEN 3401	0.352	0.170	0.125	sample 21
Paratype, adult, LM-FCEN 3402	0.398	0.182		sample 21

Description. A small, elongate and subtriangular carapace in lateral view. Subovate with pointed posterior end in dorsal view. Anterior margin well rounded with apex at mid-height and with well-developed marginal rim. Posterior margin bluntly pointed with almost subventral apex. Dorsal margin anteriorly convex, posterior straight and steeply inclined to the posterior. Ventral margin gently concave about an anteromedian oral incurvature. The marginal rim extends around the posteroventral and dorsal margins. LV slightly larger than RV with some dorsal, anterior and posterodorsal overlap. Greatest length below mid-height; greatest height at anteriorly one-third; greatest width at posterior one-third. Ornament reticulocostate. A series of seven ribs extend across the carapace from individual origin, parallel to one another and do not achieve the dorsal or ventral margins. Mid-posterolaterally, they bend round and then extend anteriorly, terminating against the smooth anteromarginal area. They resemble a series of recumbent 'U'-shapes, folded on the posterior side and concave towards the anterior. The intercostal areas are reticulate as is the wide area embraced by the recumbent 'U'. The muri of the ribs and those that defines the reticulation are perforated by pores that seem to be simple. Calcified inner lamella very wide anteriorly. CMS with adductors in a row of four and a 'U'-shaped frontal scar anterior of the second and third adductors, with two mandibular scars ventrally. Hinge gongylodont with, in the RV, the anterior socket enclosing a stepped, strongly elevated tridentine boss, a smooth anteromedian groove and single socket enclosed by a boss-like tooth posteriorly and a smooth ridge tooth dorsally and anteriorly.

Remarks. While the shape and outline of this species resemples that of other, younger members of the genus, its ornament is very different. It seem to be the oldest known species of *Heinia* by some considerable degree.

Stratigraphical range. Danian of Cerro Azul, General Roca.

Genus LOXOCONCHA Sars, 1866

Type species. *Cythere impressa* Baird, 1850

Loxoconcha sp. aff. *Loxoconcha cretacea* Alexander, 1936

Figure 8I

Material. One adult valve from sample 19. Danian.

Dimensions. Adult valve, LM-FCEN 3403, 0.425 (L), 0.226 (H).

Diagnosis. A reticulocostate species of *Loxoconcha* in which the lateral surface is dominated by ribs that, in the dorsal half of the valve are convex upwards, but in the ventral half of the valve strongly concave. Intercostal areas with large puncta between the ribs, although anteriorly and posteriorly they are crosscurrent. Anterior margin rounded but posterior caudate and upturned above mid-height.

Remarks. This species is very similar to *Loxoconcha cretacea* Alexander, 1936, from the Maastrichtian of Maryland. Due to the paucity of material and poor preservation, it became difficult to confirm the diagnostic characters of *L. cretacea*. There are subtle differences in the dorsal margin, being more elongate than Alexander's species and in its less acuminate caudal process.

Genus PALMOCONCHA Swain & Gilby, 1974

Type species. *Palmoconcha laevimarginata* Swain and Gilby, 1974

Palmoconcha similis (Bertels, 1973) comb. nov.

Figure 8J

1973 *Loxoconcha similis* Bertels, p. 327, pl. 5, figs. 5a-b.

Material. 547 specimens from samples 21, 26, 29, 31, 34, 36, 39, 40, 50, 53, 55 and 57. Danian.

Dimensions. Adult carapace, LM-FCEN 3404, 0.456 (L), 0.258 (H).

Remarks. This is clearly *Palmoconcha*, not *Loxoconcha* on the basis of shape and outline of the carapace.

Stratigraphical range. Danian of Fortín General Roca, Río Negro (Bertels 1973); Cerro Azul, General Roca.

Genus SAGMATOCYTHERE Athersuch, 1976

Type species. *Sagmatocythere napoliana* (Puri, 1963) Athersuch, 1976

Sagmatocythere? sp. 1

Figure 8K

Material. Four specimens from sample 5. Maastrichtian.

Dimensions. Adult valve, LM-FCEN 3405, 0.410 (L), 0.210 (H).

Description. Subrectangular to elongate, subromboidal in LV; more subrectangular in RV in lateral view. Anterior margin broadly rounded with apex below mid-height, posterior margin more narrowly rounded with apex well above mid-height. Dorsal margin straight, ventral margin with shallow oral incurvature and well-developed posteroventral keel. Ornament reticulocostate with large scallop and other shaped cells. Strong ventrolateral ridge in a form of three ribs which define the ventral edge of the lateral surface and which anteroventrally, inclines upwards through 90° into a single rib, which reaches the dorsal margin just anterior of the eye tubercle. A distinct lateral sulcus extends obliquely anteroventrally from the eye tubercle to about mid-height. Posteroventrally, especially in the RV, the ventrolateral rib becomes subalate. Marginal rim absent. Sexual dimorphism well-developed with males longer and proportionally less high than females.

Remarks. This species is placed in *Sagmatocythere*, as being the most appropriate genus in the Loxoconchidae to which the gongylodont hinge requires its placement.

Sagmatocythere? sp. 2

Figure 8L

Material. Three specimens from samples 29 and 34. Danian.

Dimensions. Adult valve, LM-FCEN 3406, 0.353 (L), 0.166 (H).

Diagnosis. Elongate, subrectangular, rounded anterior margin, posterior margin bluntly pointed at mid-height. Dorsal margin straight to sinuous, sloping posteriorly. Ventral margin biconvex about oral concavity. Ornament of ribs and reticulae. A strong, smooth peripheral marginal rim surrounds the free margin. A strongly anastomosing and ramifying rib extends antero-ventrally from the eye tubercle and is composed of large muri. There is a well-developed ventrolateral rib and a posterodorsal cluster of ribs making an eminence in that position, immediately ventral to which is an excavated area. The median sulcus and all other elements of the carapace are strongly reticulated.

Remarks. This species is tentatively placed in *Sagmatocythere* due to the fact that it shares some external characteristic with the referred genus. This matter will be better resolved on the acquisition of open valves. The appearance of the present species suggest it is male.

Incertae sedis

Loxoconcha (s.l.) *posterocosta* sp. nov. Ceolin and Whatley

Figure 8M-R

LSID. urn:lsid:zoobank.org:act:xxxxxxxxx

Derivation of name. L. *postero*, the back, behind; plus *costa*, a rib. With reference to the obvious single rib in the posterior area, that is parallel to the posterior margin.

Type material. Holotype: one complete carapace, LM-FCEN 3407 (Figs 8M, Q); paratypes: LM-FCEN 3408-3411 (Figs 8N; 8O; 8P; 8R).

Material. 45 specimens from samples 34 and 36. Danian.

Diagnosis. An elongate subovate loxoconchid species, characterized by a smooth lateral surface apart from a curved rib extending down from the posterior part of the dorsal rib, and parallel to the posterior margin.

Dimensions. In mm:

		L	H	W	
Holotype, female	LM-FCEN 3407	0. 398	0.205	0.178	sample 34
Paratype, female,	LM-FCEN 3408	0.408	0.213	0.175	sample 34
Paratype, male,	LM-FCEN 3409	0.429	0.235	0.167	sample 34
Paratype, female,	LM-FCEN 3410	0.401	0.194		sample 34
Paratype, male,	LM-FCEN 3411	0.471	0.245	0.194	sample 34

Description. Subquadrate (female), subrectangular (male) in lateral view. In dorsal view, hastate with margins convergent anteriorly. Anterior margin very broadly rounded with apex just below mid-height. Posterior margin poorly rounded with apex at mid-height, posterodorsal slope concave and posteroventral slope strongly convex. Dorsal margin straight between well-marked dorsal cardinal angles. Ventral margin gently convex except for oral incurvature anteroventrally. Weak marginal rims occur in both valves and a pronounced arcuate rib extends from near the posterior termination of the dorsal rib in an arc to its posteroventral termination. Surface smooth in well-preserved specimens with numerous large pores spread around the surface. In male, the oral invagination is stronger than in females. Greatest length above mid-height; greatest height at anterior cardinal angle; greatest width one-third posteriorly. Internal features not seem. Sexual dimorphism with males more elongate and narrow than females.

Remarks. Differs from *Loxoconcha bullata* Hartmann, 1956, figured in Whatley *et al*. (1997) (pl. 7, figs. 16-17) by its much straighter dorsal margin and subrectangular shape and lacking ornamentation, apart from only a posterodorsal arcuate rib. Differs from *Palmoconcha similis* (Bertels, 1973) from the Danian of Fortín General Roca, Río Negro Province, in being more elongate and in its smooth surface. The main difference is observed in males, with more concave oral incurvature than in Bertels' species.

Stratigraphical range. Danian of Cerro Azul, General Roca.

Family PECTOCYTHERIDAE, Hanai 1957

Genus KEIJIA Teeter, 1975

Type species. *Keijia demissa* (Brady, 1868*b*) Teeter 1975

Keijia circulodictyon sp. nov. Ceolin and Whatley

Figure 9A-E

LSID. urn:lsid:zoobank.org:act:xxxxxxxxx

Derivation of the name. L. *circulus* round, circle. (from Gr. *kípkoς*) ; plus Gr. *δικτυον* dictyon, net. With reference to the rounded elements of the reticulum.

Type material. Holotype: one complete carapace, LM-FCEN 3412 (Figs 9A); paratypes: LM-FCEN 3413-3416 (Figs 9B; 9C; 9D; 9E).

Material. 104 specimens, mainly adults from sample 34 and 36, Danian.

Diagnosis. A strongly built species of *Keijia* with flattened marginal rim around free margins and centrally an elevated area of strong reticulation, with deep rounded cells bearing sieve plates and strong broad muri with micropunctate microornament.

Dimensions. In mm:

	L	H	W	
Holotype, female, LM-FCEN 3412	0.419	0.426	0.182	sample 34

Paratype, female,	LM-FCEN 3413	0.408	0.215	0.175	sample 34
Paratype, female,	LM-FCEN 3414	0.406	0.211		sample 34
Paratype, female,	LM-FCEN 3415	0.402	0.207	0.170	sample 34
Paratype, male,	LM-FCEN 3416	0.408	0.215	0.169	sample 34

Description. Small, elongate, subrectangular in lateral view, also subrectangular in dorsal view with very flared anterior margin. Anterior margin broadly rounded with a smooth, thin, narrow rim that extends onto the ventral margin. Apex just below mid-height. Posterior margin diagonally subtruncated with a distinct angle dorsally and more rounded ventrally. Dorsal margin straight sloping posteriorly. Ventral margin, medianly obscured by valve tumidity and ventrolateral rib, biconvex about oral concavity. Greatest length just below mid-height; greatest height at the anterior cardinal angle; greatest width equal between cardinal angles. LV larger than RV with strongest overlap dorsally and ventrally. Very strongly ornamented with large circular reticulae, bounded by very strong muri, which bear a secondary ornament and are irregularly punctate. Centrally and anteroventrally, extremly strong muri are developed and the larger, inflated dorsal and anterior ribs parallel to the margins becomes the ventrolateral rib, a less massive, but nevertheless strong structure that terminates with a large pore conulus above the posterior surface. Large sieve plates occur in some fossae and simple pores occur on the muri but are not abundant. In dorsal view, the great strength of the marginal rib is clearly demonstrated. Sexual dimorphism pronounced with males more elongate and less inflated than females.

Remarks. Differs from *Keijia kratistos* sp. nov. in the absence of ribs, in its subcentral tubercle, and also in the nature of the reticulation and in being more rounded. Differs from

Keijia flexuosa (Bertels, 1975*a*) in its anterior rim and in the pattern of reticulation, especially anteriorly.

Stratigraphical range. Danian of Cerro Azul, General Roca.

Keijia kratistos sp. nov. Ceolin and Whatley

Figure 9F-J

LSID. urn:lsid:zoobank.org:act:xxxxxxxxx

Derivation of name. Gr. *κρατιστος*, strongest. With reference to the fact that, with its particular ornament, this species probably has strongest carapace of the genus.

Type material. Holotype: one complete carapace, LM-FCEN 3417 (Fig. 9F); paratypes: LM-FCEN 3418-3421 (Figs 9G; 9H; 9I; 9J).

Material. 411 specimens from samples 19, 21, 23, 26, 29, 31, 34, 36, 39, 40, 50 and 53. Danian.

Diagnosis. A very strongly constructed species of *Keijia* with an elevated reticulate area, surrounded by a strong, smooth, boundary rim. A number of strong mural ribs and large reticular cells of varying shape.

Dimensions. In mm:

		L	H	W	
Holotype, female,	LM-FCEN 3417	0. 464	0.241	0.178	sample 34
Paratype, female,	LM-FCEN 3418	0.422	0.226	0.175	sample 21
Paratype, female,	LM-FCEN 3419	0.502	0.253		sample 21
Paratype, female,	LM-FCEN 3420	0.459	0.250	0.206	sample 21
Paratype, male,	LM-FCEN 3421	0.461	0. 249	0.183	sample 21

Description. In lateral view, a median, elongate, subrectangular species. Subovate in dorsal view. LV larger than RV with distinct overlap dorsally and posteriorly. Anterior margin broadly rounded with a distinct but weak marginal rim without denticles. Posterior margin truncate without notable angles of truncation. Dorsal margin anteriorly straight, sinuous in posterior part. Ventral margin bilobate about a shallow oral concavity. Greatest length at about mid-height; greatest height at anterior cardinal angle; greatest width at one-third posteriorly. Ornament of very strong reticulation and ribs. A marginal rib, parallel to the anterior margin and extending ventrolaterally, obscures the ventral margin and comes to a small spinose structure posteroventrally, before extending onto the dorsal margin and eventually to the dorsal margin as a smooth rim. At the posterior cardinal angle, it changes course through 45° to form the posterior border of the elevated area. The reticulum is very strong with large cells and strong muri, which vary in being either smooth or microtuberculate. From the vertical posterior rib, a strong rib extends to the large subcentral tubercle. Below the dorsal rib a number of strong parallel muri directed antero-ventrally, always terminate at the first cell that they encounter. Sexual dimorphism pronounced with males more elongate and narrow than females.

Remarks. This species is similar to *Keijia huantraicoensis* (Bertels 1969*a*) differing in its smaller size and in the reticulation pattern being less costate, but mainly in the posterodorsal rib, and in being more reticulate.

Stratigraphical range. Danian of Cerro Azul, General Roca.

Keijia flexuosa (Bertels 1975*a*) comb. nov.

Figure 9K-N

1975*a* *Cytheromorpha*? *flexuosa* Bertels, p. 128, pl. 6, figs. 13a-b

Type material. Specimen described by Bertels, housed in the collections of the Facultad de Ciencias Exactas y Naturales in holotype LM-FCEN 602, paratypes LM-FCEN 867-868; plus four paratypes this study LM-FCEN 3422-3425 (Figs 9K; 9L; 9M; 9N).

Material. 33 specimens from samples 1, 5, 8 and 12. Maastrichtian, plus the type and other material housed in the collections of the Facultad de Ciencias Exactas y Naturales, Universidad de Buenos Aires, Argentina.

Diagnosis. A very strong reticulate *Keijia* with a marked smooth rims dorsally and anterodorsally, which deteriorates ventrally by anastomosis and ramification. Extreme anterior surface demarcated by very weak muri as opposed to those forming the reticulation. Large pore conuli with large pores posteriorly.

Dimensions. In mm:

		L	H	W	
Paratype, adult,	LM-FCEN 3422	0.604	0.312		sample 5
Paratype, adult,	LM-FCEN 3423	0.591	0.303	0.248	sample 5
Paratype, adult,	LM-FCEN 3424	0.589	0.293		sample 5
Paratype, adult,	LM-FCEN 3425	0.649	0.305	0.257	sample 8

Description. Large, elongate, subrectangular in lateral view, ovate in dorsal view and strongly compressed anteriorly with prominent, rounded posterior margin and a strong dorsal rim. The width between the cardinal angles remains approximately the same. Non-sulcate. Anterior margin asymmetrically rounded with apex well below mid-height; anterodorsal slope long and gently convex; anteroventral slope shorter and more strongly convex. Posterior margin truncated with subventral apex. Dorsal margin medianly concave, posteriorly obscured by dorsal rim. Ventral margin biconvex about a distinct oral incurvature whose apex is behind mid-length. Greatest length below mid-height; greatest height through anterior cardinal angle; greatest width medianly. Ornament essentially reticulate. A strong dorsal rim extends

anteriorly before ramifying and anastomosing subparallel to the anterior margin and onto the ventral margin. This entire rim is smooth and divided by tubercles. There is a depressed area behind this rim anteriorly, separated into two large cells by weak, narrow muri. This depressed area extends onto the ventral margin. The remainder of the valve surface is a strong reticulum with broad, smooth muri, which in the anterior part show a diagonal preference from mid-dorsal towards the anteroventral region. Fossal cells mainly circular or oval and possibly floored by sieve plates. Relatively few, simple, small pore conuli occur conjunctively on the muri. Posteriorly there are several large conuli containing large pores. Hinge pentodont. Inner lamella broad anteriorly, narrower posteriorly. CMS not seen.

Remarks. Differs from *Keijia patagonica* Whatley *et al*., 1997 from the Recent of Patagonia, in its anterior depression, different pattern of reticulation and in the presence of two posteroventral spines. This species is a very early occurrence and possibly the earliest of the genus.

Stratigraphical range. Maastrichtian of Fortín General Roca (Bertels 1975*a*) and Cerro Azul, General Roca.

Keijia huantraicoensis (Bertels, 1969*a*) comb. nov.

Figure 9O

1969*a Munseyella huantraicoensis* Bertels, p. 284, pl. IV, fig. 1a.

Material. 199 specimens from samples 14; Maastrichtian; 16, 17, 19, 21, 23, 26, 29 and 31; Danian.

Dimensions. Adult carapace, LM-FCEN 3426, 0.521 (L), 0.280 (L).

Remarks. Differs from all the other *Keijia* species in this study by having stronger ribs, mainly on the dorsal and posterodorsal margin, with the secondary reticulation being less well-developed.

Stratigraphical range. Maastrichtian and Danian of Cerro Azul, General Roca and Danian of Huantrai-co, Neuquén Province (Bertels 1969*a*).

Genus PARAMUNSEYELLA Bate, 1972

Type species. *Paramunseyella austracretacea* Bate, 1972.

Paramunseyella epaphroditus sp. nov. Ceolin and Whatley

Figure 9P-R; 10A-B

LSID. urn:Isid:zoobank.org:act:xxxxxxxxx

Derivation of name. Gr. *επαφρολίτος*, lovely, charming. An apt name for such a species.

Type material. Holotype: one compete carapace LM-FCEN 3427 (Fig. 9P); paratypes: LM-FCEN 3428-3431 (Figs 9Q; 9R; 10A; 10B).

Material. 24 specimens from samples 3, 5 and 12. Maastrichtian.

Diagnosis. A small, subtriangular species with anterior hinge ear in LV, flattened marginal rim around margins and elevated central area made up of a series of mounds ribs and riblets. Interornamental surface smooth, but bearing deep slit-like pores.

Dimensions. In mm:

		L	H	W	
Holotype, adult,	LM-FCEN 3427	0. 341	0.256	0.125	sample 3
Paratype, adult,	LM-FCEN 3428	0.328	0.178		sample 5
Paratype, adult,	LM-FCEN 3429	0.327	0.175		sample 5
Paratype, adult,	LM-FCEN 3430	0.338	0.175		sample 5
Paratype, adult,	LM-FCEN 3431	0.341	0.254	0.123	sample 5

Description. A very small, thick-shelled species of *Paramunseyella*, elongate subrectangular in lateral view. Anterior margin broadly rounded with apex below mid-height, with anterodorsal slope longer and more gently convex than anteroventral. Posterior margin

subcaudate and bluntly pointed well below mid-height. Dorsal margin straight but appearing sinuous due to periodic overhang by valve surface. Ventral margin mainly overhung by ventrolateral and/or ventral rib. Greatest length below mid-height, greatest height through eye-tubercle. Greatest width medianly. Surface ornament rugged and dominated by large tubercles, ribs and very prominent pores. The subcentral tubercle is large and subovate. There is a large tubercle situated just below the dorsal margin, just behind mid-length and another associated with the termination of the ventrolateral rib. A short, but pronounced rib extends from the eye-tubercle subparalel to the anterior margin, terminating in a wide circular pit at mid-height. Above and below this pit are several large shallow reticulae. A narrow, short, but prominent rib extends from the dorsal margin, a little behind the large dorsal tubercle, obliquely across the valve to its termination above mid-height. The dorsal rib is large, passes above the eye tubercle and extends as a peripheral rim around the anterior margin and posterodorsally, and also peripherally around the posterior margin. The remainder of the valve and the tubercles bear deep keyhole-like (cribrose) pores, most of which seems to be sieve-type, and some of which contain short calcified rod-like structures resembling setae. Sexual dimorphism not observed. Calcified inner lamella very wide anteriorly with sinuous inner margins. Hinge pentodont with all elements smooth. CMS an oblique line of four small adductors; the antennal scar not seen.

Remarks. This species differs from *Paramunseyella* sp. 5 Guzel, 2012 from the late Maastrichtian Western of Australia in shape, mainly in straight dorsal and ventral margins and in less “downturned” posterior subcaudal process. Differs from Genus A sp. Neale, 1975, which is possibly *Paramunseyella*, in the marginal and ventrolateral rims being less well-developed.

Stratigraphical range. Maastrichtian of Cerro Azul, General Roca.

Genus MUNSEYELLA Van den Bold 1957*b*

Type species. *Toulminia hyalokystis* Munsey, 1953

Munseyella costaevermiculatus sp. nov. Ceolin and Whatley

Figure 10C-F

LSID. urn:Isid:zoobank.org:act:xxxxxxxxx

Derivation of name. L. *costae*; plus *vermiculatus*, worm. With reference to the many ribs on the surface of the species, many of which are notably worm-like.

Type material. Holotype: one valve, LM-FCEN 3432 (Fig. 10C); paratypes: LM-FCEN 3433-3435 (Figs 10D; 10E; 10F).

Material. Nine specimens from samples 1, 5, 12 and 14. Maastrichtian.

Diagnosis. Species of *Munseyella* with robust rather chaotic costate ornament comprising ribs in a quasi zig-zag pattern and lacking a strong intercostal reticulation.

Dimensions. In mm:

	L	H	W	
Holotype, adult, LM-FCEN 3432	0. 422	0.224	0.155	sample 5
Paratype, adult, LM-FCEN 3433	0.428	0.232		sample 14
Paratype, adult, LM-FCEN 3434	0.420	0.228	0.153	sample 14
Paratype, adult, LM-FCEN 3435	0.416	0.208		sample 5

Description. In lateral view a small, thick-shelled, elongate, subrectangular species of *Munseyella*. Subovate in dorsal view, strongly compressed anteriorly. LV slightly larger than RV with dorsal, anterodorsal and posterodorsal overlap. Anterior margin well rounded with apex below mid-height. Posterior margin more narrowly rounded with apex below mid-height. Greatest length below mid-height; greatest height at anterior cardinal angle; greatest width at one-third posteriorly. Ornament costate. A large, peripheral rib extends around and parallel to all the margins. Posterodorsally, it ramifies with a branch descending subvertically

where it branches again, one ramus extending to the marginal rim, another anteriorly where a second very convoluted branch, extends to a mid-anterocentral position, where another branch is directed posteroventrally to unite with the marginal rib mid-ventrally. Another short branch extends towards, but does not reach the anterior margin. Another rib from the dorsal margin, proceeds very regularly below the dorsal marginal rib and terminates short of the anterior margin. Intercostal areas showing some signs of very irregular ghost reticulation. Large sieve-type pore canals and simple pores occur mainly on the elevations, but also in depressions. Internal features not seen. Sexual dimorphism not observed.

Remarks. Differs from *Munseyella laurea* Bertels, 1973, from the Danian of Fortín General Roca, Río Negro Province, in the orientation of its ribs, in having a shorter posterodorsal rib without nodes, in having a more developed posteroventral rib and poorly developed second order reticulation. It also differs from *Munseyell*a sp. Szczechura, 2001, from the Eocene of Seymour Island, in its narrower ribs, well observed in mid-carapace, and in having stronger ribs on the anteromarginal and posteromarginal margins and in the absence of two dorsomedian nodes.

Stratigraphical range. Maastrichtian of Cerro Azul, General Roca.

Genus AMEGHINOCYTHERE Whatley, Morguilevsky, Chadwick and Ramos, 1997

Type species. *Ameghinocythere reticulata* Whatley, Morguilevsky, Chadwick and Ramos, 1997.

Ameghinocythere archaios sp. nov. Ceolin and Whatley

Figure 10G-K

LSID. urn:Isid:zoobank.org:act:xxxxxxxxx

Derivation of name. Gr. *αρχαιος* archaios, from the beginning. With reference to the fact that seems to be the very oldest species of the genus.

Type material. Holotype: One complete carapace, LM-FCEN 3436 (Figs 10G, J); paratypes: LM-FCEN 3437-3438 (Figs 10H, I; 10K).

Material. 13 specimens from sample 21. Danian.

Diagnosis. An early species of *Ameghinocythere* with well-rounded anterior margin, quadrate to rectangular or rhomboidal cells as opposed to rounded in the reticulum, with pore conuli posteriorly.

Dimensions. In mm:

		L	H	W	
Holotype adult,	LM-FCEN 3436	0.611	0.304	0.233	sample 21
Paratype, adult,	LM-FCEN 3437	0.60	0.296		sample 21
Paratype, adult,	LM-FCEN 3438	0.625	0.311		sample 21

Description. Median, very elongate in lateral view. Anterior margin broadly rounded with apex well below mid-height. Anterodorsal slope long and gently convex, anteroventral shorter and more strongly convex. Posterior margin obliquely quadrate with apex well below mid-height and defined by a rounded marginal denticle. Posterodorsal slope straight and oblique, posteroventral slope strongly convex. Dorsal margin straight, strongly inclined posteriorly. Ventral margin biconvex about a very gentle oral incurvature. LV larger that RV with conspicuous overlap posteriorly and anterodorsally. Greatest length below mid-height, greatest height through anterior cardinal angle. Ornament reticulate which, in lateral view, resembles rippling waves. The muri at the end margins orientated subparallel to those margins. Simple pore conuli occur conjunctively on the muri and as a small rounded perforated tubercles in the posterior area. No apparent eye tubercle. Dorsal marginal area smooth. Hinge pentodont. Calcified inner lamella very wide anteriorly and posteroventrally. CMS not seen.

Remarks. This is a poorly preserved species. It is an important and probably the earliest representative of this genus. Differs from *Ameghinocythere reticulata* Whatley *et al*., 1997 from the Recent of the South West Atlantic, in its less pronounced anterodorsal slope, more concave ventral margin and in its more pronounced overlap posteriorly and ventrally. It is similar to ?*Ameghinocythere* cff. *Cytheromorpha*? *flexuosa* Bertels, 1975*a* identified by Szczechura (2001) from the Eocene of the Seymour Island, Antarctica by the presence of posterior pore conuli, but differs in the presence of a dorsal marginal rim in the anterodorsal region being without the pronounced slope as observed in Szczechura's species.

Stratigraphical range. Danian of Cerro Azul, General Roca.

Family TRACHYLEBERIDIDAE Sylvester-Bradley, 1948

Subfamily TRACHYLEBERIDINAE Sylvester-Bradley, 1948

Genus ALEISOCYTHEREIS gen. nov. Ceolin and Whatley

LSID. urn:lsid:zoobank.org:act:xxxxxxxxx

Derivation of name. From the Gr. *αλεισον*, aleison, a cup; plus *κύθερεις*, *Cythereis*, a common ending for cytheroid Ostracoda. With reference to the fact that many of the reticular cells in this genus contain a cup-like structure, the rims of which abut against the muri and which covers the entire solae.

Type species. *Aleisocythereis polikothonus* gen. et sp. nov.

Diagnosis. Elongate subovate with rounded anterior margin and bluntly pointed posteriorly. Eye tubercle prominent. Anterior lacking the strong marginal rim, but posterior rim very strong. Ornament reticulate with large, circular, ovate cells, with distinct rims to cup-like structures filling the solae, which are blind and lacking sieve plates. Muri relatively weak, bearing small spines, mostly perforate and with simple canals and much more rarely sieve-type. Hinge hemiamphidont.

Description. As for the type species.

Included species. *Cythereis*? *incerta* Bertels, 1975*a* is possibly a member of this genus although the dorsal margin is rather straight. However, we have tentatively included it in *Aleisocythereis* until such times as we can examine in detail its type material in Buenos Aires.

Remarks. It differs from *Hysterocythereis* gen. nov. in its much more prominent eye tubercle, the nature of the reticulation and particularly the development of the tubercles on the reticulum. It also differs in the nature of the ribs on the anterior margin, and particularly the dorsal margin, and in its paramphidont hingement. It also differs from *Sthenarocythereis* gen. nov. which, while it has an eye tubercle of similar development, differs fundamentaly in the nature of the reticulum, the muri in *Sthenarocythereis* being much larger and the reticular cells almost anything but circular.

Aleisocythereis polikothonus sp. nov. Ceolin and Whatley

Figure 10L-R

LSID. urn:lsid:zoobank.org:act:xxxxxxxxx

Derivation of name. Gr. *πολί*, many, *κοθονύς*, a cup, many cups. With reference to the large number of small cup-like structures that fill the solae in this species.

Type species. Holotype: one valve LM-FCEN 3439 (Fig. 10L); paratypes: LM-FCEN 3440-3444 (Figs 10M, N; 10O; 10P; 10Q; 10R).

Material. 94 specimens from samples 1, 3, 5, 8, 10 and 12. Maastrichtian.

Diagnosis. Lacking major anterior marginal rim although the posterior marginal rim is very strong. Ornament reticulate with cup-like solae, rather, weak muri and numerous conjunctive spines, and some large conjunctive sieve-type structures. Subcentral tubercle small and strongly eroded by the reticulum.

Dimensions. In mm:

		L	H	W	
Holotype, female,	LM-FCEN 3439	0.677	0.380		sample 5
Paratype, female,	LM-FCEN 3440	0.703	0.396		sample 5
Paratype, male,	LM-FCEN 3441	0.828	0.411		sample 5
Paratype, adult, female,	LM-FCEN 3442	0.707	0.393		sample 5
Paratype, adult, female,	LM-FCEN 3443	0.689	0.378	0.329	sample 5
Paratype, adult, male,	LM-FCEN 3444	0.791	0.359	0.325	sample 5

Description. A median, thick-shelled and subovate-elongate carapace in lateral view. Anterior margin broadly and symmetrically rounded with apex at about mid height and ventrally denticulate. Posterior margin subcaudate with apex below mid-height; posteroventral slope convex, posterodorsal slope concave in part to almost straight. Dorsal margin straight and inclined somewhat to the posterior and slightly overhung by surface ornament in posterior part. Ventral margin with broad oral concavity. In dorsal view compressed at end margins, especially anteriorly. Greatest length below mid-height; greatest height at the anterior cardinal angle; greatest width in posterior one-third. Ornament of large reticulae and with relatively subdued muri. Many of the muri are filled with large, smooth cup-like structures that abut against their walls. Most of them have smooth bottoms. The muri bear rather short tubercles with rounded extremities, some of which are perforated, while others seem to be blind. There are less tubercles antero-centrally than elsewhere. In some muri, there are a group of three or four small tubercles in the middle of which there is a small sieve-type pore. Subcentral tubercle not prominent. Eye tubercle well-developed. In internal view, there is a wide calcified inner lamella; avestibulate. Hemiamphidont hinge and ocular sinus well-developed. Antennal muscle scar ‘U’-shaped, inserted in the deep projection of subcentral tubercle. Strong sexual dimorphism with males more elongate and lower than females.

Remarks. Differs from *Cythereis*? *excellens* Bertels, 1969*a*, from the Maastrichtian of Huantrai-co, by its sinuous dorsal margin with a posterodorsal convexity, in the subcircular muri and smooth cup-like structures in the reticulation.

Stratigraphical range. Maastrichtian of Cerro Azul, General Roca.

Genus APATOLEBERIS gen. nov. Ceolin and Whatley

LSID. urn:Isid:zoobank.org:act:xxxxxxxxx

Derivation of name. Gr. *απατολεβερις* apatoleberis, from *απατελος* deceptive, illusory; plus *λεβερις*, sloughed skin. With reference to the fact that one could be deceived into considering this genus to be *Trachyleberis* Brady.

Type species. Trachyleberis noviprinceps Bertels, 1975*a*.

Diagnosis. A subrectangular genus with anterior margin rounded and posterior margin bluntly pointed, with marginal rim anteriorly and posteriorly. Surface ornamented with tubercles bearing sieve-type pores widely distributed over the valve and varying in size. These are absent from the entire periphery. Subcentral tubercle and eye tubercle well-developed. Hinge holamphidont. Frontal scar in a 'V'-shaped.

Description. As for the type species.

Included species. *Trachyleberis princeps* Bertels, 1969*a*

Trachyleberis noviprinceps Bertels, 1975*a*

? *Trachyleberis schizospinosa* Dingle, 1981

Remarks. This genus is not in any way similar to other new trachyleberid genera erected in this study. It differs from *Trachyleberis* Brady in the absence of a ventrolateral ridge, presence of marginal rim, bluntly pointed posterior end and in the absence, in internal view, of a snap-knob structure ventrally. Differs from *Actinocythereis* Puri in the absence of three well-defined spinose ribs of which the ventrolateral is ascendant. Differs from *Cythereis* Jones

in the absence of the three longitudinal ribs and in the posterior not being acuminate. The most similar taxon we have encounted in our study search of the literature is *Trachyleberis schizospinosa* Dingle, 1981 from the Alphared Formation, Agulhas Bank of Port Elizabet, southeast South Africa from Maastrichtian III, Ostracoda assembladge 4b. The present species however, is more pointed with apex above mid-heigth and althougth the tubercles are situated similarly in the two taxa, and the present species lacks the distinct ventrolateral row of tubercles of the latter. The similarities are sufficient to suggest that Dingle's species, evidently not *Trachyleberis*, belongs to a genus very similar, if not the same as *Apatoleberis* gen. nov.

Apatoleberis noviprinceps (Bertels, 1975*a*) comb. nov.

Figure 11A-E

1975*a Trachyleberis noviprinceps* Bertels. p. 104, pl. 2, figs 1–6.

1975*b Cythereis*?, Bertels, p. 345, pl. 2, figs 3, a–b; 5.

Remarks. We consider it necessary to redescribe this species, since it is now the type of a new genus.

Type material. Specimen described by Bertels, housed in the collections of the Facultad de Ciencias Exactas y Naturales in Holotype LM-FCEN 731, paratypes LM-FCEN 732-735, 605; plus five paratypes this study LM-FCEN 3445-3449 (Figs 11A; 11B; 11C; 11D; 11E).

Material. 14 specimens from samples 3, 5 and 8; Maastrichtian; plus the type and other material of Bertels housed in Facultad of Ciencias Exactas y Naturales, Laboratory of Micropaleontology, Universidad of Buenos Aires, Argentina.

Diagnosis. As for genus.

Dimensions. In mm:

	L	H	W	
Paratype, female, LM-FCEN 3445	0.879	0.488	0.410	sample 5

Paratype, female,	LM-FCEN 3446	0.868	0.507		sample 5
Paratype, male,	LM-FCEN 3447	0.895	0.456		sample 5
Paratype, female,	LM-FCEN 3448	0.875	0.488		sample 5
Paratype, female,	LM-FCEN 3449	0.897	0.458	0.413	sample 5

Description. A large, subrectangular, elongate species of *Apatoleberis*. Subhexagonal in dorsal view with compressed ends. Anterior margin symmetrically rounded with apex at mid-height, with marginal denticles. Posterior margin bluntly pointed with apex above mid-height and with small tubercles. Dorsal margin straight, slightly overhung by a tubercle in posterodorsal margin. Ventral margin almost straight with more pronounced convexity posteroventrally. LV overlaps the RV mainly at the dorsal cardinal angles. Greatest length at mid-height, greatest height at one third anteriorly and greatest width at one third posteriorly. Ornamentation tuberculospinose. Anteromarginal region with an ocular rib that extends towards the anteroventral margin, where it disappears, to reappear on the posterior margin through to the posterodorsal tubercle. Surface covered with tubercles randomly disposed and of a number of different types. Most are small, with sieve-type pores on their summits but others, with narrower terminations, are simple. These bear smaller conuli on their summit. Two further tubercles, intermediate in size between the smaller and the larger tubercles, occur mid-dorsally and between the subcentral tubercle and the most ventral of the large tubercles respectively. These have tubercular stems and concave summits surrounded by small turrets. There are three large tubercles posteriorly, aligned vertically. Subcentral tubercle well defined and bearing a group of five smaller tubercles; it has a tubercular apophosis anteroventrally. Calcified inner lamella well-developed. Hinge holamphidont. CMS with a row of four adductors and a V'-shaped antennal scar. Sexual dimorphism well-developed with males

more elongate and narrow than females and with a conspicuous reticulation on the surface among the tubercles.

Remarks. *Apatoleberis noviprinceps* (Bertels, 1975*a*) differs from *A*. *princeps* (Bertels, 1969*a*) in the absence of reticulation and the presence of tubercles on the surface.

Stratigraphical range. Maastrichtian of Fortín General Roca, Río Negro (Bertels 1975 *a*, *b*) and Cerro Azul, General Roca.

Genus MIMICOCYTHEREIS gen. nov. Ceolin and Whatley

LSID. urn:Isid:zoobank.org:act:xxxxxxxxx

Derivation of name. From L. *mimicus* (via. Gr. *μίμικός* mimikos), separate from. With reference to the fact that although species belonging to this genus have been described as *Bradleya* Hornibrook, they were simply masquerading as that genus in that they differ fundamentally in a number of characters, especially in the CMS and belong to different families.

Type species. *Bradleya*? *attilai* Bertels, 1975*a*

Diagnosis. A genus of the Trachyleberididae, short, subrectangular, with strongly rounded anterior margin and less well rounded posterior. Dorsal margin of LV with strong anterior hinge ear, lacking in RV. Remainder of dorsal margin straight, not inclined posteriorly and largely obscured by valve surface. Small posterior hinge ear in LV, ventral margin convex with very slight oral concavity. End margins both dentate. Ornament reticulocostate and tuberculate to varying degrees, with pronounced dorsal, median and ventrolateral ribs, strength of which varies between species. Reticulum with angular cells near margins more circular medianly; simple conjunctive pore conuli, strong subcentral tubercle. Eye spot absent. Hinge holamphidont.

Description. As for the type species.

Included species. *Bradleya*? *patagonica* Bertels, 1975*a*

Bradleya? *attilai* Bertels, 1975*a*

Remarks. Bertels, in 1975*a*, described three species that she assigned to *Bradleya*?. Of these, *Bradleya*? *attilai* and *Bradleya*? *patagonica* are clearly congeneric, although they obviously do not belong to *Bradleya.* The third species *Bradleya*? *argentinensi*s is a distinctly different genus, possibly related to *Oertliella* Pokorny, because it lacks any traces of the three longitudinal ribs characteristic of *Mimicocythereis*. Although Bertels classified her "*Bradleya*?" species into the Hemicytheridae, they all possess a very evident strongly developed 'V'-shaped frontal scar characteristic of Trachyleberididae. Most modern authors include *Bradleya* within the family Thaerocytheridae Hazel; others, however, prefer to consider this group as a subfamily of Hemicytheridae Puri. In any case, *Mimicocythereis* remains a Trachyleberididae due to its frontal muscle scar. The genus differs from *Cythereis* in its holamphidont hinge. *Sthenarocythereis* gen. nov., differs in lacking strong horizontal ribs and in the hinge ear in the LV and in the nature of its reticulotuberculate ornament. *Aleisocythereis* gen. nov. lacks strong horizontal ribs, and also differs fundamentally in the nature of the reticulum.

Mimicocythereis attilai (Bertels, 1975*a*) comb. nov.

Figure 11F-J

1975*a Bradleya*? *attilai* Bertels; p. 114, pl. 5, figs 6–9.

Remarks. We consider it necessary to redescribe this species, because it has now become the type of a new genus.

Type material. Holotype: specimen described by Bertels, housed in Facultad de Ciencias Exactas y Naturales in Holotype LM-FCEN 821, paratypes LM-FCEN 822-827; plus four paratypes from this study LM-FCEN 3450-3453 (Figs 11F; 11G; 11H, I; 11J).

Material. 12 specimens from samples 3, 5 and 12; Maastrichtian; plus the type and other material of Bertels housed in the collections of the Facultad de Ciencias Exactas y Naturales, Universidad de Buenos Aires, Argentina.

Diagnosis. A medium, subquadrate species of *Mimicocythereis* with a strong hinge ear in LV and very strong reticulation.

Dimensions. In mm:

		L	H	W	
Paratype, female,	LM-FCEN 3450	0. 681	0.441		sample 5
Paratype, female,	LM-FCEN 3451	0.695	0.425		sample 5
Paratype, female,	LM-FCEN 3452	1.054	0.527		sample 5
Paratype, female,	LM-FCEN 3453	0.988	0.467	0.343	sample 16

Description. In lateral view, short, subquadrate in LV; subovate in RV. Subsaggitate in dorsal view with distinct median sulcus and with anterior margin laterally, but conically compressed. Anterior margin broadly but asymmetrically rounded with apex well below mid-height and long gently convex anterodorsal and shorter, more convex anteroventral slopes. There are small denticles in the mid-anterior region. Posterior margin subtruncate to poorly rounded with apex at about mid-height and with small tubercles. Dorsal margin straight, not strongly inclined posteriorly, and obscured in posterior half by dorsal rib. In LV, there is a smaller posterior hinge ear that is absent in RV. Ventral margin gently convex and with a very weak oral incurvature, strongly overhung posteroventrally by ventrolateral rib. Greatest length at about mid-height; greatest height through anterior hinge ear; greatest width in posterior one-third. Ornament reticulocostate. A strong marginal rim comprising two rows of tubercles parallels the anterior margin. The tubercles are perforate with simple and sieve-type pores. This rib extends onto the ventral margin and re-emerges onto the posterior margin as a single row of tubercles. There is a strong dorsal rib overhanging the posterior part of the dorsal

margin, and a strong ventrolateral rib without tubercles, but with pore conuli. A median rib extends somewhat diagonally across the valve, being interrupted by the large subcentral tubercle. The reticulum is coarse with angular cells posteriorly and anteriorly and more circular cells medianly. Hinge holamphidont. Calcified inner lamella very wide anteriorly, somewhat less posteriorly. Selvage, lists and striae well-developed and numerous peripheral plications at right angles to the margin. CMS with three lower adductors closely adjacent, while the dorsal adductor is at a strong angle to the remainder and is inclined anterodorsally. Frontal scar strongly 'V'-shaped. Sexual dimorphism not observed.

Remarks. Although Bertels describes this species as possessing an eye tubercle and internal ocular sinus, we have being unable to observe these characters. This species differs from *Mimicocythereis patagonica* (Bertels, 1975*a*) in its much strong reticulation and less strongly developed lateral ribs.

Stratigraphical range. Maastrichtian of Fortín General Roca, Rio Negro Province, (Bertels 1975*a*) and Cerro Azul, General Roca.

Genus CASTILLOCYTHEREIS gen. nov. Ceolin and Whatley

LSID. urn:lsid:zoobank.org:act:xxxxxxxxx

Derivation of name. L. *castillo*, a fort or castle. With reference to the castle-like tubercles complexes, a number of which occur as part of the reticulum of this genus.

Type species. *Castillocythereis multicastrum* gen. et sp. nov.

Diagnosis. As for the type species.

Description. As for the type species.

Included species. *Castillocythereis multicastrum* gen. et sp. nov. Ceolin and Whatley

Castillocythereis albertoriccardii sp. nov. Ceolin and Whatley

Remarks. *Castillocythereis* gen. nov. differs from *Trachylebereis* Brady in the absence of an angulate posterior margin, in its dense carapace ornamentation, especially with groups of castellated turrets on the muri, and the absence of a prominent single ocular rib. It differs from *Cythereis* Jones, in the absence of the three longitudinal ribs, the strong anterior peripheral rim; in its bluntly pointed posterior end and in its poorly developed subcentral tubercle. *Apatoleberis* gen. nov. is similar to *Castillocythereis* gen. nov. in shape, but differs in its well defined anterior and posterior marginal rims, including a strong ocular rib and its prominent subcentral tubercle and in differently tuberculate carapace.

Castillocythereis multicastrum sp. nov. Ceolin and Whatley

Figure 11K-O

LSID. urn:lsid:zoobank.org:act:xxxxxxxxx

Derivation of name. L. *multi*, many; plus *castrum*, castles. With reference to the many (often circular) multi tubercular castle-like pore conuli on the surface of this species.

Type material. Holotype: one valve, LM-FCEN 3454 (Figs 11K, L); paratypes: LM-FCEN 3455-3457 (Figs 11M; 11N; 11O).

Material. 43 specimens from samples 16, 17, 19, 21 and 31. Danian.

Diagnosis. A large, subrectangular valve with reticulate surface and with groups of castellated turrets on the muri, densely distributed over the entire surface. Eye tubercle present. Hinge paramphidont.

Dimensions. In mm:

		L	H	W	
Holotype, female,	LM-FCEN 3454	0. 938	0. 529		sample 16
Paratype, female,	LM-FCEN 3455	0.988	0.587		sample 16
Paratype, male,	LM-FCEN 3456	1.054	0.527		sample 16

Paratype, female,	LM-FCEN 3457	0.988	0.586	0.467	sample 16

Description. Large, elongate subrectangular in lateral view. Subovate in dorsal view with ends largely compressed. Anterior margin broadly rounded with apex below mid-height; long regularly but gently convex, anterodorsal slope with very small marginal denticles and shorter, more convex anteroventral slope with much larger denticles. Posterior margin more narrowly rounded with apex above mid-height, with short posterodorsal slope and small posteromarginal denticles in a double row. Posteroventral slope longer, more convex and with larger denticles in double row. Dorsal margin convex above eye-tubercle, behind which this margin is straight and strongly spinose, descending abruptly into a deep sulcus parallel to the posterior margin. Ventral margin strongly spinose with a very gently oral incurvature and not overhung by valve surface or ornament. Greatest length a little above mid-height; greatest height through eye tubercle, greatest width in posterior one-third. Ornament fundamentally of a wide-open reticulum with tubercles and ribs superimposed. Three distinct ribs parallel the anterior margin; they bear the typical clusters of subcircular castellate group of tubercles, which range from having spinose club, or pestle-shape tubercles usually in groups of two to four. Those on the anterior rib are rather small. Others elsewhere on the surface, particularly medianly, are large, circular and bearing five and even seven tubercles, which surround a simple sieve-type pore. These occur conjunctively on the muri and are entirely typical of the ornament of this species. The solae are blind and all pores seems to occur centrally in the various castra. The eye tubercle is surrounded above by two arcuate rows of very small tubercles. A short median sulcus extends anteromedianly behind the eye and another separates the “highground” of the anterior from the “lowground” of the posterior margin. The subcentral tubercle is a very diffuse area of large “castles”. Calcified inner lamella very wide anteriorly, hinge paramphidont with denticulate median element. CMS with an anterior ‘V’-

shaped scar. Sexual dimorphism pronounced with males more elongate and narrower than females.

Remarks. The present species differs from *Trachyleberis huantraicoensis* Bertels, 1969*b* mainly in its ornamentation pattern that is less tuberculate and more reticulate, but with well-defined groups of castellated turrets on the muri.

Stratigraphical range. Danian of Cerro Azul, General Roca.

Castillocythereis albertoriccardii sp. nov. Ceolin and Whatley

Figure 11P-R; 12A

LSID. urn:lsid:zoobank.org:act:xxxxxxxxx

Derivation of name. Named in honour of Professor Dr. Alberto Riccardi in recognition of his important work on South American Mesozoic palaeontology, specially ammonites and for his very influential presidency of the IPU, his work with CONICET and other institutions.

Type material. Holotype: one complete carapace, LM-FCEN 3458 (Figs 11P; 12A); paratypes: LM-FCEN 3459-3460 (Figs 11Q; 11R).

Material. Ten specimens from samples 1, 3, 5, 12 and 14. Maastrichtian.

Diagnosis. A medium species with "downturned" and bluntly rounded posterior end. Second-order ornamentation well developed with strong muri and with conjunctive castellated turrets. Hinge holamphidont and pronounced eye tubercle.

Dimensions. In mm:

		L	H	W	
Holotype, carapace,	LM-FCEN 3458	0. 679	0.417	0.350	sample 3
Paratype, valve,	LM-FCEN 3459	0.726	0.438		sample 1
Paratype, valve,	LM-FCEN 3460	0.665	0.401		sample 5

Description. A medium sized slightly elongate, subquadrate species of *Castillocythereis* in lateral view. Slightly saggitate in dorsal view, narrower anteriorly, widest in posterior third and more strongly laterally compressed posteriorly than anteriorly. Anterior margin broadly, but asymmetrically rounded with apex a little below mid-height and denticulate throughout except from the extreme anterodorsal slope to the umbonate cardinal angle. Posterior margin narrowly and bluntly rounded with apex at about mid-height; posteroventral slope convex and denticulate; posterodorsal slope biconvex with a concave separation; not denticulate. Dorsal margin slightly sigmoidal, largely obscured in lateral view by dorsal rib and its ornament. Ventral margin obscured in lateral view; with oral concavity. Eye tubercle prominent and micropunctate. Sexually dimorphic with females shorter and less high than males and with a vertical rib posteriorly, clearly demarcating a smooth posteromarginal area from the elevated surface of the carapace. This structure is evidently lacking in males. There are three longitudinal ribs in the posterior part of the valve. A dorsal rib extends arcuately toward the dorsal margin and terminates posterodorsally. It contains many tubercles in a double or triple row. The tubercles are rounded and most are not perforated. A short median rib extends from the posterior dorsal rib to within one or two cells short of the median subcentral tubercle. A ventrolateral rib extends along the edge of the lateral surface, terminating at about mid-length. It bears rounded pestle-like tubercles; most are blind, some are sieve-type. The subcentral tubercle comprises a number of radiating riblets of tubercles. These are contained anteriorly by an arcuate rib. A number of ribs paralleling the anterior margin cross the lateral surface between the anterior rim and the subcentral tubercle. The eye tubercle is buttressed all around by curved rows of tubercles. Clean species shows that the reticular cells with the prominent ribs of the solae do not bear structures while intervening muri frequently bear tubercles, most of which are blind. Simple marginal pore canals occur on the intersections of the muri on the ribs, but more rarely on the muri of the reticulum. Hinge paramphidont with, in the RV a long

anterior element comprising a dentate bar comprising of seven teeth, while the posterior bar seems to bear four teeth. Median element locellate, most strongly posteriorly. The frontal CMS is a 'V'-shape.

Remarks. Differs from *Castillocythereis multicastrum* sp. nov. in its bluntly rounded posterior end, in having more developed secondary reticulation with strong muri and less densely distributed groups of castellated turrets on the muri. Differs from *Cythereis clibanarius* sp. nov. in a less pointed posterior end, less developed ribs and in having pore conuli disposed in castellated structures on the muri.

Stratigraphical range. Maastrichtian of Cerro Azul, General Roca.

Genus CYTHEREIS Jones, 1849

Type species. *Cythereis ciliate* Reuss, 1846.

Cythereis stratios sp. nov. Ceolin and Whatley

Figure 12B-F

LSID. urn:lsid:zoobank.org:act:xxxxxxxxx

Derivation of name. Gr. *στρατιο*, of soldiers. With reference to the neat line of the tubercles along the dorsal margin, which resemble soldiers on parade.

Type material. Holotype: one complete carapace, LM-FCEN 3461 (Fig. 12B); paratypes: LM-FCEN 3462-3465 (Figs 12C; 12D; 12E; 12F).

Material. 102 specimens from samples 14; Maastrichtian; 16, 17, 19, 21, 23, 26, 31, 34 and 40; Danian.

Diagnosis. *Cythereis* with three ribs bearing irregularly spatulate tubercles in straight lines. Marginally dentate at each end with strong tuberculate marginal rim.

Dimensions. In mm:

		L	H	W	
Holotype, female,	LM-FCEN 3461	0.854	0.489	0.389	sample 31
Paratype, female,	LM-FCEN 3462	0.938	0.530		sample 14
Paratype, male,	LM-FCEN 3463	0.974	0.484		sample 14
Paratype, male,	LM-FCEN 3464	0.978	0.473		sample 14
Paratype, female,	LM-FCEN 3465	0.907	0.510	0.393	sample 19

Description. Large, elongate subovate in lateral view. Very thick-shelled. In dorsal view subhexagonal with compressed extremities much modified by surface ornament. LV a little larger than RV with some overlap anteriorly and posteroventrally. Anterior margin very broadly rounded and dentate; apex near mid-height. Posterior margin bluntly rounded with apex a little below mid-height. Dorsal margin straight, entirely obscured in lateral view by dorsal rib and inclined towards posterior. Ventral margin almost straight and not obscured in lateral view. Greatest length through mid-height; greatest height through anterior cardinal angle and greatest width in posterior one-third. Ornamentation extremely robust; reticulocostate with tubercles. A strong marginal rim surrounds the anterior margin peripherally and bears marginal denticulations directed anteriorly and small castellated tubercles projected laterally. On the ventral margin, the rim becomes reduced in strength, but then becomes like that of the anterior marginal rib onto the posterior. However, at mid-height, it reduces in strength and dies out posterodorsally. A strong dorsal rib bearing very large ornate, spatulate, castellate tubercles, in military precision, extends to just behind the eye tubercle. A similar median rib extends to near the subcentral tubercle and the ventrolateral rib similarly, but less strongly constructed. This lateral structure is approximately 'L'-shaped and comprises two blocks of spatulate-sided castellate tubercles. The eye tubercle is ovate and strongly buttressed. The reticulum comprises large individual cells which are subdivided

immediately behind the anteromarginal rim. The solae are intact. The larger tubercles on the ribs and some muri, especially conjunctively, bear pores. However the majority of tubercles seem to be blind. Hinge paramphidont. Calcified inner lamella wide anteriorly and posteriorly. Antennal scar 'U'-shaped.

Remarks. This species has a hinge typical of *Cythereis* such as *Cythereis? punctatafoveolata* Majoran, 1989 (pl. 12, figs. 12-13) described from the Mid-Cretaceous of Algeria. Differs from *Cythereis trajectiones* sp. nov. in the nature of its reticulation and its more elongate ribs.

Stratigraphical range. Maastrichtian and Danian of Cerro Azul, General Roca.

Cythereis clibanarius sp. nov. Ceolin and Whatley

Figure 12G-J

LSID. urn:lsid:zoobank.org:act:xxxxxxxxx

Derivaion of name. L. *clibanarius*, a soldier clad in mail. With reference to the appearance of this species seen in lateral view, in that the ornament resembles the chain-mail armour of soldiers in Roman and Mediaeval times.

Type material. Holotype: one valve, LM-FCE 3466 (Fig. 12G); paratypes: LM-FCEN 3467-3469 (Figs 12H; 12I; 12J).

Material. Seven specimens from sample 19. Danian.

Diagnosis. *Cythereis* with strong dorsal but weaker median and ventrolateral ribs. The dorsal bearing strong clusters of club-like tubercles. Marginal rim anteriorly with rounded tubercles paralleled proximally by a similar rib also tuberculate but mural in origin. Eye tubercle strongly buttressed but not prominent.

Dimensions. In mm:

		L	H	
Holotype, female,	LM-FCEN 3466	0.803	0.444	sample 19
Paratype, female,	LM-FCEN 3467	0.970	0.500	sample 19
Paratype, male,	LM-FCEN 3468	0.952	0.456	sample 19
Paratype, female,	LM-FCEN 3469	0.785	0.441	sample 19

Description. Large, subovate in lateral view. Subhexagonal with compressed extremities in dorsal view. Anterior margin broadly rounded with apex at about mid-height. Posterior margin pointed, slightly "upturned" with apex just below mid-height, with straight to concave posterodorsal slope and straight to gently convex posteroventral slope. Dorsal margin straight, inclined posteriorly and completely obscured in lateral view by dorsal rib. Ventral margin with slight oral indentation, obscured in lateral view by ventral rib. Ornament very strong, reticulocostate and spinose. There is a distinct marginal rim, very peripheral to the anterior and posterior margins where it bears a double row of small conular denticulations of which some on the inner row are perforated terminally. A very strong dorsal rib extends from the posterior cardinal angle to a small sulcus immediately behind the eye tubercle. This rib is eroded on the lateral surface by the reticulum and comprises a number of castellate structures surrounded by blunt pore conuli, some of which are perforate. The eye tubercle, which is smooth but not prominent, is within a heavily buttressed, multiconulate area, the posterior conuli of which are considerably higher that the surface of the eye tubercle. Subcentral tubercle approximately circular, but quite irregular; it contains many conuli most of which are blind. The reticulum comprises largely, circular or ovate cells with the rims of the solae being well defined. The solae are almost all completely smooth. Some, however, have very small pores in their bases. The muri often bear usually conjunctive pores, they also bear blind conuli. There is a weakly developed median rib, somewhat arcuate in its mid-length which

terminates against the subcentral tubercle. There is a rather indistinct ventrolateral rib that extends from an anteroventral position to its termination in a large, distinct conulus, with a sieve-type pore posteroventrally. A narrow rib, formed from the muri of the reticulum, extends anteriorly from the subcentral tubercle to the anteromarginal rim. Greatest length at mid-height; greatest height at anterior cardinal angle; greatest width at one-third posteriorly. Sexual dimorphism very strong, with males more elongate than females. Hinge paramphidont. Calcified inner lamella very wide anteriorly, avestibulate. Frontal scar 'U'-shaped.

Remarks. Differs from *Cythereis stratios* sp. nov. in the less ornamented nature of the anterior and posterior rims, in the more rounded pattern of reticular cells, spinosity on the muri and in a less prominent eye tubercle. Differs from *Cythereis transkeiensis* Dingle, 1969, from the Santonian of the coast of Pondoland, South Africa, in the absence of cup-like structures in the reticule, in the posterodorsal end lacking concavity and in the presence of spines in the posteroventral region.

Stratigraphical range. Danian of Cerro Azul, General Roca.

Cythereis trajectiones sp. nov. Ceolin and Whatley

Figure 12K-P

LSID. urn:lsid:zoobank.org:act:xxxxxxxxx

Derivation of name. L. *trajectiones,* a crossing over, part way of passage of something, trajectory. With reference to the fact that this species crosses the Cretaceous–Tertiary boundary.

Type material. Holotype: one complete carapace, LM-FCEN 3470 (Fig. 12K); paratypes: LM-FCEN 3471-3474 (Figs 12L, M; 12N; 12O; 12P).

Material. 169 specimens from samples 14; Maastrichtian, 16, 17, 19 and 21; Danian.

Diagnosis. A species of *Cythereis* characterized by a very tuberculate dorsal rib and ventrolateral rib and the possession of club-like conjunctive tubercles on the muri, that also occur on the subcentral tubercle and the median rib.

Dimensions. In mm:

		L	H	W	
Holotype, female,	LM-FCEN 3470	0.662	0.475		sample 17
Paratype, female,	LM-FCEN 3471	0.639	0.384		sample 14
Paratype, female,	LM-FCEN 3472	0.661	0.384		sample 14
Paratype, male,	LM-FCEN 3473	0.666	0.323		sample 19
Paratype, female,	LM-FCEN 3474	0.698	0.387	0.324	sample 14

Description. Medium, elongate, subovate in lateral view. In dorsal view with distinct median sulcus. Greatest width about one-third length. End margins compressed. Anterior margin broadly rounded, apex a little below mid-height and anterodorsal slope slightly less convex anteroventrally. Short, strong, blunt marginal denticles. Posterior margin bluntly pointed with apex below mid-height and strongly dentate in ventral half with small strong conical marginal denticles. Dorsal margin straight sloping posteriorly and obscured by dorsal rib. Ventral margin obscured in lateral view and with slight oral inflexion. Greatest length below mid-height; greatest height through eye tubercle. LV slightly larger than RV. Ornament relatively strong, reticulo-costate and tuberculate. There is a strong dorsal rib with strong tuberculate buttresses bearing two to six conular tubercles with smooth inter-tubercular areas. The prominent oval eye tubercle is situated at the anterior end of this rib. Median rib short and tuberculate, terminating against the median sulcus, well before subcentral tubercle. Ventrolateral rib defined by rows of mainly paired tubercles terminating posteroventrally in a considerably profound sulcus. A strong marginal rim, bearing numerous tubercles in an irregular double row, parallels the anterior margin and extends onto the ventral and posterior

margins. Subcentral tubercle large with irregular outline and bearing tubercles. Intercostal areas reticulate, with muri anteriorly being directed subparallel to the anterior margin and separated by decreasingly by proximally large reticular cells. The largest cells occur between the most distal riblet and the marginal rim and are elongate ovate in shape. The remainder of the reticulation is chaotic with solae varying in shape. The area nearest to the posterior margin is not reticulate. Numerous and widespread conjugate pore conuli occur across the valve, they may be blind, simple or sieve-type pores and possibly sieve plates in the solae and on some elevations Hinge paramphidont. Calcified inner lamella very wide anteriorly, avestibulate. Frontal scar 'U'-shaped. Sexual dimorphism strong with males narrower, more elongate and less inflate than females.

Remarks. The present species has some similarities with *Cythereis*? *indocilis* Bertels 1969*a* from the Danian of Huantrai-co, Neuquén Province, differing in its better developed ribs, the presence of many conjugate pore conuli, absence of a post ocular sulcus and in the pattern of second order reticulation. This species occurs in the upper available sample in the Maastrichtian and in three samples in the Danian.

Stratigraphical range. Maastrichtian and Danian of Cerro Azul, General Roca.

Genus HENRYHOWELLA Puri, 1957

Type species. *Henryhowella evax* Ulrich and Brassler, 1904

Henryhowella (Henryhowella) nascens (Bertels, 1969*c*)

Figure 12Q-R

1969*c* *Rocaleberis nascens* Bertels, p. 163, pl. 1, fig. 1a–c.

2002 *Henryhowella* cf. *H. nascens* Miller *et al*., p. 310, fig. 9a.

Material. 56 specimens from samples 17, 19, 26, 34 and 39. Danian.

Dimensions. Adult carapace, paratype LM-FCEN 3475, (Fig. 12Q) female, 1.07 (L), 0.65 (H), LM-FCEN 3476, (Fig. 12R) male, 1.11 (L), 0.575 (H).

Remarks. Bertels erected this genus claiming that it differs from *Henyhowella* in possessing a different set of structures associate with the calcified inner lamella anteriorly. These characters, however, are common in *Henryhowell*a and do not support this generic proposition.

Stratigraphical range. Danian of Fortín General Roca, Río Negro (Bertels 1969*c*), Huantraico, Neuquén (Bertels 1973) and Cerro Azul, General Roca.

Subgenus WICHMANNELLA Bertels, 1969 new subgenus

Type species. *Wichmannella meridionalis* Bertels, 1969*c*

Remarks. The present authors do not consider that the reasons Bertels' uses to separate her genus *Wichmannella* from *Henryhowella* Puri are profound enough to warrant a separate genus. However, we believe that the differences between their respective type species are sufficient to maintain a separation at the subgenera level. Therefore, we include in *Wichmannella* all those species from the Maastrichtian and Danian assigned to it from the Neuquén Basin (Bertels 1969*b*, 1974, 1975*a*). However, Jellinek and Swanson (2003) in the discussion of their genus *Apatihowella* (*Apatihowella*) considers that Yajima's (1982) use of *Wichmannella* for *Cythere circumdentata* (Brady, 1880) is doubtful. The latter is a Recent genus from the deep southern of Pacific, while *Wichmannella* is from the Late Cretaceous–Lower Tertiary of Argentina. The present authors concur on this.

Henryhowella (Wichmannella) praealtus sp. nov. Ceolin and Whatley

Figure 13A-F

LSID. urn:lsid:zoobank.org:act:xxxxxxxxx

Derivation of name. L. *praealtus* very high. With reference to the proportionally great height of the female of this species.

Type material. Holotype: one complete carapace, LM-FCEN 3477 (Fig. 13A); paratype LM-FCEN 3478-3482 (Figs 13B; 13C; 13D; 13E; 13F).

Material. 59 specimes from samples 16, 17, 19, 21, 23 and 31. Danian.

Diagnosis. A species of *Henryhowella* (*Wichmannella*) characterized by its cup-like solae in the reticulum and numerous small, short, mostly conjunctive tubercular spines, on the muri. Eye tubercle hemispherical, large and protuberant and, in internal view, very large sieve pores.

Dimensions. In mm:

		L	H	W	
Holotype, female,	LM-FCEN 3477	1.083	0.643	0.525	sample 17
Paratype, female,	LM-FCEN 3478	1.063	0.637		sample 19
Paratype, male,	LM-FCEN 3479	1.171	0.629		sample 23
Paratype, female,	LM-FCEN 3480	1.014	0.602		sample 23
Paratype, female,	LM-FCEN 3481	1.018	0.671	0.529	sample 26
Paratype, male,	LM-FCEN 3482	1.241	0.592	0.589	sample 19

Description. A very large, subovate to subrectangular, thick-shelled species of *Henryhowella* (*Wichmannella*); subovate in dorsal view. Anterior margin very well rounded about an apex at mid-height and with marginal denticles in lower half. Subovate in dorsal view with clear median sulcus behind the eye tubercle. Posterior margin narrow and less regular, with posterodorsal slope less rounded than posteroventral part; apex a little below mid-height. Dorsal margin straight, interrupted by numerous small spines and by the large eye tubercle and its surrounding ring of spines. Ventral margin gently concave medianly with median part obscured in lateral view by valve tumidity and ventral spines. Larger spines occur

posteroventrarly. Ornamentation reticulospinose. There is a large reticulum of fairly large cells, disposed peripherally and superipherally, parallel to the margins and more randomly centrally. Solae filled with cup-like structures whose rims abut against the muri. The solae do not bear pores or sieve plates. The muri bear both simple and sieve pores and numerous spinose tubercles, often in clusters. Some are perforate but most are blind. There are faint traces of dorsal and ventrolateral ribs. There is a shallow, posteroventrally directed sulcus behind the eye tubercle and an irregularly circular subcentral tubercle. Greatest length at mid-height; greatest height at anterior cardinal angle; greatest width in posterior one-third. Sexually dimorphism with males narrower and more elongate than females. Hinge holamphidont with the posterior part of the posteromedian element strongly developed and locellate in the LV. Anteriorly, there is a vestibulum. Antennal scar large 'V'-shaped. Internal surface with numerous, larger sieve-type pores that must correspond with those situated on conjunctive muri externally.

Remarks. The present species differs from *Henryhowella* (*Wichmannella*) *meridionalis* (Bertels 1969*c*) in being longer, more subrectangular in shape and by having an irregular, rounded reticulation pattern, in contrast with *Henryhowella* (*Wichmannella*) *meridionalis* that has polygonal cells with small, conjunctive spines. It also differs from other of Bertels' species of *Wichmannella* in reticulation pattern and in carapace shape.

Stratigraphical range. Danian of Cerro Azul, General Roca.

Genus HYSTEROCYTHEREIS gen. nov. Ceolin and Whatley

LSID. urn:Isid:zoobank.org:act:xxxxxxxxx

Derivation of name. Gr. *ύστρος* hysteros, after, later; plus *Cythereis*, a well-known ostracod genus. With reference to the fact that *Cythereis* Jones is an essentially Cretaceous genus, while *Hysterocythereis* occur in both the Maastrichtian and Lower Palaeocene and is a very

possible descendent. Two other species, erroneously attributed to *Anticythereis* by Bertels (1973, 1975*a*), are also included in the present genus.

Type species. *Hysterocythereis paredros* gen. et sp. nov.

Diagnosis. A strongly reticulate genus of Trachyleberididae resembling *Cythereis* Jones, in many aspects of its morphology, but lacking the three transverse ribs on the posterior part of the lateral surface typical of that genus and also lacking a prominent subcentral tubercle. Posterior end acuminate. Hinge paramphidont. Eye tubercle small, but prominent.

Included species. *Anticythereis*? *inconnexa* (Bertels, 1973)

Anticythereis? *attenuata* (Bertels, 1975*a*)

H. *paredros* sp. nov.

H. *coinotes* sp. nov.

H. *diversotuberculatus* sp. nov.

Hysterocythereis? sp.

Remarks. Neither of the two species of Bertels included above, confirm to the generic diagnosis of *Anticythereis* Van den Bold, 1946. They do not exibit reverse overlap and they have strongly reticulate rather than punctate ornament. *Hysterocythereis* gen. nov. differs from *Sthenarocythereis* gen. nov. in the shape and nature of the solae of the reticulum and in the nature of the conjunctive tubercles in the present genus, being much smaller and less spinose. Early members of *Sthenarocythereis* have paramphidont and later members have holamphidont hingement.

Hysterocythereis paredros sp. nov. Ceolin and Whatley

Figure 13G-N

LSID. urn:Isid:zoobank.org:act:xxxxxxxxx

Derivation of name. Gr. *παρεδρος*, *paredros*, a near associate, sitting beside. With reference to the close relationship between this species and the genus *Cythereis* Jones.

Type material. Holotype: one valve, LM-FCEN 3483 (Figs 13G, L); paratypes: LM-FCEN 3484-3487 (Figs 13H; 13I, J, K; 13M; 13N).

Material. 25 specimens from sample 19 and 21. Danian.

Diagnosis. A strongly, sexually dimorphic species of *Hysterocythereis*, with strong reticulate ornament and some conjunctive tubercles, mostly as singles or doubles, but with some tubercles. Eye tubercle well-developed, subcentral tubercle very reduced.

Dimensions. In mm:

		L	H	W	
Holotype, female,	LM-FCEN 3483	0.823	0.511	0.377	sample 19
Paratype, female,	LM-FCEN 3484	0.788	0.425	0.375	sample 19
Paratype, male,	LM-FCEN 3485	0.774	0.420		sample 19
Paratype, male,	LM-FCEN 3486	0.747	0.376	0.325	sample 19
Paratype, female,	LM-FCEN 3487	0.686	0.404		sample 19

Description. A large, elongate subovate (female) to very elongate, subrectangular (male) in lateral view. In dorsal view subovate with compressed ends. Anterior margin broadly rounded and slightly extended below the ventral margin. Posterior margin bluntly rounded below mid-height, both margins dentate, especially anteriorly. Dorsal margin straight, sloping posteriorly; the dorsal cardinal angles are anteriorly pronounced and posteriorly rounded. Ventral margin biconvex about a gentle oral inflexion. Ornament reticulopunctate. The resultant reticulum is strong and the intersecting muri enclose reticular cells that range in shape from circular to oval to quadrate, rectangular and polygonal. The cells and stronger muri are orientated parallel to the free margin peripherally but much more chaotically centrally. Most of the tubercles are conjunctive and the rather short, globose tubercle occur

singly, as doubles, triples and quadruples. Many of the tubercles are blind, other bears single pores and some sieve-type pores. The pore conuli are well developed on the several ribs that parallel the anterior margins. Larger pore conuli occur on the dorsal margin. Hinge paramphidont. Frontal scar 'U'-shaped and directed anterodorsally. Calcified inner margin wide anteriorly and posteriorly with well-developed selvage.

Remarks. This species differs from *H. diversotuberculatus* sp. nov. mainly in its much stronger reticulation and tuberculation.

Stratigraphical range. Danian of Cerro Azul, General Roca.

Hysterocythereis coinotes sp. nov. Ceolin and Whatley

Figure 13O-R; 14A-C

LSID. urn:lsid:zoobank.org:act:xxxxxxxxx

Derivation of name. Gr. *κοινοτες*, sharing in common. With reference to the fact that it shares many of it biocharacters with other species of the genus.

Type material. Holotype: one valve, LM-FCEN 3488 (Fig. 13O); paratypes: LM-FCEN 3489-3492 (Figs 13P, Q, R; 14A; 14B; 14C).

Material. 73 specimens from sample 14; Maastrichtian; 16, 17 and 19; Danian.

Diagnosis. A species with spinose anterior and posterior margin, with a well-developed postocular sulcus and a reticulation pattern with cup-like cells, not perforated by sieve plates and ranging in shape from rounded to subrectangular. A few pore conuli on the muri and are of smaller size.

Dimensions. In mm:

		L	H	W	
Holotype, female,	LM-FCEN 3488	0.760	0.460		sample 16
Paratype, female,	LM-FCEN 3489	0.814	0.485		sample 16

Paratype,	male,	LM-FCEN 3490	0.889	0.416		sample 21
Paratype,	female,	LM-FCEN 3491	0.904	0.487		sample 16
Paratype,	female,	LM-FCEN 3492	0.829	0.466	0.362	sample 19

Description. A large, subrectangular species of *Hysterocythereis* subovate in dorsal view. Anterior margin broadly and symmetrically rounded with apex at mid-height. Posterior margin bluntly pointed with apex below mid-height. Dorsal margin sinuous, sloping posterodorsally and slightly obscured, in lateral view by a spinose dorsal surface. Ventral margin almost straight. Ornamentation reticulospinose with cells and muri concentrically oriented anteriorly with the most distal cells subrounded and subrectangular with cup-like fossae. Anterior and posterior margins spinose with a posterior marginal rim. A sigmoidal row starts below the eye tubercle, where it is most strongly developed and extends to a posteromedian position; less well defined in RV. Some small conjunctive tubercles can be observed in single, double or triple groups. Some bear simple pores, others are blind. The subcentral tubercle is subdued by concentrically oriented cells. Post ocular sulcus present. Hinge paramphidont. Anterior CMS in a 'U'-shape. Sexual dimorphism very strong with males more elongate and narrower than females, less spinose and with ventral margin convex.

Remarks. Differs from *Hysterocythereis diversotuberculatus* sp. nov. in the presence of the post-ocular sulcus, in having more spinose ornamentation, mainly on anterior and posterior margins; in less conjunctive spines and in the shape of cells being less diverse than in *H. diversotuberculatus*. Also differs in having a shorter anterior margin that does not extends below the ventral margin.

Stratigraphical range. Maastrichtian and Danian of Cerro Azul, General Roca.

Hysterocythereis diversotuberculatus sp. nov. Ceolin and Whatley

Figure 14D-J

LSID. urn:lsid:zoobank.org:act:xxxxxxxxx

Derivation of name. L. *diversotuberculatus*. With reference to the very diverse expression of the conjunctive tubercles on the reticulum, which varies between individual specimens and within single specimen.

Type material. Holotype: one valve, LM-FCEN 3493 (Figs 14D, I); paratypes: LM-FCEN 3494-3497 (Figs 14E, F; 14G; 14H; 14J-lost).

Material. 67 specimens from samples 21, 23, 26, 31, 34 and 36. Danian.

Diagnosis. A species of *Hysterocythereis* characterized by a reticulum in which the cells vary from circular and cup-like to quadrate, rectangular, hexagonal and polygonal, with complex grouping of small conjunctive tubercles.

Dimensions. In mm:

	L	H	W	
Holotype, female, LM-FCEN 3493	0.799	0.471	0.380	sample 21
Paratype, female, LM-FCEN 3494	0.966	0.482	0.350	sample 23
Paratype, female, LM-FCEN 3495	0.812	0.380		sample 21
Paratype, male, LM-FCEN 3496	0.911	0.320		sample 26
Paratype, female, LM-FCEN 3497 (lost)	0.809	0.456	0.319	sample 23

Description. A large, subovate (female) to subrectangular (male) specimen in lateral view. Elongate, ovate in dorsal view with very compressed end margins and carapace approximately the same in between the cardinal angles. Anterior margin very broadly rounded and extending below the ventral margin, with apex at mid-height in females, slightly below in males. Posterior margin bluntly rounded with apex at about mid-height. Dorsal margin straight, inclined to posterior, largely obscured in lateral view by spinose dorsal surface. Ventral

margin largely obscured in lateral view and with slight oral concavity. Greatest length at about mid-height; greatest height at anterior cardinal angle; greatest width equal between cardinal angles. Eye tubercle small and not prominent. Ornament very strongly reticulate. Reticular cells and muri concentrically orientated anteriorly with the most distal cells being large, but subdivided anteroventrally. The succeeding two rows of cells are smaller, but rectangular. The reticular cells in the anterior and antero-median part are circular and cup-like; while in the posterior part they are mainly quadrate to rectangular. The posterior margin has a spinose marginal rim and an area without reticulae containing some pore conuli. Virtually unvaryingly each conjunction in the reticulum bears small club-like tubercles; some single, more commonly in pairs but groups of four and six also occur, the latter resembling castellate fortifications. Some simple pores are perforated, others are blind, and some groups of blind pores seems to surround sieve-type pores. The base of the solae are without ornament or pores. Feebly well-developed subcentral tubercle. Hinge paramphidont. Inner lamella fairly wide terminally with selvage strong all around the free margin, and lists and striae developed posteriorly and posteroventrally.

Remarks. Differs from *Hysterocythereis inconnexa* (Bertels, 1973) in having different pattern of reticulation, with cells varying in shape, presence of spines at the posterior end, which is more acuminate and better developed subcentral tubercle.

Stratigraphical range. Danian of Cerro Azul, General Roca.

Hysterocythereis attenuata (Bertels, 1975*a*) comb. nov.

Figure 14K-L

1975*a Anticythereis*? *attenuata* Bertels, p. 115, pl. 5, figs 19 a–b, 20–21.

Type material. Specimens described by Bertels, housed in the collections of the Facultad de Ciencias Exactas y Naturales in Holotype LM-FCEN 842, paratypes LM-FCEN 843-846, plus two paratypes in this study LM-FCEN 3498-3499 (Figs 14K; 14L).

Material. 12 specimens from samples 3 and 5. Maastrichtian, plus the type and other material of Bertels housed in Facultad of Ciencias Exactas y Naturales, Laboratory of Micropaleontology, Universidad of Buenos Aires, Argentina.

Dimensions. Adult valve, LM-FCEN 3495, (Fig. 14K) 0.974 (L), 0.545 (H), female; LM-FCEN 3496, (Fig. 14L) 0.749 (L), 0.371 (H), male.

Diagnosis. A species of *Hysterocythereis* with posterior end pointed with five conical spines, dorsal margin convex posterodorsally and surface covered with subrounded cells, lesser anteriorly where they are subrectangular. Pore conuli less developed than in all the other species of the genus.

Description. Subovate to subtriangular in lateral view. Anterior margin broadly rounded with apex about mid-height and not extending below mid-height, dentate with short, strong, conical tubercles. Posterior margin well pointed with apex below mid-height. Dorsal margin sloping strongly posteriorly obscured by dorsal surface through most of its length in lateral view. Pronounced antero dorsal hinge ear in both valves. Ventral margin largely overhung by valve tumidity in lateral view, with slight oral inflexion. Greatest length below mid-height; greatest height through hinge ear; greatest width at one-third posteriorly. Ornament essentially reticulate plus an arcuate dorsal rib, strongly eroded by reticulum, bearing tubercles obscured by the dorsal margin. A strong rim occurs on the ventral margin above which is a gentle slope from the lateral surface. A sub-alar tubercle occurs posteroventrally. Two mural riblets extend from the eye tubercle parallel to the anterior margin. Proximal to the first of these two ribs is a single row of large rectangular cells that separates the main reticulum from the tuberculate anteromarginal rib. A double row of reticular cells separates these ribs from the second and

most proximal of the riblets originating from the eye tubercle. These riblets extend onto the ventral margin and coalesce to form the ventral rim. Reticular cells range from circular to quadrate and are chaotically distributed. Small, simple pore conuli and open pores occurs conjunctively on some conjunctions. Hinge paramphidont. Inner lamella wide on end margins. Anterior CMS scar in a 'U'-shape.

Remarks. This species from the Maastrichtian of Fortin General Roca, differs from *Hysterocythereis paredros* sp. nov. in having a more acuminate posterior end, and reticulation pattern with small subrounded solae. Its posterodorsal margin is also more convex.

Stratigraphical range. Maastrichtian of Fortín General Roca, Río Negro (Bertels, 1975*a*) and Cerro Azul, General Roca.

Hysterocythereis inconnexa (Bertels, 1973) comb. nov.

Figure 14M-N

1973 *Anticythereis*? *inconnexa* Bertels, p. 326, pl. 4, fig. 3 a–b, 4 a–b.

Type material. Specimens described by Bertels, housed in the collections of the Facultad de Ciencias Exactas y Naturales in Holotype LM-FCEN 439, paratypes LM-FCEN 470-475, plus two paratypes in this study LM-FCEN 3500-3501 (Figs 14M; 14N).

Material. Five specimens from samples 23, 26, 29 and 31. Danian; plus the type and other material of Bertels, housed in the collections of the Facultad of Ciencias Exactas y Naturales, Laboratory of Micropaleontology, Universidad of Buenos Aires, Argentina.

Dimensions. Adult carapace, LM-FCEN 3500, (Fig. 14M) 0.842 (L), 0.491 (H), female; LM-FCEN 3501, (Fig. 14N) 0.828 (L), 0.403 (H), male.

Diagnosis. A subovate species of *Hysterocythereis* with subrounded reticulae, with solae covered with cup-like structures and single conjunctive conical tubercles. Bluntly rounded posterior end and ventral margin with four horizontal riblets.

Description. As for Bertels (1973, p. 337), except to add that small club-like tubercles occur conjunctively on the muri, many are blind, others are perforate by simple pores and other by small sieve-type pores.

Remarks. Bertels described this species from the Danian of Río Negro Province. In the present study, it occurs in the Danian of samples 23, 26 and 31. This species is most similar to *Hysterocythereis diversotuberculata* sp. nov. differing essentialy in the nature of marginal rim and in the fact that *A*. *diversotuberculatus* sp. nov. has groups of two to six small club-like tubercles conjunctively on the muri of the reticulum and a very spinose dorsal rim.

Stratigraphical range. Danian of Fortín General Roca, Río Negro (Bertels, 1973) and Cerro Azul, General Roca.

Hysterocythereis? sp.

Figure 14O-P

Material. Five specimens from samples 3 and 5. Maastrichtian.

Dimensions. Adult carapace, LM-FCEN 3502, 0.94 (L), 0.402 (H); adult valve, LM-FCEN 3503, 0.694 (L); 0.391 (H).

Description. A large, subovate to subrectangular species, with anterior margin broadly and symmetrically rounded, with apex at mid-height. Posterior margin bluntly pointed with apex below mid-height. Dorsal margin almost straight declining towards posterior end. Ventral margin asymmetrical, with small oral concavity at mid-length. Greatest length below mid-height, greatest height at one-third anteriorly, greatest width at one-third posteriorly. Ornament reticulotuberculate with cells of about the same size varying in shape from ovate to subovate to quadrate, over most of the reticulum. Anteriorly, and to a lesser extent posteriorly, parallel to those margins, are large subrectangular cells in a single row. There are conjunctive, mostly single and perforate tubercles on the muri, and some in groups of four. Anterior and

posterior margins with small tubercles. Eye tubercle developed and subcentral tubercle defined by a group of six conjunctive spines. LV overlap the RV mainly in anterior and posterior margins. Hinge paramphidont. Calcified inner lamella well-developed with a large flange.

Remarks. The present species is left in open nomenclature and only tentatively within the genus because of its better developed eye tubercle, by comparison with other members of the genus. The posterior margin is of different shape and has a well developed flange, absent in others species of the genus.

Genus OERTLIELLA Pokorny, 1964

Type species. *Oertliella reticulata* (Kafka, 1886) Pokorny, 1964

Oertliella? sp.

Figure 14Q-R

Material. Five specimens from samples 3 and 5. Maastrichtian.

Dimensions. Adult valve, LM-FCEN 3504, 0.769 (L), 0.414 (H).

Diagnosis. Large, subrectangular, with anterior margin symmetrically rounded. Posterior margin bluntly pointed above mid-height. Dorsal margin straight and ventral margin slightly biconvex. Ornament reticulospinose, with reticulation ranging from small, rounded muri around entire periphery, largest centrally. There are large broken spines disposed across the valve; the only one preserved has three ramification on its top. From the posterodorsal cardinal angle, there is a spinose marginal rim that extends towards the ventral margin, where it is less well-developed, ending at the anterocardinal angle, near the well-developed eye tubercle. Subcentral tubercle slightly developed, defined by a large spine base. Hinge holamphidont. Calcified inner lamella large; CMS not seen.

Remarks. This species is left in question due to absence of a ventrolateral spinose rib present in all other species of *Oertliella*.

Genus ORTHROCOSTA gen. nov. Ceolin and Whatley

LSID. urn:Isid:zoobank.org:act:xxxxxxxxx

Derivation of name. Gr. *ορθρος*, daybreak, dawn; plus L. *costa*, rib, and *Costa* a well-known ostracod genus. With reference to the fact that this genus, which is evidently related to *Costa* Neviani, and other related genera, is an early member of this generic group.

Type species. *Orthrocosta decores* gen. et sp. nov.

Diagnosis. Subtriangular to subtrapezoidal species of *Orthrocosta* with anterior margin broadly and symmetrically rounded and acuminate posterior end. Ornamentation reticulocostate with three main ribs longitudinally and a fourth one posteriorly, almost vertically, that unites the ventral and median ribs. Eye tubercle well developed with an ocular rim anteriorly. Subcentral tubercle absent. Hinge holamphidont.

Description. As for the type species.

Remarks. This genus differs from *Protocosta* Bertels in having well-developed median and ventrolateral ribs, and, in some species, there is a vertical rib that links the posterior end of the ventrolateral rib with the posterior end of the median rib. Differs also in lateral shape, varying between subtriangular and subtrapezoidal, while species of Bertels' genus are subrectangular. Differs from the classic genus *Costa* Neviani, in its acuminate posterior end and in its very well developed ribs, with a sinuous median rib that is not recurved at the posterior. Differs from *Paracosta* Siddiqui, in general shape, in its more acuminate posterior end and in the ornamentation pattern. Also differs from *Cativella* Coryell and Fields in its non perforated ridges and in the presence of a vertical rib posteriorly that joins the median and ventrolateral ribs. Differs from *Potiguarella* Piovesan, Cabral e Colin in its pattern of reticulation, in its

three longitudinal ribs being longer and less arcuate, and in the absence of a subcentral tubercle.

Orthrocosta decores sp. nov. Ceolin and Whatley

Figure 15A-G

LSID. urn:lsid:zoobank.org:act:xxxxxxxxx

Derivation of name. L. *decores*, ornamented, elegant, beautiful. With reference to the elegance of the ornament of this attractive species.

Type material. Holotype: one complete carapace, LM-FCEN 3505 (Fig. 15A, F), paratypes: LM-FCEN 3506-3508 (Figs 15B, C; 15E; 15D, G).

Material. 19 specimens from samples 16, 17 and 19. Danian.

Diagnosis. A species with a curved median rib that is subdivided into two anteriorly. Ocular rib closely paralleling the anterior margin and extending across the ventral surface.

Dimensions. In mm:

		L	H	W	
Holotype, female,	LM-FCEN 3505	0. 936	0. 552	0.428	sample 16
Paratype, female,	LM-FCEN 3506	0.899	0.525		sample 16
Paratype, male,	LM-FCEN 3507	1.04	0.531	0.392	sample 16
Paratype, female,	LM-FCEN 3508	0.891	0.489		sample 16

Description. A large, thick-shelled, subtrapezoidal species in lateral view, subhexagonal in dorsal view with ends extremities strongly compressed and slightly compressed medianly in RV. Anterior margin broadly and symmetrically rounded with marginal denticles, especially anteroventraly. Apex at mid-height. Posterior margin strongly pointed at mid-height with marginal denticles posteroventrally. The dorsal margin obscured by a flared rib with is eroded

into a series of reentrants by strong reticulation. This rib extends dorsal to the eye tubercle and unites with the anterior peripheral rib. All the ribs are similarly affected by the reticulation. There is a third rib in the ventral region. The second and third ribs do not achieve the anterior and posterior margins. An ocular rib extend from the eye tubercle and, closely paralleling the anterior margin, then extends across the ventral surface and in so doing obscures that margin in lateral view. It further extends closely parallel to the posterior margin before becoming lost in the elevated posterior structure of the dorsal rib. Immediately below this elevated structure, the median rib extends in a slightly arcuate curve, obliquely across the valve to its termination, one reticulum short of the marginal ocular rib. From this median rib, shortly after its inception, a narrow rib extends ventrally to a position one reticulum above the ventral marginal rib, where it bend through 45° and extends in an arc towards the termination of the median rib. Between the median rib and this latter rib, a series of riblets extend antero ventrally, the strongest being the anterior. Intercostal areas strongly reticulate. The reticulae are largest on the flank of the ribs. The muri are rather narrow and do not normally bear spines. Some perforate tubercles occur but very rarely. Solae are smooth and lack pore or sieve plates. Some sieve pores occurs on muri but very few. Internal features not seen. Sexual dimorphism present with males more elongate and narrower posteriorly than females.

Remarks. Differs from *Orthrocosta* sp. in its less elongate and acuminate posterior end, in the more strongly developed features of the ribs, mainly in the anterior margin that connects to the eye tubercle and in the well developed anterior subdivision of the median rib.

Orthrocosta atopos sp. nov. Ceolin and Whatley

Figure 15H-M

LSID. urn:Isid:zoobank.org:act:xxxxxxxxx

Derivation of name. Gr. ατοπος atopos*,* strange, out of place*.* With reference to two strange elements of the ornament (the box-like structure in the dorsal rib and the arcuate riblet above the ventrolateral rib) that are most unusual and entirely characteristic of the species of *Orthrocosta.*

Type material. Holotype: one complete carapace, LM-FCEN 3509 (Fig. 15H); paratypes: LM-FCEN 3510-3512 (Figs 15I, J; 15K, L; 15M).

Material. 40 specimens from samples 26, 29, 31, 34, 36, 40, 50, 53, and 55. Danian.

Diagnosis. An elongate, subtriangular species of *Orthrocosta* with a very strong median rib extending diagonally across most of the lateral surface. Dorsal rib less well-developed; ventrolateral rib, short convex upwards and irregular. Eye tubercle prominent, intercostal reticulation strong with circular, oval, triangular and quadrate cells.

Dimensions. In mm:

		L	H	W	
Holotype, female,	LM-FCEN 3509	0.904	0.452	0.301	sample 26
Paratype, female,	LM-FCEN 3510	0.804	0.440	0.410	sample 29
Paratype, male,	LM-FCEN 3511	0.904	0.452	0.285	sample 26
Paratype, male,	LM-FCEN 3512	0.787	0.373		sample 34

Description. Elongate subtriangular in lateral view; subhexagonal with compressed ends in dorsal view. Thick-shelled and strongly ornamented. LV larger than RV, with overlap well developed around much of the free margin. Anterior margin broadly rounded with strong spatulate marginal denticles. Greatest height below mid-height in female and at mid-height in male. Posterior margin bluntly pointed at about mid-height. Dorsal margin straight, inclined to the posterior, but greatly obscured, in lateral view, by the dorsal ornament. Ventral margin with a slight oral concavity. Greatest length at about mid-height; greatest height just anterior of the eye tubercle. Ornament reticulocostate with some blunt, terminally performed, pestle-

like, conjunctive tubercle. There are three principal ribs: one extends from the prominent hemicircular eye tubercle paralleling the anterior margin and bearing very strong spatulate marginal tubercles. This becomes the ventrolateral rib and extends onto the posterior margin, where it loses it identity in an eminence with five tubercles, and then extends upwards to form the dorsal rib. A ventral rib extends below this lateral rib, and a median rib extends diagonally across the valve to terminate at two cells distance from the anterior ocular rib. In its posteromedian part, an unusual rib extends upwards in an arc from the ventrolateral rib. The dorsal rib, which extends above the eye, forms a box-like structure immediately behind that organ and is very well seen in the male paratype. A second, but double box-like structure occurs immediately above the posterior termination of the median rib. Intercostal ornament of large, somewhat chaotically distributed reticulae, in which the circumference limits of the solae are clearly marked by a circular or oval rim. The median rib is eroded by the adjacent solae given it a serpentine outline. Very large reticular cells parallel the ocular-ventrolateral-posterior margin and dorsal ribs. Some muri and the median rib seems to bear sieve-type pores. Internal details imperfectly seen. Calcified inner lamella narrow with holamphidont hinge. CMS not seen. Sexual dimorphism strongly pronounced with male being more elongate and lower than female.

Remarks. The present species differ from *Orthrocosta phantasia* sp. nov. in having an arcuate and shorter rib anteroventrally that initiates in a group of four modified reticular cells, while *O. phantasia* has a continuous and concave ventrolateral rim.

Stratigraphical range. Danian of Cerro Azul, General Roca.

Orthrocosta phantasia sp. nov. Ceolin and Whatley

Figure 15N-R; 16A

LSID. urn:lsid:zoobank.org:act:xxxxxxxxx

Derivation of name. Gr. φαντασια, phantasia *"*an image of the imagination*"*. With reference the very unusual appearance of this species, particularly in the development of its dorsal rib.

Type material. Holotype: one complete carapace, LM-FCEN 3513 (Fig. 15N); paratypes: LM-FCEN 3514-3516 (Figs 15O, P; 15Q; 15R; 16A).

Material. 54 specimens from samples 12 and 14; Maastrichtian; 16, 17, 19, 21, 26 and 34; Danian.

Diagnosis. Subtriangular species of *Orthrocosta* with strongly flared dorsal, ventrolateral and ventral ribs. Median rib distinct and extending across the valve surface. Eye tubercle pronounced and linked to tuberculate marginal rim, extending onto ventral surface. Anteroventral and posteroventral margins strongly dentate. Intercostal reticulation strong and eroding flanks of ribs.

Dimensions. In mm:

		L	H	W	
Holotype, female,	LM-FCEN 3513	0.899	0.503		sample 21
Paratype, female,	LM-FCEN 3514	0.841	0.446	0.403	sample 29
Paratype, male,	LM-FCEN 3515	0.826	0.405		sample 31
Paratype, female,	LM-FCEN 3516	0.884	0.503		sample 21

Description. A large, subrectangular to subtriangular species in lateral view, fairly thick-shelled; subhexagonal with compressed ends in dorsal view. Anterior margin very broadly, but asymmetrically rounded, with apex well below mid-height; anterodorsal slope gently curved, anteroventral slope more convex. Margin bearing large tubular and spatulate denticles. Posterior margin subcaudate and appearing upturned due to posteroventral slope being convex and the posterodorsal slope being slightly concave. Very large marginal denticles posteroventrally. Dorsal margin straight, strongly inclined to the posterior and

completely obscured, in lateral view, by the large, very flared dorsal rib. Ventral margin almost entirely obscured by strong ventral rib. Greatest length below mid-height, greatest height at the anterior cardinal angle. Ornament reticulocostate with small, usually conjunctive tubercles on the muri. Most of which are terminally perforated while others seem blind. There are five ribs. A dorsal rib extends from anterior to the dorsal posterior cardinal angle passing dorsal to the eye tubercle which is a large complex structure comprising a vertically directed blade-like tubercle and two posteriorly directed, more tubular tubercles. The dorsal rib is strongly flared and separated into two long rectangular cells by near vertical muri. This rib is perforated by what seems to be simple, normal pore canals, some of which are situated on the flanks of the muri, although the majority pass through their crest. The median rib, depending on the individual specimen, is straight or sinuous, but to a degree always eroded by the reticulum on its flanks, with variable consequences of corrugation. This rib terminates two cells from the anteromarginal rib and one cell below the large structure at the posterior cardinal angle. The ventrolateral rib extends from a posterior ventrolateral process, a two bladed structure, approximately one-third of the distance from the posterior margin to a similar structure approximately one-quarter of the distance from the anterior margin. It is concave, very flared and blade-like in lateral view. From the posterior end of this rib, a short, ill-defined riblet extends dorsally to the median rib. The fourth rib, the ventral rib, is slightly longer than the ventrolateral rib to which it is subparallel as it is also to the ventral margin. It is flared and divided into rectangular to quadrate cells by vertical muri. From the large, prominent, oval eye tubercle, a flared rib with large cells dorsally and multiple cells ventrally, parallels the anterior margin. All these ribs, or the tubercles they bear, are perforated by simple pore canals. The muri of the reticulum are strong and bear usually conjunctive tubercles, that range from subspinate to cylindrical; most are terminally perforate. The cells

are smooth and seem to lack sieve-pores. CMS not seen. Hinge holamphidont but not strongly developed. Calcified inner lamella rather feebly developed.

Remarks. Differs from *Protocosta spinosa* Bertels, 1975*a* from the Maastrictian of Fortín General Roca, in its well-developed ribs, mainly medianly and ventrally.

Stratigraphical range. Maastrichtian and Danian of Cerro Azul, General Roca.

Orthrocosta sp.

Figure 16B

Material. One specime from sample 17. Danian.

Dimensions. Adult valve, LM-FCEN 3517, 1.019 (L), 0.552 (H).

Description. A very large, subtriangular species of *Orthrocosta* with a very well rounded but asymmetrical anterior margin, bearing in its lower half very strong marginal denticles. Posterior caudate with a slightly upturned apex at about mid-height and with strong tubercles on ventral dorsal slope. Dorsal rib crest-like, strongly reticulate with large reticulum over lateral surface that erode the flanks of the ribs. Strong dorsal rib. Median rib divides at subcentral tubercle, which has smaller, rounder reticulae, into a rib that defines the dorsal limit; another which defines the ventral limit and the central rib that passes through the subcentral tubercle. Internal features as for genus.

Remarks. Differs from *Orthrocosta phantasia* sp. nov. by the presence of a subdivided median rib, by the posterior end being longer and acuminate and with the anterior and posterior ends being almost smooth.

Genus PETALOCYTHEREIS gen. nov. Ceolin and Whatley

LSID. urn:Isid:zoobank.org:act:xxxxxxxxx

Derivation of name. Gr. πεταλος petalos of leaves; plus *κύθερεις Cythereis,* a common ending used for cytheroid Ostracoda. With reference to the petalloid outline of the reticular cells in this genus.

Type species. *Petalocythereis schilleri* (Bertels, 1973)

Diagnosis. A median to large member of the Trachyleberididae, subovate, with small, subdued eye tubercle. Free margins surrounded by mural ribs bearing tubercles, but lacking strong marginal rims. Strongly reticulate ornament, muri ranging from smooth to strongly microtuberculate and from bearing numerous spinose tubercles to rather few. Shape of reticular cells petaloid. Hinge paramphidont. Anterior CMS in a 'U'-shape.

Description. As for the type species.

Included species. *Afranticythereis shilleri* (Bertels, 1995)

Afranticythereis venusta (Bertels, 1995)

Remarks. This genus differs from *Cythereis* Jones in lacking three longitudinal ribs. It differs from *Apatihowella* Jellinek and Swanson 2003, which lacks an eye, although there are some similarities in the nature of the conjunctive tubercular spines on the respectives muri. *Sthenarocythereis* gen. nov. differs from *Petalocythereis* in its much stronger muri, much larger eye tubercle and its very strong marginal rim. *Petalocythereis* also differs from *Anticythereis* Van den Bold, in that the latter genus has reversed overlap (RV over LV). Although Carbonel and Johnson (1989) had included all Bertels species erroneously in *Afranticythereis*, that genus differs from *Petalocythereis* in the presence of a vestibulum and subcentral tubercle, and in the ornamentation pattern without spines. *Anebocythereis* Bate, differs in its hemimerodont hinge, narrow inner lamella and anterior CMS in a 'V'-shape.

Petalocythereis schilleri (Bertels, 1973) comb. nov.

Figure 16C-G

1973 *Anticythereis schilleri* Bertels, p. 326, pl. 4, figs 5 a–d, 6 a–b.

1995 *Afranticythereis schilleri* Bertels-Psotka, p. 168, pl. 2, fig. 16.

Type material. Holotype: specimens described by Bertels, housed in Facultad de Ciencias Exactas y Naturales, in Holotype LM-FCEN 476, paratypes 477-479, plus the paratypes from this study LM-FCEN 3518-3521 (Figs 16C; 16D; 16E; 16F, G).

Material. 220 specimens from samples 16, 17, 19, 21, 23, 26, 31 and 34. Danian; plus the type and other material of Bertels housed in the collections of Facultad de Ciencias Exactas y Naturales, Laboratory of Micropaleontology, Univerisidad de Buenos Aires, Argentina.

Remarks. We consider it necessary to rediagnose and redescribe this species, as it is now the type species of a new genus.

Diagnosis. A subovate, strongly tuberculate species of *Petalocythereis* gen. nov. Tubercles mostly single and conjunctive on muri. Muri smooth. Solae petaliform in shape.

Dimensions. In mm:

		L	H	
Holotype, female,	LM-FCEN 3518	0.825	0.506	sample16
Paratype, female,	LM-FCEN 3519	0.950	0.512	sample 16
Paratype, male,	LM-FCEN 3520	0.916	0.561	sample 19
Paratype, male,	LM-FCEN 3521	0.977	0.497	sample 23

Description. A large, thick-shelled species, subovate in lateral view. Subovate in dorsal view but medially constricted with posterior half strongly inflated. Valves subequal with little overlap. Anterior margin broadly rounded, bearing strong but with short, terminally perforate marginal denticles; apex at about mid-height. Posterior margin more narrowly rounded, strongly denticulate and apex at about mid-height. Dorsal margin straight but overhung by numerous, perforate tubercles. Ventral margin largely obscured by valve tumidity and tubercular spines. Well-developed oral invagination seen in internal view. Surface ornament

strongly reticulospinose. Around the entire periphery, the muri are preferentially oriented concentrically parallel to the margins. This preference become less apparent distal from the margins and the central part is almost without this influence. In all parts, the solae are occupied by large sieve plates rather deeply inserted. These are quadrifoil embayments of greater or lesser intensity and separated by spike-like "headlands", probably the product of celation. The muri are strong and often bear conjunctive spiny tubercles. The spines are terminally perforate and probably bore, in life, a single seta. Some tubercles occur as "doubles" and others are quadruple. Associated with the tubercles on the muri, are small sieve-type pores flush with the surface. There are no horizontal ribs. Eye tubercle small. Internally, the calcified inner lamella is strongly developed, particularly anteriorly and mid-posteriorly and is avestibulate. Hinge modified paramphidont with, in the RV, the terminal element showing evidence of divisions into a number of denticles on a boss-like bar. Central muscle scar with a 'U'-shaped frontal. A small internal ocular sinus occurs below the anterior terminal element of the hinge. Sexually dimorphic with males notably more elongate than females.

Remarks. Differs from *Anebocythereis amoena* Bate, 1972 from the Campanian of the Carnavon Basin, Australia, in its more rounded shape, less well-developed eye tubercle, more strongly developed muri and spines and in its paramphidont hinge.

Stratigraphical range. Danian of Fortín General Roca, Río Negro (Bertels 1973) and Cerro Azul, General Roca.

Petalocythereis venusta (Bertels, 1975*a*) comb. nov.

Figure 16H-L

1975*a* *Anticythereis venusta* Bertels, p. 114, pl. 5, figs 10-16.

1995 *Afranticythereis venusta* Bertels, p. 168, pl. 2, fig. 15.

Type material. Holotype: specimens described by Bertels, housed in Facultad de Ciencias Exactas y Naturales, in Holotype LM-FCEN 608, paratypes: LM-FCEN 828-837; plus the four paratypes from this study LM-FCEN 3522-3525 (Figs 16H, L; 16I; 16J; 16K).

Material. 60 specimens from samples 1, 3, 5, 8 and 12. Maastrichtian, plus the type and other material of Bertels housed in the collections of Facultad de Ciencias Exactas y Naturales, Laboratory of Micropaleontology, Univerisidad de Buenos Aires, Argentina.

Dimensions. In mm:

		L	H	W	
Paratype, female,	LM-FCEN 3522	0.687	0.445	0.365	sample 5
Paratype, female,	LM-FCEN 3523	0.663	0.422	0.355	sample 1
Paratype, female,	LM-FCEN 3524	0.729	0.453		sample 5
Paratype, male,	LM-FCEN 3525	0.831	0.444		sample 5

Diagnosis. Subovate with strong anterior hinge ear in LV. Much more tuberculate posteriorly than anteriorly. Muri micro-tuberculate. Solae petaliform.

Description. A median, thick-shelled, ovate ostracod. Anterior margin broadly but asymmetrically rounded with the anterodorsal slope longer and much less strongly rounded than the anteroventral slope, the latter being more strongly curved and bearing strong, terminally perforated marginal denticles. Apex somewhat below mid-height. Posterior margin bluntly rounded with apex at mid-height. Dorsal margin straight but largely obscured by valve surface. Ventral margin appears straight in lateral view due to the presence of a strong ventrolateral rib. Greatest length at about mid-height; greatest height at the anterior cardinal angle, greatest width in posterior one-third. Ornament reticulate and spinose peripherally, especially dorsally. Particularly around the free margin, the muri are preferentially oriented parallel to the margins, strongly enough to resemble peripheral riblets. The muri are strongly

secondarily ornamented with micro-"ropey"riblets than extend along the muri more than crossing them. This is most strongly developed anteriorly although it also occurs elsewhere. Particularly posteriorly, the muri bear rather small tubercles most of which are terminally perforate, these are largely absent medianly. The solae contain deeply recessed sieve plates and many are quadrilobate. What appear to be other small sieve-type plates occur on the muri. Eye tubercle well-developed, but not prominent. Internally the hinge seems to be paramphidont as distinct teeth can be seen on the terminal element of the RV. Calcified inner lamella wide, avestibulate. The frontal muscle scar is 'U'-shaped. A well-developed ocular sinus occurs below the anterior terminal element of the hinge. Sexual dimorphism with male more elongate, more pointed posteriorly and with the ventral margin biconvex about a mid-ventral concavity.

Remarks. Differs from *Petalocythereis schilleri* (Bertels, 1973) in that spines only occur on anterior and posterior surfaces, and in the shape of the dorsal and ventral margins, this being more evident in males than females.

Stratigraphical range. Maastrichtian of Fortín General Roca, Río Negro (Bertels 1975*a*) and Cerro Azul, General Roca.

Genus PHILONEPTUNUS Whatley, Millson and Ayres, 1992

Type species. *Cythereis gravezia* Hornibrook, 1952

Philoneptunus? sp.

Figure 16M-N

Material. Ten specimens from sample 5. Maastrichtian.

Dimensions. Adult valve, LM-FCEN 3526, 0.640 (L), 0.353 (H).

Description. A median, subovate carapace in lateral view. Anterior margin broadly rounded with a marginal rim that extends from an anterodorsal to the posterodorsal region and, which

below mid-height, is closely strongly reentrant with structures forming approximately triangular elevations. These are distally nodose and perforate, probably representing the exit of true radial pore canals. Posterior margin truncate and straight at just about mid-height. Dorsal margin convex and subumbonate anterodorsally, straight and declining steeply posterior. The ventral margin is weakly biconvex about a long weakly indented oral concavity. The dorsal rib is broad and low and is marked by a number of large, but low pore conuli. An anteroventrally directed median sulcus occur approximately mid-dorsally. The ventrolateral rib is strongly developed and extends diagonally, from an anteroventral position, across the ventral margin to form the posteromarginal rim. Surface smooth. CMS with 'V'-shaped antennal scar.

Remarks. The generic status of this species is somewhat in question due to the absence of one of the three ribs as required in the generic diagnosis.

Genus STHENAROCYTHEREIS gen. nov. Ceolin and Whatley

LSID. urn:lsid:zoobank.org:act:xxxxxxxxx

Derivation of name. Gr. σθεναρος, strong, mighty; plus *κύθερεις*, *Cythereis.* With reference to its extremely strong and ornate carapace.

Type species. *Anticythereis arcana*, Bertels 1975*a*

Diagnosis. Large, thick-shelled, elongate subovate genus of the Trachyleberididae with very strongly reticulate ornament, in which strong muri and solae, that range in shape from circular, trefoil to polygonal, and contain large inserted sieve plates. Large strong eye tubercle, very strong anterior and posterior marginal rims. Multituberculate dorsal rib and similar ventrolateral and ventral ribs. Many conjunctive tubercles, single or paired, bearing simple pores; more rarely sieve-type. Subcentral tubercle prominent. Paramphidont or holamphidont hinge and large 'U'-shape frontal scar.

Description. As for the type species.

Included species. *Anticythereis arcana* Bertels 1975*a*

Sthenarocythereis erymnos sp. nov.

Remarks. This genus is erected to embrace two species, one of which was placed in *Anticythereis* by Bertels, the other is new. Both species are manifestly not *Cythereis*, lacking three major longitudinal ribs and in possessing heavily complex reticulae. This genus differs from *Aleisocythereis* gen. nov. in that the latter possesses a reticulum in which the solae are circular or ovate. *Anebocythereis* Bate, 1972 has a hemimerodont hinge and narrow inner lamella. It differs from *Petalocythereis* gen. nov. in lacking a strong, ornate marginal rim and in lacking petaloid solae in the reticulum. Also *P. schilleri* (Bertels) is much more strongly spinose and *P. venusta* (Bertels) has a strong micro-ornament on the muri. The species identified by Bertels as *Anticythereis arcana*, cannot belong to that genus mainly because the valves have normal overlap, and quite different ornament. The two species of this genus bear different hinge, *S. arcana* being holamphidont while *S. erymnos* is paramphidont. This is not necessarily surprisingly, given that at this time, there was rapid evolution in the amphidont hinge towards the more efficient holamphidont variety.

Sthenarocythereis arcana (Bertels, 1975*a*) comb. nov.

Figure 16O-R; 17A-B

1975*a* *Anticythereis arcana* Bertels. p. 115, pl. 5, 19 a–b, 20–21.

Remarks. Although this species was described by Bertels (1975*a*), now that it has become the type species of a new genus, it is necessary to redescribe and rediagnose.

Type material. Holotype: specimens described by Bertels, housed in Facultad de Ciencias Exactas y Naturales, in Holotype 838; paratypes LM-FCEN 839-841, plus the three paratypes from this study 3527-3529 (Figs 16O, 17B; 16P, Q, R; 17A).

Material.18 specimens from sample 14, Maastrichtian; plus the type and other material of Bertels housed in the collections of the Facultad de Ciencias Exactas y Naturales, Laboratory of Micropaleontology, Univerisidad de Buenos Aires, Argentina.

Dimensions. In mm:

		L	H	W	
Paratype, adult,	LM-FCEN 3527	0. 662	0.475	0.241	sample 14
Paratype, adult,	LM-FCEN 3528	0.719	0.394		sample 14
Paratype, adult,	LM-FCEN 3529	0.716	0.368		sample 14

Diagnosis. An elongate species, subovate with extremely strong reticulate ornament, with strong peripheral rims at each end and ovate to polygonal reticular cells with strong tubercles, mainly conjunctive, single paired or multiple. Hinge holampidont.

Description. A large, thick-shelled ostracod, subrectangular in lateral view, elongate in dorsal view. Anterior margin broadly and symmetrically rounded with small, blunt marginal denticles and apex a little below mid-height. Posterior margin bluntly pointed with apex just above mid-height and with short, concave posterior dorsal slope and longer convex posterior ventral slope. Dorsal and ventral margins straight and subparallel. LV larger than right with overlap at end margins and dorsally. Greatest length above mid-height, greatest height at anterior cardinal angle, greatest width medianly. Surface strongly reticulate with distal reticulae parallel to the free margins. Muri polygonal, strong, smooth with rounded profile. They bear numerous rounded pestle-like tubercles often occurring in pairs or triplets, frequently conjunctive. Most seem blind but others are terminally perforate. Sieve-type pores also occur on the muri, frequently conjunctively. Reticulae varying in shape, largest and most elongate occur anteroventrally and posteriorly. Elsewhere, they range from circular, bifid, trefoil, quadrifoil to irregularly hexagonal. Most of the solae seem to have large inserted sieve plates. Valve surface with three longitudinal ribs. The dorsal rib, which is very peripheral, and

well-defined with a well-developed series of multiple tubercles along its length. The ventrolateral rib is similar; although the median rib, strongest in posterior half is less well-developed. Subcentral tubercle with very strong large irregularly, but poorly defined smooth area. Eye tubercle prominent. Internally, the calcified inner lamella is wide with a very narrow anterior vestibulum. Central muscle scar insert in the sub-central depression with a large obliquely orientated 'U'-shape frontal scar. The hinge is holamphidont, robustly developed with a smooth anteromedian element and stepped anterior tooth in the right valve. Sexual dimorphism not observed.

Remarks. This species differs from *Sthenarocythereis erymnos* sp. nov. in the nature and aspect of its reticulation, in its strong peripheral rims on the end margins and in the less strong tuberculate dorsal rib.

Stratigraphical range. Maastrichtian of Fortín General Roca, Río Negro (Bertels 1975*a*) and Cerro Azul, General Roca.

Sthenarocythereis erymnos sp. nov. Ceolin and Whatley

Figure 17C-G

LSID. urn:lsid:zoobank.org:act:xxxxxxxxx

Derivation of name. Gr. *ερυγνος* erymnos, strong, fortified. With reference to the very strong ornament of reticulum and conjunctive spines and tubercles.

Type material. Holotype: one complete carapace, LM-FCEN 3530 (Fig. 17C); paratypes: LM-FCEN 3531-3534 (Figs 17D; 17E; 17F; 17G).

Material. 92 specimens from samples 1, 3, 5 and 12. Maastrichtian.

Diagnosis. A strongly reticulocostate species of *Sthenarocytereis* with the reticulum around the margins comprising muri that are preferentially orientated to those margins. Subcentral tubercle very strongly developed with a ramifying extension dorsally. Eye tubercle strongly

developed. Anterior and posterior marginal rims not strongly developed, but strongly denticulate antero and posteroventrally. Hinge paramphidont.

Dimensions. In mm:

		L	H	W	
Holotype, female,	LM-FCEN 3530	0.733	0.477		sample 3
Paratype, female,	LM-FCEN 3531	0.725	0.437		sample 5
Paratype, male,	LM-FCEN 3532	0.905	0.457		sample 3
Paratype, male,	LM-FCEN 3533	0.875	0.446		sample 5
Paratype, female,	LM-FCEN 3534	0.734	0.386	0.386	sample 5

Description. A large, thick-shelled ostracod, subrectangular in lateral view, subovate in dorsal view with compressed extremities. Valves subequal with LV overlap the RV mainly in ventral region. Anterior margin broadly rounded with apex at mid-height and denticulate. Posterior margin subcaudate with apex at mid-height. Dorsal margin straight but overhung by valve tumidity and ornamentation. The ventral margin is obscured by valve tumidity; oral invagination is well seen internally. Greatest height at the anterior cardinal angle. The surface is strongly reticulate with rather short, mostly conjunctive mural spines; less developed centrally. Peripherally, the muri have a circular orientation parallel to the margins. This orientation is largely lost centrally. The muri bear rather small tubercles that are terminally blind and these are largely absent medianly. The solae contain deeply recessed sieve plates and of mostly trefoil or quatrefoil pattern. The muri also bear smaller sieve-type pores. Only in the extreme posterior is this pattern of ornamentation absent. Subcentral tubercle largely low and strongly reflected internally. Eye tubercle well-developed. Calcified inner lamella very wide; avestibulate. Central muscle scar in subcentral tubercle depression. Frontal scar very large and ‘U’-shaped. Hinge clearly paramphidont. Internal eye-sinus well-developed

and positioned below the anterior element of the hinge. Strong sexual dimorphism with males more elongate and lower than females.

Remarks. *Sthenarocythereis erymnos* sp. nov. differs from *Sthenarocythereis arcana* (Bertels, 1975*a*) in that the reticulation pattern that is less strongly developed, although fossae are somewhat similar in both species.

Stratigraphical range. Maastrichtian of Cerro Azul, General Roca.

Genus VEENIA Butler and Jones, 1957

Type species. *Cythereis ozanana* Israelsky, 1929

Veenia tumida (Bertels, 1975*a*)

Figure 17H

1975*a* *Veenia (Nigeria) tumida* Bertels, p. 123, pl. 4, fig. 7.

1995 *Nigeria tumida* Bertels-Psotka, p. 167, pl. 2, fig. 8

Material. Five specimens from samples 5 and 12. Maastrichtian.

Dimensions. Adult valve, LM-FCEN 3535, 0.941 (L), 0.594 (H).

Stratigraphical range. Maastrichtian of Fortín General Roca, Río Negro (Bertels 1975*a*) and Cerro Azul, General Roca.

Subfamily BUNTONIINAE Apostolescu, 1961

Genus HUANTRAICONELLA Bertels, 1968*a*

Type species. *Huantraiconella prima* Bertels, 1968*a*

Huantraiconella costata (Bertels, 1975*c*) comb. nov.

Figure 17I

1975*c* *Harringtonia costata* Bertels, p. 263, pl. 1, fig. 1, a–b.

1968*a* *Huantraiconella prima* Bertels, p. 254, pl. 1, figs 1, a–c; 2, a–b.

Material. 22 specimens from samples 16, 17, 21, 26 and 40. Danian.

Dimensions. Adult carapace, LM-FCEN 3536, 0.821 (L), 0.497 (H).

Remarks. We do not consider that *Harringtonia* (Bertels, 1975*c*) differs in any significant manner from *Huantraiconella* Bertels, 1968*a* and we therefore, subsume the former within the latter.

Stratigraphical range. Danian of Fortín General Roca, Río Negro, (Bertels 1975*b*) and Cerro Azul, General Roca.

Subfamily UNICAPELLINAE Dingle, 1981

Genus UNICAPELLA Dingle, 1980

Type species. *Unicapella sacsi* Dingle, 1980

Unicapella? sp.1

Figure 17J

Material. Two complete carapaces from sample 3. Maastrichtian.

Dimensions. Carapace, LM-FCEN 3537: 0.941 (L), 0.596 (H).

Diagnosis. Large, elongate, subrectangular in lateral view. Anterior margin broadly rounded with apex below mid-height. Posterior margin subcaudate with apex a little above ventral margin. Dorsal margin straight, overhung by dorsal rib and posterodorsal tubercle. Ventral margin very gently sinuous. LV larger than RV especially anterodorsally. Ornament with several large tubercles, with large free marginal rim and ventrolateral rib. Subcentral tubercle well developed. Eye tubercle present and a hinge ear in LV. A deep conical depression occurs on the anterior margin. Surface coverd with a net of small circular meshes. Internal features not seen.

Remarks. Differs from *Unicapella sacsi* Dingle, 1980 from the Campanian of Richard Bay, South Africa, in the absence of spines, in the anterior and posterior marginal rims being less

strongly developed and in the reticulation pattern that is absent at anterior and posterior ends. Differs from *Curfsina kafkai kafkai* Pokorny, 1967, from Cretaceous of Czech Republic in a less developed marginal rim and in the absence of a median rib. Also in *C. kafkai kafkai* the intercostal surface is smooth.

Unicapella? sp. 2

Figure 17K

Material. Six specimens from samples 16, 17, 19 and 21. Danian.

Dimensions. Adult carapace, LM-FCEN 3538, 0.840 (L), 0.342 (H).

Diagnosis. Large, elongate subrectangular in lateral view. Irregularly subovate with compressed terminal end margins (especial anteriorly) in dorsal view. Anterior margin broadly rounded with apex at mid-height and strongly denticulate, posterior bluntly rounded with apex well below mid-height and denticulate. Dorsal margin straight, rising to dorsal cardinal angle. Ventral margin straight. Ornamentation reticulocostate and very irregular. Subcentral tubercle large. Five structures, the dentate antero and posteromarginal rims, the ventrolateral rib, the median rib and a short, but prominent rib extends near ventically from a posterodorsal position, are all well-developed. Intercostal area, particularly posteriorly, with circular and oval reticulae. Few normal pore canal, mostly simple. Internal features not seen.

Remarks. This species is left in question due to the absence of spines on its surface, absence of a hinge ear in LV at anterocardinal angle, in being larger in size than the type species of genus (L: 0.60, H: 0.33). Differs from *Unicapella*? sp. 1 in the nature of its reticulation and in the absence of a hinge ear in LV.

Subfamily *incertae sedis*

Genus CLINOCYTHEREIS Ayress and Swanson, 1991

Type species. *Clinocythere australis* Ayress and Swanson, 1991

Clinocythereis sp.

Figure 17L

Material. Four specimens from samples 17 and 21. Danian.

Dimensions. Adult carapace, LM-FCEN 3539, 0.397 (L), 0.175 (H).

Description. Small, elongate subtriangular, with LV slightly larger than RV. Anterior margin rounded, posterior margin subcaudate, slightly "upturned" with concave posterodorsal slope. Surface smooth except for four short parallel longitudinal ribs on the ventrolateral surface.

Remarks. Differs from the type species *Clinocythereis australis* Ayress and Swanson, 1991, from the Oligocene of New Zealand in that the caudal process is less "downturned" and by the presence of four small ribs ventrolaterarly. It also differs from *C*. aff. *C*. *australis* Bergue *et al*., 2006 from the Quaternary of the Santos Basin, Brazil in the same characteristics as Ayres and Swanson's species.

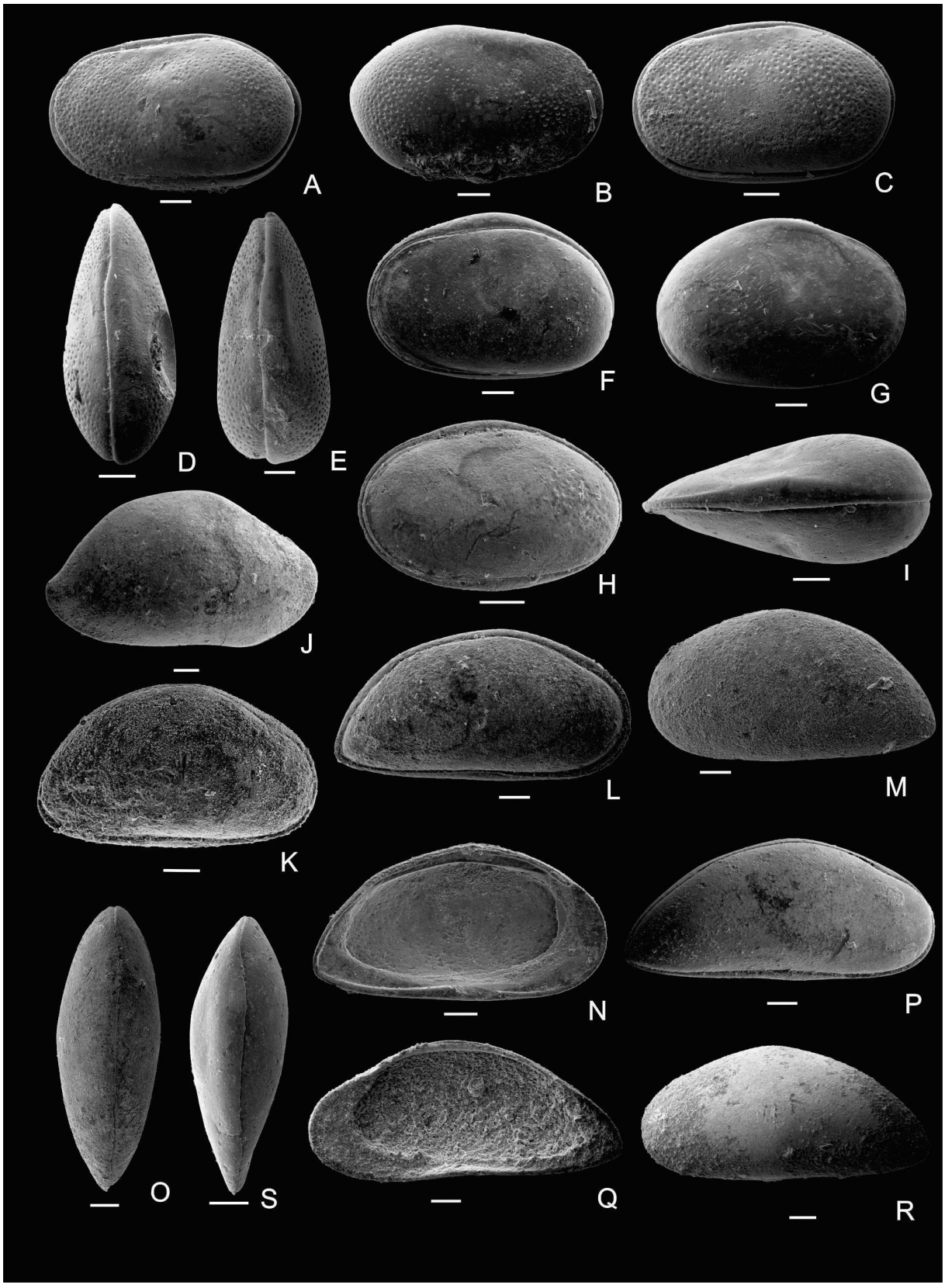
A
B
C
D
E
F
G
H
I
J
K
L
M
N
O
P
Q
R
S

FIG. 3. Photomicrographs of Ostracoda from the Cerro Azul section, Neuquén Basin. All scale bars represent 100 μm. A-E, *Cytherella saraballentae* sp. nov.; A, B, holotype, LM-FCEN 3232, A, adult carapace, female, left lateral view; B, right lateral view; C, D, paratype, LM-FCEN 3233, C, adult male carapace, right lateral view; D, dorsal view; E, paratype, LM-FCEN 3234, male, dorsal view. F-I, *Cytherella semicatillus* sp. nov.; F, G, I, holotype, LM-FCEN 3235, F, adult female carapace, left lateral view; G, right lateral view, I, dorsal view; H, paratype, LM-FCEN 3236, juvenile carapace, left lateral view. J, *Bairdoppilata* sp., LM-FCEN 3237, adult valve, right lateral view. K, *Bairdoppilata*? sp. LM-FCEN 3238, adult carapace, right lateral view. L-O, *Paracypris bertelsae* sp. nov.; L, O, holotype, LM-FCEN 3239, L, adult carapace, right lateral view; O, dorsal view; M, paratype, LM-FCEN 3240, adult valve, left lateral view; N, paratype, LM-FCEN 3241, adult valve, internal view. P-S, *Paracypris imaguncula* sp. nov; P, S, holotype, LM-FCEN 3242, P, adult carapace, right lateral view; S, dorsal view; Q, paratype, LM-FCEN 3243, adult valve, internal view; R, paratype, LM-FCEN 3244, adult valve, left lateral view.

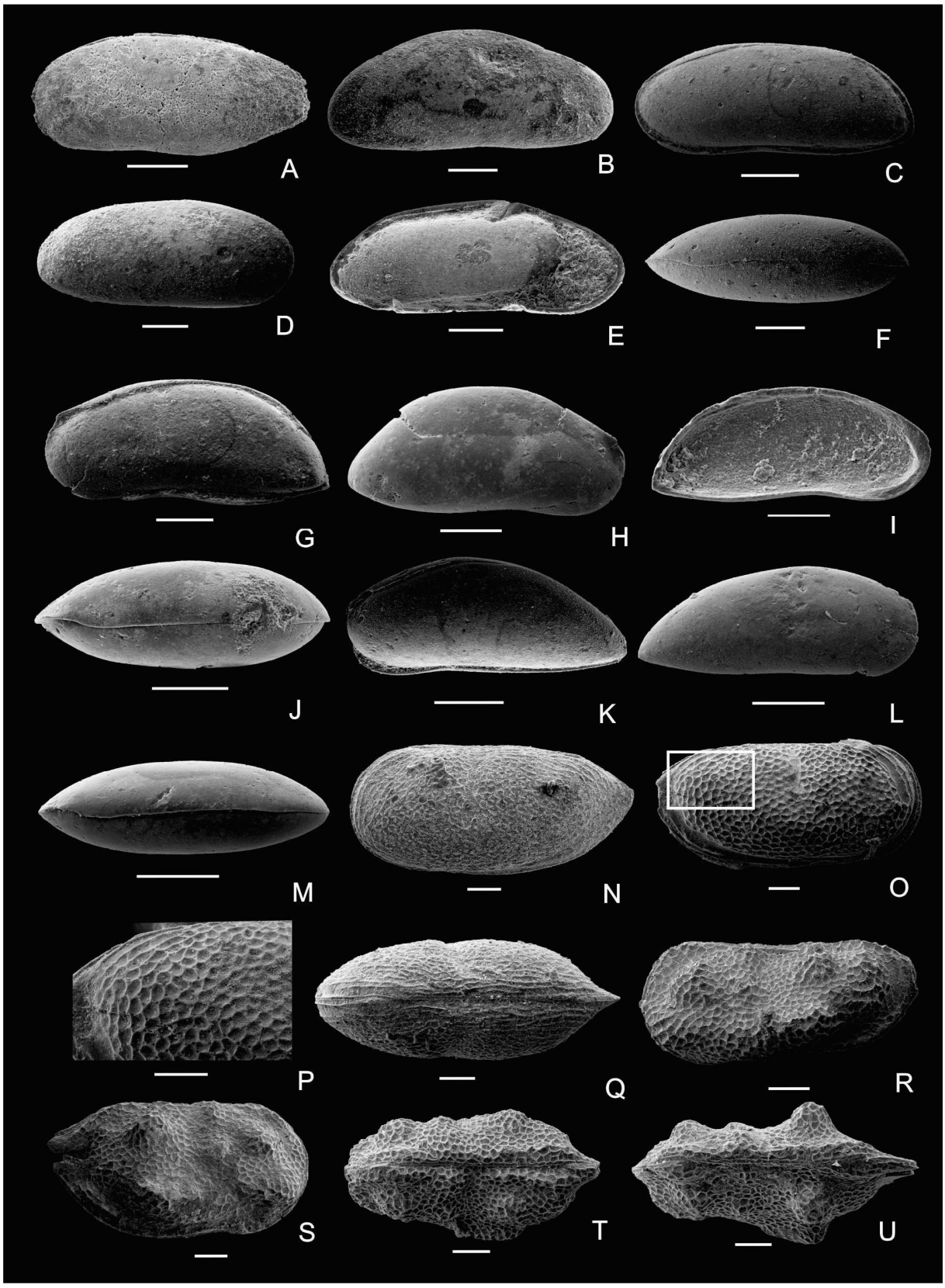
A
B
C
D
E
F
G
H
I
J
K
L
M
N
O
P
Q
R
S
T
U

FIG. 4. Photomicrographs of Ostracoda from the Cerro Azul section, Neuquén Basin. All scale bars represent 100 μm. A, *Paracypris*? sp., LM-FCEN 3245, adult carapace, left lateral view. B, *Aglaiocypris*? sp., LM-FCEN 3246, adult valve, right lateral view. C-F, *Argilloecia abnormalis* sp. nov.; C, holotype, LM-FCEN 3247, adult carapace, left lateral view; D, paratype, LM-FCEN 3248, adult valve, right lateral view; E, paratype, LM-FCEN 3249, adult valve, internal view; F, paratype, LM-FCEN 3250, adult carapace, dorsal view. G-J, *Argilloecia concludos* sp. nov.; G, holotype, LM-FCEN 3251, adult carapace, left lateral view; H, paratype, LM-FCEN 3252, juvenile carapace, right lateral view; I, paratype, LM-FCEN 3253, juvenile valve, internal view; J, paratype, LM-FCEN 3254, juvenile carapace, dorsal view. K-M, *Argilloecia hydrodynamicus* sp. nov., K, holotype, LM-FCEN 3255, adult carapace, left lateral view; L, paratype, LM-FCEN 3256, juvenile valve, right lateral view; M, paratype, LM-FCEN 3257, juvenile, carapace, dorsal view. N-Q, *Bythoceratina cheleutos* sp. nov.; N, Q, holotype, LM-FCEN 3258, N, adult carapace, left lateral view; Q, carapace, dorsal view; O, P, paratype, LM-FCEN 3259, O, adult carapace, right lateral view; P, detail of ornamentation. R-U, *Bythoceratina rocana* (Bertels 1973) comb. nov.; R, T, paratype, LM-FCEN 3260, R, adult, female carapace, left lateral view; T, dorsal view; S, U, paratype, LM-FCEN 3261, S, adult male carapace, right lateral view; U, dorsal view.

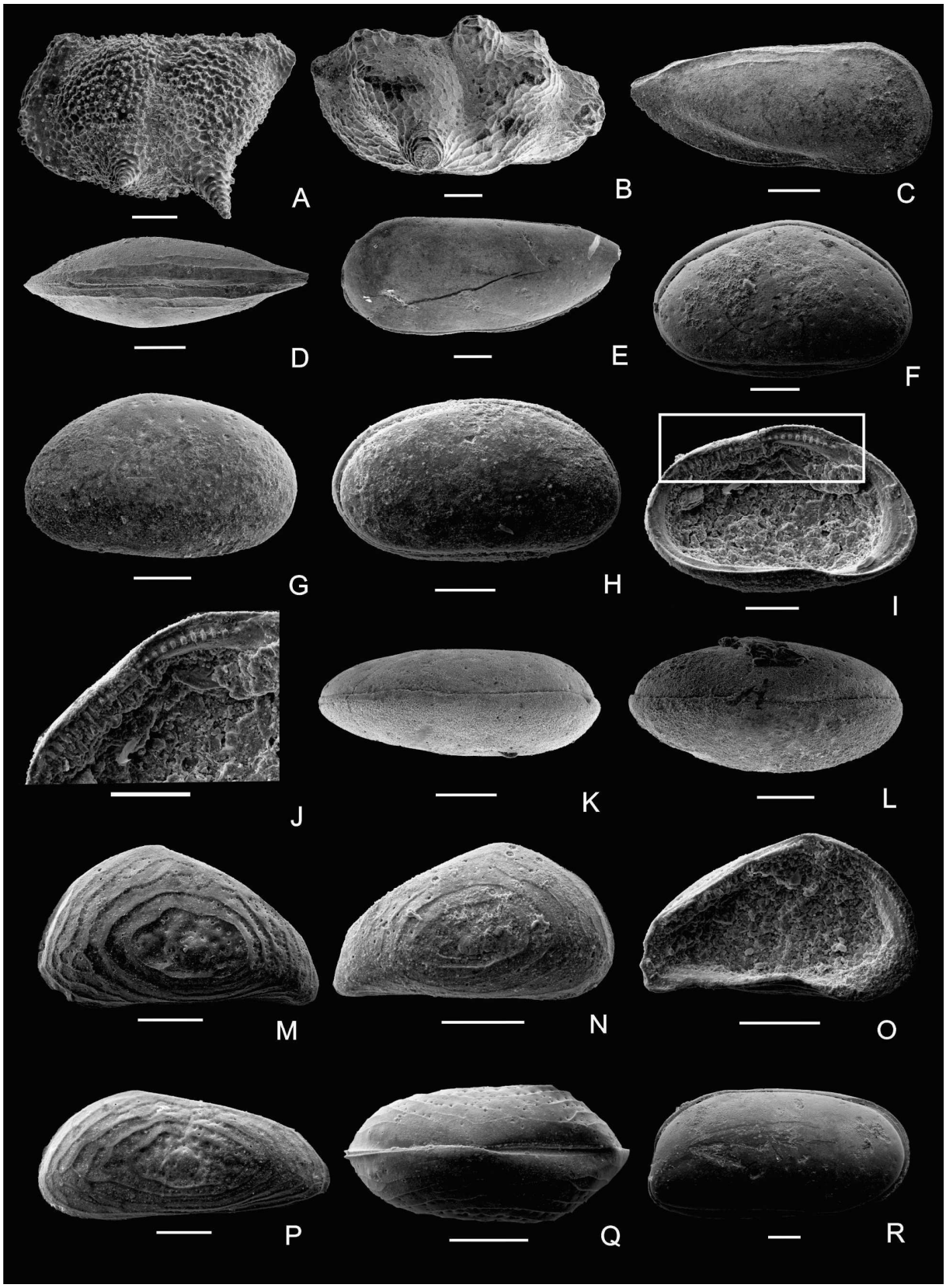
A
B
C
D
E
F
G
H
I
J
K
L
M
N
O
P
Q
R

FIG. 5. Photomicrographs of Ostracoda from the Cerro Azul section, Neuquén Basin. All scale bars represent 100 μm. A, *Bythoceratina* sp. aff. *Bythoceratina scaberrima* (Brady 1887), LM-FCEN 3262 (lost), adult valve, left lateral view. B, *Bythoceratina* sp., LM-FCEN 3263, adult valve, right lateral view. C-D, *Pseudocythere* sp., LM-FCEN 3264, C, adult carapace, right lateral view; D, dorsal view. E, *Thanycythere* sp.; LM-FCEN 3265, adult carapace, left lateral view. F-L, *Phelocyprideis acardomesido* gen. et sp. nov.; F, holotype, LM-FCEN 3266, carapace, female, right lateral view; G, paratype, LM-FCEN 3267, female valve, left lateral view; H, paratype, LM-FCEN 3268, adult male carapace, right lateral view; I, J, paratype, LM-FCEN 3269, I, female valve, internal view; J, detail of alternamerodont hinge; K, paratype, LM-FCEN 3270, adult male carapace, dorsal view; L, paratype, LM-FCEN 3271, adult female carapace, dorsal view. M-Q, *Eucythere dinetos* sp. nov., M, holotype, LM-FCEN 3272, adult female valve, left lateral view; N, paratype, LM-FCEN 3273 female, juvenile valve, right lateral view; O, paratype, LM-FCEN 3274, adult female valve, internal view; P, paratype, LM-FCEN 3275, adult male valve, left lateral view; Q, paratype, LM-FCEN 3276, carapace, female, dorsal view. R, *Krithe crepidus* sp. nov., holotype, LM-FCEN 3277, adult carapace, right lateral view.

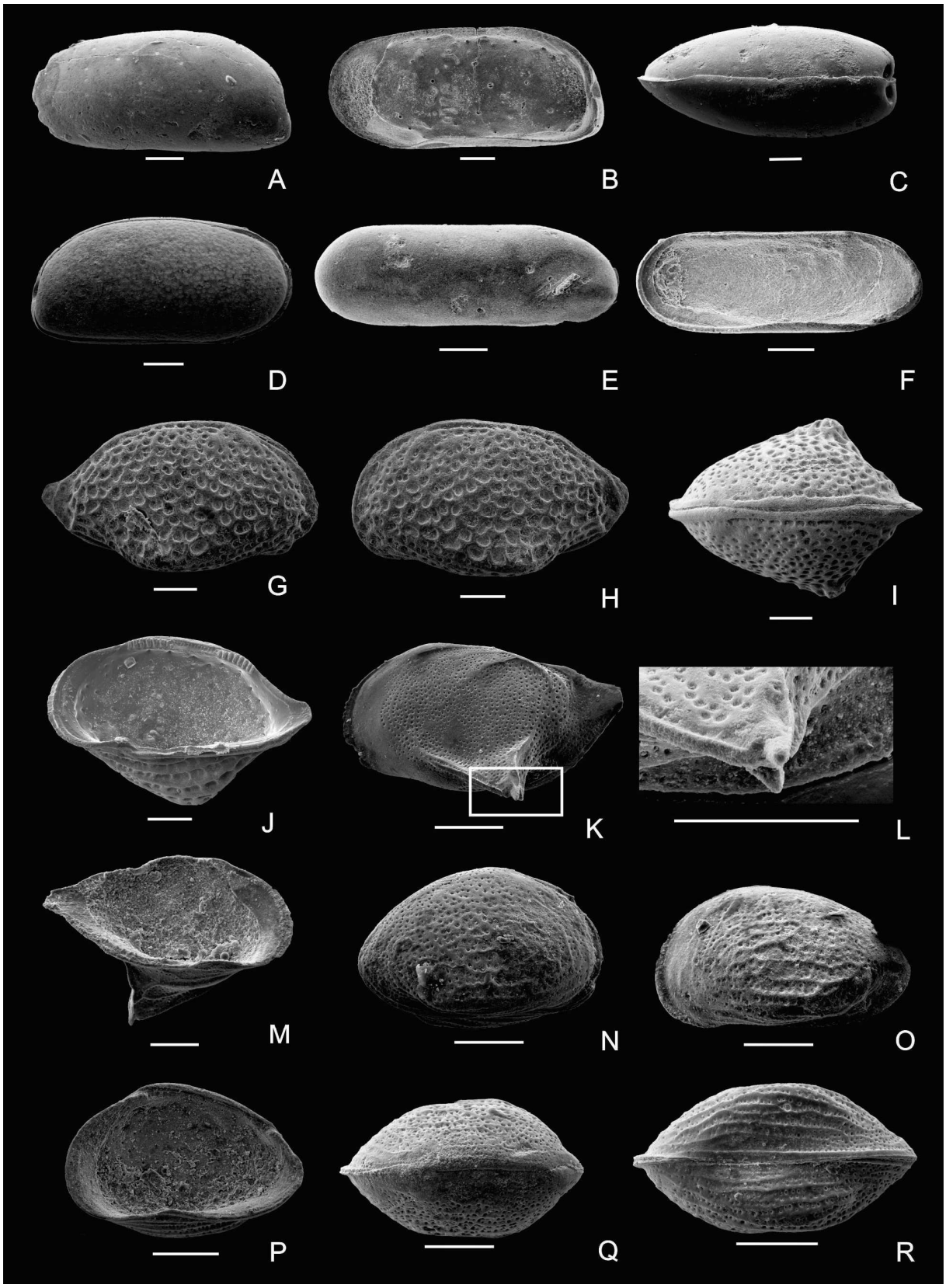
A
B
C
D
E
F
G
H
I
J
K
L
M
N
O
P
Q
R

FIG. 6. Photomicrographs of Ostracoda from the Cerro Azul section, Neuquén Basin. All scale bars represent 100 μm. A-C, *Krithe crepidus* sp. nov., A, paratype, LM-FCEN 3278, adult valve, left lateral view; B, paratype, LM-FCEN 3279, adult valve, internal view; C, holotype LM-FCEN 3277, dorsal view. D, *Krithe* sp., LM-FCEN 3280, adult carapace, right lateral view. E-F, *Copytus* sp., LM-FCEN 3281, E, adult valve, right lateral view; F, internal view. G-J, *Cytheropteron hyperdictyon* sp. nov.; G, holotype, LM-FCEN 3282, adult valve, right lateral view; H, paratype, LM-FCEN 3283, adult valve, left lateral view; I, paratype, LM-FCEN 3284, adult carapace, dorsal view; J, paratype, LM-FCEN 3285, adult valve, internal view. K-M, *Cytheropteron bidentinos* sp. nov., K, L, holotype, LM-FCEN 3286, K, adult valve, left lateral view; L, detail of the spine; M, paratype, LM-FCEN 3287, adult valve, internal view. N-R, *Cytheropteron translimitares* sp. nov., N, Q, holotype, LM-FCEN 3288, N, adult carapace, right lateral view; Q, dorsal view; O, paratype, LM-FCEN 3289, adult valve, left lateral view; P, paratype, LM-FCEN 3290, adult valve, internal view; R, paratype, LM-FCEN 3291, adult carapace, ventral view.

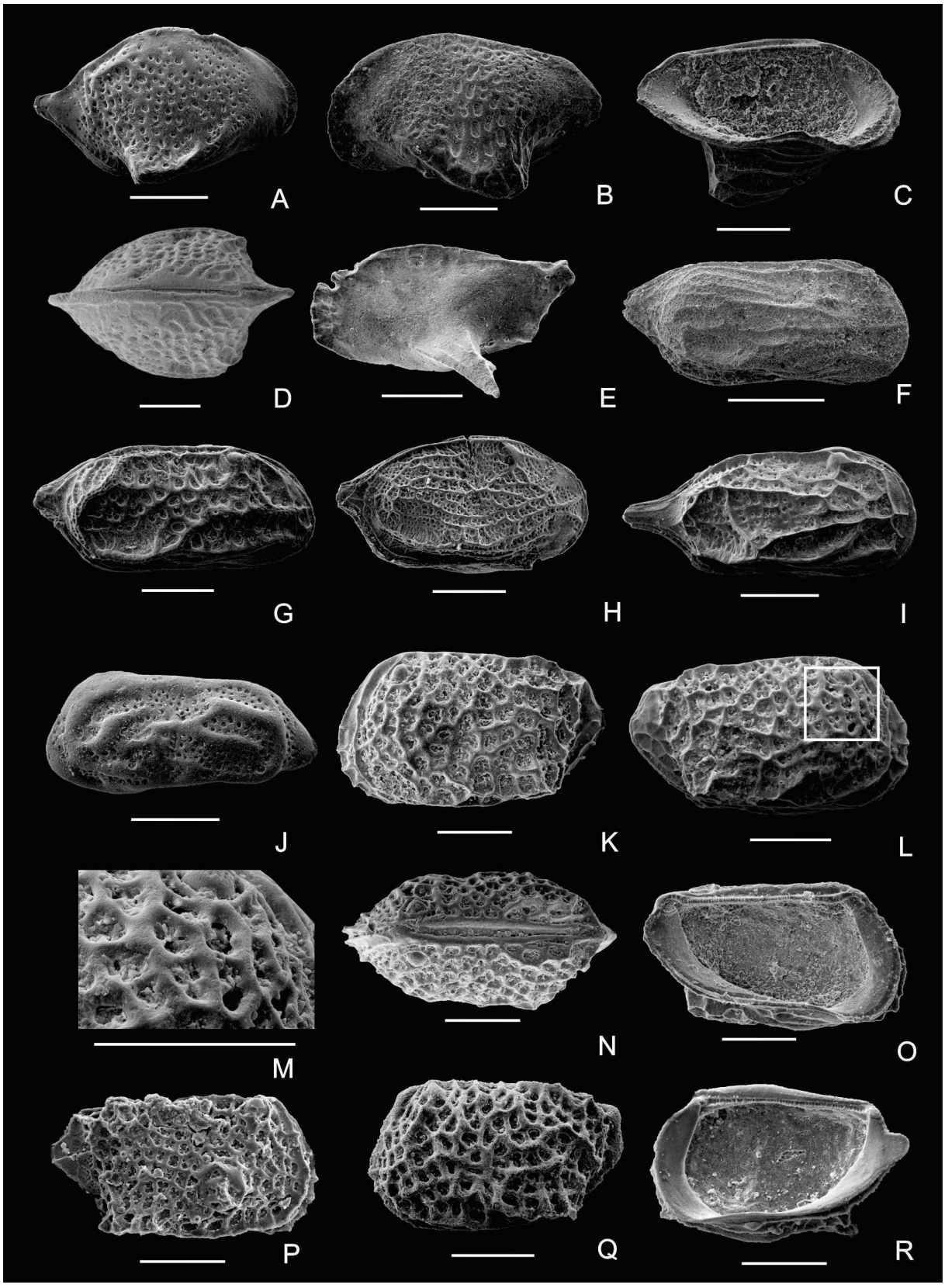
A
B
C
D
E
F
G
H
I
J
K
L
M
N
O
P
Q
R

FIG. 7. Photomicrographs of Ostracoda from the Cerro Azul section, Neuquén Basin. All scale bars represent 100 μm. A, *Cytheropteron* sp., LM-FCEN 3292, valve, right lateral view. B-D, *Aversovalva glochinos* sp. nov., B, holotype, LM-FCEN 3293 (lost), adult valve, left lateral view; C, paratype, LM-FCEN 3294, adult valve, internal view; D, paratype, LM-FCEN 3295, adult carapace, dorsal view. E, *Pedicythere* sp., LM-FCEN 3296, adult valve, left lateral view. F, *Semicytherura argentinensis* (Bertels, 1974), LM-FCEN 3297, adult carapace, right lateral view. G, *Semicytherura* sp. 1, LM-FCEN 3298, adult carapace, right lateral view. H, *Semicytherura* sp. 2, LM-FCEN 3299, adult carapace, right lateral view. I, *Semicytherura* sp. 3, LM-FCEN 3300, adult carapace, right lateral view. J, *Semicytherura*? sp., LM-FCEN 3301, adult valve, left lateral view. K-O, *Eucytherura stibaros* sp. nov., K, holotype, LM-FCEN 3302, adult carapace, left lateral view; L, M, N, paratype, LM-FCEN 3303, L, adult carapace, right lateral view; M, detail of ornamentation; N, dorsal view; O, paratype, LM-FCEN 3304, adult valve, internal view. P, *Eucytherura* sp. 1, LM-FCEN 3305 (lost), adult valve, right lateral view. Q-R, *Eucytherura* sp. 2, LM-FCEN 3306, Q, adult valve, left lateral view; R, internal view.

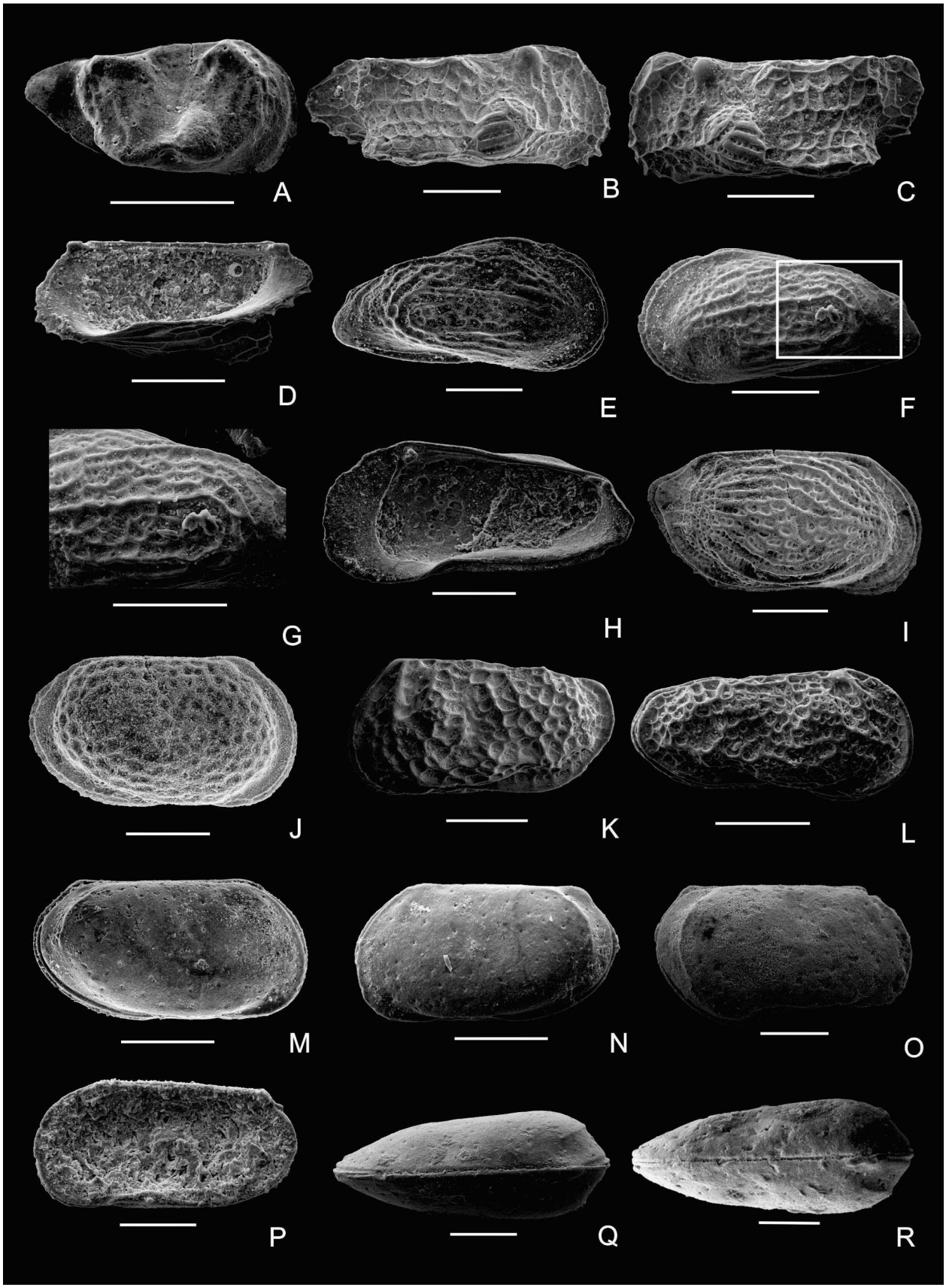
A
B
C
D
E
F
G
H
I
J
K
L
M
N
O
P
Q
R

FIG. 8. Photomicrographs of Ostracoda from the Cerro Azul section, Neuquén Basin. All scale bars represent 100 μm. A, *Hemiparacytheridea* sp., LM-FCEN 3307 (lost), adult valve, right lateral view. B-D, *Hemingwayella verrucosus* sp. nov.; B, holotype, LM-FCEN 3308 (lost), adult valve, right lateral view; C, paratype, LM-FCEN 3309, juvenile valve, left lateral view; D, paratype, LM-FCEN 3310, adult valve, internal view. E-H, *Heinia prostatopleuricos* sp. nov.; E, holotype, LM-FCEN 3400, adult carapace, right lateral view; F, G, paratype, LM-FCEN 3401, F, adult carapace, left lateral view; G, detail of the ribs; H, paratype, LM-FCEN 3402, adult valve, internal view. I, *Loxoconcha* sp. aff. *Loxoconcha cretacea* Alexander, 1936, LM-FCEN 3403, adult valve, right lateral view. J, *Palmoconcha similis* (Bertels, 1973), LM-FCEN 3404, adult female carapace, right lateral view. K, *Sagmatocythere*? sp. 1, LM-FCEN 3405, adult valve, left lateral view. L, *Sagmatocythere*? sp. 2, LM-FCEN 3406, adult carapace, right lateral view. M-R, *Loxoconcha* (s.l.) *posterocosta* sp. nov., M, Q, holotype, LM-FCEN 3407, M, adult female carapace, right lateral view; Q, dorsal view; N, paratype, LM-FCEN 3408, adult female carapace, left lateral view; O, paratype, LM-FCEN 3409, adult male carapace, right lateral view; P, paratype, LM-FCEN 3410, adult female valve, internal view; R, paratype, LM-FCEN 3411, adult male carapace, dorsal view.

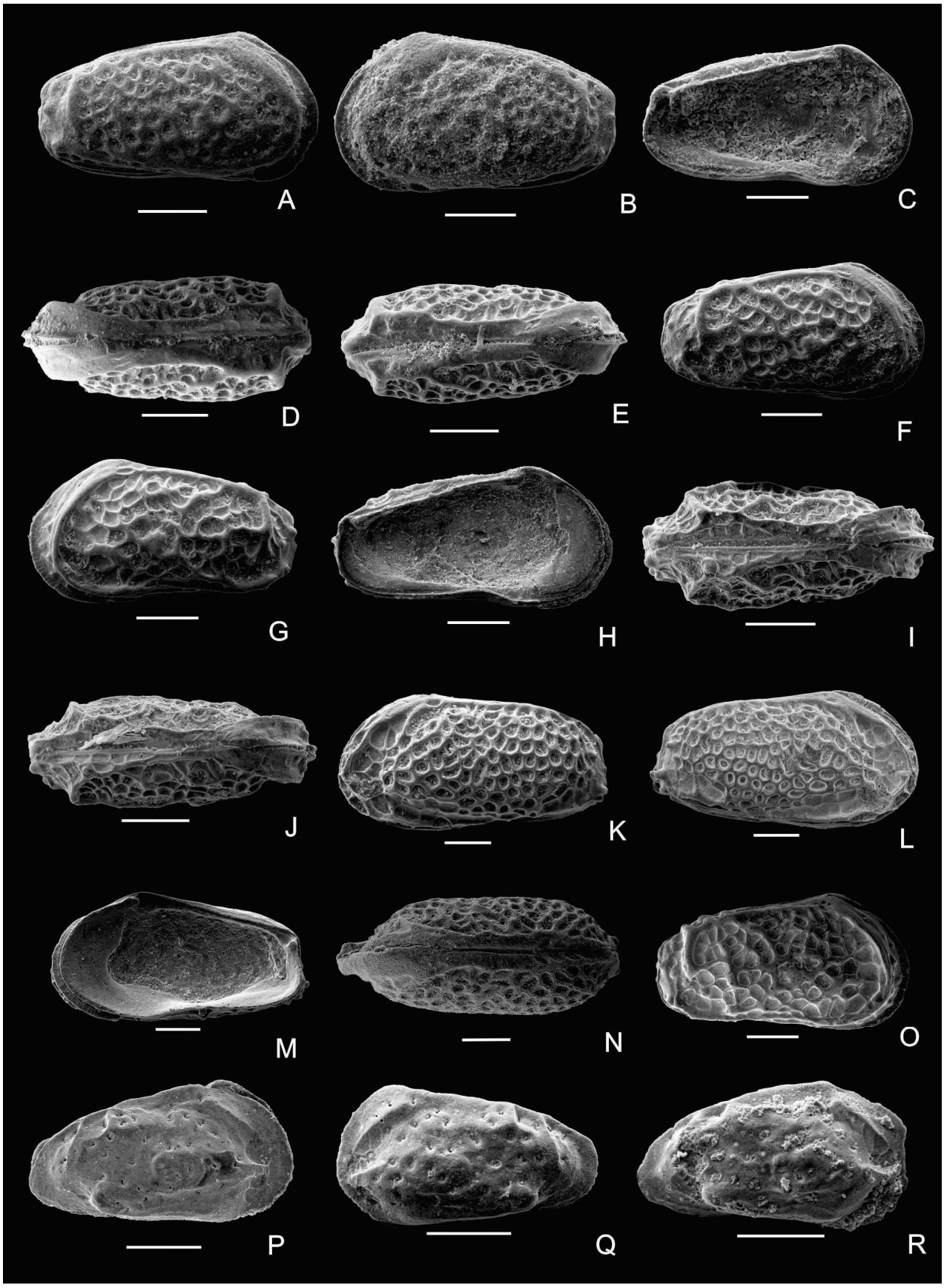
A
B
C
D
E
F
G
H
I
J
K
L
M
N
O
P
Q
R

FIG. 9. Photomicrographs of Ostracoda from the Cerro Azul section, Neuquén Basin. All scale bars represent 100 μm. A-E, *Keijia circulodictyon* sp. nov., A, holotype, LM-FCEN 3412, adult female carapace, right lateral view; B, paratype, LM-FCEN 3413, adult female carapace, left lateral view; C, paratype, LM-FCEN 3414, adult female valve, internal view; D, paratype, LM-FCEN 3415, adult female carapace, dorsal view; E, paratype, LM-FCEN 3416, adult carapace, male, dorsal view. F-J, *Keijia kratistos* sp. nov., F, holotype, LM-FCEN 3417, adult female carapace, right lateral view; G, paratype, LM-FCEN 3418, adult female carapace, left lateral view; H, paratype, LM-FCEN 3419, adult valve, internal view; I, paratype, LM-FCEN 3420, adult female carapace, dorsal view; J, paratype, LM-FCEN 3421, adult male, carapace, dorsal view. K-N, *Keijia flexuosa* (Bertels 1975*a*) comb. nov.; K, paratype, LM-FCEN 3422, adult carapace, left lateral view; L paratype, LM-FCEN 3423, adult carapace, right lateral view; M, paratype, LM-FCEN 3424, adult valve, internal view, N, paratype, LM-FCEN 3425, adult carapace, dorsal view. O, *Keijia huantraicoensis (*Bertels, 1969*a*) comb. nov.; LM-FCEN 3426, adult female carapace, right lateral view. P-R, *Paramunseyella epaphroditus* sp. nov.; P, holotype, LM-FCEN 3427, adult carapace, right lateral view; Q, paratype, LM-FCEN 3428, adult valve, left lateral view; R, paratype, LM-FCEN 3429, adult valve, right lateral view.

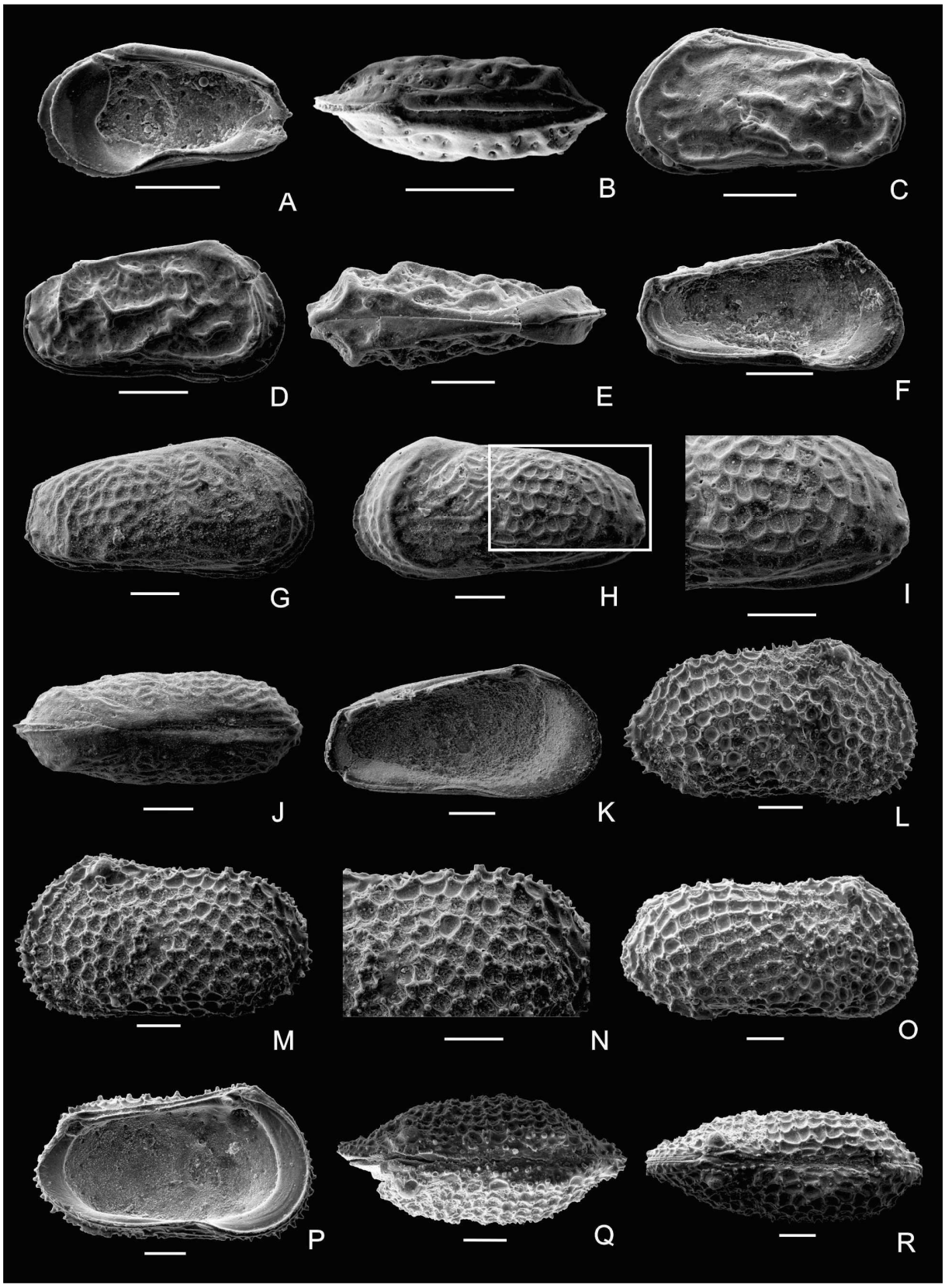
A
B
C
D
E
F
G
H
I
J
K
L
M
N
O
P
Q
R

FIG. 10. Photomicrographs of Ostracoda from the Cerro Azul section, Neuquén Basin. All scale bars represent 100 μm. A-B, *Paramunseyella epaphroditus* sp. nov.; A, paratype, LM-FCEN 3430, adult valve, internal view; B, paratype, LM-FCEN 3431, adult carapace, dorsal view. C-F, *Munseyella costaevermiculatus* sp. nov.; C, holotype, LM-FCEN 3432, adult carapace, left lateral view; D, paratype, LM-FCEN 3433, adult carapace, right lateral view; E, paratype, LM-FCEN 3434, adult carapace, dorsal view; F, paratype, LM-FCEN 3435, adult valve, internal view. G-K, *Ameghinocythere archaios* sp. nov.; G, J, holotype, LM-FCEN 3436, G, adult carapace, right lateral view; J, dorsal view; H, I, paratype, LM-FCEN 3437, H, adult valve, left lateral view; I, detail of reticulation; K, paratype, LM-FCEN 3438, adult valve, internal view. L-R, *Aleisocythereis polikothonus* sp. nov., L, holotype, LM-FCEN 3439, adult female valve, right lateral view; M, N, paratype, LM-FCEN 3440, M, female, left lateral view; N, detail of a cup-like structure; O, paratype, LM-FCEN 3441 adult male valve, right lateral view; P, paratype, LM-FCEN 3442, adult female valve, internal view; Q, paratype, LM-FCEN 3443, adult female carapace, dorsal view; R, paratype, LM-FCEN 3444, adult male carapace, dorsal view.

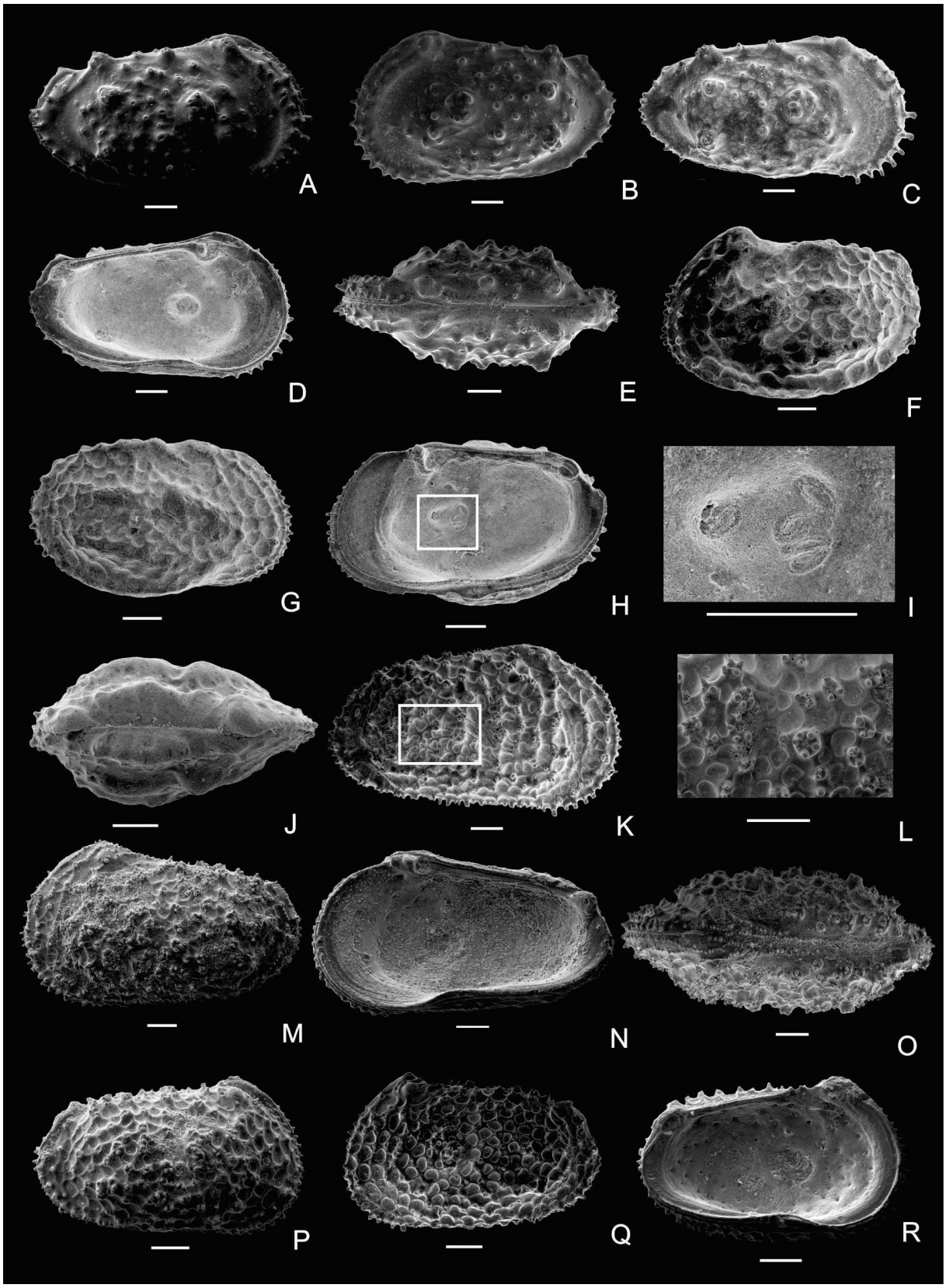
A
B
C
D
E
F
G
H
I
J
K
L
M
N
O
P
Q
R

FIG. 11. Photomicrographs of Ostracoda from the Cerro Azul section, Neuquén Basin. All scale bars represent 100 μm. A-E, *Apatoleberis noviprinceps* (Bertels, 1975*a*) comb. nov.; A, paratype, LM-FCEN 3445, adult female carapace, right lateral view; B, paratype, LM-FCEN 3446, adult female valve, left lateral view; C, paratype, LM-FCEN 3447, adult male, right lateral view; D, paratype, LM-FCEN 3448, adult female valve, internal view; E, paratype, LM-FCEN 3449, adult female carapace, dorsal view. F-J, *Mimicocythereis attilai* (Bertels, 1975*a*) comb. nov.; F, paratype, LM-FCEN 3450, adult female valva, left lateral view; G, paratype, LM-FCEN 3451, adult female valve, right lateral view; H, I, paratype, LM-FCEN 3452, H, adult female valve, internal view; I, detail of CMS; J, paratype, LM-FCEN 3453, adult female carapace, dorsal view. K-O, *Castillocythereis multicastrum* gen. et sp. nov.; K, L, holotype, LM-FCEN 3454, K, adult valve, right lateral view; L, multi tubercular castle-like pore conuli; M, paratype, LM-FCEN 3455, adult male valve, left lateral view; N, paratype, LM-FCEN 3456, adult male valve, internal view; O, paratype, LM-FCEN 3457, adult female carapace, dorsal view. P-R, *Castillocythereis albertoriccardii* sp. nov.; P, holotype, LM-FCEN 3458, adult carapace, right lateral view; Q, paratype, LM-FCEN 3459, adult valve, left lateral view; R, paratype, LM-FCEN 3460, adult valve, internal view.

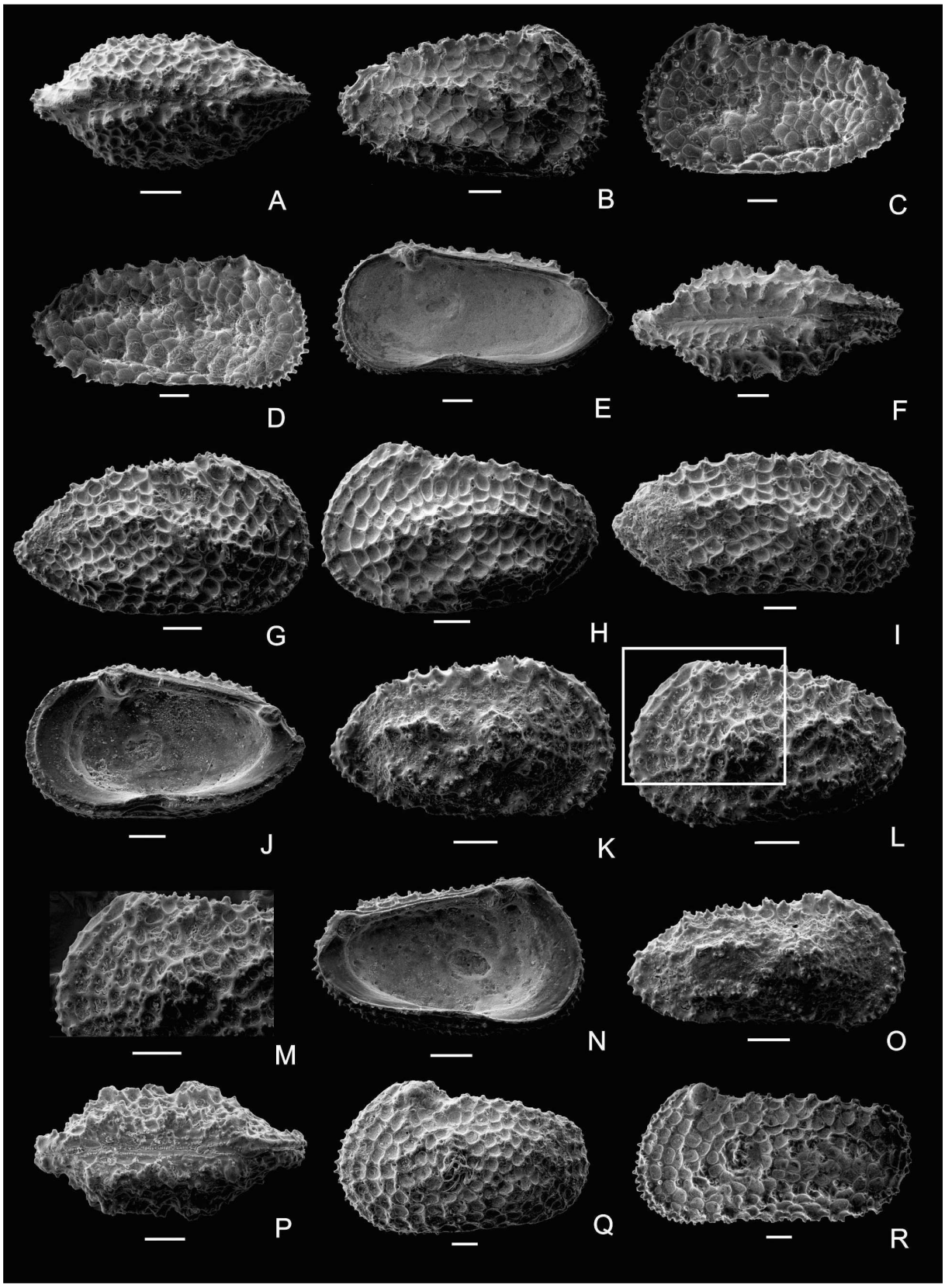
A
B
C
D
E
F
G
H
I
J
K
L
M
N
O
P
Q
R

FIG. 12. Photomicrographs of Ostracoda from the Cerro Azul section, Neuquén Basin. All scale bars represent 100 μm. A, *Castillocythereis albertoriccardii* sp. nov.; holotype, LM-FCEN 3458, adult carapace, dorsal view. B-F, *Cythereis stratios* sp. nov.; B, holotype, LM-FCEN 3461, adult female carapace, right lateral view; C, paratype, LM-FCEN 3462, adult female valve, left lateral view; D, paratype LM-FCEN 3463, adult male valve, right lateral view; E, paratype, LM-FCEN 3464, adult male valve, internal view; F, paratype, LM-FCEN 3465, adult female carapace, dorsal view. G-J, *Cythereis clibanarius* sp. nov., G, holotype, LM-FCEN 3466, adult female valve, right lateral view; H, paratype, LM-FCEN 3467, adult female valve, left lateral view; I; paratype, LM-FCEN 3468, adult male valve, right lateral view; J, paratype, LM-FCEN 3469, adult female valve, internal view. K-P, *Cythereis trajectiones* sp. nov.; K, holotype, LM-FCEN 3470, adult female valve, right lateral view; L, M, paratype, LM-FCEN 3471, L, adult female valve, left lateral view; M, detail of ornamentation; N, paratype, LM-FCEN 3472, adult female valve, internal view; O, paratype, LM-FCEN 3473, adult male valve, right lateral view; P, paratype, LM-FCEN 3474, adult carapace, dorsal view. Q-R, *Henryhowella* (*Henryhowella*) *nascens* (Bertels, 1969*c*); Q, paratype, LM-FCEN 3475, adult female valve, left lateral view; R, paratype, LM-FCEN 3476, adult male valve, left lateral view.

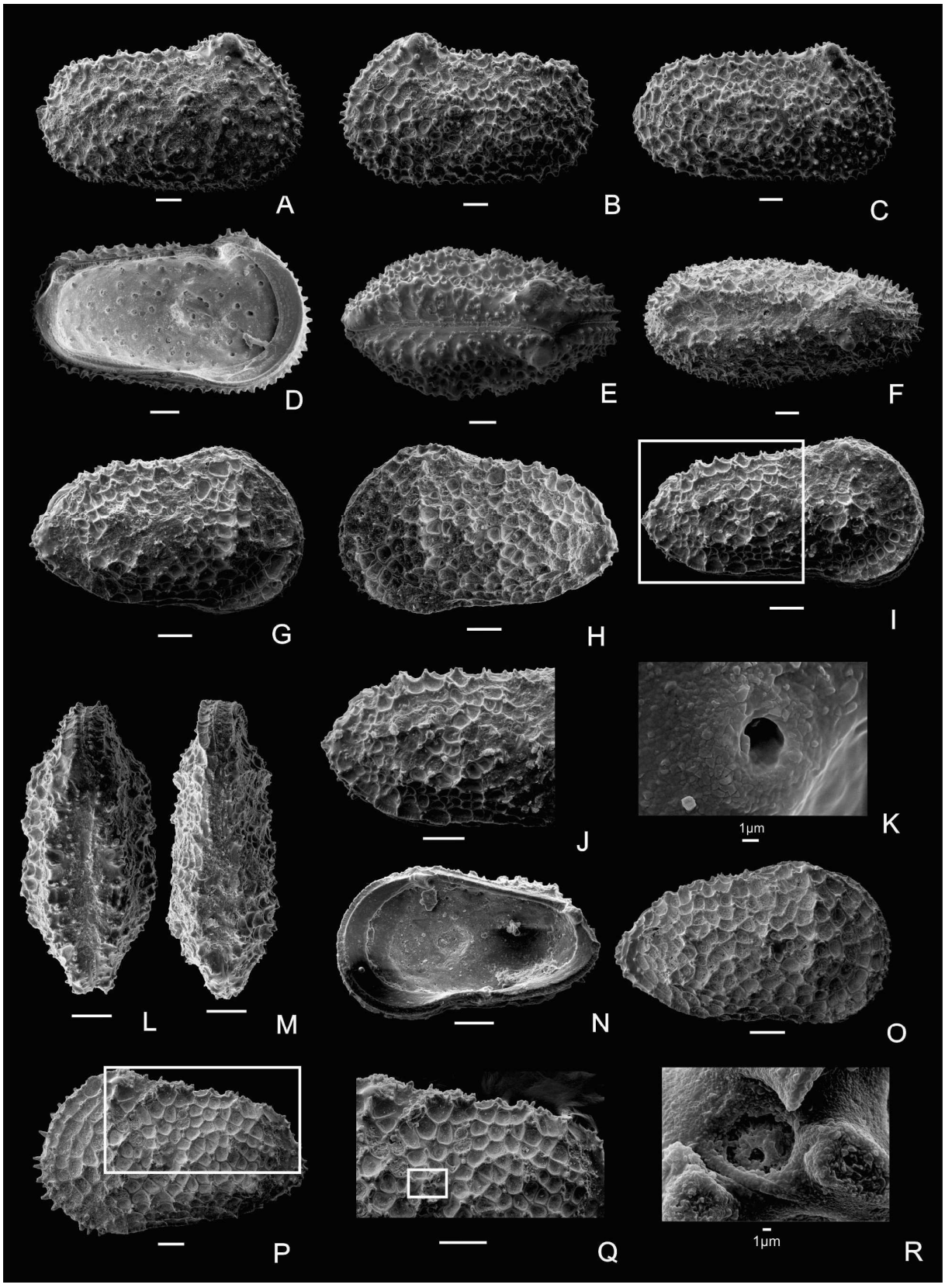
A
B
C
D
E
F
G
H
I
J
1µm
K
L
M
N
O
P
Q
1µm
R

FIG. 13. Photomicrographs of Ostracoda from the Cerro Azul section, Neuquén Basin. All scale bars represent 100 μm, except those in K and R, which are 1 μm. A-F, *Henryhowella (Wichmannella) praealtus* sp. nov.; A, holotype, LM-FCEN 3477, adult female carapace, right lateral view; B, paratype, LM-FCEN 3478, adult female carapace, left lateral view; C, paratype, LM-FCEN 3479, adult male valve, right lateral view; D, paratype, LM-FCEN 3480, adult female valve, internal view; E, paratype, LM-FCEN 3481, adult female carapace, dorsal view; F, paratype, LM-FCEN 3482, adult male carapace, dorsal view. G-N, *Hysterocythereis paredros* gen. et sp. nov.; G, L, holotype, LM-FCEN 3483, G, adult female carapace, right lateral view; L, dorsal view; H, paratype, LM-FCEN 3484, adult female carapace, left lateral view; I, J, K, paratype, LM-FCEN 3485, I, adult male carapace, right lateral view; J, detail of ornamentation, K, simple pore; M, paratype, LM-FCEN 3486, adult male carapace, dorsal view; N, paratype, LM-FCEN 3487, adult female valve, internal view. O-R, *Hysterocythereis coinotes* sp. nov.; O, holotype, LM-FCEN 3488, adult female valve, right lateral view; P, Q, R, paratype, LM-FCEN 3489, P, female valve, left lateral view, Q, detail of ornamentation; R, sieve-type pore.

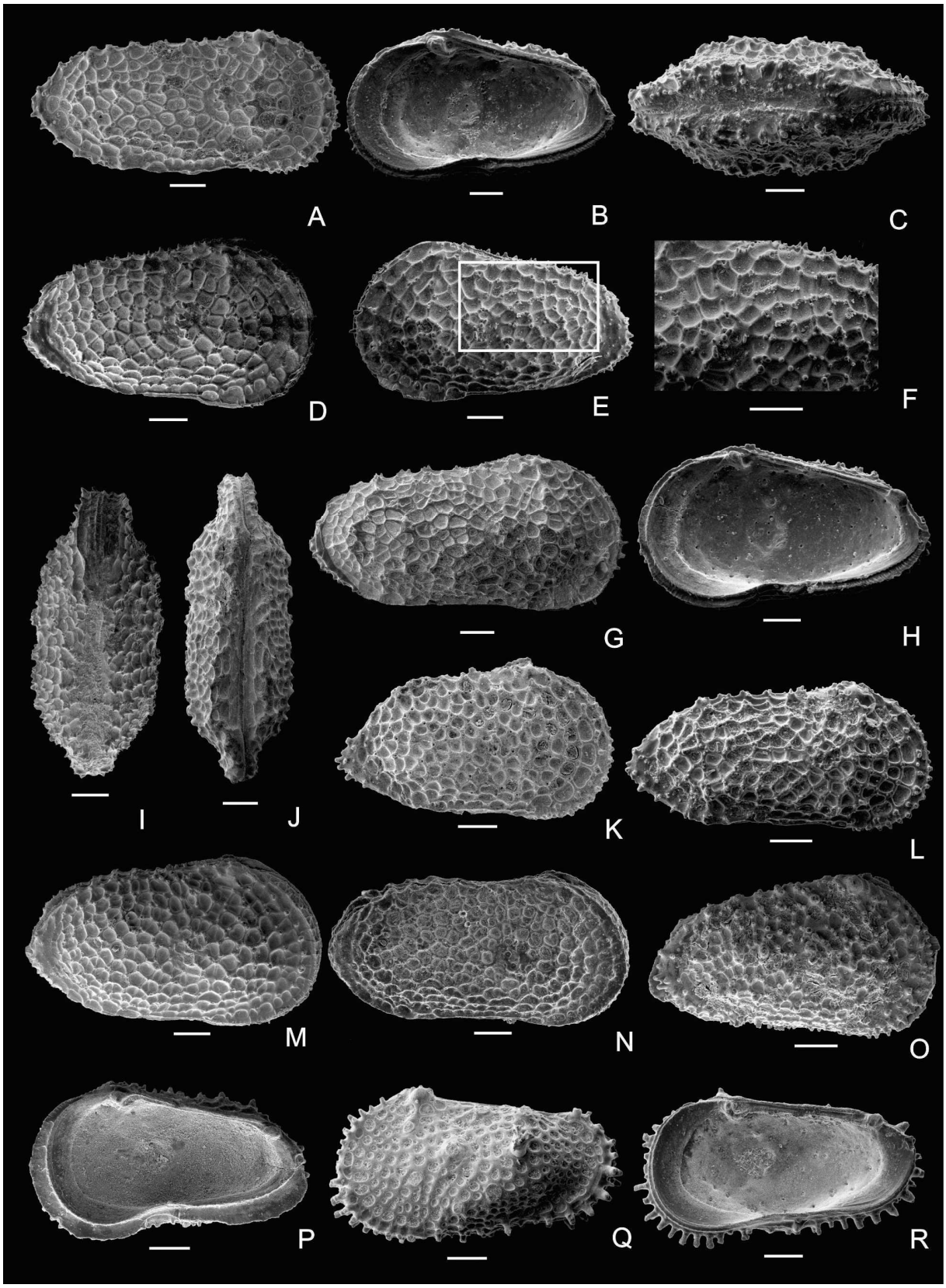
A
B
C
D
E
F
G
H
I
J
K
L
M
N
O
P
Q
R

FIG. 14. Photomicrographs of Ostracoda from the Cerro Azul section, Neuquén Basin. All scale bars represent 100 μm. A-C, *Hysterocythereis coinotes* sp. nov.; A, paratype, LM-FCEN 3490, adult male valve, right lateral view; B, paratype, LM-FCEN 3491, adult female valve, internal view; C, paratype, LM-FCEN 3492, adult female carapace, dorsal view. D-J, *Hysterocythereis diversotuberculatus* sp. nov.; D, I, holotype, LM-FCEN 3493, D, adult female carapace, right lateral view; I, dorsal view; E, F, paratype, LM-FCEN 3494, E, adult female carapace, left lateral view; F, detail of ornamentation; G, paratype, LM-FCEN 3495, adult male valve, right lateral view; H, paratype, LM-FCEN 3496, adult female valve, internal view; J, paratype, LM-FCEN 3497 (lost), adult male carapace, dorsal view. K-L, *Hysterocythereis attenuata* (Bertels, 1975*a*); K, paratype, LM-FCEN 3498, adult female valve, right lateral view; L, paratype, LM-FCEN 3499, adult male valve, right lateral view. M-N, *Hysterocythereis inconnexa* (Bertels, 1973); M, paratype, LM-FCEN 3500, adult female carapace, right lateral view; N, paratype, LM-FCEN 3501, adult male carapace, right lateral view. O-P, *Hysterocythereis*? sp., LM-FCEN 3502, O, adult carapace, right lateral view, P, LM-FCEN 3503, adult valve, internal view. Q-R, *Oertliella*? sp., LM-FCEN 3504, Q, adult valve, left lateral view; R, internal view.

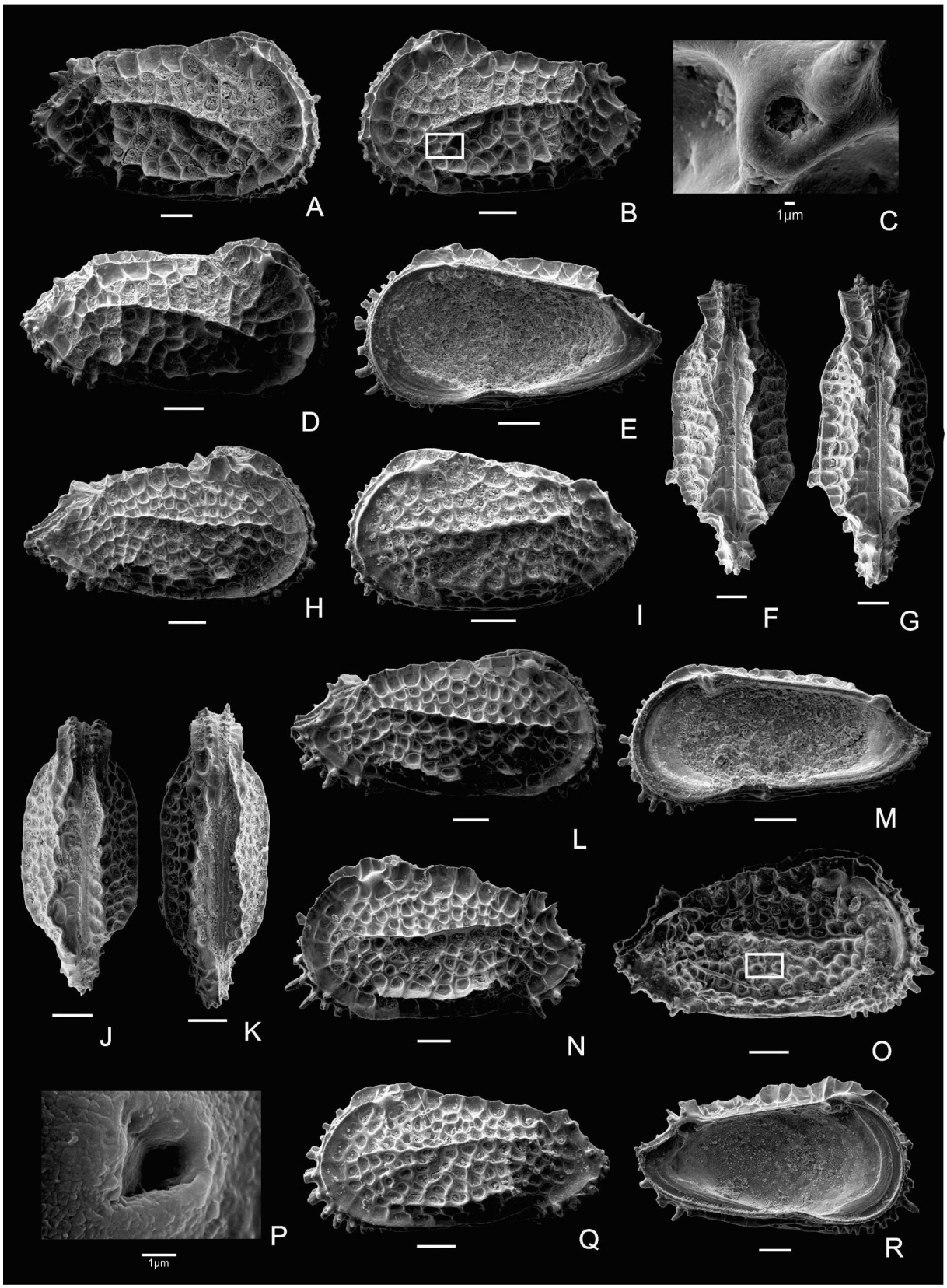
A
B
1µm
C
D
E
F
G
H
I
J
K
L
M
N
O
P
1µm
Q
R

FIG. 15. Photomicrographs of Ostracoda from the Cerro Azul section, Neuquén Basin. All scale bars represent 100 μm, except those in C and P, which are 1 μm. A-G, *Orthrocosta decores* sp. nov.; A, F, holotype, LM-FCEN 3505, A, adult female carapace, right lateral view, F, dorsal view; B, C, paratype, LM-FCEN 3506, B, adult female valve, left lateral view; C, sieve-type pore; D, G, paratype, LM-FCEN 3507, D, adult male carapace, right lateral view, G, dorsal view; E, paratype, LM-FCEN 3508, adult female valve, internal view. H-M, *Orthrocosta atopos* sp. nov.; H, holotype, LM-FCEN 3509, adult female carapace, right lateral view; I, J, paratype, LM-FCEN 3510, I, adult female carapace, left lateral view; J, dorsal view; K, L, paratype, LM-FCEN 3511, K, dorsal view; L, adult male carapace, right lateral view; M, paratype, LM-FCEN 3512, adult male valve, internal view. N-R, *Orthrocosta phantasia* sp. nov.; N, holotype, LM-FCEN 3513, adult female valve, left lateral view; O, P, paratype, LM-FCEN 3514, O, adult female carapace, right lateral view, P, simple pore, Q, paratype, LM-FCEN 3515, adult male valve, left lateral view; R, paratype, LM-FCEN 3516, adult female valve, internal view.

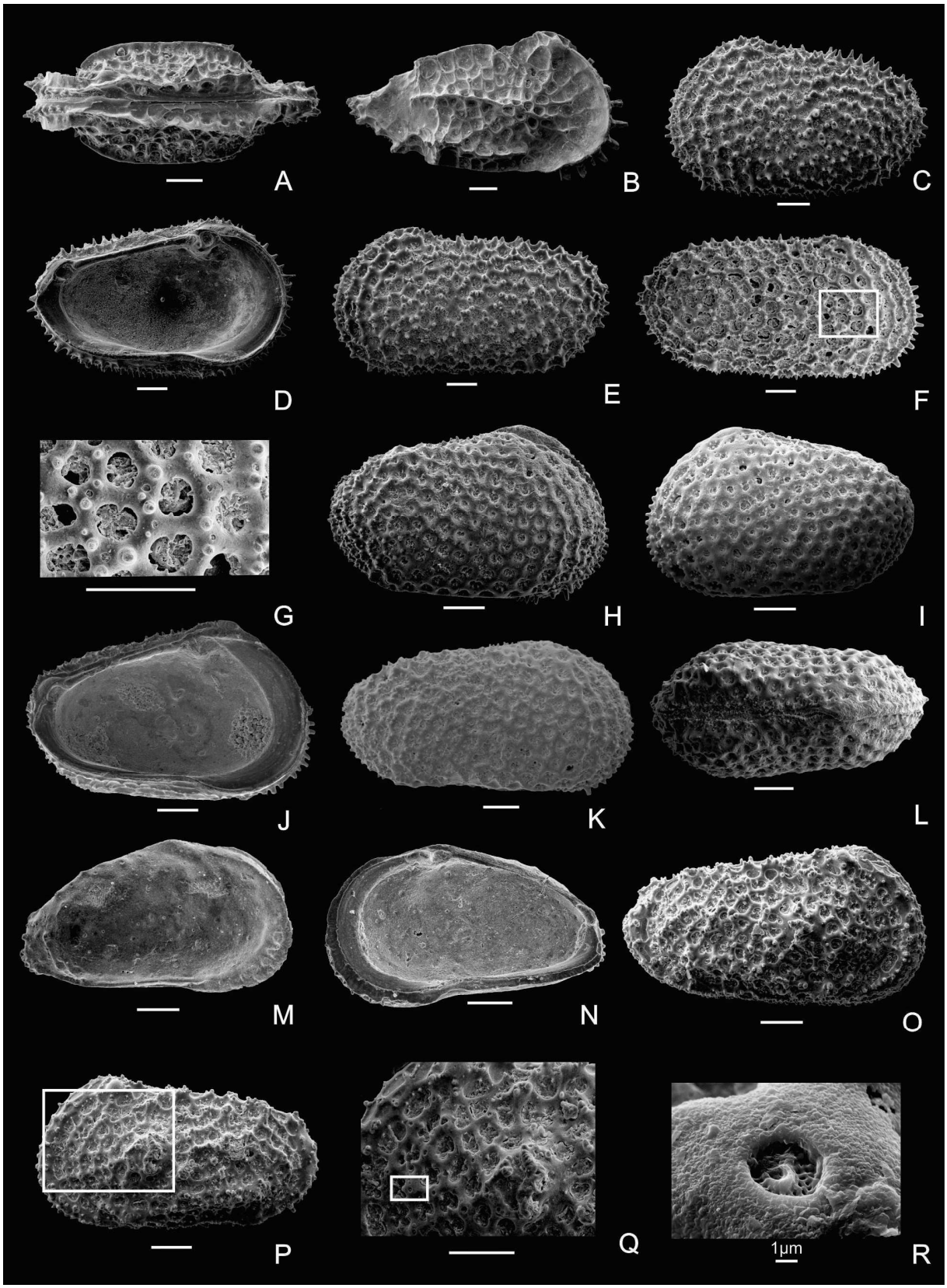
A
B
C
D
E
F
G
H
I
J
K
L
M
N
O
P
Q
R
1µm

FIG. 16. Photomicrographs of Ostracoda from the Cerro Azul section, Neuquén Basin. All scale bars represent 100 μm, except that in R, which is 1 μm. A, *Orthrocosta phantasia* sp. nov., paratype, LM-FCEN 3514, adult female carapace, dorsal view. B, *Orthrocosta* sp., LM-FCEN 3517, adult valve, right lateral view. C-G, *Petalocythereis schilleri* (Bertels 1973) comb. nov.; C, paratype, LM-FCEN 3518, adult female valve, left lateral view; D, paratype, LM-FCEN 3519, adult female valve, internal view; E, paratype, LM-FCEN 3520, adult male valve, left lateral view; F, G, paratype, LM-FCEN 3521, F, adult male valve, right lateral view; G, detail of petaliform shape of the solae. H-L, *Petalocythereis venusta* (Bertels, 1975*a*) comb. nov.; H, L, paratype, LM-FCEN 3522, H, adult female carapace, right lateral view; L, dorsal view; I, paratype, LM-FCEN 3523, adult female carapace, left lateral view; J, paratype, LM-FCEN 3524, adult female valve, internal view; K, paratype, LM-FCEN 3525, adult male valve, right lateral view. M-N, *Philoneptunus*? sp.; LM-FCEN 3526, M, adult valve, right lateral view; N, internal view. O-R, *Sthenarocythereis arcana* (Bertels, 1975*a*) comb. nov.; O, paratype, LM-FCEN 3527, adult carapace, right lateral view; P, Q, R, paratype, LM-FCEN 3528, P, adult valve, left lateral view; Q, detail of ornamentation, R, sieve type pore.

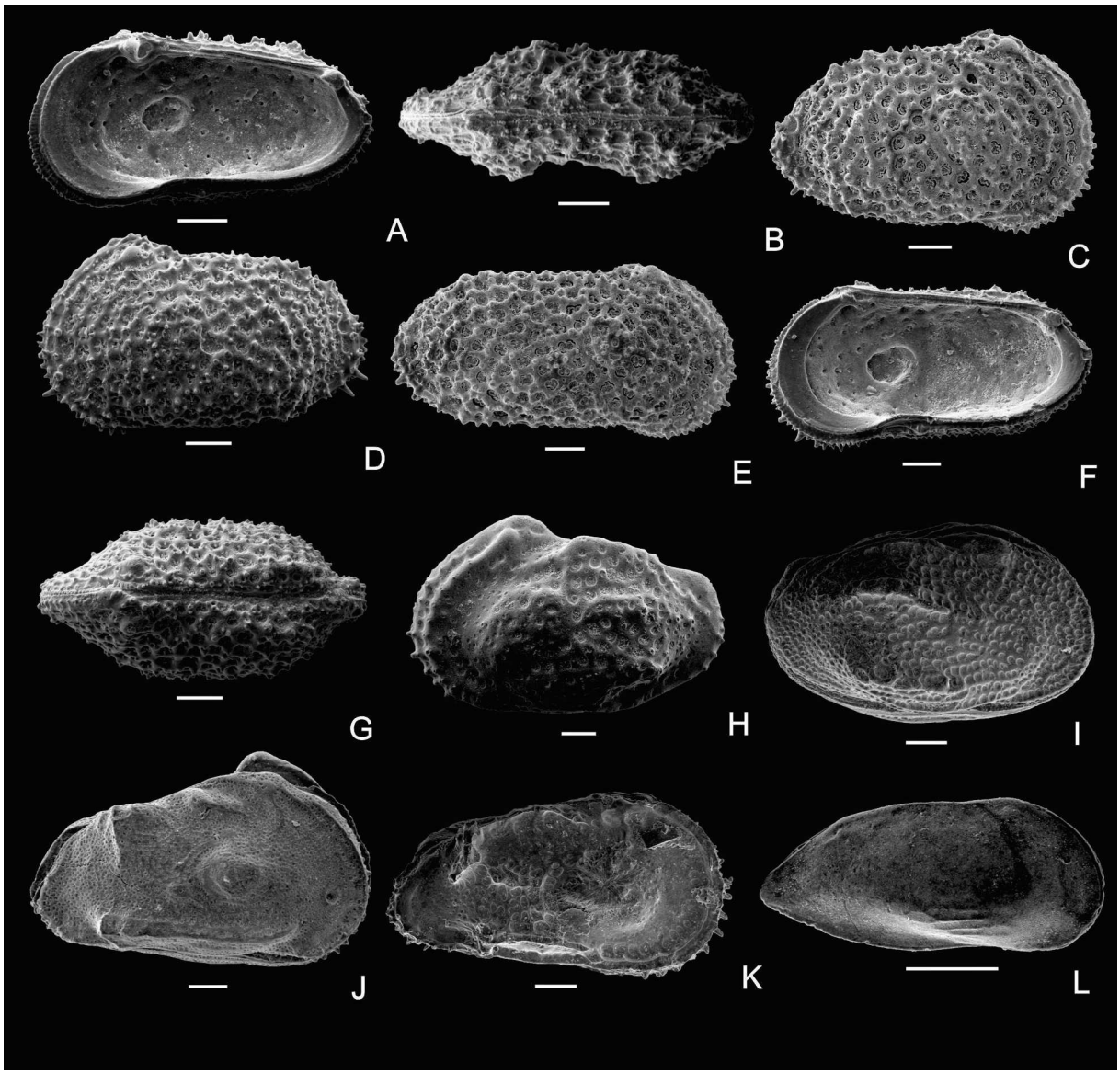

FIG. 17. Photomicrographs of Ostracoda from the Cerro Azul section, Neuquén Basin. All scale bars represent 100 μm. A-B, *Sthenarocythereis arcana* (Bertels, 1975*a*) comb. nov.; A, paratype, LM-FCEN 3529, adult valve, internal view; B, paratype, LM-FCEN 3527, dorsal view (broken). C-G, *Sthenarocythereis erymnos* gen. et sp. nov., C, holotype, LM-FCEN 3530, adult female valve, right lateral view; D, paratype, LM-FCEN 3531, adult female valve, left lateral view; E, paratype, LM-FCEN 3532, adult male valve, right lateral view; F, paratype, LM-FCEN 3533, adult male valve, internal view; G, paratype LM-FCEN 3534, adult female carapace, dorsal view. H, *Veenia tumida* (Bertels, 1975*a*), LM-FCEN 3535, adult female valve, left lateral view. I, *Huantraiconella costata* (Bertels, 1975*b*) comb. nov.,

LM-FCEN 3536, adult carapace, right lateral view; J, *Unicapella*? sp.1; LM-FCEN 3537, adult carapace, right lateral view. K, *Unicapella*? sp. 2; LM-FCEN 3538, adult carapace, right lateral view. L, *Clinocythereis* sp.; LM-FCEN 3539, adult carapace, right lateral view.

THE NATURE OF THE FAUNA

In essence, there are three faunas: the Maastrichtian, the Danian and that which is both Maastrichtian and Danian. Each of these faunas has certain characteristics, some of which can be conveyed in simple statistics, others in taxonomic appreciation.

Maastrichtian.

From the seven samples studied from the Maastrichtian, 53 species belonging to 33 genera were recovered. Of these, 18 species were previously described; 19 species are new and 12 species are left in *nomina aperta* due to either poor preservation or paucity of material. Experience shows that the majority that these species in open nomenclature will eventualy be described as new. Therefore, there is in the Maastrichtian of the Neuquén Basin, a total potential of some 31 new species. This newness is further emphasized by our discovery of six new genera.

Danian.

Twenty samples were collected from the Danian of the Cerro Azul section and these yielded 81 species belonging to 40 genera. Of these 81 species, 27 are previously described, 32 are new and 19 are left *nomina aperta*. Of these, however most or all must be new, as time eventually will show, so that the Danian has a potential of some 59 new species. The newness of this fauna is further emphasized by the seven new genera that we have erected from the Danian in this study.

Both Maastrichtian and Danian.

A total of 21 species belonging to 16 genera occur in both the Maastrichtian and Danian. Given the alledgely catastrophic effects on both vertebrate and invertebrate faunas of events at the K-T boundary, this is a surprisingly high number and percentage (18,6%) of fauna to have survived and crossed the boundary.

Of the 21 species crossing the boundary, the number of the samples in which they occur in the Maastrichtian ranges between one and four (mean 1.80) and the number of samples in which they occur in the Danian, ranges from one to 15 (mean 6.61). This later figure illustrates that this is not a chance phenomenon but that these species evolved in the Maastrichtian and passed the boundary with no ill-effects in order to be able to flourish in the Danian.

Another study will commence shortly to analyse in greater detail the nature of the effect on the Ostracoda of the K-T boundary from four additional outcrop localities in the Neuquén Basin.

The taxonomic and evolutionary aspects of the two faunas: Maastrichtian and Danian.

Maastrichtian. Table 1 lists the Maastrichtian fauna and it can be seen to be very diverse, containing Platycopids (7.5%), marine Cyproidea (5.6%) but overwhelmingly Cytheroidea (86.8%). In terms of number of species within the Cytheroidea, certain families, such as the Cytheruridae and the Pectocytheridae are very well represented. The latter probably better so than in any other Maastrichtian deposit known to the authors. However, it is the Trachyleberididae that are so totally dominant, representing by 24 species (45.3%) of the fauna and more than 50 per cent of all Cytheroidea.

Notable is that eight species of the 24 trachyleberid species belong to new genera (33.3%). These are: *Apatoleberis*, *Mimicocythereis*, *Castillocythereis*, *Orthrocosta*, *Hysterocythereis*, *Petalocythereis* and *Sthenarocythereis* and comprise a very considerable body of hitherto undescribed taxa.

Details of what can be called an evolutionary explosion of these trachyleberid genera in both the Maastrichtian and Danian, are discussed separately in this section.

Danian. The Danian fauna of this study (Table 2) is even more richly endowed than the Maastrichtian and even more diverse, as shown below:

The Cytherellidae are represented by four species (4.9%) and the Bairdiidae by two species (2.4%), both rather low figures. However, while the marine Cyproidea comprise eight species (9.8%), the remainder of the fauna are Cytheroidea (79%), of these Bythocytheridae six species (7.6%) and Nodoconchiinae (subfam. nov. in press) (5.1%). However, these newly found taxa are of great importance in allowing us to understand the fossil history of the previously monotypic Antarctic genus *Nodoconcha*.

The subfamily Cytherideinae with the single taxon *Phelocyprideis acardomesido* gen. et sp. nov. is numerically and in percentage terms insignificant; however, it represents a genus with a entirely new hinge type and is a precursor of the Pleistocene and Recent *Cyprideis* Jones. The Krithinae and Neocytheridinae together, with three species make up (3.7%), but the two subfamilies of Cytheruridae, however, with 12 species, make up the substantial percentage of 14.8 per cent.

Exceeding the Loxoconchidae, which with four species make up only 4.9 per cent of the Pectocytheridae have only five species (6.2%), but they are nonetheless numericaly abundant and form a significant and important component of the fauna, in representing well-developed early members of the two genera *Keijia* and *Ameghinocythere*. Once again, however with 29 species (35.8%) the Trachyleberididae truly dominate the Cytheroidea and the new genera *Sthenarocythereis*, *Castillocythereis*, *Hysterocythereis*, *Petalocythereis* and *Orthrocosta* represent a dynamical evolutionary component within the family which will be discussed below.

The Trachyleberididae

The Trachyleberids that we have encountered in this study include two new species of *Cythereis*. Bertels (1969*a*, 1975*a*) had already described another three species of the same age. We encountered one new species of the genus *Henryhowella* which we consider is in fact the subgenus *Wichmannella* (Bertels, 1969*c*).

Of some importance zoogeographicaly, we encoutered two species in very small number of the genus *Unicapella* described by Dingle (1980) from the Campanian of Richard Bay, South Africa. We encountered a single species of *Veenia* Butler and Jones, *Veenia tumida* (Bertels, 1975*a*), a single species of *Philoneptunus*? sp. Whatley, Millson and Ayres, 1992 and another single specimen of a species that we tentatively included in *Oertliella* Pokorny.

One of the new genera of trachyleberidid is *Apatoleberis* gen. nov, (ex. *Trachyleberis*, Bertels 1975*a*). This clearly is not *Trachyleberis*, lacking all the basic features of that genus (Brandão *et al*. 2013). Similarly, Bertels (1975*a*) described the species *Bradleya*? *attilai*. However, since because of its musculature, this species is clearly a trachyleberidid while *Bradleya* is usually classified in the Thaerocytheridae Hazel, we have named this species *Mimicocythereis* gen. nov.

Orthorocosta gen. nov. has three new species, *O. phantasia*, *O. atopos* and *O. decores* plus *Orthrocosta* sp. We make the assumption that this genus is somehow ancestral to *Costa* Neviani although the evidence for this is not entirely convincing.

The five new genera *Aleisocythereis*, *Castillocythereis*, *Hysterocythereis*, *Sthenarocythereis* and *Petalocythereis* form an interesting and complicated complex of genera. We cannot be certain of their ancestry in the Maastrichtian, but despite the fact that they all lack three transverse ribs in the posterior part that carapace and not all have paramphidont hinges, we suspect that the ancestor was *Cythereis* Jones. They differ from *Cythereis* not just in those features mentioned above, but also in the nature of the reticulum,

which is always strongly and very diversely developed. Indeed it is the principal characteristic on which both genera and species are classified in this group.

All of these genera originated in the Maastrichtian where they appear quite suddenly and without any direct evidence for their ancestry. From their first appearance they already exhibit a great diversity in the nature of the reticulum. For example, *Castillocythereis* already has its ornament which includes the strong fortress-like complexes of tubercles and *Sthenarocythereis* appears with its extremely strong muri and mural tubercles surrounding reticular cells ranging in shape from circular to polygonal and enclosing strong sieve plates. Similarly *Aleisocythereis* with its large circular, reticular cells containing distinct cup-like structures, *Hysterocythereis* with its large open reticular cells and poor development of the mural tubercles; and *Petalocythereis* with its numerous petal-shaped reticular cells all appear suddenly with these structures fully developed.

This is an almost unrivalled example of such rapid diversity. All these genera, except *Aleisocythereis*, continue up into the Danian where they are a significant component of the fauna. Within these five genera, it is very difficult to find a particular relationship. Perhaps the closest relationship is between *Sthenarocythereis* and *Petalocythereis*, but it is impossible on either stratigraphical or morphological grounds to propose which of the two is the ancestor. Although beyond the scope of the present paper, it is interesting to wonder what the fate of this vigorous group of rapidly evolving trachyleberids was, since there seems to be no trace of them in post-Danian deposits in Argentina or elsewhere. We hope, in a detailed survey of the Maastrichtian and Danian of other outcrops in the Neuquén Basin, to find evidence which will help to resolve this enigma.

Family CYTHERELLIDAE Sars, 1866
Cytherella saraballentae sp. nov.
Cytherella semicatillus sp. nov.
Cytherella terminopunctata Holden, 1964
Cytherelloidea spirocostata Bertels, 1973
Family PARACYPRIDIDAE Sars, 1923
Paracypris imaguncula sp. nov.
Family PONTOCYPRIDIDAE Müller, 1894
Argilloecia abnormalis sp. nov.
Argilloecia concludus sp. nov.
Superfamily CYTHEROIDEA Baird, 1850
Family BYTHOCYTHERIDAE Sars, 1826
Bythoceratina sp. aff. *Bythoceratina scaberrima* (Brady 1887)
Family CYTHERIDAE Baird, 1850
Subfamily NODOCONCHIINAE subfam. nov.
Nodoconcha? sp.
Family CYTHERIDEIDAE Sars, 1925
Subfamily EUCYTHERINAE Puri, 1954
Eucythere dinetos sp. nov.
Subfamily KRITHINAE Mandelstam, 1958
Krithe crepidus sp. nov.
Copytus sp.
Family CYTHERURIDAE Müller, 1894
Cytheropteron translimitares sp. nov.
Cytheropteron sp.
Aversovalva glochinos sp. nov.
Pedicythere sp.
Semicytherura sp. 3
Eucytherura stibaros sp. nov.
Eucytherura sp. 2
Hemiparacytheridea sp.
Family LOXOCONCHIDAE Sars, 1925
Sagmatocythere? sp. 1
Family PECTOCYTHERIDAE Hanai, 1957
Keijia flexuosa (Bertels, 1975*a*) comb. nov.
Keijia huantraicoensis (Bertels, 1969*a*) comb. nov.
Paramunseyella epaphroditus sp. nov.
Munseyella costaevermiculatus sp. nov.
Munseyella minima Bertels, 1975*a*
Family TRACHYLEBERIDIDAE Sylvester-Bradley, 1948
Actinocythereis tuberculata Bertels, 1974
Aleisocythereis polikothonus sp. nov.
Apatoleberis noviprinceps (Bertels, 1975*a*) comb. nov.
Mimicocythereis attilai (Bertels, 1975*a*) comb. nov.
Castillocythereis albertoriccardii sp. nov.
Cythereis stratios sp. nov.
Cythereis incerta (Bertels, 1975*a*)
Cythereis rionegrensis (Bertels, 1975*a*)
Cythereis trajectiones sp. nov.
Henryhowella (Henryhowella) splendida Bertels, 1975*a*
Henryhowella (Wichmannella) meridionalis (Bertels, 1969*c*)
Hysterocythereis attenuata (Bertels, 1975*a*) comb. nov.
Hysterocythereis coinotes gen. et sp. nov.
Hysterocythereis? sp.
Oertliella ? sp.
Oertliella exquisita Bate, 1972
Orthrocosta phantasia sp. nov.
Petalocythereis venusta (Bertels, 1975*a*) comb. nov.
Philoneptunus ? sp.
Sthenarocythereis erymnos sp. nov.
Sthenarocythereis arcana (Bertels, 1975*a*) comb. nov.
Unicapella? sp.1
Veenia tumida (Bertels, 1975*a*)
Sphaeroleberis? *abnormalis* Bertels, 1975*a*
Subfamily BUNTONIINAE Apostolescu, 1961
Togoina cretacea Bertels, 1975*a*
Togoina argentinensis Bertels, 1975*a*
Nigeria punctata Bertels, 1975*a*

Table 1. Maastrichtian ostracod fauna from Cerro Azul section with all identified species in this work.

Family CYTHERELLIDAE Sars, 1866
Cytherella saraballentae sp. nov.
Cytherella semicatillus sp. nov.
Cytherella terminopunctata Holden, 1964
Cytherelloidea spirocostata Bertels, 1973
Family BAIRDIIDAE Sars, 1888
Bairdoppilata sp.
Bairdoppilata? sp
Family PARACYPRIDIDAE Sars, 1923
Paracypris bertelsae sp. nov.
Paracypris imaguncula sp. nov.
Paracypris? sp.
Paracypris jonesi Bonnema, 1941.
Aglaiocypris? sp.
Family PONTOCYPRIDIDAE Müller, 1894
Argilloecia abnormalis sp. nov.
Argilloecia hydrodynamicus sp. nov.
Superfamily CYTHEROIDEA Baird, 1850
Family BYTHOCYTHERIDAE Sars, 1826
Bythocythere costata Bertels, 1973
Bythoceratina cheleutos sp. nov.
Bythoceratina rocana (Bertels, 1973) comb. nov.
Bythoceratina sp.
Pseudocythere sp
Tanycythere sp.
Family CYTHERURIDAEMüller, 1894
Subfamily Nodoconchiinae subfam. nov.
Nodoconcha polytorosa sp. nov.
Nodoconcha sanniosis sp. nov.
Nodoconcha upsilon sp. nov.
Ectonodoconcha lepidotus gen. et sp. nov.
Family CYTHERIDEIDAE Sars, 1925
Subfamily CYTHERIDEINAE Sars, 1925
Phelocyprideis acardomesido sp. nov.
Subfamily EUCYTHERIDEINAE Puri, 1954
Eucythere dinetos sp. nov
Subfamily KRITHINAE Mandelstam, 1958
Krithe crepidus sp. nov.
Krithe sp.
Subfamily NEOCYTHERIDEIDINAE Puri, 1957
Copytus sp.
Family CYTHERURIDAE Müller, 1894
Cytheropteron hyperdictyon sp. nov.
Cytheropteron bidentinos sp. nov.
Cytheropteron translimitares sp. nov.
Aversovalvaglochinos sp. nov
Semicytherura argentinensis (Bertels, 1974) comb. nov.
Semicytherura sp. 1
Semicytherura sp. 2
Semicytherura sp. 3
Semicytherura? sp.
Eucytherura stibaros sp. nov.
Eucytherura sp. 1
Hemingwayella verrucosus sp. nov.
Family LOXOCONCHIDAE Sars, 1925
Heinia prostratopleuricos sp. nov.
Loxoconcha sp. aff.*Loxoconcha cretacea* Alexander, 1936
Palmoconcha similis (Bertels, 1973)
Sagmathocythere? sp. 2
Loxoconcha (s.l.)*posterocosta* sp. nov.
Family PECTOCYTHERIDAE, Hanai 1957
Keijia circulodictyon sp. nov.
Keijia kratistos sp. nov.
Keijia huantraicoensis (Bertels, 1969) comb. nov.
Keijia flexuosa(Bertels, 1975) comb. nov.
Ameghinocythere archaios sp. nov.
Family TRACHYLEBERIDIDAE Sylvester-Bradley, 1948
Subfamily TRACHYLEBERIDINAE Sylvester-Bradley, 1948
Actinocythereis biposterospinata Bertels, 1973
Actinocythereis indigena Bertels, 1969
Actinocythereis rex Bertels, 1973
Castillocythereis multicastrum sp. nov.
Cythereis stratios sp. nov.
Cythereis clibanarius sp. nov.
Cythereis trajectiones sp. nov
Henryhowella (Henryhowella) nascens (Bertels, 1969*c*)
Subgenus WICHMANNELLA Bertels, 1969*c* subgen. nov.
Henryhowella (Wichmannella) praealtus sp. nov.
Henryhowella (*Wichmannella*) *meridionalis* (Bertels, 1969*c*)
Hysterocythereis paredros sp. nov.
Hysterocythereis coinotes sp. nov.
Hysterocythereis diversotuberculatus sp. nov.
Hysterocythereis inconnexa (Bertels, 1973) comb. nov.
Neoveenia argentinensis Betels, 1969*c*
Orthrocosta decores sp. nov.
Orthrocosta atopos sp. nov.
Orthrocosta phantasia sp. nov.
Orthrocosta sp.
Petalocythereis schilleri (Bertels, 1973) comb. nov.
Trachyleberis weiperti Bertels, 1969*a*
Unicapella? sp. 2
Subfamily BUNTONIINAE Apostolescu, 1961
Togoina argentinensis Bertels, 1975*a*
Togoina australis Bertels, 1968
Togoina semiinornata Bertels, 1975*a*
Huantraiconella costata (Bertels, 1975*c*) comb. nov.
Huantraiconella prima Bertels, 1973
Subfamily *INCERTAE SEDIS*
Clinocythereis sp.

Table 2. Danian ostracod fauna from Cerro Azul section with all identified species in this work.

CONCLUSION

Although this study is based on only one of the five localities of Maastrichtian and Danian strata in the Neuquén Basin available to us, we have been surprised at the richness and diversity of the fauna we have encountered. The total fauna comprises 113 species belonging to 54 genera and of these, nine genera and 38 species are new. The fauna is dominated by Cytheroidea and these are dominated by the Trachyleberididae. A group of five new trachyleberid genera *Aleisocythereis*, *Castillocythereis*, *Hysterocythereis*, *Sthenarocythereis* and *Petalocythereis*, which may have evolved from *Cythereis* Jones, are discriminated principally on the nature of the reticulum which varies greatly within the group, but is always strongly reticulate. The ultimate fate of this group is of as great interest as is their origin. We intend at the earliest opportunity to investigate the other four outcrop localities with the aim to resolving these outstanding problems, and also to encounter additional material of the many species in open nomenclature, so that can be properly named and described.

Aknowledgements.This study forms part of the Ph.D thesis project of the first author, financially supported by a Padre Milton Valente Scholarship of the Universidade do Vale do Rio dos Sinos – Unisinos. This study was partially formed at Aberystwyth University during a Ph.D. internship of the first author in the summer of 2014, supported by Conselho Nacional de Desenvolvimento Científico e Tecnológico (CAPES – Proc. BEX 2696/14-2). The authors thanks to Michele Goulart da Silva for the SEM images, Dr. Telma Musso from the Universidad of Comahue, Neuquén, Argentina, for her help in the field and particularly, to Dr. Charlie Bendall and Dr. Caroline Maybury of Aberystwyth University, UK for all their help in the construction of this paper. Thanks are also due to Dr. Adrian Wood of the University of Coventry and to Professor Richard Dingle of Cambridge for very useful

comments. The first author thanks to Dr. Cristianini Trescastro Bergue and the others colleagues of itt-Fossil- Technological Institute on Micropaleontology for all their support in this research. Funding for this study has been also partially financed with the Grant UBACyT 20020110100170BA. This paper is contribution number R-158 of the Instituto de Estudios Andinos "Don Pablo Groeber" (IDEAN). Gerson Fauth thanks CNPq (The Brazilian Scientific and Technology Developing Council) for the grant (proc. 308544/2012-9). This paper is dedicated in memory of the late Dr. Sara Ballent, who was the original mentor of this project. May she Rest in Peace. Robin Whatley, as always, thanks Mary for her continuing inspiration and guidance.

DATA ARCHIVING STATEMENT

Data for this study are available in the [Dryad Digital Repository]:

http://dx.doi.org/10.5061/dryad.[NNNN]

REFERENCES

AGUIRRE-URRETA, B., TUNIK, M., NAIPAUER, M., PAZOS, P., OTTONE, E., FANNING M. and RAMOS V. A. 2011. Malargüe Group (Maastrichtian-Danian) deposits in the Neuquén Andes, Argentina: Implications for the onset of the first Atlantic transgression related to Western Gondwana break-up. *Gondwana Research*, **19**, 482-494.

ALEXANDER, C. I. 1934. Ostracoda of the Midway (Eocene) of Texas. *Journal of Paleontology*, **8** (2), 206–237.

--- 1936. Ostracoda of the Genera Eucythere, Cytherura, Eucytherura, and Loxoconcha from the Cretaceous of Texas. *Journal of Paleontology*, **10** (8), 689–694.

ANDREU, B., LEBEDEL, V., WALLEZ, M-J., LÉZIN, C. and ETTACHFINI, El. M. 2013. The Upper Cenomanian-Lower Turonian carbonate plataform of the Preafrican Trough, Morrocco: Biostratigraphical, paleoecological and paleobiogeographical distribution of ostracod. *Cretaceous Research*, **45**, 216–246.

ATHERSUCH, J. 1976. On *Sagmatocythere napoliana* (Puri). *Stereo-Atlas of ostracod shells*, **3** (21), 117–124.

AYRESS, M.A. and SWANSON, K.M. 1991. New fossil and Recent genera and species of Cytheracean Ostracoda (Crustacea) from South Island, New Zealand. *New Zealand Natural Sciences*, **18**, 1–18.

BAIRD, W. 1838. The Natural History of the British Entomostraca: part 4. *Magazine of Zoology and Botany*, **2** (8), 132–144.

--- 1850. *The Natural history of the British Entomostraca*. Ray Society, London, 364 pp.

BALLENT, S., CONCHEYRO, A., NÁÑEZ, C., PUJANA, I., LESCANO, M., CARIGNANO, A. P., CARAMÉS, A., ANGELOZZI, G. and RONCHI, D. 2011. Microfósiles Mesozoicos y Cenozoicos. *In* LEANZA, H. A., ARREGUI, C., CARBONE, O., DANIELI, J. C. and VALLÉS J. M. (eds). *XVIII Congresso Geológico*

Argentino, Neuquén. Geología y recursos naturales de la provincia del Neuquén, 489–528 pp.

BATE, R. H. 1972. Upper Cretaceous Ostracoda from the Carnarvon Basin Western Australia. *Special papers in Palaeontology*, **10**, (1–5), 1–85.

BERGUE, C. T., COSTA, K. B., DWYER, G. and MOURA, C. A. 2006. Bathyal Ostracode diversity in the Santos Basin, Brazilian southeast margin: response to Late Quaternary climate changes. *Revista Brasileira de Paleontologia*, **9** (2), 201–210.

--- FAUTH, G., VIEIRA, C. E. L. and SANTOS, A. S. 2011. New species of *Fossocytheridea* Swain & Brown, 1964 (Ostracoda, Crustacea) in the Upper Cretaceous of Santos Basin, Brazil. *Revista brasileira de paleontologia*, **14** (2), 149–156.

BERTELS, A. 1968*a*. *Huantraiconella* N. Gen. (Ostracoda, Buntoniinae) del Terciario Inferior (Daniano) de Argentina. *Ameghiniana*, **5** (7), 252–253.

--- 1968*b*. Micropaleontologia y Estratigrafia del Limite Cretacico-Terciario em Huantrai-co (Provincia del Neuquén). Ostracoda. Part one, *Ameghiniana*, **5** (8), 279–288.

--- 1969*a*. Micropaleontologia y Estratigrafia del Limite Cretacico-Terciario em Huantrai-co (Provincia del Neuquén). Ostracoda. Part two. *Ameghiniana*, **6** (4), 253–290.

--- 1969*b*. Estratigrafia del Limite Cretacico-Terciario en Patagônia Septentrional. *Revista de la Asociación Geológica Argentina,* **24** (1), 40–54.

--- 1969*c*. Rocaleberidinae, nueva subfamília (Ostracoda, Crustacea) del Limite Cretacico-Terciario de Patagonia Septentrional (Argentina). *Ameghiniana*, **4** (2), 146–171.

--- 1973. Ostracodes of the Type locality of the Lower Tertiary (lower Danian) Rocanian Stage and Roca Formation of Argentina. *Micropaleontology*, **19** (3), 308–340.

--- 1974. Upper Cretaceous (lower Maastrichtian?) ostracodes from Argentina. *Micropaleontology*, **20** (4), 385–397.

--- 1975*a*. Upper Cretaceous (middle Maastrichtian) ostracodes of Argentina. *Micropaleontology*, **21** (1), 97–130.

--- 1975*b*. Ostracode ecology during the Upper Cretaceous and Cenozoic in Argentina. *Bulletins of American Paleontology*, **65** (282), 317–351.

--- 1975*c*. "Harringtonia" gen. nov. (Ostracoda, Crustacea) y nuevas especies del Terciarico de la Republica Argentina. *Ameghiniana*, **12** (3), 59–279.

--- POSOTKA. 1995. The Cretaceous-Tertiary boundary in Argentina and its ostracodes. Ostracoda and Biostratigraphy, *Riha*, 163–170 pp.

BOLD, W. A. VAN DEN. 1946. Contribution to the study of Ostracoda with special reference to the Tertiary and Cretaceous microfauna of the Caribbean region. Published PhD thesis, RIJKS University of Utrecht. 167 pp.

--- 1957*a*. Ostracoda from the Paleocene of Trinidad. *Micropaleontology*, **3** (1), 1–18.

--- 1957*b*. Oligo-Miocene Ostracoda from Southern Trinidad. *Micropaleontology*, **3** (3), 231–254.

--- 1960. Eocene and Oligocene Ostracoda of Trinidad. *Micropaleontology*, **6** (2), 145–196.

--- 1985. *Heinia*, a new genus oof ostracoda from the Gulf of Mexico and the Caribbean. *Journal of Paleontology*, **59** (1), 1–7.

BONNEMA, J. H. 1940. Ostracoden aus der Kreide des untergrundes der Nordoestlichen Niederlande, teil 2. *Natuurhistorisch maandblad*, **29** (12), 129–132.

BOOMER, I., WHATLEY, R., BASSI, D., FUGAGNOLI, A. and LORIGA, C. 2001. An Early Jurassic oligohaline ostracod assemblage within the marine carbonate platform sequence of the Venetian Prealps, NE Italy. *Palaeogeography, Palaeoclimatology, Palaeoecology*, **166**, 331–344.

BRADY, G.S. 1866. Notes on Entomostraca collected by A. Haly in Ceylon. *Journal Linnean Society*, **19**, 293–317.

--- 1867. A synopsis of the Recent British Ostracoda. *The intellectual observer*, **12** (2), 110–130.

--- 1868*a*. A monograph of the Recent British Ostracoda. *Transactions of the Linnean Society of London*, **26** (2), 353–495.

---1868*b*. Descriptions of Ostracoda. *In* FOLIN, A. G. L. de, and PERIER, L. 1867/1871 A: *Les fonds de la Mer, Etude Internationale sur les particularities vouvelles des regions sous-marines*. Livraison **1** (1), 4–7.

--- (1880). Report on the Ostracoda dredged by H.M.S. Challenger during the Years 1873-1876. *Report on the scientific results of the voyage of H.M.S. Challenger. Zoology*, **1** (3), 1–184.

--- and ROBERTSON, D. 1872. Contributions to the study of the Entomostraca – 6: on the distribution of the British Ostracoda. *Annals and Magazine of Natural History*, Series 4, **3** (17), 353–374.

BRANDÃO, S. N., YASUHARA, M., IRIZUKI, T. and HORNE, J. D. 2013. The ostracod genus *Trachyleberis* (Crustacea; Ostracoda) and its type species. *Marine Biodiversity*. DOI 10.1007/s12526-013-0163-6.

CABRAL, M. C., LORD, A., BOOMER, I., LOUREIRO, I. and MALZ, H. 2014. *Tanycythere* new genus and its significance for Jurassic ostracod diversity. *Journal of Paleontology*, **88** (3), 519–530.

CARBONNEL, G. and JOHNSON, A. K. 1989. Les Ostracodes Paleogenes du Togo: Taxonomie, Biostratigraphie. Apports dans L'Organisation et L'Evolution du Bassin. *Geobios*, **22** (4), 409–443.

CEOLIN, D., FAUTH, G. and COIMBRA, J. C. 2011. Cretaceous-Lower Paleogene Ostracods from the Pelotas Basin, Brazil. *Palaeobiodiversity and Palaeoenvironments*, **91**, 111–128.

COLIN, J.-P. 1987. Étude systématique dês ostracodes de Ia Formation dês Madeleines (Danien du Senegal). *Cahiers de Micropaléontologie*, **2** (3–4), 13–143.

--- and HOCHULI, P. A. 1992. Biostratigraphie de Ia Formation de 1'Aschia-Tinamou (Crétacé Supérieur), Niger oriental: Implications paléogéographiques. *In* CURNELLE, R. (ed.). *I^er^ Colloque de Stratigraphie et de Paléogéographie dês bassins sedimentaires Ouest-Africains*. Géologie Africaine, 255–273 pp.

CORYELL, H. N., SAMPLE, C. H. and JENNINGS, P. H. 1935. *Bairdoppilata*, a new genus of Ostracoda, with two new species. *American Museum Novitates*, **777**, 1–5.

CRANE, M. J. 1965. Upper Cretaceous ostracodes of the Gulf Coast Area. *Micropaleontology*, **11** (2), 191–254.

DEL RÍO C. J., CONCHEYRO, A. and MARTÍNEZ, S. 2011. The Maastrichtian-Danian at General Roca (Patagonia, Argentina): a reappraisal of the chronostratigraphy and biostratigraphy of a type locality. *Neues Jahrbuch Geoogie Paläontologie Abhandlungen*, **259** (2), 129–156.

DINGLE, R. V. 1969. Upper Senonian ostracods from the coast of Pondoland, South África. *Transactions of the Royal Society of South Africa*, **4** (38), 347–385.

--- 1980. Marine Santonian and Campanian ostracods from a borehole at Richards Bay, Zululand. *Annals of the South African Museum,* **82**, 1–70.

--- 1981. The Campanian and Maastrichtian Ostracoda of South-East Africa. *Annals of the South African Museum*, **85**, 1–181.

--- 1984. Mid-Cretaceous ostracoda from Southern Africa and the Falkland Plateau. *Annals of the South American Museum*, part 3, **93**, 98–211.

--- LORD, A. R. and BOOMER, I. D. 1990. Deep-water Quaternary Ostracoda from the continental margin off South-Western Africa (SE Atlantic Ocean). *Annals of the South African Museum*, **99** (9), 245–366.

EAGAR, S. H. 1965. Ostracoda of the London clay (Ypresian) in the London Basin-1: Readiing district. *Revue de Micropaleontologie*, **8** (1), 505–528.

ECHEVARRÍA, A. E. 1986. Presencia de *Copytus* (Ostracoda, Crustacea) en el Cretacico Superior de Chubut, Argentina. I*V Congreso Argentino de Paleontologia y Bioestratigrafia*. Actas 3, Mendoza, 163–167 pp.

--- 1987. Ostracodos de la Formacion Carmen Silva, Miembro Superior (Mioceno Inferior), Isla Grande de Tierra del Fuego, Argentina, part I. *Ameghiniana*, **24** (1–2), 129–139.

EDWARDS, R. A. 1944. Ostracoda from the Duplin Marl (Upper Miocene) of North Carolina. *Journal of Paleontology*, **18** (6), 505–528.

FAUTH, G., SANTOS, A. S. dos., VIEIRA, C. E. L., BERGUE, C. T., MUSACCHIO, E. A., FERREIRA, E. P., ESCAMILLA, J. H., CARVALHO, M. A., VIVIERS, M. C. and BAECKER-FAUTH, S. 2013. Bioestratigrafia integrada do Cretáceo Superior da Bacia de Santos: ostracodes, carófitas e palinomorfos. *Boletin de Geociência*, *Petrobras*, Rio de Janeiro, **20** (1/2), 229–258.

GRÜENDEL, J. 1975. Zur Taxonomie Und Phylogenie Der Unterfamilie Paracytherideinae Puri, 1957 (Cytherocopina, Ostracoda). *Zeitschrift Fuer Geologische Wissenschaften*, **3** (7), 971–983.

GUZEL, M. 2012. Paleobiogeographic significance of Jurassic and Cretaceous Western Australian ostracod faunas. Unpublished PhD thesis, Deakin University, Melbourn. Australia, 371 pp.

HARTMANN, G. 1956. Weiter neue marine Ostracoden aus Brazilian. *Beitrage zur Neotropischen Fauna, Jena*, **1** (1), 19–62.

HERRIG, E. 1963. Neue Ostracoden-Arten aus der weissen schreibkreide der Insel Ruegen (Unter-Maastricht). Wissenchaftliche Zeitschirift der Ernst-Moritz-Arndt-Universitaet Greifswald, Matematisch-Naturwissenschaftliche Reihe, **12** (3–4), 289–325.

HORNIBROOK, N. B. 1952. Some New Zealand Tertiary Marine Ostracoda useful in stratigraphy. *Transactions of the Royal Society of New Zealand*, part 2, **81**, 303–311.

HOLDEN, J. C. 1964. Upper Cretaceous Ostracods from California. *Palaeontology*, **7** (3) 393–429.

HOWELL, A. J., SCHWARZ, E., SPALLETTI, A. L. and VEIGA, G. D. 2007. The Neuquén Basin: an overview. *In* VEIGA, G. D., SPALLETTI, A. L., HOWELL, A. J. and SCHWARZ, E. (eds). *The Neuquén Basin, Argentina. A case study in Sequence Stratigraphy and Basin Dynamics*. Geological Society, London, Special Publications, **252,** 1–14.

ISRAELSKY, M. C. 1929. Upper Cretaceous Ostracods from Arkansas, *In*: SPOONER, W. C. and AL, 1929: *Stratigraphy and Structure of the Gulf Coastal Plain of Arkansas*. Bulletin, Arkansas Geological Survey 2 (Supplement) 1–29.

JELLINEK, T. and SWANSON, K. M. 2003. Report on the taxonomy, biogeography and phylogeny of mostly living benthic Ostracoda (Crustacea) from deep-sea samples (Intermediate Water depths) from the Challenger Plateau (Tasman Sea) and Campbell Plateau (Southern Ocean), New Zealand. *Abhandlungen der Senckenbergischen Naturforschhenden Gesellchaft Frankfurtam Main*, **558**,1–339.

---1857*a*. A monograph of the Tertiary Entomostraca of England. *Annual Volumes (Monographs) of the Palaeontographical Society,* **9**, 1–68.

KAFKA, J. 1886. Kritisches Verzeichniss der Ostracoden der Boehmischen Kreideformation. Sitzungsberichte, Koeniglich-Boehmische Wissenschaftliche Gesellschaft, Mathematisch-naturwissenschaftliche classe: *Vestinik, Ceska spolecnost nauk, trida mathematicko-prirodovedecka*. **1885**, 51–57.

MAJORAN, S. 1989. Mid-Cretaceous Ostracoda of Northern Algeria. *Fossils and Strata*, **27**, 1–67.

McKENZIE, K. G., REYMENT, R. A. and REYMENT, E. R. 1993. Eocene Ostracoda from the Browns Creek Clays at Browns Creek and Castle Cove, Victoria, Australia. *Revista Española de Paleontologia*, **8** (1), 75–116.

MILLER, C. G., RICHTER, M. and DO CARMO, D. A. 2002. Fish and ostracod remains from the Santos Basin (Cretaceous to Recent), Brazil. *Geological Journal*, **37**, 297–316.

MOORE, R. C. and PITRAT, C. W. 1961. Crustacea: Ostracoda. *In* MOORE, R. C. (ed.). *Treatise on Invertebrate Paleontology, Part Q, Arthropoda 3*. Geological Society of America, Boulder, CO, and University of Kansas Press, Lawrence KS, 465 pp.

MUNSEY, G. C. 1953. A Paleocene Ostracoda fauna from the Coal Bluff marl member of the Naheola Formation of Alabama. *Journal of Paleontology*, **27** (1), 1–20.

MUSSO, T., CONCHEYRO, A. and PETTINARI, G. 2012. Mineralogía de arcillas y nanofósiles calcáreos de las formaciones Jagüel y Roca em el sector oriental del Lago Pellegrini, Cuenca Neuquina, República Argentina. *Andean Geology*, **39** (3), 511–540.

NEALE, J. 1975. The Ostracod fauna from the Santonian chalk (Upper Cretaceous) of Gingin, Western Australia. *Special Papers in Palaeontology*, **16**, 1–111.

NEUFVILLE, E. M. H. 1973. Upper Cretaceous Paleogene Ostracoda from the South Atlantic.Publications from the Palaeontological Institution of the University of Uppsala, Special volume **1**,1–523.

NORMAN, A. M. 1865. Report on the Crustacea of Deep-Sea Dredging off the coasts of Northumberland and Durham. *Transactions of the Natural History Society of Northumberland, Durham and Newcastle-upon- Tyne*, **1**, 12–29.

PIOVESAN, E. K., CABRAL, M. C., COLIN, J-P., FAUTH, G. and BERGUE, C. T. 2014. Ostracodes from the Upper Cretaceous deposits of the Potiguar Basin, northeastern Brazil: taxonomy, paleoecology and paleobiogeography. Part 1. *Carnets de Géologie* [*Notebooks on Geology*]. **14** (12), 211–252.

POKORNY, V. 1964. *Oertliella* and *Spinicythereis*, new otracode genera from the Upper Cretaceous. *Vestnik Ustredniho Ustavu Geologickeho*, **39** (4), 283–284.

--- 1967. The Genus Curfsina (Ostracoda, Crustacea) from the Upper Cretaceous of Bohemia, Czechoslovakia. *Acta Universitatis Carolinae, Geologica*, Praha, **4**, 375–379.

PURI, H. S. 1963. Preliminary Notes on the Ostracoda of the Gulf of Napoles. *Experientia*, **19** (7), 368–373.

REUSS, A. E. 1846. Die Versteinerungen der Böhmischen Kreide Formation. *Schweizerbart*, *Stuttgart*, **2**, 59–148.

RODRÍGUEZ, M. E. 2011. El grupo Malargüe (Cretácico Tardío-Paleógeno Temprano) em la Cuenca Neuquina. *In*: Relatório del XVIII Congresso Geológico Argentino, Neuquén, *Geología y recursos naturales de la Província del Neuquén*. 245–264p.

RÖEMER, F. A. 1840. Die Cytherinen des Molasse-Gebirges. *Neues Jahrbuch fuer Mineralogy, Geognosie, Geologie und Petrefaktenkunde*, **1838** (5) 514–519.

SANGUINETTI, Y. T. 1979. Miocene ostracodes of the Pelotas Basin, State of Rio Grande do Sul, Brasil. *Pesquisas*, **12**, 119–187.

SARS, G. O.1866. Oversigt af Norges Marine Otracoder. *Forhandlinger I Videnskabs-Selskabet I Cristiania*, **1865**, 1–130.

SKOGSBERG, T. 1939. A new genus and species of marine ostracods from South Georgia. *Proceedings of the California Academy of Science*, *Series 4*, **23** (27), 415–425.

SWAIN, F. M. and BROWN, P. M. 1964. Cretaceous Ostracoda from wells in the southeastern United States. *Bulletin of North Carolina Department of Conservation and Development*, **78**, 1–55.

--- and GILBY, J. M. 1974. Marine Holocene Ostracoda from the Pacific coast of North and Central America. *Micropaleontology*, **20** (3), 257–353.

SZCZECHURA, J. 2001. Ostracods from the Eocene of Seymour Island, Antarctic Peninsula. *Palaeontologia Polonica*, **60**, 157–181.

TEETER, J. W. 1975. Distribution of Holocene marine Ostracoda from Belize. *In* WANTLAND, K. F. and PUSEY, W. C. III (eds). *Belize shelf carbonate sediments, clastic sediments and ecology*. American Association of Petroleum Geologists, studies in Geology, Tusla (Oklahoma), **2**, 400–499.

TIBERT, N. E., COLIN, J. P., LECKIE, R. M. and BABINOT, J. P. 2003. Revision of the ostracode genus *Fossocytheridea* Swain & Brown, 1964: Mesozoic ancestral root for the modern eurytopic *Cyprideis* Jones. *Micropaleontology*, **49**, 205–230.

ULIANA, M. A. and DELLAPÉ, D. A. 1981. Estratigrafia y evolucion paleoambiental de la sucesion Maestrichtiano-Eoterciaria Del Engolfamento Neuquino (Patagonia Septentrional). *VII Congresso Geológico Argentino*, *San Luis*. Actas III, 673–711.

ULRICH, E. O. and BASSLER, R. S. 1904. Systematic paleontology of the Miocene deposits of Maryland. *Maryland Geological Survey*, **2**, 98–130.

WHATLEY, R. C. and COLES, G. P. 1987. The Late Miocene Quaternary Ostracoda of Leg 94, Deep Sea Drilling Project. *Revista Española de Micropaleontologia* **19**, 33–98.

--- and MASSON. 1980. The ostracod genus *Cytheropteron* from the Quaternary and Recent of Great Britain. *Revista Española de Micropaleontologia*, **11** (2), 223–277.

--- MILLSON, K. and AYRES, M. 1992. *Philoneptunus*, a new Ostracod genus from the Cainozoic of Australasia. *Revista Española de Micropaleontologia*, **24** (3), 43–62.

--- MOGUILEVSKY, A., TOY, N., CHADWICK, J. and RAMOS, M. I. F. 1997. Ostracoda from the Southwest Atlantic. Part III. The littoral fauna from between Tierra del Fuego and the Rio de la Plata. *Revista Española de Micropaleontología*, **29**, 5–83.

4.2 Artigo 2

Título

The Nodoconchiinae, a new Subfamily of Cytheridae (Crustacea, Ostracoda).

Autores

Daiane Ceolin*[1], Robin Whatley[2], Gerson Fauth[1] & Andrea Concheyro[3]

[1]Instituto Tecnológico de Micropaleontologia - itt Fossil, Universidade do Vale do Rio dos Sinos-UNISINOS, Avenida Unisinos, 950, CEP 93022-000, São Leopoldo-RS, Brazil.

[2]Micropalaeontology Research Group, Institute of Earth Sciences, Aberystwyth University, Aberystwyth, Cardiganshire SY23 3DB, United Kingdom

[3]IDEAN - Instituto de Estudios Andinos "Don Pablo Groeber". Consejo Nacional de Investigaciones Científicas y Técnicas. Facultad de Ciencias Exactas y Naturales, Universidad de Buenos Aires. Pabellón II. Ciudad Universitaria. CP 1428. Buenos Aires, Argentina.

*Corresponding author (e-mail:daianeceolin@yahoo.com.br)

Periódico

Submetido ao *Journal of Micropaleontology*

OBS: o artigo se encontra formatado de acrodo com as normas da revista.

The Nodoconchiinae, a new Subfamily of Cytheridae (Crustacea, Ostracoda).

Daiane Ceolin*[1], Robin Whatley[2], Gerson Fauth[1] & Andrea Concheyro[3]

[1]Instituto Tecnológico de Micropaleontologia - itt Fossil, Universidade do Vale do Rio dos Sinos-UNISINOS, Avenida Unisinos, 950, CEP 93022-000, São Leopoldo-RS, Brazil

[2]Micropalaeontology Research Group, Institute of Earth Sciences, Aberystwyth University, Aberystwyth, Cardiganshire SY23 3DB, United Kingdom

[3]IDEAN - Instituto de Estudios Andinos "Don Pablo Groeber". Consejo Nacional de Investigaciones Científicas y Técnicas. Facultad de Ciencias Exactas y Naturales, Universidad de Buenos Aires. Pabellón II. Ciudad Universitaria. CP 1428. Buenos Aires, Argentina.

*Corresponding author (e-mail:daianeceolin@yahoo.com.br; daiaceolin@unisinos.br)

ABSTRACT - The new subfamily Nodoconchiinae of the Cytheridae Baird, is erected to accommodate three genera: *Austrocythere* Hartmann, *Nodoconcha* Hartmann and *Ectonodoconcha* gen. nov. *Austrocythere* seems to be known only from the type species *A. reticulotuberculata* Hartmann, from its type locality in the Antarctic and from the Antarctic Oligocene. *Nodoconcha*, however, apart from its original record by Hartmann from the Antarctic as *Nodoconcha minuta*, has also been encountered in the Oligocene of the Antarctic. In the present study, we have identified seven species of *Nodoconcha* from the Maastrichtian and Danian of the Neuquén Basin, together with a new genus from the Danian, *Ectonodoconcha lepidotus* gen. et sp. nov. The new species of *Nodoconcha* are *N. polytorosa* sp. nov, *N. sanniosis* sp. nov and *N. upsilon* sp. nov. and *Nodoconcha*? sp. that is the possible ancestor of the entire group. Previously described species now placed in the genus are: *N.*

paleocenica (Bertels), *N. jaguelensis* (Bertels) and *Nodoconcha* sp. (Bertels). The *Nodoconcha* species are divided into the Minuta and Upsilon groups.

KEYWORDS: *Ostracoda*, *Nodoconchiinae*, *Evolution*, *Maastrichtian-Danian*, *Neuquén Basin.*

INTRODUCTION

There have being some subsequent records of *Austrocythere reticulotuberculata* Hartmann from the Recent of Holm Bay Lützow, East Antarctic (Yasuhara *et al*. 2007) and Oligocene CRP-2/2A and CRP-3 Drill holes, Victoria Land Basin, Antarctic (Dingle & Majoran, 2001). On the other hand, *Nodoconcha* has being recorded by various authors as early as the Oligocene (Lower Miocene of New Zealand, Milhau, 1993; Victoria Land Basin, Antarctic, Dingle, 2000, and King George, Antarctic, Blaszyk, 1987).

Hartmann (1989a) described two new genera, *Austrocythere* and *Nodoconcha* from the Oligocene and Recent. These genera were encountered in extremely cold conditions in the Antarctic. Hartmann classified *Austrocythere* as Cytheridae (1987? *Cytheride* sp.; 1989a, *Austrocythere reticulotuberculata*). He found it in South Georgia, Lavoisier Island and Adelaide Island, at water depths between 116 and 215 m. The type locality of *Austrocythere* is South Georgia.

The genus *Nodoconcha* was classified by Hartmann (1997) *incertae sedis*, although every indication from his early work is that it belongs to the Cytheridae (Hartmann, 1989a). The type species *Nodoconcha minuta* Hartmann, has been recorded from the Antarctic Peninsula, South Georgia, South Orkneys, Lavoisier Island, Hope Bay, Adelaide Island,

between 185–370 m depth (Hartmann, 1988, 1989 a, b, 1990), Ross Island (Briggs, 1978) and also from Lützow-Holm Bay (Yasuhara *et al*. 2007).

The antiquity of the occurrence of *Nodoconcha*, is confirmed and extended into the Maastrichtian and Danian in the present study. The new occurrence of seven species of *Nodoconcha* in the Neuquén Basin, a well-known basin for its rich fossil content, represents a place of species cluster and migration route for many species (Whatley & Ballent, 1996; Ballent & Whatley, 2006, 2007; Piovesan *et al*., 2012, Ceolin *et al*. in press).

The aim of this paper is to present new species of *Nodoconcha*, belonging to our new subfamily Nodoconchiinae, some of them previously identified as "*Cytherura*?" and "*Wolburgia"* by Bertels (1973, 1974) and to demonstrate possible evolutionary trends and relationship with the Recent occurrences of this genus.

Geological setting

The Neuquén Basin is located in West-Central Argentina between latitudes 32º and 40ºS. It is developed in the provinces of Mendoza, Neuquén, Río Negro and La Pampa. In latitude 35ºS, the basin extends to form the Neuquén embayment that comprises 600 km of extension in a North-South direction and 300-400 km East-West. It has a maximum thickness of 7.000 m of marine and non-marine sedimentary rocks, ranging from the late Jurassic to the Palaeocene (Concheyro *et al*. 2002; Howell *et al*., 2007; Aguirre-Urreta *et al*., 2011) (Figure 1).

The marine sediments from the Cerro Azul section (S38°50'48", W67°52'20"), a relatively new site for micropaleontological studies in the eastern sector of Lake Pellegrini, Neuquén Basin, were deposited during the first transgression from the Atlantic Ocean in the Late Maastrichtian-Lower Danian (Jagüel Formation) and Danian (Roca Formation). The

samples are composed of calcareous siltstones and claystones and according to Musso *et al*. (2012), the samples from the Jagüel Formation have an homogeneous lithology of grey calcareous mudstone. An alternation of carbonate rocks and greenish grey calcareous mudstones characterise the Roca Formation and the base of the referred formation was defined, according to criteria adopted by Uliana & Dellape (1981), by the first appearance of organogenic limestone. The age of the samples was determined by calcareous nannofossils (Musso *et al.* 2012).

Material and methods

Were studied 27 samples, seven from the Maastrichtian and 20 from the Danian, from the Cerro Azul section. Approximately 20 g of dried rock was crushed and soaked in 200 mL of a hydrogen peroxide solution (H_2O_2) for 24 hours, at a concentration of 35 per cent. Residues were then washed and divided into grain fractions 63, 180, and 250 μm and dried at 60 ºC. All ostracods were hand-picked under a stereo microscope from each size fraction. Selected specimens were imaged by scanning electron microscopy (SEM), in a EVO MA15 Zeiss microscope.

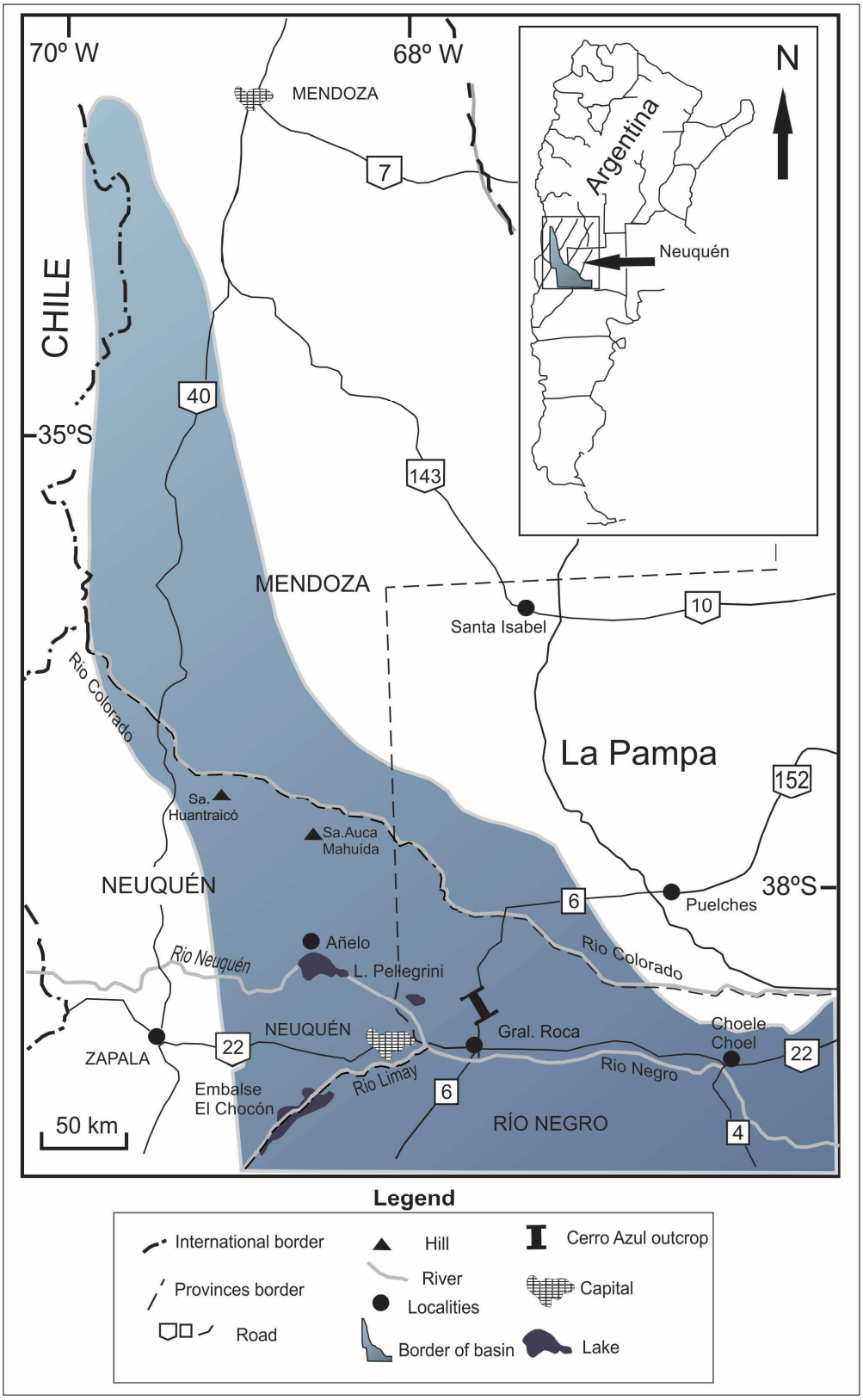

Fig. 1. Location map of Neuquén Basin with the position of the Cerro Azul section.(Modified from Del Río *et al*. 2011).

SYSTEMATIC DESCRIPTION

The suprageneric classification adopted is that proposed by Moore and Pitrat (1961) with some modifications. In the systematic descriptions, the following conventions are employed: L: length; H: height; W: width, RV: right valve, LV: left valve, CMS: central muscle scar. All dimensions are in mm. Size, based on length, is as follows: very small (<0.400 mm), small (0.410–0.500 mm), medium (0.510–0.700 mm), large (0.710–0.900 mm), very large (>0.900 mm). Type and figured specimens are deposited in the collections of the Facultad de Ciencias Exactas y Naturales, Laboratorio de Micropaleontología, Buenos Aires, Argentina, under their respective catalogue numbers LM-FCEN 3210-3231.

Subfamily Nodoconchiinae subfam. nov. Ceolin & Whatley

This group form a distinct entity within the family Cytheridae. In their ornamentation and carapace organization, they are quite different from other Cytheridae.

The Cytherinae, those members of the family not in Nodoconchiinae subfam. nov., such as *Cythere* O.F. Müller and *Loxocythere* Hornibrook, are a group of ovate, subovate, often ventrolateraly tumid genera which usually do not bear tubercles, nor strong sulcae and there is an essential similarity about them in carapace morphology and ornamentation. It would be very difficult to accommodate the taxa we include in the Nodoconchiinae, with the other members of the Cytheridae. Therefore, we feel justified in erecting this new subfamily and including within it the genera *Austrocythere* Hartmann, *Nodoconcha* Hartmann and *Ectonodoconcha.*

This new subfamily first appears in the Maastrichtian and ranges through to the Recent in the form of *Austrocythere* and *Nodoconcha*.

Class **Ostracoda** Latreille, 1806

Order **Podocopida**, Müller, 1894

Suborder **Podocopina** Sars, 1866

Family **Cytheridae** Baird, 1850

Subfamily **Nodoconchiinae** new subfamily

Genus *Nodoconcha* Hartmann, 1989

Minuta group

Nodoconcha minuta Hartmann, 1989

(Pl. 1, fig. 1)

1978 "*Roundstonia*" sp. Briggs: 29, figs 2-12.

1988 *Cytheride*, Hartmann: 149, pl. 1, fig. 8.

1989a *Nodoconcha minuta* gen et sp. nov., Hartmann: 218-219, figs 42-49b.

1989b *Nodoconcha minuta* Hartmann: p. 251.

1990 *Nodoconcha minuta* Hartmann: 211-121, figs 70-71; pl. VII, figs 63-65.

2000 *Nodoconcha minuta* Hartmann. Dingle: 489, fig. f.

2001 *Nodoconcha* aff. *N. minuta* Hartmann. Dingle & Majoran: 31.

Description. A medium to large species of the Nodoconchiinae subfam. nov., subovate in lateral view. Anterior margin well rounded and extending below ventral margin; posterior margin with apex above mid-height with a long keel-like posteroventral slope. Dorsal margin straight, overhung ocularly, medianly and posteromedianly by valve ornament. Ventral margin biconvex about a distinct oral incurvature; in the centre of which internally, is a circular snap-knob. Ornament of tubercles and reticulation. There is a small eye tubercle below and behind which is a large tubercle behind mid-length on the dorsal margin and projecting beyond it is another, smaller tubercle. These two latter tubercles are separated by a

distinct diagonally forwards inclined median sulcus. Between these two tubercles and close to the dorsal margin, there are two small circular tubercles *en echelon* and a further two small tubercles occur posteriorly to the posteromedian tubercle. Three tubercles, all of the same size, and approximately the same size as the posteromedian tubercle, occur on a ventrolateral rib in a shallow concave upwards curve. The summits of all five tubercles bear a very fine reticulation within the larger reticulation that covers the entire valve surface, except the extreme end margins, and much of that reticulation is itself secondarily reticulate but not as finely as on the summit of the tubercles. Hinge antimerodont with, in the right valve, the anterior terminal element is a dentate bar with three large teeth and one small proximal tooth while the posterior terminal element bears five teeth; the median element is a finely locellate groove. CMS not seen. Inner lamella vestibulate at either end with well-developed selvage anteriorly.

Remarks. Dingle & Majoran (2001) recorded *N*. aff. *N*. *minuta* Hartmann from the Oligocene of Antarctic, but neither described nor illustrate it. We, therefore, are unable to compare it with none of the species in Minuta group nor with *N*. *minuta* Hartmann, but we believe that this species belongs to *N*. *minuta*.

Nodoconcha polytorosa sp. nov. Ceolin & Whatley

(Pl. 1, figs. 2-9)

Derivation of name. Gr. *πολύς*, many, numerous; plus L. *torus*, elevation, protuberance, "many tubercles" referring to the numerous rounded tubercles that occur on the carapace of this species.

Holotype. One complete carapace, LM-FCEN 3210.

Paratypes. LM-FCEN 3211- 3214.

Material. 47 specimens from samples 16, 17, 19, 21, 23, 26, 29, 34, 39 and 53. Danian.

Diagnosis. A small species of *Nodoconcha* characterized by a ventrolateral rib on which three small tubercles are disposed longitudinally and a double posteromedian rib on the dorsal margin. An anterior marginal ridge extends from the anterior cardinal angle to an anteroventral position. Surface of the carapace strongly punctate and reticulate in part.

Dimensions.

				L	H	W	Sample
Holotype,	LM-FCEN 3210,	♀	carapace	0.462	0.240	0.213	23
Paratype,	LM-FCEN 3211,	♀	carapace	0.424	0.227	0.201	17
Paratype,	LM-FCEN 3212,	♂	carapace	0.585	0.235	0.192	23
Paratype,	LM-FCEN 3213,	♀	valve	0.490	0.272		17
Paratype,	LM-FCEN 3214,	♂	carapace	0.434	0.211	0.187	21

Description. Subrectangular in lateral view with rounded end margins. In dorsal view, subovate with compressed extremities, mainly anteriorly, which is somewhat flared. Shell of medium thickness. Anterior margin broadly rounded, more narrowly below mid-height. Posterior more narrowly rounded with apex above mid-height. Dorsal margin straight but overhung in posterior part by a tubercle. Ventral margin biconvex about an anterocentral oral concavity and obscured in lateral view by valve tumidity, more prominent in males, in which posteroventral keel is better developed. Dorsal cardinal angle pronounced, especially anteriorly. LV larger than RV with some overlap anteroventrally and from mid-posterior to posteroventral. Greatest length at mid-height; greatest height at both anterior cardinal angles; greatest width in posterior one-third. Ornamentation reticulopunctate, more pronounced in anterior and posterior areas. A pronounced, mainly smooth marginal rim extends peripherally around the free and dorsal margins. There is a distinct ventrolateral rib, which bears three longitudinally disposed tubercles. This rib divides into two with the lower rib overhanging the ventral surface and terminating anteroventrally. An irregular, sinuous rib extends from the eye

tubercle adjacent to the dorsal rim to a posterodorsal complex. Two tubercles occur anterodorsally and posterodorsally. A distinct subvertical median sulcus extends ventrally to the ventrolateral rib. A smaller, post-ocular sinus separates the eye-tubercle from the anterodorsal tubercle. Apart from some smooth ribs and the marginal rim, the carapace is covered by small puncta, which also occur on the flanks and summit of some tubercles. The reticulation is more or less confined to the anterior and posterior and it is not preferentially oriented. Normal pore canals are simple, most on the elevation of muri or the tubercles. Large, simple pore conuli occur across the valve, especially posteriorly. Hinge antimerodont. In the left valve, the anterior terminal element is a biloculate socket in which the two locules are disposed obliquely, with the proximal one above the distal. The entire socket is buttressed by an anti-slip structure ventrally. The posterior terminal element is a curved, loculate socket with six smaller loculae. The median element is a long, strongly denticulate bar with numerous relatively long circular denticles. Calcified inner lamella very wide posteroventrally; avestibulate. Radial pore canal not seen. CMS imperfectly seen. The position of the larger tubercles are reflected internally. Sexual dimorphism with males more elongate and less inflated at posterior one-third than females.

Remarks. Differs from *Nodoconcha minuta* Hartmann in being slightly smaller, in possessing, as well as a median sulcus, a post-ocular sulcus and in its ornament, which is much more punctate than *N. minuta*. It also has a much better developed marginal rim, particularly anteriorly. A further difference is that in *N. polytorosa* sp. nov. the posteomedian tubercle is a double structure unlike the single structure of *N. minuta*.

Nodoconcha sanniosis sp. nov. Ceolin & Whatley

(Pl. 1, figs. 10-17)

Derivation of name. L. *sanniosis* "one who makes faces". Which reference to the rather face-like appearance of the ornamentation on the surface of the lateral tubercles.

Holotype. One complete carapace, LM-FCEN 3215.

Paratypes. LM-FCEN 3216-3219.

Material. 43 specimens from samples 34, 36, 39, 40 and 53. Danian.

Dimensions.

				L	H	W	Sample
Holotype,	LM-FCEN 3215,	♀	carapace	0.462	0.240	0.212	34
Paratype,	LM-FCEN 3216,	♀	carapace	0.410	0.210	0.211	34
Paratype,	LM-FCEN 3217,	♂	carapace	0.502	0.243	0.170	34
Paratype,	LM-FCEN 3218,	♀	valve	0.441	0.217		26
Paratype,	LM-FCEN 3219,	♂	carapace	0.452	0.201	0.18	34

Diagnosis. A small species characterized by a group of five tubercles, three of which are disposed ventrolaterally and whose ornament is mask-like. Surface reticulopunctate.

Description. Small, subrectangular in lateral view. Subovate in dorsal view. Shell of medium width. Anterior margin broadly rounded with apex at mid-height. Anteroventrally there are small, blunt, rounded, marginal denticles. Posterior margin bluntly pointed with apex at mid-height. Dorsal margin straight but overhung in posterior part by ornament. Ventral margin bi-convex about shallow anterocentral oral concavity and not obscured by valve tumidity. LV overlaps the RV, mainly on posterior and ventral margins. Dorsal cardinal angles distinct. Ornamentation reticulotuberculate. The reticulum posteriorly is extremely coarse due to the fact that most of the muri have been enlarged into strong ribs that are chaotically disordered across the ventral surface. Except anterodorsally, there are relatively few interconnecting muri so that in most of area there are no reticular cells. The muri, especially posteriorly, bear simple pores on small conuli. Anteriorly, the muri are less strong and there is a genuine reticulum where much larger conuli and perforations occur distally. There are five large

tubercles on the carapace surface plus an eye tubercle. The two largest tubercles on the dorsolateral surface have flanks that are ornate with a distinct reticulation pattern, in a group of three mask-like structures on each tubercle. They are separated from each other by a vertical median sulcus and the anterior-most of these is separated by the post ocular sinus from a strongly buttressed eye tubercle. Three smaller tubercles occur in a line posteroventrally, the largest being anterior. Each tubercle is surrounded dorsally by an inverted "U"-shaped rib and centrally comprises several short, horizontal striae. From the eye tubercle, a sinuous ribs extends close and parallel to the dorsal rib onto a posterodorsal complex above the posterodorsal tubercle, and from this complex, a strong mural rib extends ventrally and eventually joins the ventrolateral rib. A strong, smooth marginal rim surrounds the entire valve margin. Rare sieve-type pores present mainly in anterior region. Greatest length near mid-height; greatest height in posteriorly third. Hinge antimerodont with median element in LV a long, strongly denticulate bar with numerous relatively strong circular denticles. Calcified inner lamella very wide posteroventrally; avestibulate. Radial pore canals not seen. CMS with four adductors in a vertical line and a single oval frontal scar. The position of the larger tubercle are reflected internally. Sexual dimorphism pronounced with males more elongate and less inflated than females.

Remarks. This species differ from *Nodoconcha polytorosa* sp. nov. in the better developed pattern of reticulation and in the absence of a strong ventrolateral rib that join the three tubercles.

Nodoconcha sp. (Bertels, 1974)

(Pl. 1, fig. 18)

1974 *Cytherura*? sp. Bertels: 392, pl. 2, figs 12 a-b.

Type material. One carapace from Bertels' material, LM-FCEN 706, from Lower Jagüelian Substage (Lower Maastrichtian?), Fortín General Roca. Rio Negro Province. Argentina.

Dimensions. L: 0.429, H: 0.220, W: 0.20.

Diagnosis and Remarks. An elongate subrectangular species of Nodoconchiinae typified by reticulotuberculate ornament. Unlike any others species of genus, the chain of the three ventrolateral tubercles is extending onto the anterior marginal surface with a further two tubercles. The reticulation is rather irregular and variable. In places there seems to be a micro ornament between the two tubercles and the reticulation. Marginal rim better developed than *N. minuta* Hartmann, but much less well developed than *N. polytorosa* sp. nov. However, this is clearly a member of Minuta group.

Upsilon group

Nodoconcha upsilon sp. nov. Ceolin & Whatley

(Pl. 2, figs. 1-7)

Derivation of name. Gr. *υπσιλον*, upsilon, with reference to the reclining 'U'-shape of the lobe that surrounds the median sulcus.

Holotype. One complete carapace, LM-FCEN 3220.

Paratypes. LM-FCEN 3221-3225.

Material. 62 specimens from samples 29, 31, 34, 36, 39, 50, 55 and 57.

Dimesions.

				L	H	W	Sample
Holotype,	LM-FCEN 3220,	♀	carapace	0.528	0.274	0.139	34
Paratype,	LM-FCEN 3221,	♀	carapace	0.461	0.227	0.137	34
Paratype,	LM-FCEN 3222,	♂	carapace	0.540	0.258	0.125	34
Paratype,	LM-FCEN 3223,	♂	valve	0.491	0.251		26
Paratype,	LM-FCEN 3224,	♂	carapace	0.515	0.152	0.198	34
Paratype,	LM-FCEN 3225,	♀	carapace	0.589	0.251	0.275	34

Diagnosis. A medium species of *Nodoconcha* characterized by the reclining 'U'-shaped lobe that surrounds the median sulcus and the fact that ventrolateral tubercles are not developed. Ornament irregular reticulation.

Description. Subrectangular in lateral view with rounded end margins; in dorsal view subovate with compressed extremities, especially anteriorly. Females more inflated in posterior one-third than males. Moderately thick-shelled. Anterior margin broadly rounded, most narrowly below mid-height. Posterior margin more narrowly rounded with apex above mid-height. Both end margins bear very small marginal denticles on their ventral edges. Dorsal margin straight and overhung only by the posterior dorsal tubercle. Ventral margin biconvex, about an anterocentral oral concavity and not obscured in lateral view. Dorsal cardinal angles pronounced, especially posteriorly. LV larger than RV with some overlap posterodorsally and anterodorsally. Greatest length at mid-height; greatest height at anterior cardinal angle and in the position of the posterodorsal tubercle; greatest width in posterior one-third. Ornamentation reticulopunctate. There is a distinct oblique median sulcus the base of which is largely smooth, it terminates just below mid-height. Another, longer oblique postocular sulcus also largely smooth extends from just behind the small, but prominent, eye tubercle. Anteroventrally, it is bridged by a small elevated area that is reticulated. A large, reclined 'U'-shaped lobe surrounds the median sulcus. It expands posterodorsally into a long, irregular tubercle that overreaches the dorsal margin. Another elongate tubercular area extends anteroventrally from near the eye tubercle, which, in some specimens bears a rib from just above mid-height. Some specimens have small tubercles close to the ocular rib. The reticulation is strongly developed and in most individuals, the horizontal muri are strongest, giving rise to small, longitudinal riblets. These are often pronounced on the summits of the larger tubercles. Normal pore canals of two types: one on the muri that are small, simple and

mainly conjunctive, and the others, larger in the solae and clearly sieve-type. Hinge antimerodont. In the left valve, the anterior terminal element is a bi-loculate socket in which the two loculae, are disposed obliquely, with the proximal above the distal. The entire socket is buttressed by an anti-slip structure ventrally. The posterior terminal element is a curved loculate socket with six smaller loculae. The median element is a long, strongly denticulate bar with numerous relatively large circular denticles. In the anterior part of the median element, there are larger denticles than other parts. Calcified inner lamella very wide posteroventrally; anteriorly the inner lamella and line of concrescence seems coincident and there is no vestibulum. Radial pore canal not seen. CMS as for family, the anterior scar is ovate. Sexual dimorphism with males more elongate than females.

Remarks. Bertels' species, (1973, Danian) *Nodoconcha paleocenica* (ex. *Wolburgia*) differs in lacking the type of reticulation of the present species and the structures paralleling the anterior margin. In addition, the 'U'-shaped elevation surrounding the median sulcus is incomplete in Bertels' species. The two species also differ in dorsal view. There are also many other smaller differences in ornamentation.

Nodoconcha paleocenica (Bertels, 1973)

(Pl. 2, figs 8-9)

1973 *Wolburgia*? *paleocenica* Bertels: 332, pl. 5, figs 12a-b, 13.

Type material. Two carapaces and two valves from Bertels' material. Holotype LM-FCEN 515; paratypes LM-FCEN 516-517 from Roca Formation of Fortín General Roca, Río Negro Province, Argentina.

Dimensions. Paratypes LM-FCEN 516-517, L: 0.446, H: 0.226, W: 0.175.

Description. An elongate subovate species of *Nodoconcha* with distinct marginal rim and two strong lobe-like structures somewhat resembling certain species of the Palaeozoic Palaeocopida. These two lobes which are distinctively rounded dorsally and are joined ventrally to form a large 'U'-shaped structure. Both the two lobes and the remainder of the shell surface are distinctly punctate.

Remarks. This species differs from *N. upsilon* sp. nov., to which group it clearly belongs, by the fact that in *N. upsilon* the ornament is distinctly reticulate while in *N. paleocenica* (Bertels, 1973) it is punctate. Also in *N. upsilon* the dorsal termination of the lobes are not rounded and the post-ocular sulcus is in two distinct parts separated by a ridge. The lower part of this sulcus is absent in *N. paleocenica*. There are also many other differences in the ornament of the two species, such as, the divergence into two of the anteromarginal rim in *N. upsilon*.

Others species

Nodoconcha jaguelensis (Bertels, 1974)

(Pl. 2, figs. 10-11)

1974 *Cytherura*? *jaguelensis* Bertels: 392, pl. 2, figs 10 a-b, 11.

Type material. Two carapaces and two valves from Bertels' material. Holotype LM-FCEN 703; paratypes LM-FCEN 705 from lower beds of the Upper member of the Jagüel Formation, Fortín General Roca , Rio Negro Province. Argentina. Approximately 67°32'W; 39°00'S.

Dimensions. Paratype LM-FCEN 704, L: 0.382, H: 0.187, W: 0.157.

Diagnosis. A very elongate, subrectangular species of *Nodoconcha* with anterior margin obliquely rounded. Surface reticulotuberculate with the third tubercle on the upper ramus of

the ventrolateral rib absent or only feebly developed. Posterodorsal tubercle not well defined. Intertubercular area posterocentrally with horizontal or oblique riblets.

Description. A small, elongate carapace, subrectangular in lateral view, subovate in dorsal view with well-defined median sulci. Anterior margin well rounded with apex at about mid-height and with dorsal part of anterodorsal slope straight to almost concave. Posterior margin narrow, bluntly pointed with apex at mid-height. On the posterodorsal slope, there is a small concavity while the posteroventral is convex. Dorsal margin straight and only slightly overhung mid-posteriorly by small nodose inflation. Anterior and posterior cardinal angles well defined. Ventral margin biconvex about slight oral concavity. Greatest height at anterocardinal angle, greatest length at mid-height, greatest width at one third posteriorly. Ornamentation reticulotuberculate, with an irregular reticulum that covers the entire surface, except anteriorly. It is very chaotic posterodorsally with a tendency for the muri to be preferentially oriented ventrally while more medianly, they are orientated laterally. A ventrolateral rib at joins three small, poorly defined, horizontally aligned tubercles. A median sulcus disposed almost vertically that separates the antero and posterodorsal tubercles. The posterior one poorly defined. A small, post ocular sulcus is also developed. Eye tubercle small and close to valve margin and with small ocular rib. Marginal rim rather weakly developed. Other features not seen. Sexual dimorphism present with males more elongate and narrower than females.

Remarks. Differs from *Nodoconcha sanniosis* sp. nov. in the absence of an exclusive ornamentation on the tubercles, the absence of reticulation on the anterior margin and less well-defined tubercles, specially the most posterior on the ventrolateral rib. Differs from *Nodoconcha polytorosa* sp. nov. in its more elongate shape, more developed reticulation pattern and larger nodes, mainly antero and posterodorsally.

Nodoconcha? sp.

(Pl. 2, fig. 12)

Material. Five poorly preserved specimens from sample 5, Maastrichtian.

Dimensions. Holotype LM-FCEN 3226, L: 0.347, H: 0.260.

Description. Elongate subtriangular in lateral view; anterior margin rounded with apex below mid-high. Posterior margin subtruncate with apex at about mid-height. Dorsal margin straight and sloping posteriorly; obscured by sinuous ribs on the dorsal surface. Ventral margin with large, shallow oral concavity. There are two large sulci, a median and a post ocular, both extending forward diagonally. Ornament reticulate with muri around free margins parallel to those margins with short intervening ribs giving rise to numerous largely circular, but some quadrate reticule. The base of all sulci are smooth. A sinuous ventrolateral rib bears distinct swellings and another occurs on the dorsal margin posteromedianlly. Internal features not seen.

Remarks. While this species lacks, for example, the three ribs in a curved row ventrolaterally, the site of the ribs exist putatively as does the site of the posteromedian rib. We believe this to be an ancestor of *Nodoconcha* and we have used that name questionably. It is our intention in the very near future to seek further material examples of the species in the Maastrichtian of the Neuquén Basin.

Genus *Ectonodoconcha* gen. nov. Ceolin & Whatley

Derivation of name. Gr. *εκτο* ecto, without, away; plus *Nodoconcha*. With reference to the fact that, although related, this species is of a genus different from *Nodoconcha*.

Type species. *Ectonodoconcha lepidotus* sp. nov. Ceolin & Whatley

Diagnosis. As for the type species.

Remarks. It differs from species of *Nodoconcha* in lacking large nodes posteroventrally and in its massively strong reticulation. However we believe that this genus is a probable early Danian offshoot of the Nodoconchiinae.

Ectonodoconcha lepidotus sp. nov. Ceolin & Whatley

(Pl. 2, figs. 13-17)

Derivation of name. Greek *λεπϊδωτος* lepidotus; covererd in scales. With reference to the fact that in the posterior half of the valve, the reticulae are rather like fish-scales.

Type material. One complete carapace, LM-FCEN 3227.

Paratypes. LM-FCEN 3228-3231.

Material. 20 complete carapaces from samples 21, 23, 29, 34, 36 and 40. Danian.

Diagnosis. A genus of Nodoconchiinae gen. nov. with strongly developed smooth ventrolateral keel. Strong ventrolateral rib, becoming almost alate anterior of mid-length. Ornament of extremely strong reticulation with circular, ovate and quadrate cells and strong subcentral tubercle, which is also reticulate. Reticulae in very like scales of a carp. Smooth rim around free margins. Eye partially ornamented.

Dimensions.

				L	H	W	Sample
Holotype,	LM-FCEN 3220,	♀	carapace	0.453	0.253	0.175	23
Paratype,	LM-FCEN 3221,	♀	carapace	0.369	0.20	0.125	29
Paratype,	LM-FCEN 3222,	♂	carapace	0.404	0.206	0.153	36
Paratype,	LM-FCEN 3223,	♂	carapace	0.384	0.20	0.151	36
Paratype,	LM-FCEN 3225,	♀	carapace	0.440	0.225	0.199	26

Description. Small, elongate subrhomboidal in lateral view. In dorsal view, both end margins are splayed due to the angle of the peripheral rims. The alar process is not prominent in this view, although the tubercle immediately below and behind the eye is very prominent.

Anterior margin widely and evenly rounded about mid-height. Posterior margin more narrowly rounded, asymmetrical with apex above mid-height and very long, gently curved ventral slope. Dorsal margin straight, slightly obscured posteriorly by valve surface. Ventral margin irregularly biconvex with marked oral incurvature, largely obscured by alar process. LV larger than RV with overlap around the entire margin, especially at the dorsal cardinal angles and posteroventrally. Greatest length above mid-height; greatest height medianly; greatest width at one-third posteriorly. Eye tubercle large and overreaching the dorsal margin. A strong smooth marginal rim with a small denticle anteriorly, occurs peripherally at both end margins. Ornament of extremely strong reticulae, embracing cells ranging in shape from circular through oval to quadrate and polygonal; and giving an aspect of the scales of such fish as carp, bass or mullet. Small simple pores, mostly conjunctive, occur on the muri and there are small pore conuli elsewhere. Some pore conuli in the solae are apparently sieve-type. The ornament extends onto the alar process and covers an elevated area immediately posteroventral to the eye tubercle. Internal features not seen.

Remarks. Differs from *Nodoconcha polytorosa* sp. nov., in the absence of ventrolateral and posterodorsal tubercles and in the pattern of the fish-scale like reticulation.

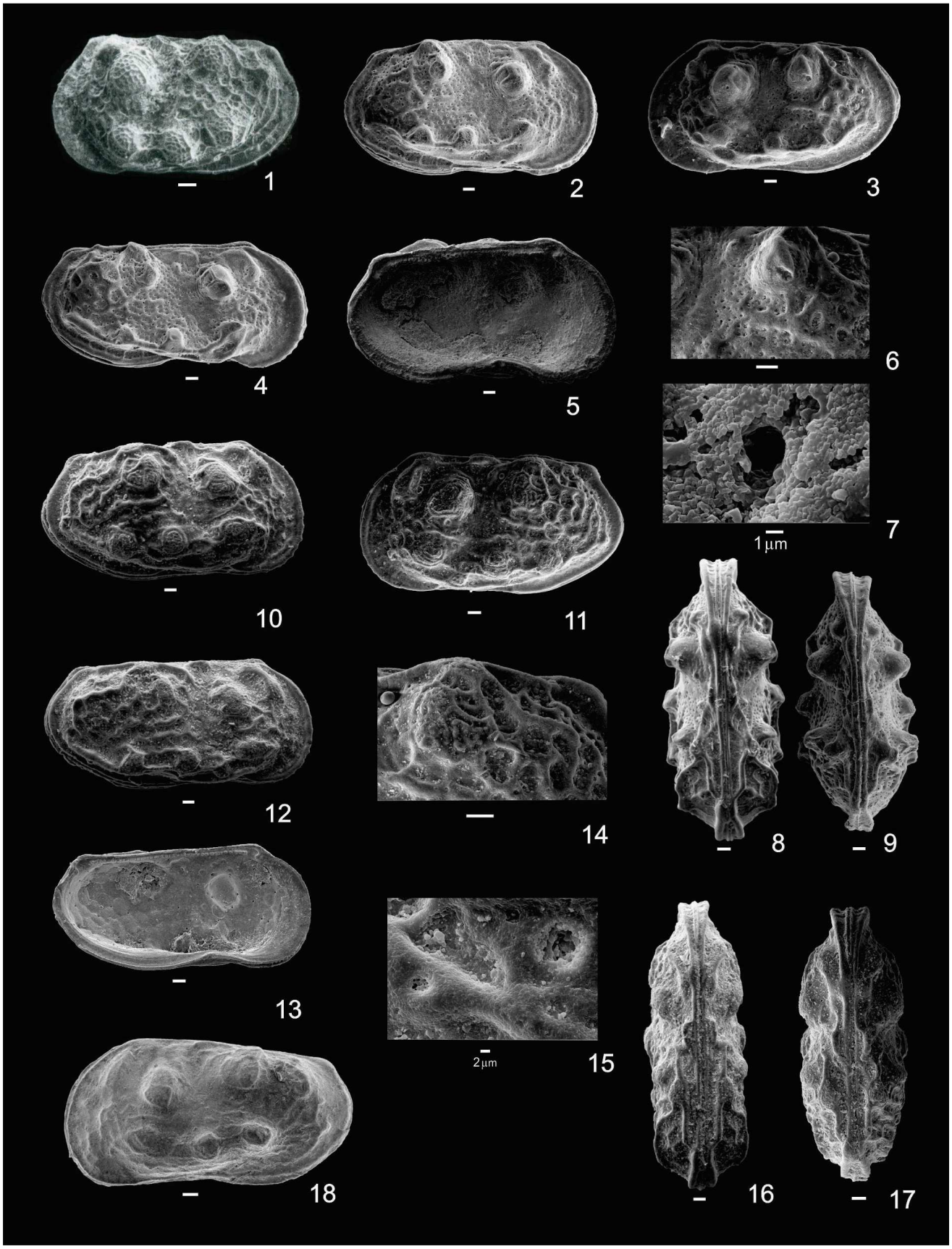
1
2
3
4
5
6
7
1 µm
10
11
12
14
8
9
13
2 µm
15
16
17
18

Explanation of Plate 1. Scale bars are 20 µm. **fig. 1.** *Nodoconcha minuta* Hartmann, 1989, valve, left view. **figs 2-9.** *Nodoconcha polytorosa* sp. nov., **2**, holotype LM-FCEN 3210, carapace, right view, female, **3**,**6-7,** paratype LM-FCEN 3211, **3**, carapace, left view, female, **6**, detail of ornamentation, **7**, detail of simple pore, **4**, paratype LM-FCEN 3212, carapace, male, dorsal view, **5**, paratype LM-FCEN 3213, internal view, female, **8**, paratype, LM-FCEN 3214, dorsal view, male, **9**, holotype LM-FCEN 3210, dorsal view, female. **figs. 10-17.** *Nodoconcha sanniosis* sp. nov., **10**, holotype LM-FCEN 3215, carapace, right view, female, **11**, paratype LM-FCEN 3216, female, carapace, left view, **12**, **16**, paratype LM-FCEN 3217, carapace, male, right view, **13**, paratype, LM-FCEN 3218, valve, male, internal view, **14-15**, paratype LM-FCEN 3218, **14**, detail of mask-like reticulation, **15**, detail of sieve-type pore, **16**, paratype LM-FCEN 3217, carapace, male, dorsal view, **17**, paratype LM-FCEN 3219, carapace, female, dorsal view, **18**. *Nodoconcha* sp. (Bertels, 1974), carapace, left view.

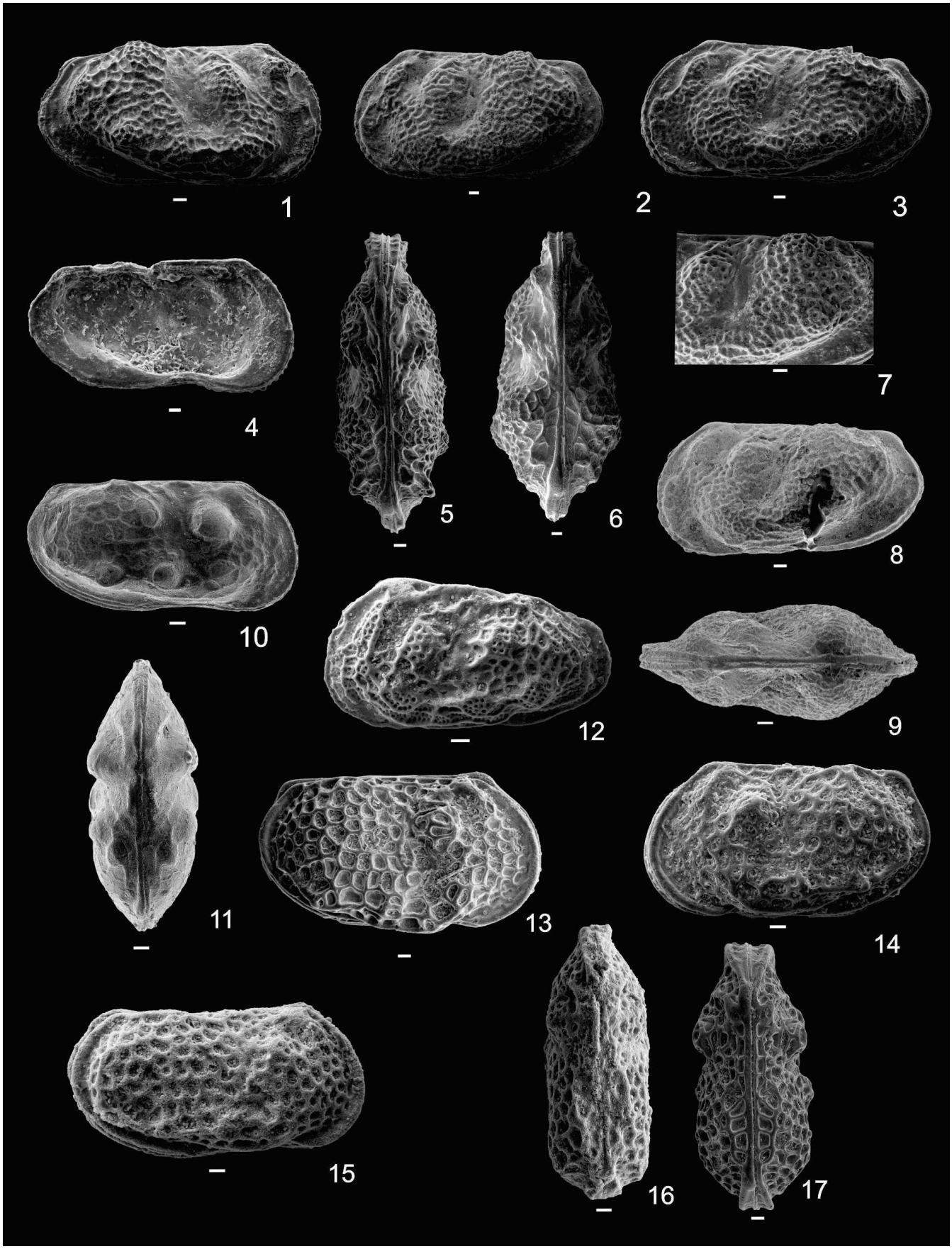
1
2
3
4
5
6
7
8
9
10
11
12
13
14
15
16
17

Explanation of Plate 2. Scale bars are 20 µm. **figs. 1-7.** *Nodoconcha upsilon* sp. nov., **1**, holotype LM-FCEN 3220, carapace, female, right view, **2**,**7**, paratype LM-FCEN 3221, **2,** female, carapace, left view, **7**, detail of reticulation, **3**, paratype LM-FCEN 3222, male, left view, carapace, **4**, paratype LM-FCEN 3223, valve, female, internal view, **5**, paratype LM-FCEN 3224, male, carapace, dorsal view, **6**, paratype LM-FCEN 3225, female, dorsal view, **8**-**9.** *Nodoconcha paleocenica* (Bertels, 1973), **8**, female, carapace, left view, **9**, female, carapace, dorsal view, **10-11**. *Nodoconcha jaguelensis* (Bertels, 1974), **10**, carapace, female, right view, **11**, female, carapace, dorsal view, **12**, *Nodoconcha*? sp., LM-FCEN 3226, valve, left view, **13-17**. *Ectonodoconcha lepidotus* gen. et sp. nov., **13**, holotype LM-FCEN 3227, carapace, female, right view, **14**, paratype, LM-FCEN 3228, carapace, female, left view, **15**, paratype LM-FCEN 3229, carapace, male, right view, **16**, paratype LM-FCEN 3230, male, carapace, dorsal view, **17**, paratype LM-FCEN 3231, female, carapace, dorsal view.

EVOLUTIONARY HISTORY OF THE NODOCONCHIINAE

The new evidence presented in this paper allows us to demonstrate that this subfamily has a long and varied phylogenetical history dating from the Lower Maastrichtian to the present day.

Austrocythere

Austrocythere seems to exist as a single species. *A. reticulotuberculata* Hartmann is from the Oligocene to Recent. Both records are all from the Antarctic and all from cold water (Blaszyk, 1987; Dingle & Majoran, 2001).

Nodoconcha

By contrast with *Austrocythere*, the genus *Nodoconcha* is represented by a number (7) of species as well as the type species *N. minuta* Hartmann (see fig. 4). The Minuta group which comprises, in stratigraphical order, *Nodoconcha* sp. of Bertels, 1974, *N. polytorosa* sp. nov., *N. sanniosis* sp. nov. and *N. minuta* Hartmann, represents what seems to be a cladogenesis within four species (fig. 5).

Nodoconcha sp. (Bertels, 1974) which overall is somewhat similar to *N. minuta,* ranges from Lower to Upper Maastrichtian within the Jagüel Formation of Neuquén. This seems to give rise to *N. polytorosa* sp. nov., which first appears early in the Danian and extends well into the late Danian, Roca Formation. This in turn is thought to be ancestral to *N. sanniosis* sp. nov., which first appears in the Danian, Roca Fm. but does not survive this formation. With respect to *N. minuta,* which first appears in the Oligocene, it is difficult to determine, whether it evolved from *N. sanniosis* or *N. polytorosa*. In terms of morphology, either one could be the ancestor. *Nodoconcha* sp. aff. *N. minuta* is reported from the Miocene

Ross Sea by Dingle (2000). However, since it is neither described nor illustrated, we are unable to comment on its possible status.

N. jaguelensis (Bertels, 1974), which has approximately the same Maastrichtian biochron as *Nodoconcha* sp. (Bertels, 1974), can either be seen as a potential ancestor of the Minuta group, or as a short lived descendent from either that group or a common ancestor. The same can be said of *Nodoconcha*? sp. in that it could be either the ancestor of *Nodoconcha* sp. (Bertels, 1974) or a derivative form from a common ancestor. While it lacks many of the biocharacters of the Minuta group, it shares enough, notably the two major sulci and the posterodorsal tubercle, to denote a close relationship.

Two closely related species are *N. paleocenica* (Bertels, 1973) from the early Danian, Jagüel Formation to the late Danian, Roca Formation and *N. upsilon* sp. nov., with a more restricted biochron within in the middle and upper Danian. The two species are noted for a 'U'-shaped structure in their ornament and constitute the Upsilon group. It is thought that *N. paleocenica* (Bertels, 1973) may have evolved from *Nodoconcha*? sp. and *N. upsilon* sp. nov. from *N. paleocenica* (Bertels, 1973).

Lastly, a species that we have placed in the subfamily, differs sufficiently from *Nodoconcha* to demand separate generic state. This is *Ectonodoconcha lepidotus* gen. et sp. nov., a genus that appear early in the Danian and just survives to the upper part of the Danian. Although it evidently derives from *Nodoconcha*, we are unable to state with any degree of certainly from which of the two groups mentioned above.

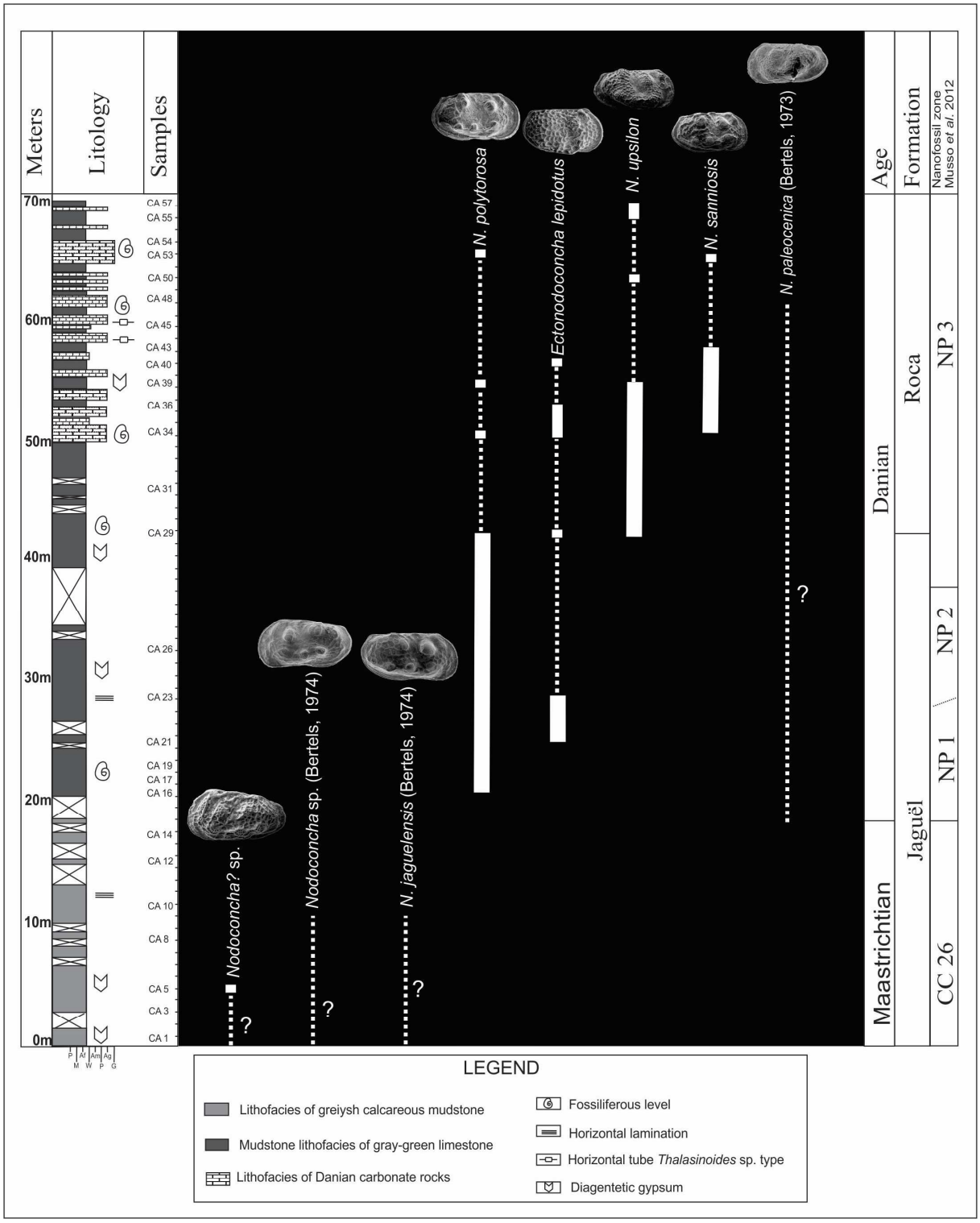

Fig. 4. Stratigraphical distribution of Minuta and Upsilon groups and *Ectonodoconcha* gen. nov.

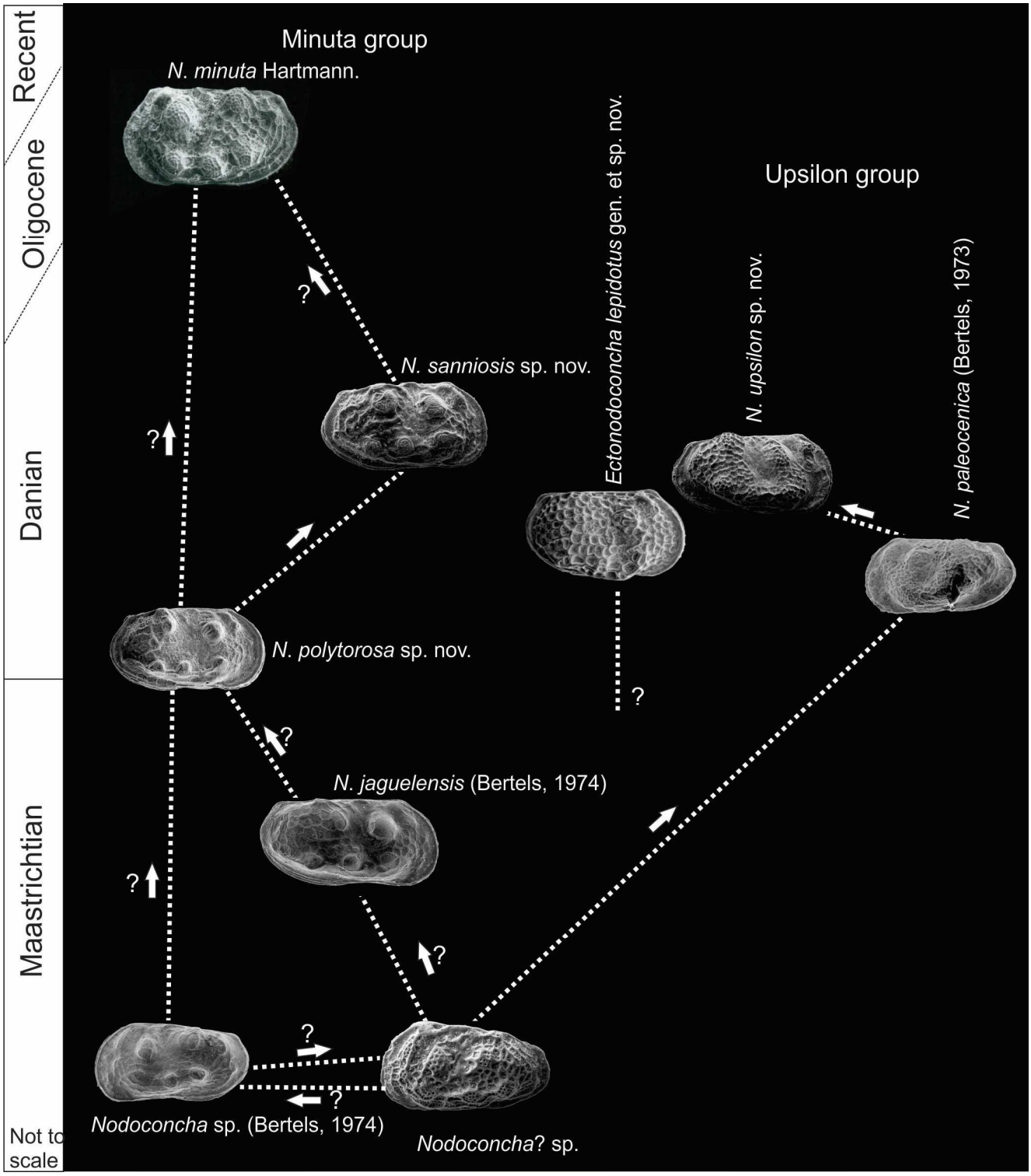

Fig. 5. Evolutionary trend of Nodoconchiinae subfam. nov.

CONCLUSIONS

The Nodoconchiinae subfam. nov. are a close-knit group of three genera *Austrocythere* Hartmann, *Nodoconcha* Hartmann and *Ectonodoconcha* gen. nov. There arose in the Maastrichtian where they rapidly diversified, survived the Cretaceous-Tertiary boundary event and continued to proliferate in the Danian. They seem to have declined somewhat in the later Paleocene and are represented today by only two species *Austrocythere reticulotuberculata* Hartmann and *Nodoconcha minuta* Hartmann.

One of the areas of our future work in the Upper Cretaceous-Tertiary strata of Neuquén basin will be to seek more evidence on the early origins of this group, which we presently believe to reside in either species *Nodoconcha*? sp. or *N. jaguelensis* (Bertels, 1974).

AKNOWLEDGEMENTS

This study forms part of the Ph.D thesis project of the first author, financially supported by a Padre Milton Valente Scholarship of the Universidade do Vale do Rio dos Sinos – Unisinos. This study was partially formed at Aberystwyth University during a Ph.D. internship of the first author supported by Conselho Nacional de Desenvolvimento Científico e Tecnológico (CAPES – Proc. BEX 2696/14-2). The authors thanks Dr[a]. Andrea Caraméz from Universidad de Buenos Aires-UBA and Dr[a]. Telma Musso from Universidad Nacional del Comahue, Neuquén, Argentina, for some SEM images and for their help in the field; to Dr. Charlie Bendal for help in matters concerning Aberystwyth and to Dr. Caroline Maybury for all her help in the construction of this paper. Professor Richard Dingle is thanked for useful information. Funding for this study has been also partially financed with the Grant UBACyT 20020110100170BA. This paper is contribution number R-157 of the Instituto de

Estudios Andinos "Don Pablo Groeber" (IDEAN). Gerson Fauth thanks CNPq (The Brazilian Scientific and Technology Developing Council) for the grant (proc. 308544/2012-9). This paper is dedicated in memory of Sara Ballent, who was the mentor of this project. May she Rest in Peace. Robin Whatley thanks Mary for her guidance and inspiration.

REFERENCES

Aguirre-Urreta, B., Tunik, M., Naipauer, M., Pazos, P., Ottone, E., Fanning M. & Ramos, V.A., 2011. Malargüe Group (Maastrichtian-Danian) deposits in the Neuquén Andes, Argentina: Implications for the onset of the first Atlantic transgression related to Western Gondwana break-up. *Gondwana Research*, **19**, 482-494.

Ballent, S., & Whatley, R., 2006. The Mesozoic ostracod genus *Arculicythere* Grekoff: further evidence for the southern Gondwana seaway. *Cretaceous Research,* **27**: 728-734.

Ballent, S., & Whatley, R., 2007. The distribution of the Gondwanine ostracod *Rostrocytheridea* Dingle: palaeozoogeographical implications. *Geological Journal,* **42:** 113-125.

Bertels, A. 1973. Ostracodes of the Type locality of the Lower Tertiary (Lower Danian) Rocanian Stage and Roca Formation of Argentina. *Micropaleontology*, **19** (3): 308-340.

Bertels, A. 1974. Upper Cretaceous (Lower Maastrichtian?) ostracodes from Argentina. *Micropaleontology*, **20** (4): 385-397.

Blaszyk, J. 1987. Ostracods from the Oligocene Polonez Cove Formation of King George Island, West Antarctica. *Palaeontologia Polonica,* **49:** 63-81.

Briggs, M. W. 1978. Ostracoda from the Pleistocene Taylor Formation, Ross Island, and the Recent of the Ross Sea and McMundo Sound region, Antarctica. *Antarctic Journal of the United States*, **13**: 27-29.

Concheyro, A., Nañez, C. & Casadío, S. 2002. El Límite Cretácico-Paleógeno em Trapalcó, província de Río Negro, Argentina: ¿una localidad clave en América del Sur? XV *Congresso Geológico Argentino*. El Calafate. Actas: 590-595.

Del Río, C. J., Concheyro, A. & Martínez, S. 2011. The Maastrichtian-Danian at General Roca (Patagonia, Argentina): a reappraisal of the chronostratigraphy and biostratigraphy of a type locality. *Neues Jahrbuch Geoogie Paläontologie Abhandlungen*, **259/2**: 129-156.

Dingle, R. V. 2000. Ostracoda from CRP-1 and CRP-2/2A, Victoria Land Basin, Antarctica. *Terra Antartica,* **7:** 479-492.

Dingle, R. V. & Majoran, S. 2001. Palaeo-climatic and -biogeographical implications of Oligocene Ostracoda from CRP-2/2A and CRP-3 drillholes, Victoria Land Basin, Antarctica. *Terra Antarctica,* **8:** 369-382.

Hartmann, 1987. Antarktische benthische Ostracoden II. Auswertung der Fahrten der "Polarstern" Ant. III/2 und der Reisen der "Walther Herwig" 68/1 und 2. 2. Teil: Elephant Island und Bransfield Straße. *Mitteilungen aus dem Hamburgischen zoologischen Museum und Institut,* **84:** 115-156.

Hartmann, 1988. Antarktische benthische Ostracoden III. Auswertung der Reise des FFS "Walther Herwig" 68/1. 3. Teil: Süd-Orkney-Inseln. *Mitteilungen aus dem Hamburgischen zoologischen Museum und Institut,* **85:** 141-162.

Hartmann, G. 1989a. Antarktische benthische Ostracoden IV. Auswertung der während der Reise von FFS "Walther Herwig" (68/1) bei Süd-Georgien gesammelten Ostracoden. *Mitteilungen aus dem Hamburgischen zoologischen Museum und Institut,* **86:** 209-230.

Hartmann, G. 1989b. Antarktische benthische Ostracoden V. Auswertung der Sudwinterreise von FS "Polarstern" (Ps 9/V-1) im Bereich Elephant Island und der Antarktischen Halbinsel. *Mitteilungen aus dem Hamburgischen zoologischen Museum und Institut,* **86:** 231-288.

Hartmann, G. 1990. Antarktische benthische Ostracoden VI. Auswertung der Reise der "Polarstern" Ant. VI-2 (1. Teil, Meiofauna und Zehnerserien) sowie Versuch einer

vorläufigen Auswertung aller bislang vorliegenden Daten). *Mitteilungen aus dem Hamburgischen zoologischen Museum und Institut,* **87:** 191-245.

Hartmann, G. 1997. Antarktische und Subantarktische Podocopa (Ostracoda). In: Wagele J.W. & Sieg J. (eds), *Synopses of the Antarctic Benthos,* **7,** Koenigstein, Koeltz Scientific Books, 355pp.

Howell, A. J., Schwarz, E., Spalletti, A. L. & Veiga, G. D. 2007. The Neuquén Basin: an overview. In: Veiga, G. D., Spalletti, A. L., Howell, A. J. & Schwarz, E. (eds), *The Neuquén Basin, Argentina. A case study in Sequence Stratigraphy and Basin Dynamics*. Geological Society, London, Special Publications, **252:** 1-14.

Milhau, B. 1993. Nouveaux ostracodes du Miocène inférieur de Nouvelle-Zélande. *Geobios,* **26:** 161-200.

Moore, R. C. & Pitrat, C. W. 1961. Crustacea: Ostracoda. In: Moore, R. C. (ed.). *Treatise on Invertebrate Paleontology, Part Q, Arthropoda 3*. Geological Society of America, Boulder, CO, and University of Kansas Press, Lawrence KS, 465 pp.

Musso, T., Concheyro, A. & Pettinari, G. 2012. Mineralogía de arcillas y nanofósiles calcáreos de las formaciones Jagüel y Roca em el sector oriental del Lago Pellegrini, Cuenca Neuquina, República Argentina. *Andean Geology*, **39** (3): 511-540.

Piovesan, E. K., Ballent, S. & Fauth, G. 2012. Cretaceous palaeogeography of southern Gondwana from the distribution of the marine ostracod *Majungaella* Grekoff: New data and review. *Cretaceous Research* **37**:127-147.

Uliana, M. A. & Dellapé, D. A. 1981. Estratigrafia y evolucion paleoambiental de La sucesion Maestrichtiano-Eoterciaria Del Engolfamento Neuquino (Patagonia Septentrional). *VII Congresso Geológico Argentino*, *San Luis*. Actas iii, 673-711.

Whatley, R. & Ballent, S. 1996. A review of the Mesozoic ostracod genus *Progonocythere* and its close allies. *Palaeontology,* **39:** 919-939.

Yasuhara, M., Kato, M., Ikeya, N. & Seto, K. 2007. Modern benthic ostracodes from Lützow-Holm Bay, East Antarctica: paleoceanographic, paleobiogeographic, and evolutionary significance. *Micropaleontology*, **53** (6): 469-496.

5 INTERPRETAÇÃO PALEOECOLÓGICA COM BASE EM OSTRACODES PARA A SEÇÃO DE CERRO AZUL

5.1 Evidências de predação

Os ostracodes fazem parte da dieta de vários organismos aquáticos como bivalves, anfíbios, peixes, dentre outros (Reyment & Elewa 2003, Ruiz *et al*. 2010). Os primeiros estudos detalhados da predação por gastrópodes em ostracodes foram feitos por Reyment (1963, 1966a,b) que analisou os ostracodes do Cretáceo–Paleógeno da Nigéria (Reyment *et al*. 1987).

Na seção de Cerro Azul, das 27 amostras estudadas, 17 continham espécimes de ostracodes com marcas de predação, tanto em amostras maastrichtianas quanto danianas (Fig.12). Estas marcas, de acordo com Reyment *et al*. (1987), possivelmente são originadas por gastrópodes carnívoros das famílias dos Naticídeos e Muricídeos. Em condições de ambiente equilibrado, os gastrópodes, principalmente os Naticídeos, são predadores de moluscos (documentadas desde o Cretáceo), tendo os ostracodes como uma opção secundária de alimento. No caso da eliminação de um organismo chave para o equilíbrio da cadeia alimentar, fato que geralmente ocorre em eventos de extinção, a população de moluscos pode ser diminuída ou eliminada, tornando os ostracodes a principal opção alimentar para os gastrópodes, principalmente os juvenis que rapidamente atacam tanto ostracodes adultos quanto os instars menores (Kelley e Hansen 1993, Lipps e Culver 2002).

De maneira geral, os níveis de predação registrados na seção de Cerro Azul apresentam certa ciclicidade. No Maastrichtiano, a predação é observada em três níveis sendo que a maior quantidade ocorre na última amostra (CA 14). No entanto, o aumento na incidência de predação é registrada no Daniano, principalmente nas amostras CA 26, CA 34 e CA 36 (Fig. 12). Kelley e Hansen (1993) encontraram uma tendência semelhante em fósseis da América do Norte, onde observaram um padrão de mortalidade moderada causada pela predação no Cretáceo, uma diminuição no limite K–Pg e um aumento substancial no Paleoceno inferior, sugerindo que este padrão de níveis de predação possa estar relacionado com o distúrbio ambiental advindo do evento de extinção. No trabalho desenvolvido no Texas, utilizando ostracodes do Cretáceo, Paleógeno e Holoceno, Maddocks (1988) relatou que um dramático aumento na predação por Naticídeos ocorreu do Campaniano até o limite

K–Pg, produzindo altos índices de mortalidade em adultos durante o Paleoceno. O mesmo aumento no Paleoceno foi documentado por Reyment *et al*. (1987) na Nigéria.

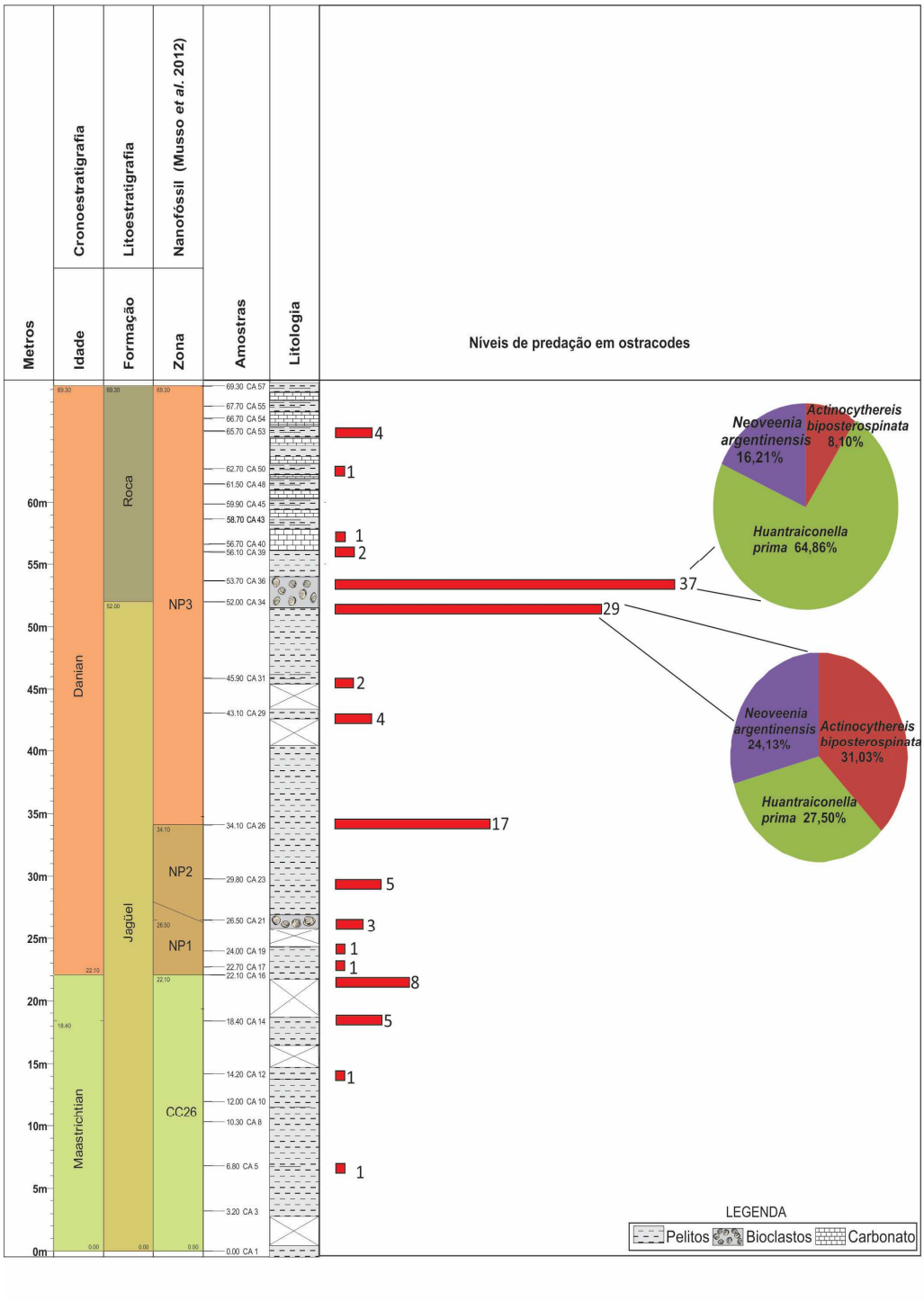

Figura 12: Distribuição dos níveis de predação na seção de Cerro Azul. No gráfico em pizza os dados percentuais das espécies mais predadas nos respectivos níveis.

Um fator que deve ser levado em consideração ao analisar uma fauna com evidências de predação, são os hábitos dos possíveis predadores para poder determiná-los, uma vez que os ostracodes fazem parte da dieta alimentar de vários animais. Os Muricídeos apresentam hábitos epifaunais e comem cadáveres combinando a ação química com raspagem. Já os Naticídeos atacam as presas na superfície e as carregam para o sedimento para serem consumidas. Estes perfuram a carapaça com o uso da rádula, um processo puramente mecânico. Reyment *et al*. (1987) realizaram um experimento para determinar a razão pela qual os ostracodes, seres tão ágeis, se tornam presas relativamente fáceis para os gastrópodes. Observaram que, quando os ostracodes são tocados sutilmente, diminuem o movimento e por isso, são facilmente imobilizados e envolvidos pela mucosa secretada pelo gastrópode que contém uma substância anestésica.

Maddocks (1988) em estudo de uma assembleia de ostracodes do Cretáceo–Holoceno do Texas, determinou 20 diferentes tipos de marcas de predação feitas por gastrópodes, denominando-as de *Icnophena*. As marcas encontradas nos ostracodes de Cerro Azul apresentam forma similar as *Icnophena* B, G, I, L, M e N. De acordo com Maddocks (1988) *Phenon* B e M são produzidas por gastrópodes em geral, G, I e L podem estar associados com alterações sedimentares ou diagenéticas e N, são produzidas por Naticídeos (Fig.13). Ao analisar os tipos de predação registrados para o Maastrichtiano de Cerro Azul, 30% da fauna predada apresentou marcas prováveis de ataque por Naticídeos, sendo que 70% das demais marcas foram causadas pelos outros fatores mencionados anteriormente. Já no Daniano, este dado é praticamente inverso, com 69,5% dos espécimes predados pelo ataque de Naticídeos e 30,5% pelos demais fatores.

Este é um dado interessante se comparado com o aumento de riqueza e abundância da fauna de Naticídeos registrada no Paleógeno por Griffin & Pastorino (2013) na região da Patagônia argentina. Embora os demais moluscos (principal presa dos Naticídeos e Muricídeos) também tenham sua diversidade mais alta no Paleoceno, a riqueza dos Naticídeos também aumentou de quatro espécies no Cretáceo para 14 no Daniano (Del Río *et al*. 2007, Stilweel 2003). Este fato pode explicar o domínio da *Icnophena* N em Cerro Azul. Já a presença de múltiplas marcas na carapaça pode expressar uma tentativa de defesa da presa ou pode indicar uma ineficiência de ataque do predador, segundo Maddocks (1988) (Fig. 13).

Na pedreira Poty foi observada uma predominância de predação por Naticídeos e um aumento desta no Paleógeno. Entretanto a predação ocorreu com maior incidência em espécies de carapaças lisas, principalmente do gênero *Cytherella* (Fauth *et al*. 2005).

Reyment *et al*. 1987 sugere que os ostracodes grandes e com carapaças lisas são preferidos para serem predados. Em Cerro Azul a maior quantidade de icnophenas foi encontrada em espécies com carapaças ornamentadas, mas isto é compreensível pela menor proporção de espécies com carapaças lisas (15,9%) se comparada às ornamentadas (84%). Além disso, os níveis com predação mais significativa no Daniano coincidem com os níveis de bioclastos e, entre os ostracodes predados, as espécies mais afetadas foram *Huantraiconella prima* Bertels, 1968, *Actinocythereis biposterospinata* Bertels, 1973 e *Neoveenia argentinensis* Bertels, 1969c. Do total de espécies predadas nas duas amostras que correspondem aos níveis de bioclastos (CA 34 e CA 36), estas três representam um percentual aproximado de 80% (Fig. 12).

As possíveis explicações para estas ocorrências seria que a predação nestas espécies poderia estar relacionada a um controle populacional, visto que são registrados os maiores picos de abundância das mesmas nestas amostras, confirmando a relação natural presa x predador (Maddocks 1988). O nível de bioclastos representaria a redução de disponibilidade de alimento pela diminuição da principal fonte de nutrição e, por consequência, os maiores níveis de predação estariam ali representados; ou estes maiores níveis teriam sido gerados pelos eventos de tempestades que remobilizaram estas carapaças e valvas e as concentraram nestas amostras; ou ainda, poderia significar uma predação *post mortem* uma vez que, mesmo não sendo identificadas evidências de predação pelos Muricídeos (as marcas são similares), estes apresentam hábitos detritívoros e poderiam ter predado estes ostracodes logo após a morte. Além disso a alta quantidade de fragmentos de ostracodes nestas amostras também pode estar relacionada com a predação como sugerido por Maddocks (1988).

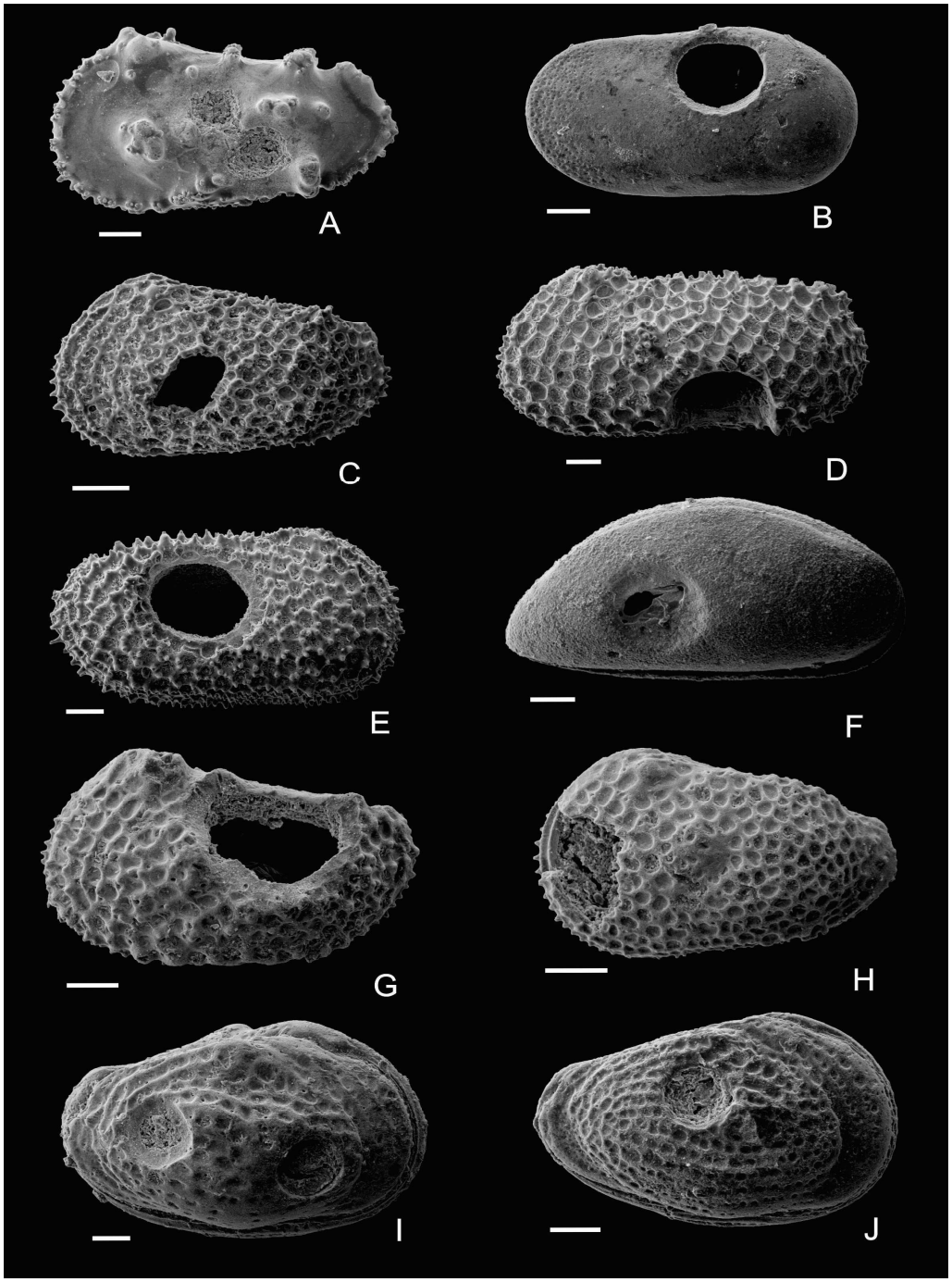

Figura 13: Tipos de marcas de predação (baseado em Maddocks 1988). A, *Phenon* B, *Actinocythereis biposterospinata* Bertels, 1973, c, Daniano; **B**, *Phenon* N, *Cytherella terminopunctata* Holden, 1964, ve, Maastrichtiano; **C**, *Phenon* G, *Cythereis trajectiones* sp. nov., juvenil (A-7), ve, Maastrichtiano; **D**, *Phenon* N, *Henryhowella* (*Wichmannella*) *meridionalis* (Bertels, 1969c) comb. nov., macho, c, Maastrichtiano; **E**, *Phenon* N, *Petalocythereis schilleri* (Bertels, 1973) comb. nov., macho, c, Daniano; **F**, *Phenon* I, *Paracypris bertelsae*, sp. nov., c, Daniano; **G**, *Phenon* M, *Neoveenia argentinensis* Bertels 1969c, ve, Daniano; **H**, *Phenon* L, *Neoveenia argentinensis* Bertels, 1969c, juvenil (A-7), c, Daniano; **I-J**, *Phenon* N, *Huantraiconella prima* 1968a; **I**, c, Daniano; **J**, juvenil (A-8), Daniano. Escala 100µm. c: carapaça, ve: valva esquerda.

5.2 Interpretação paleoambiental para a seção de Cerro Azul.

5.2.1 MAASTRICHTIANO

De uma maneira geral, a fauna de ostracodes identificada na seção de Cerro Azul é composta por espécies tipicamente de ambiente marinho normal. O Maastrichtiano é representado por sete amostras e compreende 53 espécies (destas 19 são novas), que apresentam hábitos bentônicos.

Ao analisar o intervalo amostral CA 3 à CA 5, é possível observar a primeira ocorrência de 30 espécies. Esse intervalo é marcado pelo pico de abundância das espécies *Aleisocythereis polikothonus* sp. nov., *Petalocythereis venusta* (Bertels, 1975a) comb. nov., *Sthenarocythereis erymnos* sp. nov. e *Cytherelloidea spirocostata* (Bertels, 1973). Este pico, mais expressivo na amostra CA 5 (Fig. 14) pode refletir uma transgressão que também foi observada a partir do estudo de nanofósseis e foraminíferos planctônicos no Maastrichtiano de Trapalcó, Río Negro, Argentina (Concheyro *et al*. 2002) e é corroborada pelo predomínio de minerais compostos por esmectita geralmente associados a este tipo de evento, sugerindo um ambiente de plataforma média (Musso *et al*., 2012).

Especialmente o pico de abundância da espécie *Cytherelloidea spirocostata* Bertels, 1973, uma espécie considerada termofílica (Sohn 1962), pode indicar um ambiente marinho de águas quentes, com profundidades variando entre 150 e 300 m, corroborando a interpretação proposta por Bertels (1975c) para a região de Huantrai-co, baseada em foraminíferos planctônicos. Além disso, das 53 espécies identificadas no Maastrichtiano, 27 pertencem à família Trachyleberididae, cujas espécies preferem viver em ambientes plataformais internos a externos (de acordo com o modelo proposto por Suguio 2003), com águas rasas e com maior nível de circulação, devido às suas carapaças fortemente ornamentadas, espessas e predomínio de tubérculo ocular. Essas características permitem a essas espécies suportar as condições de maior energia de um ambiente de águas rasas, dentro da zona fótica, protegendo-as contra a destruição (Whatley 1983, Whatley e Boomer 1995). Damotte & Fleury (1987), que estudaram os ostracodes do limite K–Pg na Algéria também encontraram um padrão semelhante de abundância das espécies da família Trachyleberididae no Maastrichtiano, porém em um ambiente de plataforma média a externa.

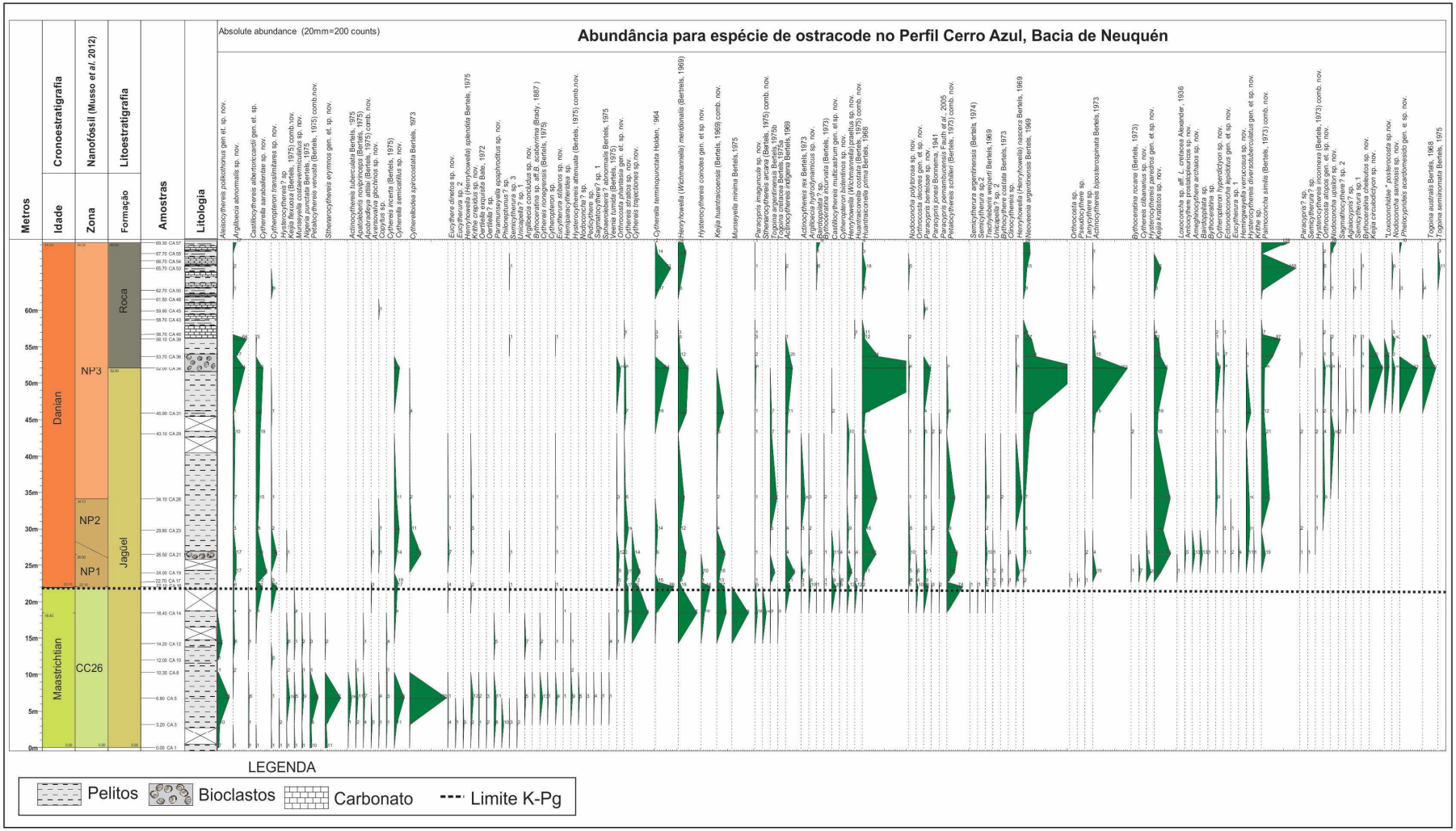

Figura 14: Abundância faunística de ostracodes em Cerro Azul.

Uma ocorrência interessante é a presença da espécie *Bythoceratina* aff. *B. scaberrima* que apresenta clara afinidade à *Bythoceratina scaberrima* (Brady, 1887) que ocorre em águas profundas do Terciário ao Recente em todo o mundo. É de se levar em consideração que ambos os taxa, tão similares morfologicamente, não teriam vivido em um mesmo ambiente. Uma explicação poderia ser a possibilidade desta espécie ter sido transportada para dentro do ambiente marinho raso por bioturbação (com. verb. Concheyro 2014), ou pelo evento de transgressão, até porque foi encontrado apenas um espécime desta espécie, e seu registro é coincidente com o provável evento transgressivo sugerido para este intervalo.

5.2.2 MAASTRICHTIANO-DANIANO

A transição entre o Maastrichtiano e o Daniano em Cerro Azul, determinado pelo zoneamento bioestratigráfico de nanofósseis calcários apresentado por Musso *et al*. (2012), ocorre entre as amostras CA 14 e CA 16. A passagem K–Pg é marcada por uma considerável mudança na fauna de ostracodes em termos de abundância e riqueza, além da presença de espécies sobreviventes [considere-se para o termo riqueza a quantidade de espécies de um determinado local ou amostra (Dias 2004)]. Nas duas últimas amostras do Maastrichtiano, CA 12 e CA 14, observa-se o último registro de 17 espécies (Fig. 15). Este dado pode indicar um momento de crise ambiental relacionado ao evento de extinção. Vários estudos que abordam o limite K–Pg (e.g., Bown 2005, Alegret 2007, Keller *et al*. 2012, Robertson *et al*. 2013, Punekar *et al*. 2014), inclusive na Bacia de Neuquén (Scasso *et al*. 2005, Keller *et al*. 2007, Musso *et al*. 2012) retratam algo semelhante. Estes estudos sugerem que houve uma redução no suprimento de alimento disponível no ambiente, resultante do colapso sofrido pelo plâncton em função dos eventos vulcânicos e do impacto do meteorito, que levaram à Terra um período de escuridão e ao chamado "impacto de inverno" (Robertson *et al*. 2013). A alta concentração de poeira, fuligem e aerossóis de sulfato por um intervalo de seis meses ou anos, teria gerado um período de escuridão e a consequente extinção nos ambientes aquáticos pela eliminação da fotossíntese.

Por outro lado, a última amostra do Maastrichtiano (CA 14) é marcada pelo aparecimento de 11 espécies, sendo que destas, oito sobreviveram ao momento de crise e seguiram no Daniano. Destas, duas espécies *Hysterocythereis coinotes* sp. nov e *Cythereis trajectiones* sp nov. registram a última ocorrência logo após o evento de extinção e podem

representar as espécies *r*-estrategistas ou espécies oportunistas, que são as capazes de sobreviver em ambientes perturbados e que apresentam um ciclo biológico curto (Odum 2004) (Fig. 16). No limite K–Pg, exemplos de espécies *r*-estrategistas são mencionados por vários autores, principalmente em estudos com foraminíferos planctônicos e nanofósseis calcários (MacLeod *et al*. 1997, Keller & Pardo 2004, Keller 2005, Punekar *et al*. 2014).

De um total de 113 espécies identificadas em Cerro Azul, 28,32% são exclusivamente maastrichtianas, 18,58% destas são consideradas sobreviventes, e 53% são danianas. O padrão de extinção, se levada em consideração a diferença de percentagens entre as espécies exclusivamente maastrichtianas e as sobreviventes (9,74%), pode indicar que não foi um evento catastrófico de grande magnitude. O mesmo padrão foi constatado por Damotte (1993) na Algéria, África do Norte. Segundo Maddocks (1985) devido ao hábito infaunal dos ostracodes bentônicos, que se alimentam mais de organismos e partículas em suspensão do que do próprio plâncton, a extinção não teria sido tão catastrófica para eles como foi para os demais grupos. Como sugerido por Robertson *et al*. (2013) os organismos que se alimentam de detritos podem sobreviver por mais tempo sem a fotossíntese. Sendo assim, os ostracodes teriam sido afetados tardiamente, tendo tempo para reestruturar a comunidade. Entretanto Bertels, que realizou estudos com ostracodes no Maastrichtiano (1974, 1975a) e no Daniano (1973) da Argentina, sugeriu que a fauna de ostracodes e foraminíferos do Cretáceo teria sido completamente substituída no Daniano. Ao analisar a fauna presente em Cerro Azul, foi verificado que algumas espécies, até então identificadas somente para o Daniano, tem seu primeiro registro já no Maastrichtiano [e.g., *Cytherelloidea spirocostata* Bertels, 1973*, Keijia huantraicoensis* (Bertels, 1969a), *Henryhowella* (*Wichmannella*) *meridionalis* (Bertels, 1969), *Cytherella terminopunctata* Holden, 1964)].

Outro dado importante registrado por alguns autores que estudaram o limite K–Pg com ostracodes, são os níveis de predação nas carapaças. Estes parecem ter aumentado nas amostras do limite e, como discutido no item 5.1, tiveram um expressivo aumento no Daniano (Maddocks 1985, Reyment *et al*. 1987, Fauth *et al*. 2005).

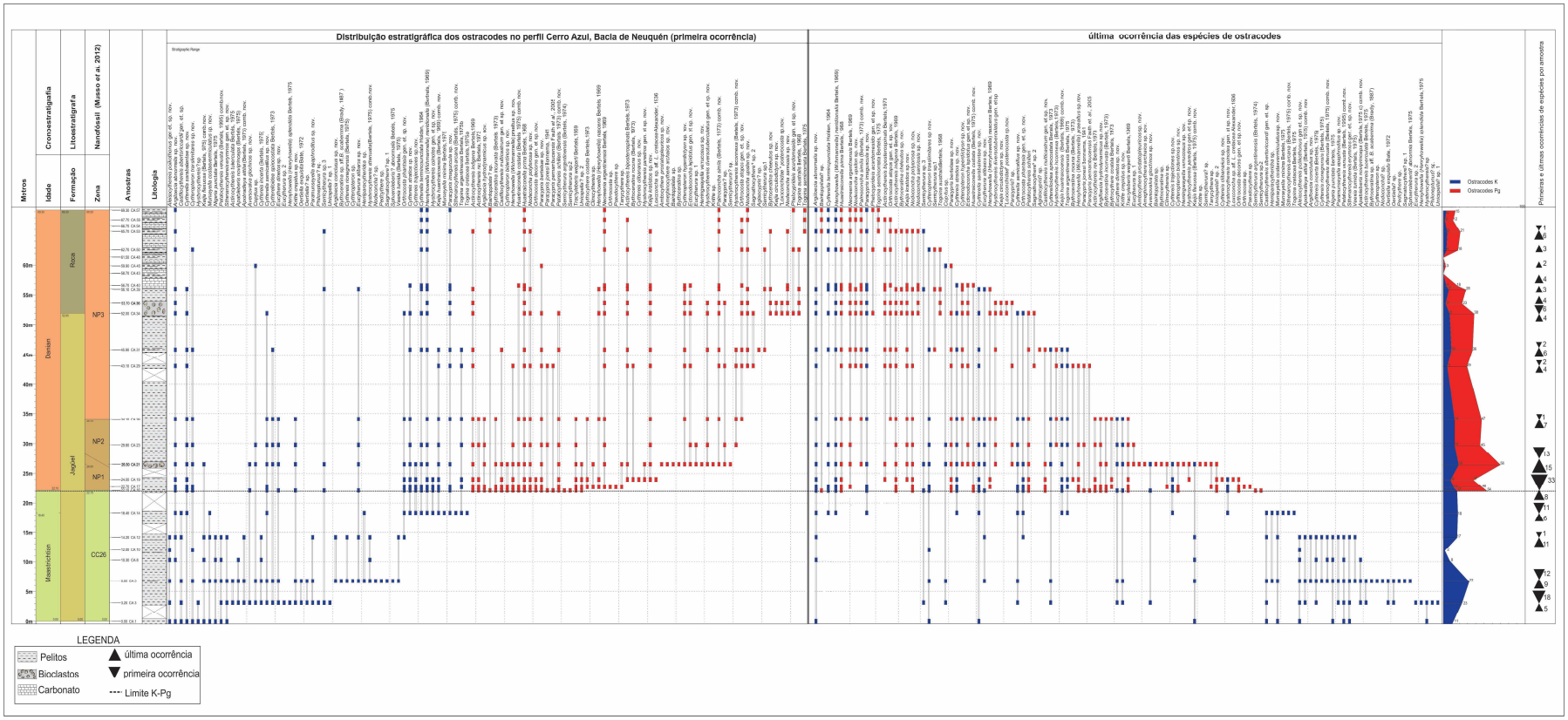

Figura 15: Distribuição estratigráfica das espécies de ostracodes em Cerro Azul.

5.2.3 DANIANO

O intervalo do Daniano em Cerro Azul contém 81 espécies e, destas, 32 são novas, representando o intervalo com maior abundância e riqueza. A família mais abundante é a Trachyleberididae com 38% de representatividade na fauna.

No intervalo entre as amostras CA 16 e CA 21, 46 espécies têm seu primeiro aparecimento e 23 desaparecem (Fig. 15). Este aumento na riqueza e abundância, que é expresso principalmente por *Cytherelloidea spirocostata* Bertels, 1973, *Keijia huantraicoensis* (Bertels, 1969b), *Huatraiconella prima* Bertels, 1968, *Petalocythereis schilleri* (Bertels, 1973) e *Keijia kratistos* sp. nov., pode refletir a ocupação de novos nichos disponibilizados em decorrência da extinção das espécies, e também indica o reestabelecimento de condições favoráveis ao desenvolvimento das mesmas, como luminosidade, disponibilidade de alimento e temperatura. Este "boom" de diversidade presente no Daniano pode estar vinculado ao rápido aumento de temperatura global registrado no final do Maastrichtiano que continua no Daniano, e que poderia estar associado ao vulcanismo ocorrido em várias regiões no mundo (Barrera & Huber 1990, Smit 1990, Li & Keller 1998, Punekar *et al*. 2014). Especialmente na Bacia de Neuquén, o clima mais quente no Daniano é bem documentado (Casadío 1998, Aguirre-Urreta *et al*. 2008, Musso *et al*. 2012). Por outro lado, o nível de última ocorrência de 23 espécies neste mesmo intervalo, principalmente na amostra CA 21, pode indicar ainda a existência de um possível estresse ambiental remanescente do evento, pois destas, 13 espécies surgem e desaparecem na mesma amostra com pequenos picos de abundância (Fig. 15).

Nas amostras CA 21, CA 34 e CA 36 são registrados picos de abundância de espécies de ostracodes justamente nos níveis de bioclastos (Fig. 14). Os bioclastos presentes em Cerro Azul podem representar depósitos de tempestades de curta duração gerados em ambientes de plataforma interna a externa. A configuração destes depósitos apresenta um ordenamento caótico, com valvas côncavas voltadas para cima, empilhadas e também com valvas articuladas, refletindo um rápido soterramento dos mesmos (Barrio 1990, Musso *et al*. 2012). Dessa forma, é possível inferir que estes picos, caracterizados pela abundância das espécies *Huantraiconella prima* Bertels, 1968a, *Neoveenia argentinensis* Bertels, 1969c e *Actinocythereis biposterospinata* Bertels, 1973 representam um momento de maior energia no

ambiente, com remobilização e concentração das carapaças pelas tempestades. Além disso, destaca-se a presença conjunta de uma maior quantidade de fragmentos de valvas de ostracodes nestas amostras.

O gênero *Huantraiconella* é reconhecido por Bertels (1968a) como um possível fóssil guia para a Bacia de Neuquén por apresentar sua ocorrência restrita ao Daniano. Em Cerro Azul, a presença deste gênero com duas espécies, *Huantraiconella prima* Bertels, 1968a e *Huantraiconella costata* (Bertels, 1975b) na primeira amostra do Daniano reforça esta hipótese.

No intervalo amostral que compreende a Formação Roca, é observado uma considerável diminuição na abundância e na riqueza faunística como pode ser observado pela sequência de níveis com últimas ocorrências de ostracodes que se sobrepõe aos níveis de aparecimento de novas espécies (Fig. 15). Se observarmos o intervalo entre as amostras CA 36 e CA 53, 22 espécies têm suas últimas ocorrências e apenas um surgimento. Esta redução, acompanhada pelo predomínio de ostracodes preservados como moldes (amostras CA 43, 45 e 48) e também por sinais de dissolução das carapaças (amostras CA 50, CA 55 e CA 57), indica possíveis alterações neste ambiente, como mudança na disponibilidade de carbonato de cálcio, que influencia na agradação ou degradação da ornamentação das carapaças, ou ainda alterações na temperatura e profundidade da lâmina d'água (Peypouquet *et al*. 1988). Vários trabalhos realizados na Formação Roca sugerem que este é um ambiente marinho raso em fase gradual de regressão (Barrio 1990, Casadío 1998, Rodrigues 2011). O aumento na quantidade de minerais I/S (ilita/esmectita) detectado por Musso *et al*. (2012) indica um ambiente relativamente quente e seco, alternado com períodos de umidade e com maior energia durante o Daniano superior. A presença de recifes de coral e moluscos também corroboram estas condições (Leanza & Hugo 1985, Casadío 1998) além da já mencionada maior abundância de representantes da família de ostracodes Trachyleberididae. Somando-se a isso, as associações de foraminíferos provenientes desta formação sugerem um ambiente de plataforma média, com profundidade possivelmente variando de 80 a 100 m (Bertels 1975c, Nañez & Concheyro, 1996 Keller *et al*. 2007).

Por outro lado, a maior concentração dos argilominerais mencionada por Musso *et al*. (2012) pode estar relacionada ao aumento da atividade vulcânica no setor oeste da bacia, como resultado do levantamento tectônico, no final do Maastrichtiano e no Daniano, advindos

dos movimentos iniciais para a formação da atual Cordilheira dos Andes, representando a fase Laramica.

Com o intuito de verificar qual é o tipo de preservação dos moldes de ostracodes, foi aplicado um teste qualitativo para a identificação da presença de sílica e/ou carbonato de cálcio nesses moldes. Como os ostracodes são compostos por carbonato de cálcio, foi adicionado sobre o molde algumas gotas de solução de ácido clorídrico (HCl 10%) onde não foi observada qualquer reação ou desprendimento (Fig. 16A), o que comprovou a inexistência de carbonato de cálcio. Também foi testada a hipótese destes terem sido substituídos por sílica aplicando-se algumas gotas da solução de ácido fluorídrico (HF 20%). Como resultado, a solução de ácido fluorídrico reagiu e dissolveu quase que por completo o molde do ostracodes (Fig. 16B). Neste caso, a hipótese de alteração da composição química da água pela atividade vulcânica deve ser considerada.

O pico de abundância das espécies *Cytherella terminopunctata* e *Palmoconcha similis* associado com a redução na abundância e riqueza das demais espécies, pode ser indicativo de pequenos eventos de flutuações no nível do mar, considerando-se que estas sejam mais tolerantes a estas variações ambientais e preferiram viver em ambientes mais rasos (Yamaguchi & Hamiya 2007, Mazzini *et al*. 2011).

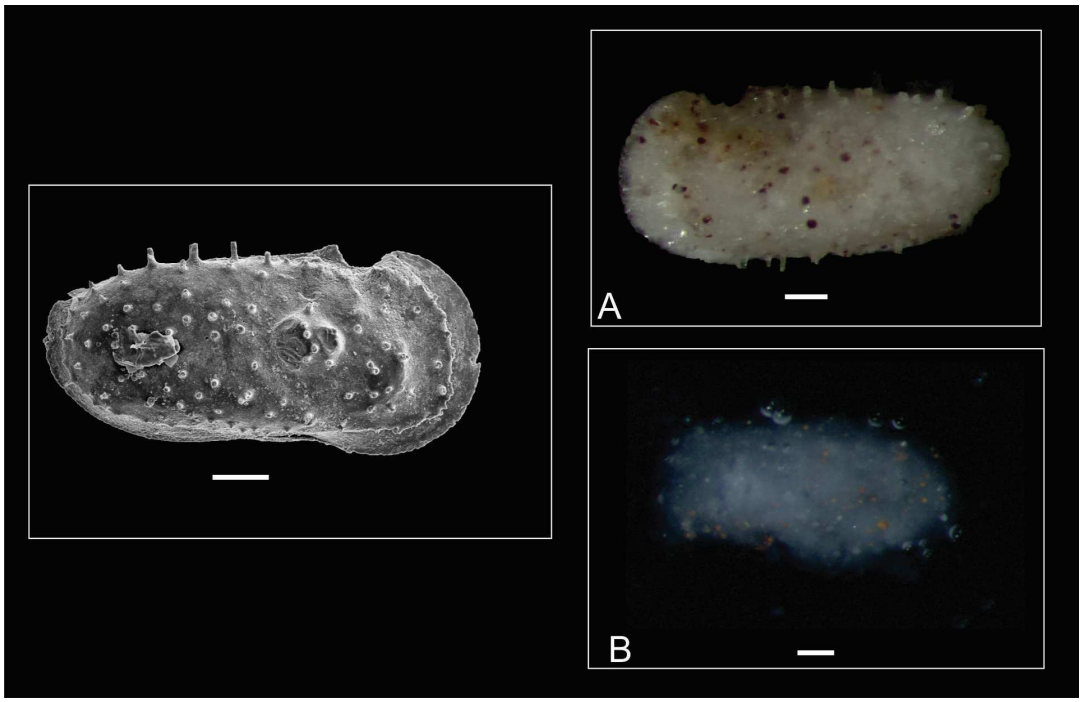

Figura 16: Dissolução do molde de ostracodes por ácido fluorídrico. A, ação do ácido clorídrico**. B,** dissolução do mesmo molde após a adição de ácido fluorídrico. Escala 100µm.

6 CONCLUSÕES E PERSPECTIVAS FUTURAS

Em 27 amostras estudadas no intervalo Maastrichtiano–Daniano, foram identificadas 113 espécies, pertencentes à 51 gêneros e 11 famílias, sendo descritos 10 gêneros novos, 41 espécies novas, uma nova subfamília, Nodoconchiinae, além de um novo tipo de charneira, alternamerodonte. As novas espécies descritas foram: *Cytherella saraballentae*, *Cytherella semicatillus*, *Paracypris bertelsae*, *Paracypris imaguncula*, *Argilloecia abnormalis, Argilloecia concludus*, *Argilloecia hydrodynamicus*, *Bythoceratina cheleutos*, *Phelocyprideis acardomesido* (novo gênero e espécie), *Eucythere dinetos*, *Krithe crepidus*, *Cytheropteron hyperdictyon*, *Cytheropteron bidentinos*, *Cytheropteron translimitares*, *Aversovalva glochinos*, *Eucytherura stibaros*, *Hemingwayella verrucosus*, *Heinia prostratopleuricos*, *Loxoconcha* (s.l.) *posterocosta*, *Keijia circulodictyon*, *Keijia kratistos*, *Paramunseyella epaphroditus*, *Munseyella costaevermiculatus*, *Ameghinocythere archaios*, *Aleisocythereis polikothonus*, *Castillocythereis multicastrum* (novo gênero e espécie), *Castillocythereis albertoriccardii*, *Cythereis stratios*, *Cythereis clibanarius*, *Cythereis trajectiones*, *Henryhowella (Wichmannella) praealtus*, *Hysterocythereis paredros* (novo gênero e espécie), *Hysterocythereis coinotes*, *Hysterocythereis diversotuberculatus*, *Orthrocosta decores* (novo gênero e espécie), *Orthrocosta atopos*, *Orthrocosta phantasia*, *Sthenarocythereis erymnos* (novo gênero e espécie), *Nodoconcha polytorosa*, *Nodoconcha sanniosis*, *Nodoconcha upsilon* e *Ectonodoconcha lepidotus* (novo gênero e espécie). Outros quatro gêneros novos *Aleisocythereis*, *Apatoleberis*, *Mimicocythereis* e *Petalocythereis* foram propostos para acomodar espécies previamente descritas por Bertels para a Bacia de Neuquén, mas que também foram registrados em Cerro Azul.

A partir do refinamento taxonômico realizado na seção de Cerro Azul, pode-se considerar que a Bacia de Neuquén tenha sido um centro de especiação, pois foi registrado um expressivo aumento na abundância e riqueza de espécies, principalmente nas amostras danianas, que sucedem o evento de extinção. Além disso, foram identificadas somente 30 espécies comuns com as previamente descritas por Bertels.

De maneira geral, a fauna de ostracodes presente em Cerro Azul caracteriza um ambiente marinho de plataforma média a externa, com profundidade não maior que 200 m no Maastrichtiano, e que foi progressivamente raseando no Daniano.

O evento de extinção não pode ser considerado de grande magnitude, pois o surgimento de 11 novas espécies na amostra que antecede este evento, e o considerável número de últimas ocorrências na amostra anterior (CA 12), fornece indícios de uma fauna que estava em declínio e que apresenta sinais de recuperação. Por outro lado, se desconsiderássemos o posicionamento do limite K–Pg proposto pelos nanofósseis calcários (Musso *et al*. 2012) para esta seção, poderíamos sugerir que o evento de extinção estaria logo acima da amostra CA 14.

A presença de moldes de ostracodes substituídos por sílica e por espécimes com diferentes graus de dissolução, corroboram a existência de um ambiente mais raso na Fm. Roca, com profundidade não maior que 100 m. Além disso, a atividade vulcânica advinda dos movimentos iniciais para a formação da atual Cordilheira dos Andes, no setor oeste da bacia, influenciou na composição química da água.

Pretende-se, em um futuro próximo, analisar detalhadamente o intervalo entre as amostras CA 14 e CA 16, objetivando o refinamento do posicionamento do limite, pois existe um significativo desaparecimento de espécies entre as amostras CA 12 e CA 14 e um aparecimento de 41 novas espécies na amostra CA 16. Além disso, há a possibilidade de analisar o material de outros quatro perfis, o que poderá contribuir para uma melhor compreensão de como este evento de extinção afetou a fauna de ostracodes na Bacia de Neuquén.

REFERÊNCIAS

Abdelkader B.O., Salem B.H., Donze P., Maamouri A.L., Méon H., Robin É., Rocchia R., Froget L. 1997. The K/T stratotype section of El Kef (Tunisia): Events and biotic turnovers. *Geobios*, **21**: 235-245.

Aguirre-Urreta M.B., Casadío S., Cichowolski M., Lazo G.D., Rodríguez D.L. 2008. Afinidades paleobiogeográficas de lós invertebrados cretácicos de La Cuenca Neuquina. *Ameghiniana* **45** (3): 591-611.

Aguirre-Urreta B., Tunik M., Naipauer M., Pazos P., Ottone E., Fanning M., Ramos V.A. 2010. Malargüe Group (Maastrichtian-Danian) deposits in the Neuquén Andes, Argentina: Implications for the onset of the first Atlantic transgression related to Western Gondwana break-up. *Gondwana Research* doi:10.1016/j.gr.2010.06.008.

Albertão G. 1994. A possible tsunami deposit at the Cretaceous-Tertiary boundary in Pernambuco, Northeastern Brazil. *14º International Sedimentological Congress*, 1-3.

Albertão G.1996. O limite Cretáceo-Terciário no Brasil e no mundo: visão geral e fatores causais. *In*: Boletim do 4º Simpósio sobre o Cretáceo do Brasil, 9-13.

Albertão G.A.A., Koutsoukos E.A.M., Regali M.P.S., Attrep Jr. M., Martins Jr. P.P. 1994. The Cretaceous-Tertiary boundary in Southern low-latitude regions: preliminary study in Pernambuco, northeastern Brazil. *Terra Nova*, **6:** 366-375.

Alegret L. 2007. Recovery of the deep-sea floor after the Cretaceous-Paleogene boundary event: The benthic foraminifera record in the Basque-Cantabrian basin and in southeastern Spain. *Palaeogeography*, *Palaeoclimatology*, *Palaeoecology*, **255:** 191-194.

Alegret L., Molina E., Thomas E. 2001. Benthic foraminifera at the Cretaceous-Tertiary boundary around the Gulf of Mexico. *Geology*, **29** (10): 891-894.

Alegret L., Molina E., Thomas E. 2003. Benthic foraminiferal turnover across the Cretaceous-Paleogene boundary at Agost (southeastern Spain): paleoenvironmental inferences. *Marine Micropaleontology*, **48**: 251-279.

Alegret L., Thomas E., Lohmann K.C. 2012. End-Cretaceous marine mass extinction not caused by productivity collapse. PNAS, **109** (3): 728-732.

Alvarez L.W. 1983. Experimental evidence that an asteroid impact led to the extinction of many species 65 million years ago. *Geology*. **80**: 627-642.

Alvarez L.W. 1987. Mass extinctions caused by large bolide impacts. *Phisics Today*, **87**: 25-33.

Alvarez L.W., Alvarez W., Asaro F., Michel H.V.1980a. Extraterrestrial Cause for the Cretaceous-Tertiary Extinction. *Science*, **208** (4448): 1095-1108.

Alvarez L.W., Alvarez W., Asaro F., Michel H.V. 1980b. Extraterrestrial Cause for the Cretaceous-Tertiary Extinction: experimental results and theoretical interpretation of experimental evidence that an asteroid impact led to extinction of many species 65 million years ago. *Science*, **208** (4448): 1095-1980.

Alvarez W., Asaro W.L., Michel V.H. 1982. Current status of the i,pact yheory for the terminal Cretaceous extinction. *Geological Society of America. Special Paper*, **190**: 305-315.

Alvarez W., Claeys P., Kieffer S.W. 1995. Emplacement of Cretaceous-Tertiary Boundary Shocked Quartz from Chicxulub Crater. *Science*, **269**: 930-935.

AMS, 2014. Meteor terminology. American Meteor Society. Disponível em: http://www.amsmeteors.org. Acessado em 27 nov 2014.

Apesteguía S. & Ares R. 2010. Las extinciones em massa. *In*: V. Mazzini (ed). *Vida em Evolución, La Historia Natural vista desde Sudamérica*, p.: 41-48.

Arregui C., Carbone O., Leanza H.A. 2011. Contexto Tectosedimentario. *In*: Geología y recursos naturales de la Provincial del Neuquén. *Relatorio del XVIII Congreso Geológico Argentino*. 29-62 p.

Arthur M.A., Zachos J.C., Jones D.S. 1987. Primary productivity and the Cretaceous/Tertiary boundary event in the Oceans. *Cretaceous Research*, **8:** 43-54.

Aumond G.N, Kochhann K.G.D, Florisbal L.S., Fauth S.B., Bergue C.T., Fauth G. 2009. Maastrichtian-Early Danian Radiolarian and Ostracodes from ODP Site 1001B, Caribean Sea. *Revista Brasileira de Paleontologia*, **12** (3): 195-210.

Baksi A.K., Byerly G.R., Chan L-H. 1994. Intracanyon flows in the Deccan province, India? Case history of Rajahmundry Traps. *Geology*, **22**: 605-608.

Barreda V., Susana P., John A.C.Jr. 2004. Vegetacional disruption at the Cretaceous-Paleogene boundary in Neuquén, Argentina: evidence from pores and pollen. *In*: X Reunión Argentina de Sedimentología. San Luis, *Resumenes Contribuciones Simposio K/T*, 185-186 p.

Barrera E. & Huber B. 1990. Evolution of Antarctic waters during the Maaastrichtian: Foraminifera oxygen and carbon isotope ratios, Leg 113. *Proceedings of the Ocean Drilling Program, Scientific Results*, **113**: 813-827.

Barrera E. & Keller G. 1994. Productivity across the Cretaceous/Tertiary boundary in high latitudes. *Geological Society of America Bulletin*, **106:** 1254-1266.

Barrio C.A. 1990. Late Cretaceous-Early Tertiary sedimentation in a semi-arid foreland basin (Neuquén Basin, western Argentina). *Sedimentary Geology*, **66**: 255-275.

Benton M.J. & Harper D.A.T. 2009. Mass extinctions and biodiversity loss. *In*: M.J. Benton & D.A.T Harper (eds). *Introduction to Paleobiology and the Fossil Record*. British Library, UK, 592p.

Benton M.J. 2001. Biodiversity through time. *In*: D.E. Briggs & P.R. Crowther (eds.). *Palaeobiology II*. Oxford: Blackwell, p. 212-220.

Bernaola G. & Monechi S. 2007. Calcareous nannofossil extinction and survivorship across the Cretaceous–Paleogene boundary at Walvis Ridge (ODP Hole 1262C, South Atlantic Ocean). *Palaeogeography*, *Palaeoclimatology*, *Palaeoecology*, **255:** 132-156.

Bertels A. 1964. Micropaleontologia del Paleoceno de General Roca (Província de Rio Negro). *Revista del Museo de La Plata*, Palentología, **4**, (**23**): 125-199.

Bertels A. 1968a. *Huantraiconella* N. Gen. (Ostracodea, Buntoniinae) del Terciario Inferior (Daniano) de Argentina. *Ameghiniana*, **5**, 252-253.

Bertels A. 1968b. Micropaleontologia y estratigrafia del Limite Cretacico-Terciario em Huantrai-co (Provincia del Neuquén). Ostracoda. Parte II. *Ameghiniana*, **6**, (4): 253-290.

Bertels A. 1969. Rocaleberidinae, nueva subfamilia (Ostracoda, Crustacea) del Limite Cretacico-Terciario de la Patagonia Setentrional. *Ameghiniana*, **6**, (2): 116-171.

Bertels A. 1970. Los foraminíferos planctônicos de la cuenca Cretacico-Terciaria em Patagonia septentrional (Argentina), con consideraciones sobre la estratigrafia de Fortín General Roca (Provincia de Rio Negro). *Ameghiniana*, **1**: 1-56.

Bertels A. 1973. Ostracodes of the Type locality of the Lower Tertiary (Lower Danian) Rocanian Stage and Roca Formation of Argentina. *Micropaleontology*, **19** (3): 308-340.

Bertels A. 1974. Upper Cretaceous (Lower Maastrichtian?) ostracodes from Argentina. *Micropaleontology*, **20** (4): 385-397.

Bertels A. 1975a. Upper Cretaceous (middle Maastrichtian) ostracodes of Argentina. *Micropaleontology*, **21** (1): 97-130.

Bertels A. 1975b. "Harringtonia" Gen. Nov. (Ostracoda, Crustacea) y nuevas espécies del Terciarico de la Republica Argentina. *Ameghiniana*, **7** (3): 259-279.

Bertels A. 1975c. Ostracode ecology during the Upper Cretaceous and Cenozoic in Argentina. *Bulletin of American Paleonology*, **65** (282): 317-351.

Bertels A. 1980. Estratigrafía y Foraminíferos (Protozoa) bentónicos del limite Cretácico-Terciárico em la área tipo de la Formación Jagüel, província del Neuquén, República Argentina. *In*: *Segundo Congreso Argentino de Paleontogía y Bioestratigrafía y Primer Congreso Latinoamericano de Paleontología*, **2:** 47-92.

Bertels-Posotka A. 1995. The Cretaceous-Tertiary boundary in Argentina and its ostracodes. Ostracoda and Biostratigraphy, *Riha* (ed). 163-170 p.

Bohor B.F., Foord E.E., Modreski P.J. Triplehorn D.M. 1984. Sedimentological Evidence for an Impact Event at the Cretaceous-Tertiary Boundary. *Science*, **224:** 867-868.

Bohor F.B., Modreski P.J. Foord E.E. 1987. Schocked Quartz in the Cretaceous-Tertiary.

Bourgeois J., Hansen A.T. Wiberg P.L. 1988. A Tsunami Deposit at the Cretaceous-Tertiary Boundary in Texas. *Science* **241:** 567-570.

Bown P. 2005. Selective calcareous nannoplancton survivorship at the Cretaceous-Tertiary boundary. *Geology*, **33** (8): 653-656.

Bramlette M.N. 1965. Massive Extinctions in Biota at the End of Mesozoic Time. *Science*, **148** (1): 696-1699.

Brenchley P.J. & Harper D.A.T. 1998. Evolutionary paleoecology of the marine biosphere. *In*: Brenchley P.J. & Harper D.A.T. (Eds). *Paleoecology: Ecosystems, Environments and Evolution*. Ed.1º Editora Chapman & Hall. p.:303-357.

Browers E.M. & De Deckker P. 1993. Late Maastrichtian and Danian ostracodes faunas from Northern Alaska: reconstructions of environment and paleogeography. *Palaios*, **8**: 40-154.

Camacho H.H. 1992. Algunas consideraciones acerca de la transgresión marina paleocena em la Argentina. *Miscelanea de la Academia Nacional de Ciencias*, **85**: 1-41.

Canudo J.I., Keller G., Molina E. 1991. Cretaceous/Tertiary boundary extinction pattern and faunal turnover at Agost and Caravaca, S.E. Spain. *Marine Micropaleontology*, **17:** 319-341.

Carignano A.P. 2011. Sistemática y Paleoecología de Foraminifera (Protista) y Ostracoda (Crustacea) del Cretácico Superior-Paleoceno de Argentina en ambientes marino transicionales y continentales. Tese de Doutorado, Facultad de Ciencias Naturales y Museo, Universidad Nacional de la Plata (não publicado).

Carter N.L., Officer C.B. Drake C.L. 1990. Dynamic deformation of quartz and feldspar: clues to causes of some natural crises. *Tectonophysics*, **171:** 373-391.

Casadío S. 1998. Las ostras del Límite Cretácico-Paleógeno de la Cuenca Neuquina (Argentina). Su importancia bioestratigráfica y paleobiogeográfica. *Ameghiniana*, **35** (4): 449-471.

Casadío S. & Leanza A.H. 1991. *Eubaculites Argentinicus* (Weaver) (Cephalopoda-Ammonoidea) del Maastrichtiano del oeste central de la Argentina. *Revista de La Asociacion Geologica Argentina*. **XLVI** (1-2): 26-35.

Casadío S., Griffin M., Parras A. 2005. *Camptonectes* and *Plicatula* (Bivalvia, Pteiomorphia) from the Upper Maastrichtian of northern Patagonia: paleobiogeographic implications. *Cretaceous Research,* **26**: 507-524.

Casadío S., Griffin M., Parras A., Concheyro A., Feldmann R., Gasparini Z. Parma S.G. 2004. Biotic and environmental changes across the Cretaceous/Paleogene boundary in Patagonia. *In*: X Reunión Argentina de Sedimentologia, San Luis. *Resumenes*. 187-188p.

Casadío S. Parras A., Concheyro A. Pires M. 1998. El diacronismo de la sedimentación carbonática em la Cuenca Neuquina durante la transición Cretácico-Paleógena. *In*: *VII Congresso Argentino de Paleontologia y Bioestratigrafia (Bahia Blanca).* 126p.

Ceolin D., Fauth G. Coimbra J.C. 2011. Cretaceous-Lower Paleogene Ostracods from the Pelotas Basin, Brazil. *Palaeobiodiversity and Palaeoenvironments*, **91:** 111-128.

Cisowski S.M. & Fuller M. 1986. Cretaceous Extinction and Wildfires. *Letters*, **234:** 261-262.

Claeys P., Kiessling W., Alvarez W. 2002. Distribution of Chicxulub ejecta at the Cretaceous-Tertiary boundary. *Geological Society of America*. Special Paper**, 356:** 55-68.

Coccioni R. & Galeotti S. 1994. K-T boundary extinction: Geologically instantaneous or gradual event? Evidence from deep-sea benthic foraminifera. *Geology*, **22**: 779-782.

Colin J.P., Tambareau Y. Krasheninnikov V.A. 1998. Maastrichtian and Paleocene ostracodes assemblages of Mali (Western Africa). Dela-Opera Sazu 4. *Razr*, **34** (2): 273-345.

Concheyro, A. 1995. Nanofósiles calcareous del Cretácico Superior y Paleógeno de Patagonia, Argentina. Tese de Doutorado, Universidade de Buenos Aires, 384p. (não publicado).

Concheyro A. 2004. High resolution biostratigraphy K–Pg boundary from northern Patagonia, Argentina. *In*: X Reunión Argentina de Sedimentología, San Luis. *Resúmenes Contribuciones Simposio K/T*, 189 p.

Concheyro A. & Nañez C. 1994. Microfossils and Bioestartigraphy of the Jagüel and Roca Formations (Maastrichtian-Danian), province of Neuquén. Reunion de Comunicaciones. *Ameghiniana*, **4:** 31.

Concheyro A., Nañez C., Casadío S. 2002. El Límite Cretácico-Paleógeno em Trapalcó, província de Río Negro, Argentina: ¿una localidad clave en América del Sur? *In*: XV Congresso Geológico Argentino. El Calafate. *Actas*: 590-595.

Concheyro A. & Villa G. 1996. Maestrichtian-Danian (K/P) calcareous nannofossils in the Liu Malal section. Northern Patagonia, Argentina. *Paleopelagos*, **6:** 281-297.

Coutillot V., Besse J., Vandamme D., Montigny R., Jaeger J.J., Cappetta H. 1986. Deccan flood basalts at the Cretaceous/tertiary boundary? *Earth and Planetary Science Letters*, **80:** 361-374.

Damotte R. 1991. Sur la faune d'Ostracodes des dépôsits marins au passage crétacé-tertiaire dans la vallée du Tilemsi (nord Mali). *Cahiers de Micropaléontologie* **6** (1): 5-19.

Damotte R. 1993. Late Cretaceous and early Tertiary ostracodes from North Africa. *Cretaceous Research*, **14**: 39-47.

Damotte R. & Fleury J.J. 1987. Ostracodes maastrichtiens et paléocènes du Djebel Dyr, près de Tebessa, (Algerie orientale). *In*: X Colloque Africain de Micropaléontologie; B, Le Mesozoique. *Geologie Mediterranéenne*, **14** (2): 87-107.

Del Río C.J., Concheyro A., Martínez S. 2011. The Maastrichtian-Danian at General Roca (Patagonia, Argentina): a reappraisal of the chronostratigraphy and biostratigraphy of a type locality. *Neues Jahrbuch Geoogie Paläontologie Abhandlungen*, **259/2**: 129-156.

Del Río C.J., Martínez S.A., Stilwell D.J., Concheyro A. 2007. Paleontology of the Cerros Bayos section, Roca Formation (Danian), La Pampa Province, Argentina. *Alcheringa*, **31**: 241-269.

Dias S.C.2004. Planejando estudos de diversidade e riqueza: uma abordagem para estudantes de graduação. *Acta Scientiarum. Biological Sciences*, **26** (4): 373-379.

Donze P., Colin J.P., Damotte R., Oertli H.J., Peypouquet J.P., Said R. 1982. Les Ostracodes du Campanien terminal à l'Èocène inférieur de la coupe du Kef, Tunisie Nord-Occidentale. *Bulletin des Centres de Researches Exploration-Production Elf-Aquitain*, **6**: 273-335.

Ellwood B.B., MacDonald W.D., Wheeler C., Benoist, S.L. 2003. The K-T boundary in Oman: identified using magnetic susceptibility field measurements with geochemical confirmation. *EPSL*, **206:** 529-540.

Erickson D.J. & Dickson S.M. 1987. Global trace-element biogeochemistry at the K/T boundary: Oceanic and biotic response to a hypothetical meteorite impact. *Geology*, **15:** 1014-1017.

Erwin D.H. 1990. End-Permian. *In:* D.E.G. Briggs & P.R. Croether. *Palaeobiology: A Synthesis*, Australia, 1ª ed. Cap. 13, 187-190.

Fauth G., Colin J.P., Koutsoukos E.A.M. Bengston P. 2005. Cretaceous-Tertiary boundary ostracodes from Poty Quarry, Pernambuco, northeastern Bazil. *Journal of South American Earth Sciences*, **19:** 285-305.

Fernández M., Martin J., Casadío S. 2008. *Mosasaurus* (Reptilia) from the late Maastrichtian (Late Cretaceous) of northern Patagonia (Río Negro, Argentina). *Journal of South American Earth Sciences*, **25**: 176-186.

Gamper M.A. 1977. Acerca del Limite Cretacico-Terciario en Mexico. *Revista* **1** (1): 23-27.

Ganapathy R., Brownlee D.E., Hodge P.W. 1978. Silicate spherules from Deep-Sea sediments: Confirmation of Extraterrestrial Origin. *Science*, **201:** 1119-1121.

Gartner S. & Keany J. 1978. The terminal Cretaceous event: A geological problem with an oceanographic solution. *Geology*, **8** (12): 708-712.

Gartner S. & McGuirk J.P. 1979. Terminal cretaceous Extinction Scenario for a Catastrophe. *Science*, **206:** 1272-1276.

Gasparini Z., Casadío S., Fernández M., Salgado L. 2001. Marine reptiles from the Late Cretaceous of northern Patagonia. *Journal of South American Earth Sciences*. **14:** 51-60.

Gasparini Z., Salgado L., Parras A. 2007. Late Cretaceous plesiosaurs from northern Patagonia, Argentina. *Geological Journal*, **42:** 185-202.

Gradstein F.M., Ogg J.G., Schmitz M.D., Ogg G.M. (Eds.) 2012. *The Geologic time scale 2012*. V. 2, 437-1129 pp.

Grice K., Changquin C., Gordon D.L., Böttcher M.E., Twitchett R.J., Grosjean E., Summons R.E., Turgeon S.C., Dunning W., Jin Y. 2005. Photic Zone Euxinia During the Permian-Triassic Superanoxic Event. *Science*, **307:** 706-709.

Griffin M. & Pastorino G. 2013. Cenozoic *Ampullinidae* and *Naticidae* (*Mollusca, Gastropoda*) from Patagonia, Argentina. *Journal of Paleontology*, **87** (3): 502-525.

Groeber P. 1946. Observaciones geológicas a lo largo del meridiano 70°. I Hoja de Chos Malal. *Revista de la Sociedad Geológica Argentina*, 177-208.

Guernet C. & Danelian T. 2006. Ostracodes bathyaux du Crétacé terminal-Éocène moyen em Atlantique tropical (Palteau de Demerara, Leg 207). *Revue de Micropaléontologie*, **49:** 215-225.

Hallam T. 2005. Catastrophes and lesser calamities: The causes of mass extinctions. Oxford University Press, 226p.

Hallan A. 1987. End-Cretaceous Mass Extinction Event: Argument for Terrestrial Causation. *Science*, **238:** 1237-1242.

Hansen T., Farrad B.R., Montgomery H.A., Billman G.H., Blechschmidt G. 1987. Sedimentology and Extinction Patterns across the Cretaceous-Tertiary boundary interval in East Texas. *Cretaceous Research*, **8:** 229-252.

Hay W.W. 2008. Evolving ideas about the Cretaceous climate and ocean circulation. *Cretaceous Research*, **29**: 725-753.

Hildebrand R.A., Penfield G.T., Kring D.A., Pilkington M., Camargo Z.A., Jacobsen S.B. 1991. Chicxulub crater: A possible Cretaceous/Tertiary boundary impact crater on the Yucatán Peninsula, Mexico. *Geology*, **19**: 867-871.

Howell A.J., Schwarz E., Spalletti A.L., Veiga G.D. 2007. The Neuquén Basin: an overview. *Geological Society, London*, Special Publications, **252**:1-14.

Holden J.C. 1964. Upper Cretaceous pstracods from California. *Palaeontology*, **7**: 393-429.

Hsü K.J., Judith W.H., Mackenzie A., Weissert H., Perch-Nielsen K., Oberhänsli H., Kelts K., LaBrecque J., Tauxe L., Krähenbühl U., Percival F.S., Wright R., Karpoff A.M., Petersen N., Tucker P., Poore R.Z., Gombos A.M., Pisciotto K., Carman M.F.,

Schreiber E. 1982. Mass Mortality and Its Environmental and Evolutionary Consequences. *Science*, **216** (4543): 249-255.

Isozaki Y., Shimizu N., Yao J., Zhansheng J., Matsuda T. 2007. End-Permian extinction and volcanism-induced environmental stress: The Permian-Triassic boundary interval of lower-slope facies at Chaotian, South China. *Palaeogeography, Palaeoclimatology, Palaeoecology*, **252:** 218-238.

Jablonski D. & Raup D. 1995. Selectivity of End-Cretaceous Marine Bivalve Extinctions. *Science*, **268:** 389-391.

Javoy M. & Courtillot V. 1989. Intense acid volcanism at the Cretaceous-Tertiary boundary. *Earth and Planetary Science Letters*, **94:** 409-416.

Jiang S., Bralower T.J., Patzkowsky M., Kump L.R., Schueth J.D. 2010. Geographic controls on nannoplankton extinction across the Cretaceous/Paleogene boundary. *Nature Geoscience*.1-6.

Kaiser S.I., Steuber T., Becker T.R., Joachimski M.M. 2006. Geochemical evidence for major environmental change at the Devonian-Carboniferous boundary in Carnic Alps and the Rhenish Massif. *Palaeogeography, Palaeoclimatology, Palaeoecology*, **240:** 146-160.

Kastner M., Asaro F., Michel H.V., Alvarez W., Alvarez L.W. 1984. The precursor of the Cretaceous-Tertiary Clays at Stevens Klint, Denmark, and DSDP Hole 465A. *Science*, **226:** 137-143.

Kauffman, E.G. & Harries, P.J. 1996. Las consecuencias de la extinction en masa: prediciones para la supervivencia y regeneración em ecossistemas antigos y modernos. *In:* Tusquets (Ed). *La lógica de las extinciones*. Metatemas 42, J. Augustí (Ed.), Barcelona, 17-64.

Keller G. 1988. Extinction, Survivorship and Evolution of Planktic Foraminifera across the Cretaceous/Tertiary Boundary at El Kef, Tunisia. *Marine Micropalentology*, **13:** 239-263.

Keller G. 1989. Extended Cretaceous/Tertiary boundary extinctions and delayed population change in planktonic foraminifera from Brazos River, Texas. *Paleoceanography,* **4** (3): 287-332.

Keller G. 1993. The Cretaceous-Tertiary boundary transition in the Antarctic Ocean and its global implications. *Marine Micropaleontology*, **21:** 1-45.

Keller G. 2003. Biotic effects of impacts and volcanism. *Earth and Planetary Science Letters*, **215**: 249-264.

Keller G. 2005. Biotic effects of late Maastrichtian mantle plume volcanism: implications for impacts and mass extinctions. *Lithos*, **79**: 317-341.

Keller G. 2008. Cretaceous climate, volcanism, impacts, and biotic effects. *Cretaceous Research*, **29**: 754-771.

Keller G. Adatte T., Burns S.T., Tantawy A.Z. 2002. High-stress paleoenvironment during the late Maastrichtian to early Paleocene in Central Egypt. *Palaeogeography, Palaeoclimatology, Palaeoecology*, **187:** 35-60.

Keller G. Adatte T., Hollis C., Ordóñez M., Zambrano N.J., Stinnesbeck W., Aleman A., Hale-Erlich. 1997. The Cretaceous/Tertiary boundary event in Ecuador: reduced biotic effects due to eastern boundary current setting. *Marine Micropaleontology*, **31:** 97-133

Keller G., Adatte T., Browmick P.K., Upadhyay H., Dave A., Reddy A.N., Jaiprakash B.C. 2012. Nature and timing of extinctions in Cretaceous-Tertiary planktic foraminifera preserved in Deccan intertrappean sediments of the Krishna-Godavari. *Earth and Planetary Science Letters*, **341-344:** 211-221.

Keller G., Adatte T., Gardin S., Bartolini A., Bajpai. 2008. Main Deccan volcanism phase ends near the K-T boundary: Evidence from the Krishna-Godavari Basin, SE India. *Earth and Planetary Science Letters*, **268:** 293-311.

Keller G., Adatte T., Tantawy A.A., Berner Z. Stinnesbeck W., Stueben D., Leanza H.A. 2007. High stress late Maastrichtian - Early Danian palaeonvironment in the Neuquén Basin, Argentina. *Cretaceous Research* **28:** 939-960.

Keller G., Barrera E., Mattson E. 1993. Gradual mass extinction, species survivorship, and long-term environmental changes across the Cretaceous-Tertiary boundary in high latitudes. *Geological Society of America Bulletin*, **105:** 979-997.

Keller G., Li L., MacLeod N. 1995. The cretaceous-Tertiary boundary stratotype section at El Kef, Tunisia: how catastrophic was the mass extinction? *Palaeogeography, Palaeoclimatology, Palaeoecology*, **119**: 221-254.

Keller G. & Pardo A. 2004. Disaster opportunists *Guembellitrinidae*: index for environmental catastrophes. *Marine Micropaleontology*, **53**:83-16.

Keller G., Rhowmick P.K., Upadhyay H., Dave A., Reddy A.N. Jaiprakash B.C., Adatte T. 2011. Deccan Volcanism Linked to the Cretaceous-Tertiary Boundary Mass Extinction: New Evidence from ONGC Wells in the Krishna-Godavari Basin. *Journal Geological Society of India*, **78:** 399-428.

Keller G., Stinnesbeck W., Adatte T., Stueben D. 2003. Multiple impacts across the Cretaceous-Tertiary boundary. *Earth Science Reviews*, 62: 327-363.

Kelley, P.S. & Gurov, E., 2002. Boltysh, another end-Cretaceous impact. *Meteoritics & Planetary Science*, **37:** 1031-1043.

Kelley P.H. & Hansen T.A. 1993. Evolution of predator-prey behavior: Naticid gastropods and their molluscan prey. In: M. Nitecki & J. Kitcheli (eds.). *Evolution of Animal Behavior: Paleontological and Field Approaches*. Oxford University Press, 88-110 p.

Kent D.V. 1981. Asteroid Extinction Hypothesis. *Science*, 211:650.

Kiessling W., Scasso R. Aberhan M., Riz L., Weidemeyer S. 2006. A Maastrichtian microbial reef and associated limestones in the Roca Formation of Patagonia (Neuquén Province, Argentina). *Fossil Record,* **9** (2): 183-197.

Koutsoukos E.A.M. 1997. Meteorites: Origin of the Solar System, Meteorite Impact and Evolution. Heidelberg, 1-10.

Koutsoukos E.A.M. 2005. The K-T boundary. *In*: E.A.M. Koutsoukos. *Applied Stratigraphy*, Editora Springer, **23:** 147-178.

Kring D.A. 2007. The Chicxulub impact event and its environmental consequences at the Cretaceous-Tertiary boundary. *Palaegeography, Palaeoclimatology, Palaeoecology,* **255**: 4-21.

Krug A., Jablonski D., Valentine J.W. 2009. Signature of the End-Cretaceous Mass Extinction in the Modern Biota. *Science*, **323:** 767-771.

Kyte F. 2002. Tracers of extraterrestrial component in sediments and inferences for Earth's accretion history. *Geological Society of America*, special paper **356**: 21-38.

Lavina, E.L. & Fauth, G. 2011. Evolução Geológica da América do Sul nos últimos 250 Milhões de anos. *In:* C.J.B Carvalho & E.A.B. Almeida. *Biogeografia da América do Sul*. Editora Roca. p.: 3-13.

Leanza H. & Hugo C. 1985. Los biohermas osteros de la Formacion Roca (Paleoceno) em el sudoeste de la provincia de La Pampa, Argentina. *Ameghiniana*, **21** (2-4): 143-149.

Li L. & Keller G. 1998. Abrupt deep-sea warming at the end of the Cretaceous. *Geology*, **26**: 995-999.

Lipps J.H. & Culver S.J. 2002. The trophic role of marine microorganisms through time. *Paleontological Society Papers*, **8**: 69-92.

López-Oliva J.G., Kelelr G., Stinnesbeck W. 1998. El Límite Cretácico/Terciario (K/T) en el noreste de México-extinción de foraminíferos plactónicos. *Revista Mexicana de Ciencias Geológicas*, **15** (1): 109-113.

Macdougall J.D. 1988. Seawater Strontium Isotopes, Acid rain, and the Cretaceous-Tertiary boundary. *Reports*, **239:** 485-487.

MacLeod N. 2003. The causes of Phanerozoic extinctions. *Evolution on Planet Earth.* p. 253-277.

MacLeod N., Rawson P.F., Forey P.L., Banner F.T., Boudagher-Fadel M.K., Bown P.R., Burnett J.A., Chambers P., Culver S.E., Evans S.E., Jeffery C., Kaminski M.A., Lord A.R., Milner A.R., Morris N., Owen E., Rosen B.R., Smith A.B., Taylor P.D., Urquhart E., Young J.R. 1997. The Cretaceous-Tertiary biotic transition. *Journal of the Geological Society, London,* **154:** 265-292.

Maddocks R.F. 1985. Ostracoda of Cretaceous-Tertiary contact sections in central texas. *Gulf Coast association of Geological Societies, Transactions*, **35:** 445-456.

Maddocks R.F.1988. One hundred million years of Predation on Ostracods: The Fossil Record in Texas. *In*: T. Hanai, N. Ikeya, K. Ishizaki (eds). *Evolutionary biology of Ostracods*. Developments in Palaeontology and Stratigraphy, **11**: 367-657.

Malumián N. 1999. La sedimentación y el volcanismo terciarios en la Patagonia Extraandina. Geología Argentina*, Anales*, **29** (18): 557-612.

Martínez-Ruíz F., Bernasconi S., McKenzie J.A. 1994. Paleoceanographic changes across the Cretaceous-Tertiary boundary: carbono and nitrogen isotope stratigraphy at the Agost section, Spain. *Mineralogical Magazine*, **58A:** 561-562.

Martini. E. 1971. Standard Tertiary and Quaternary calcareous nannoplankton zonation. *In*: Farinacci A. (ed.). *Proceedings of the 2nd Planktonic Conference*, Rome, 739-785.

Mazzini I., Faranda C., Giardini M., Giraudi C. Sadori L. 2011. Late Holocene palaeoenvironmental evolution of the Roman harbour of *Portus*, Italy. *Journal of Paleolimnomogy*, **46**: 243-256.

McLean D.M. 1985. Deccan Traps Mantle degassing in the Terminal Cretaceous Marine Extinctions. *Cretaceous Research*, **6:** 235-259.

Molina E., Alegret L., Arenillas I., Arz J.,Gallala N.,Hardenbold J.,Salis K.von.,Steurbaut E., Vandenberghe N., Zaghbib-Turki D. 2006. The Global Boundary Stratotype Section and Point for the base of the Danian Stage (Paleocene, Paleogene, "Tertiary", Cenozoic) at El Kef, Tunisia-Original definition and revision. *Episodes*, **29** (4): 263-273.

Moore R.C. & Pitrat C.W. 1961. Crustacea: Ostracoda. *In*: R.C. Moore (ed.). *Treatise on Invertebrate Paleontology, Part Q, Arthropoda 3*. Geological Society of America, Boulder, CO, and University of Kansas Press, Lawrence KS, 465 pp.

Musso T., Concheyro A., Pettinari G. 2012. Mineralogía de arcillas y nanofósiles calcáreos de las formaciones Jagüel y Roca em el sector oriental del Lago Pellegrini, Cuenca Neuquina, República Argentina. *Andean Geology*, **39** (3): 511-540.

Nañez C. & Concheyro A. 1996. Limite Cretacico-Paleogeno. Geologia y Recursos Minerales del departamento Añelo. Província del Neuquén, República Argentina, 129-150 p.

Nañez C. & Malumián N. 2008. Paleobiogeografía y Paleogeografía del maastrichtiense marino de la Patagonia, Tierra Del Fuego y la plataforma continental Argentina, según sus foraminíferos bentônicos. *Revista Española de Paleontología*, **23** (2): 273-300.

Odum E.P. 2004. Fundamentos de Ecologia. Fundação Calouste Gulbenkian, 7ª ed. Lisboa, 927pp.

Officer C.B. & Drake C.L. 1983. The Cretaceous-Tertiary transition. *Science*, **219**:1383-1390.

Officer C.B. & Drake C.L. 1985. Cretaceous-Tertiary Extinctions-Alternative Models. *Science*, **230:** 1294-1295.

Olempska E. 1997. Changes in benthic ostracod assemblages across the Devonian-Carboniferous boundary in the Holy Cross Mountains, Poland. *Acta Paleontologica Polonica*, **42:** 291-332.

Olssom R.K., Miler K.G., Browning J.V., Habib D., Sugarman P.J. 1997. Ejecta layer at the Cretaceous-Tertiary boundary, Bass River, New Jersey (Ocean Drilling Program Leg 174AX). *Geology*, **25** (8): 759-762.

Ortega-Huertas M., Martínez-Ruíz F., Oddone M., Palomo I. 2002. REE behaviour across the Cretaceous-Tertiary boundary. *Mineralogical Magazine*, **58A:** 674-675.

Palamarkzuk S. 2002. Maastrichtian dinoflagellates from the Jagüel Formation, Neuquén Province, Argentina. *Palynology*, **26**: 272p.

Palamarkzuk S. 2006. Bajada de Jagüel, Neuquén province, Argentina: complete or incomplete K/Pg boundary section? Philadelphia Annual Meeting. Geological Society of America *Abstracts with Programs*, **38** (7): 297p.

Pälike H. 2013. Impact and Extinction. *Science*, **339:** 655-656.

Papú O.H., Prámparo M.B., Nañez C., Concheyro A. 1999. Palinología y Micropaleontología de la Formación Jagüel (Maastrichtiano-Daniano), Perfil Opaso, Cuenca Neuquina, Argentina. Simposio Paleogeno de América del Sur (Buenos Aires, 1996), Actas Susecretaría de Minería de La Nación, Serivicio Geológico Minero Argentino, *Anales* **33**: 17-31.

Parma S.G. & Casadío S. 2005. Upper Cretaceous-Paleocene echinoids from northern Patagonia, Argentina. *Journal of Paleontology*, **79** (6): 1072-1087.

Parras A.M., Casadío S., Pires M. 1998. Secuencias depositacionales Del Grupo Malargüe y El Límite Cretácico-Paleógeno, em el Sur de la Provincia de Mendoza, Argentina. *Asociación Paleontológica Argentina*. Publicación Especial 5, Buenos Aires. 61-69p.

Perch-Nielsen K. 1985. Mesozoic calcareous nannofossils. *In*: Bolli H.H., Saunders J.B. Perch-Nielsen K. (eds.). *Plankton Stratigraphy*, Cambridge, 329-426.

Peypouquet J.P., Carbonnel P. Ducasse O., Tölderer-Farmer M., Lété C. 1988. Environmentally Cued Polymorphism of Ostracods *In:* H. Tetsuro., N. Ikeya., K. Ishizaki. *Developments in Paleontology and Stratigraphy- Evolutionary biology of ostracoda: its fundamentals applications,* **11***:* 1003-1019.

Prámparo M.B. & Papú O.H. 2006. Late Maastrichtian dinoflagellate cysts from the Cerro Butaló section, southern Mendoza province, Argentina. *Journal of Micropaleontology*, **25**: 23-33.

Punekar J., Mateo P., Keller G. 2014. Effects of Deccan volcanism on paleoenvironment and planktic foraminifera: A global survey. *Geological Society of America Special Papers*, doi:10.1130/2014.2505(04).

Renne P.R., Deino A.l., Hilgen F.J., Kuiper K.F., Mark D.F., Mitchell W.S., Morgan L.E., Mundil R., Smit J. 2013. Time Scales of Critical Events around the Cretaceous-Paleogene boundary. *Science***, 39:** 684-687.

Reyment R.A., 1963. Studies on Nigerian Upper Cretaceous and Lower Tertiary Ostracoda: part 2: Danian, Paleocene and Eocene Ostracoda. *Stockholm Contributions in Geology*, **10:** 1-286.

Reyment R.A. 1966a. Preliminary observations on gastropod predation in the western Niger Delta. *Palaeogeography, Palaeoclimatology, Palaeoecology*, **2**: 81-102.

Reyment R.A. 1966b. Studies on Nigerian Upper Cretaceous and Lower Tertiary Ostracoda. Part 3. Stratigraphical, palaeoecological and biometrical conclusions. *Stockholm Contributions in Geology*, **14:** 1-151.

Reyment R.A. & Elewa A.F. 2003. Predation by Drills on Ostracoda. *In*: P.H. Kelley, M. Kowalewski., A. Thor (eds.). *Predator-Prey Interactions in the Fossil Record*. Plenun Publishers, New York. Chapter 4, 93-111 p.

Reyment R.A., Reyment E.R., Honigstein A. 1987. Predation by boring gastropods on Late Cretaceous and early Palaeocene ostracodes. *Cretaceous Research*, **8**:189-209.

Ridley M. 2006. Extinção e irradiação. *In*: M. Rydley (ed.) *Evolução*.Artmed, 3ª ed.Porto Alegre. p. 663-695.

Robert C. & Chamley H., 1990. Paleoenvironmental significances of clay mineral associations at the Cretaceous-Tertiary passage. *Palaeogeography, Palaeoclimatology, Palaeoecology*, **79:** 5205-219.

Robertson D.S, William M.L., Sheehan P.M., Toom O.B. 2013. K–Pg extinction patterns in marine and freshwater environments: The impact winter model. *Journal of Geophysycal Research: Biogeosciences*, **118**: 1006-1014.

Rodrigues M.F. 2011. El grupo Malargüe (Cretácico Tardío-Paleógeno Temprano) em la Cuenca Neuquina. *In*: Relatório del XVIII Congresso Geológico Argentino, Neuquén, *Geología y recursos naturales de la Província del Neuquén*. 245-264p.

Rodrigues G.B. & Fauth G., 2013. Isótopos estáveis de carbono e oxigênio em ostracodes do Cretáceo: metodologias, aplicações e desafios. *Terrae Didatica*, **9:** 34-49.

Rodrigues G.B., Fauth G., Santos R.V., Koutsoukos E.A., Colin, J.P. 2014. Tracking paleoecological and isotopic changes through the K–Pg boundary from marine ostracodes: The Poty quarry section, notheastern Brazil. *Cretaceous Research*, **47:** 105-116.

Ruddiman W.R. 2008. Greenhouse Climate. *In:* W.F. Freeman & Company. *Earth's Climate past and future*. 2ªed., New York. cap. 5, p.81-95.

Ruiz F., Abad M., González-Regalado M.L., Civis J., González-Delgado J.A., García E.X.M., Toscano A. 2010. Predation on Neogene ostracodes of southwestern Spain. *Rivista Italiana di Paleontologia e Stratigrafia*, **116** (2): 253-260.

Ryder G. 1996. The unique significance and origin of the Cretaceous-Tertiary boundary: Historical context and burdens of proof. *Geological Society of America*, **307:** 31-38.

Said-Benzarti R. 1988. Les Ostracodes Du Campanien superior à I'Yprésien de la coupe d'Ellès (Tunisie du Centre Nord)-Biostratigraphie, Paléoécologie et Paléobiologie. *In*: S. Crasquin-Soleau, E. Braccini, F. Lethiers. *What about Ostracoda!* Actes du 3º Congrès Européen des Ostracodologistes. **20:** 197-211.

Scasso R.A., Concheyro A.; Kiessling W., Aberhan M., Hecht L., Medina F., Tagle R. 2005. A tsunami deposit at the Cretaceous/Paleogene boundary in the Neuquén Basin of Argentina. *Cretaceous Research*, **26**: 283-297.

Schulte *et al*. 2010. The Chicxulub Asteroid Impact and Mass Extinction at the Cretaceous-Paleogene Boundary. *Science*, **327:** 1214-1218.

Scotese C.R. 2011. Paleomap Project. Disponível em: www.scotese.com. Acessado em 19 nov 2014.

Signor P.W. & Lipps J.H., 1982. Sampling bias, gradual extinction patterns and catastrophes in the fossil record. *Geological Society of America*, **190:** 291-296.

Skelton P., 2003. *The Cretaceous World*. Cambridge University Press. Cambridge, United Kingdom, 360p.

Slipper I.J. 1997. Turonian (Late Cretaceous) Ostracoda from Dover, south-east England (BL). PhD thesis, University of Greenwich. p. 433.

Smit J., 1990. Meteorite impact, extinctions and the Cretaceous-Tertiary Boundary. *Geologie en Mijnbouw*, **69:**187-204.

Smith A.B. 1994. *Systematics and the fossil record: documenting evolutionary patterns*.- Blackwell, London.

Smith C.C. 1997. The Cretaceous-Tertiary boundary at Moscow Landing West-Central Alabama. *Gulf Coast Association of Geological Societies Transactions*, XLVII: 533-539.

Smit J., Romein A.J.T. 1985. A sequence of events across the Cretaceous-Tertiary boundary. *Earth and Planetary Science Letters*, **74**:155-170.

Sohn I.G. 1962. The Ostracode Genus *Cytherelloidea*, a possible indicator of paleotemperature. *Geological Survey Research*, **162:** 144-147.

Sohn I.G., Berclan J.M., Peck R.E. 1965. Ostracods. *In*: Kummel B.& Raup D. (eds) *Handbook of Paleontological Techniques*, W.H. Freeman & Co. 77-89pp.

Stewart, S.A. & Allen, J.P., 2002. A 20-km-diameter multi-ringed impact structure in the North Sea. *Nature*, **418:** 520-523.

Stilweel J.D. 2003. Patterns of biodiversity and faunal rebound following the K-T boundary extinction event in Austral Palaeocene molluscan faunas. *Palaeogeography, Palaeoclimatology, Palaeoecology*, **195**: 319-356.

Stüben D., Kramar U., Berner Z., Stinnesbeck W., Keller G., Adatte T. 2002. Trace elements, stable isotopes, and clay mineralogy of the Elles II K-T boundary section in Tunisia: indications for sea level fluctuations and primary productivity. *Palaeogeography*, *Palaeoclimatology*, *Palaeoecology*, **178:** 321-345.

Suguio K. 2003. Ambientes de sedimentação marinhos. *In*: Suguio K. *Geologia Sedimentar*, 1ªed. Cap. 8, 205-287.

Surlyk F. 1999. Cretaceous-Tertiary (Marine). *In:* Briggs D.E.G & Croether P.R. *Palaeobiology: A Synthesis*, Australia, 1ª ed. Cap.12, 198-203.

Tantawy A.A., Keller G., Adatte T., Stinnesbeck W., Kassab A., Schulte P. 2009. Maastrichtian to Paleocene depositional environment of the Dakhla Formation, Western Desert, Egypt: sedimentology, mineralogy, and integrated micro-and macrofossil biostratigraphies. *Cretaceous Research*, **22:**795-827.

Tappan H. 1979. Protistan evolution and extiction at the Cretaceous-Tertiary boundary. *II. Proceedings, Cretaceous-Tertiary boundary events*, University of Copenhagen, p.13-21.

Uliana M.A. & Bidde K.T. 1988. Mesozoic-Cenozoic Paleogeographic and geodynamic evolution of southern South America. *Revista Brasileira de Geociências*, **18** (2): 172-190.

Uliana M.A. & Dellapé D.A. 1981. Estratigrafia y evolucion paleoambiental de La sucesion Maestrichtiano-Eoterciaria Del Engolfamento Neuquino (Patagonia Septentrional). *VII Congresso Geológico Argentino*, San Luis. Actas III: 673-711.

Ward W.C., Keller G., Stinnesbeck W., Adatte T. 1995. Yucatán subsurface stratigraphy: Implications and constraints for the Chicxulub impact. *Geology*, **23:** 876-877.

Whatley R. & Boomer I. 1995. Authochthonous and Allochthonous Quaternary Ostracoda from Site 893, Santa Barbara Basin. *Proceedings of the Ocean Drilling Program. Scientific Results*, **146**: 251-294.

Whatley R. 1983. The application of Ostracoda to palaeoenvironmental analysis. *In*: R.F Maddocks (ed). *Applications of Ostracoda*. Univeristy of Houston, Geoscience. 51-77.

Wignall P.B. 2001. Large igneous provinces and mass extinctions. *Earth-Science Reviews*, 53:1-33.

Windle D.W., Kendall P.C. Gretton W.H., 1971. Terminal Cretaceous Events. *Nature*, **230:**318-320.

Wolbach W. S., Lewis E.S., Anders E., 1985. Cretaceous Extinctions: Evidence for Wildfire and Search for Meteoritic Material. *Science*, **230:**167-170.

Worsley T., 1974. The Cetaceous-Tertiary boundary event in the Ocean. *Society of Economic Paleontologists and Mineralogists*, **20:** 94-125.

Yalcin H. & Bozkaya O., 1996. A new discovery of the Cretaceous/Tertiary Boundary from the Tethyan Belt, Hekimhan Basin, Turkey: Mineralogical and Geochemical Evidence. *International Geology Review*, **38:** 759-767.

Yamaguchi T. & Hamiya T. 2002. Oligocene-Miocene ostracodes assemblages with the genus *Palmoconcha* from Japan. *Journal of Paleontology*, **81** (4):632-642.

Zoller W.H., Parrington J. R., Kotra P.J., 1983. Iridium Enrichment in Airborne Particles from Kilauea Volcano: January 1983. *Science*, **222:** 1118-1121.